

Effects of Alternate Blowing Agents on the Aging of Closed-Cell Foam Insulation

by

Melissa C. Page

B.S., Northeastern University (1987)

Submitted to the Department of Mechanical Engineering
in partial fulfillment of the requirements for the degree of

Master of Science

at the

MASSACHUSETTS INSTITUTE OF TECHNOLOGY

June 1991

© Massachusetts Institute of Technology 1991

Signature of Author
Department of Mechanical Engineering
May 20, 1991

Certified by
Leon R. Glicksman
Professor of Thermal Sciences and Building Technology
Thesis Supervisor

Accepted by
ARCHIVES
Ain A. Sonin
Chairman, Departmental Committee on Graduate Studies

MASSACHUSETTS INSTITUTE
OF TECHNOLOGY

JUN 12 1991

Blank Page

Effects of Alternate Blowing Agents on the Aging of Closed-Cell Foam Insulation

by

Melissa C. Page

Submitted to the Department of Mechanical Engineering
on May 20, 1991, in partial fulfillment of the
requirements for the degree of
Master of Science

Abstract

International agreements limiting the production of chlorofluorocarbons are having an impact on the rigid foam insulation industry. Shortages of the most common foam blowing agent, CFC-11 (a chlorofluorocarbon), has motivated a worldwide search for alternate blowing agents. The rate of thermal conductivity drift (*aging*) of foams blown with any viable alternate must be at least comparable to aging characteristics of CFC-11 blown foams.

Aging is modeled using measurements of mass transfer rates of gases in and structural characteristics of foam samples from board stock. A transient, constant-volume, sorption method that measures both gas diffusion and solubility is used to quantify the permeability of air constituents and blowing agents (CFC-11, HCFC-123, HCFC-141b) in samples of foams blown with either CFC-11, HCFC-123 or HCFC-141b. Measurements of foam cell size, cell wall thickness and density are used to characterize mass distribution in the foam.

Results indicate that foams blown with the alternates tend to have a higher percent of solid polymer in the cell walls compared to CFC-11 blown foams. There is also an indication that alternate blown foams have higher solid polymer permeability. The more permeable solid polymer and more material in the cell walls have canceling effects in terms of the resulting aging rates. Tests at high temperatures indicate that the diffusion coefficients of the three blowing agents are similar in magnitude. Results extrapolated to room temperature indicate that the alternate blowing agents will not significantly increase aging rates in these foams.

Thesis Supervisor: Leon R. Glicksman

Title: Professor of Thermal Sciences and Building Technology

Acknowledgements

Thanks to Professor L.R. Glicksman for his support and guidance through this, lifelong dream come true, opportunity to study at M.I.T. Deep gratitude to my mother, my sister and friends for their endless encouragement. I'm glad that my co-workers at R. G. Van-derweil Engineer urged me to return to school. My inspiration came from the memory of my father.

By generously sharing their ideas and experiences, my colleagues in the M.I.T. Heat Transfer Lab, in particular Tim Brehm and the members of the "Foam Group", enriched mine. I am grateful to Pat Griffin for help in computer related aspects and to KC for logistical aide. Heart-felt appreciation to Tiny and Norm in the machine shop for their helping hands with nuts and bolts problems.

This research was partially sponsored by the Mobay Chemical Company. Special thanks to the people there, G.F. Baumann, K.W. Dietrich, R.E. Weidemann and J.F. Szabat, who made this work possible and shared the insight of their experience. Through the efforts of D.L. McElroy funding was also provided by Oak Ridge National Laboratory. I would like to acknowledge D. Chen and D. Bhattacharjee of Dow Chemical for allowing me to use their test apparatus. Some of the results quoted were obtained in related projects sponsored by Dow Chemical Company and by the United States Department of Energy.

Contents

Abstract	3
Acknowledgements	4
Nomenclature	9
1 Introduction	19
1.1 What is Foam Insulation?	20
1.2 The CFC Issue	23
1.3 The Alternates	25
1.4 Focus of this Research	30
2 Characterization of Foam Structure	31
2.1 Determination of Percent Of Solid Polymer in Cell Walls	33
2.2 Determination of Cell Wall Thickness	36
2.3 Determination of Average Cell Diameter	38
2.4 Density Measurements	39
3 Transient Sorption Method for Permeability Measurement	41
3.1 Analysis of Physical Model	42
3.2 Analytical Solution	50
4 Test Apparatus and Procedure	61
4.1 Hardware	61
4.2 Data Acquisition	69

4.3	Experimental Procedures	70
5	Error and Uncertainty	81
5.1	Estimation of Measurement Uncertainty	82
5.2	Uncertainty in Permeability Test Results	90
6	Results and Discussion	101
6.1	Test Results for Air Components.	104
6.2	Percent of Solid Polymer in Cell Wall, P_{cw}	107
6.3	Solid Polymer Diffusion Coefficients, D_{sp}	109
6.4	Test Results: Blowing Agents	111
6.5	Aging Predictions	114
7	Conclusions and Recommendations	127
7.1	Conclusions	127
7.2	Recommendations	128
7.3	Future Work	129
	References	133
A	Alternate Blowing Agent Information	137
A.1	HCFC-123	139
A.2	HCFC-141b	148
B	Scanning Electron Microscope Photographs	153
C	Foam Geometry Calculations	177
D	Apparatus Information and Calibrations	185
E	Supplementary Information on Tested Foams	189
F	Transient Sorption Test Data	193

F.1	Foam No. 1	197
F.2	Foam No. 2	215
F.3	Foam No. 14	233
F.4	Foam No. 15	249
F.5	Foam No. 16	257
F.6	Foam No. 17	275
F.7	Foam No. 18	295

Nomenclature

A	Cross-sectional area of foam sample
D_{eff}	Foam effective diffusion coefficient
\hat{D}	Normalized diffusion coefficient
D_g	Foam diffusion coefficient
D_{sp}	Solid polymer diffusion coefficient
C_1	Initial gas concentration in test chamber
C_2	Gas concentration in test chamber after pressure change
C_{eff}	Foam effective concentration
C_g	Concentration of gas in foam cell or chamber
C_{sp}	Concentration of gas in the solid polymer
d	Diameter of foam sample
d_c	Average diameter of foam cell
E_D	Activation energy of diffusion
E_P	Activation energy of permeation
G	Equilibrium sorption parameter
K_{eff}	Foam effective solubility ratio S_{eff}/S_g
K_{sp}	Solid polymer solubility ratio S_p/S_g
k_G	Thermal conductivity of the cell gas
k_R	Thermal conductivity due to radiation
k_S	Thermal conductivity of the solid matrix
k_{sp}	Thermal conductivity of the solid polymer
k_T	Total effective foam thermal conductivity

$\langle l \rangle$	Average distance between foam cell walls
L_{eff}	Effective half-thickness of foam sample
m	Slope of best-fit line
\bar{P}	Non-dimensional gas pressure in test chamber
\bar{P}_∞	Equilibrium non-dimensional gas pressure in test chamber
P_1	Initial absolute pressure in test chamber
P_{cw}	Percent of polymer in foam cell walls
P_i	Partial pressure of gas species i
$P_{e,eff}$	Foam effective permeability
$P_{e,sp}$	Solid polymer permeability
R	Specific gas constant
R_d	Correction factor for sample deformation
S_{eff}	Foam effective solubility coefficient
S_g	Solubility coefficient for gas in foam cells
S_N	Standard deviation of a set of N measurements
S_{sp}	Solubility coefficient for gas in solid polymer
S_V	Foam cell surface to volume ratio
T	Absolute temperature
t_{cw}	Thickness of foam cell walls
T_{STP}	Standard absolute temperature (298°K or 536.4°R)
v	Voltage output of absolute pressure transducer
V_f	Volume of foam sample
V_{gm}	Volume of in test chamber with sample deformation
V_g	Volume of gas surrounding foam sample in test chamber
V_T	Total volume of test chamber
x	Space coordinate in foam sample
z	Non-dimensional space coordinate in foam sample

α_n	Eigenvalues for the solution of the model equations
δ	Foam void fraction
ΔH	Heat of solution
ΔP	Imposed pressure change in test chamber
ϵ	Absolute uncertainty interval
ρ_f	Density of foam
ρ_g	Density of gas
ρ_{sp}	Density of solid polymer
σ	Standard deviation of sample population
τ	Non-dimensional time coordinate
τ_0	Intercept of best-fit line
ξ	Fractional uncertainty interval

Blank Page

List of Figures

1-1	The Foam Aging Process.	20
1-2	Closed Cell Foam Insulation.	21
1-3	1986 Global CFC Use.	24
2-1	SEM Micrographs Showing: Typical Foam Cell Matrix, Strut and Cell Wall.	32
2-2	Technique used to obtain specimen for SEM.	35
2-3	Typical SEM Photograph Used in Lineal Analysis.	37
2-4	Typical SEM Photograph Used to Determine Cell Wall Thickness.	38
3-1	Conceptual Schematic of Transient Sorption Chamber and Sample.	42
3-2	Visualization of Concentration Gradients in Foam	45
3-3	Plot of analytical solution showing $P(\tau, G)$ for a range of G	54
3-4	Diagram of mapping from $\bar{P}(t)$ and $\bar{P}_G(\tau)$ curves to the τ vs. t plane.	55
4-1	Schematic of the Test Apparatus.	62
4-2	Cutaway View of Constant Volume Test Chamber.	63
4-3	Apparatus with 3 Chambers Built by Brehm.	66
4-4	Apparatus Built for This Research.	66
4-5	“Potting” on Transducer Electrical Connections.	67
4-6	Transient Sorption Test Sample Preparation.	70
4-7	Schematic of Chamber Volume Measurement setup.	72
4-8	Deformation of Preconditioned Sample Due to Low Internal Pressures	76

5-1	Uncertainty in τ as a Function of τ and G.	95
6-1	$\text{Log}(D_{eff})$ vs. $1/T$ Plot for Test Results All Foams, CO_2 Test Gas.	104
6-2	A comparison of P_{cw} for Different Foams.	109
6-3	Comparison of CO_2 Solid Polymer Diffusivities at 80°C	111
6-4	$\text{Log}(D_{eff})$ vs. $1/T$ Plot of Blowing Agent Test Results.	112
6-5	Test results for Foam 18, $\text{Log}(D_{eff})$ vs. $1/T$ for 6 test gases.	116
6-6	Foam 18 Aging Model Cell Gas Pressures	118
6-7	Foam 18 Aging at 25°C and 70°C , Predicted and Measured Conductivity.	119
6-8	Foam 18 Initial Aging (Detail of Figure 6-7).	119
6-9	Cross Section of the Bayer Igloo.	121
6-10	Igloo Aging, Predicted and Measured	123
6-11	Igloo Cell Gas Partial Pressure vs. Time.	123
6-12	Possible Locations of Igloo K-Factor Measurement Sample.	125
7-1	Foam Panel Schematic.	130
7-2	Aging of CFC-11 Blown Foam vs. CO_2 Blown Foam	130
B-1	S.E.M. Photographs Foam No. 1 Parallel Diffusion.	154
B-2	S.E.M. Photographs Foam No. 1 Perpendicular Diffusion.	155
B-3	S.E.M. Photographs Foam No. 2 Parallel Diffusion.	156
B-4	S.E.M. Photographs Foam No. 2 Perpendicular Diffusion.	157
B-5	S.E.M. Photographs Foam No. 14 Parallel Diffusion.	158
B-6	S.E.M. Photographs Foam No. 14 Perpendicular Diffusion.	159
B-7	S.E.M. Photographs Foam No. 15 Parallel Diffusion.	160
B-8	S.E.M. Photographs Foam No. 15 Perpendicular Diffusion.	161
B-9	S.E.M. Photographs Foam No. 16 Parallel Diffusion.	162
B-10	S.E.M. Photographs Foam No. 16 Parallel Diffusion.	163
B-11	S.E.M. Photographs Foam No. 16 Perpendicular Diffusion.	164
B-12	S.E.M. Photographs Foam No. 16 Perpendicular Diffusion.	165

B-13 S.E.M. Photographs Foam No. 16 Perpendicular Diffusion.	166
B-14 S.E.M. Photographs Foam No. 16 Perpendicular Diffusion.	167
B-15 S.E.M. Photographs Foam No. 17 Parallel Diffusion.	168
B-16 S.E.M. Photographs Foam No. 17 Perpendicular Diffusion.	169
B-17 S.E.M. Photographs Foam No. 18 Parallel Diffusion.	170
B-18 S.E.M. Photographs Foam No. 18 Parallel Diffusion.	171
B-19 S.E.M. Photographs Foam No. 18 Parallel Diffusion.	172
B-20 S.E.M. Photographs Foam No. 18 Parallel Diffusion.	173
B-21 S.E.M. Photographs Foam No. 18 Perpendicular Diffusion.	174
B-22 S.E.M. Photographs Igloo Foam Parallel Diffusion.	175
B-23 S.E.M. Photographs Igloo Foam	176
F-1 $\text{Log}(D_{eff})$ versus $1/T$ for all test results, Foam 1.	197
F-2 CO_2 , 80°C Data Plot Sample 1A.	198
F-3 CO_2 , 60°C Data Plot Sample 1A	200
F-4 CO_2 , 40°C Data Plot Sample 1A	202
F-5 O_2 , 80°C Data Plot Sample 1A.	204
F-6 O_2 , 61°C (Test A) Data Plot Sample 1A	206
F-7 O_2 , 61°C (Test B) Data Plot Sample 1A	208
F-8 O_2 , 61°C (Test C) Data Plot Sample 1A	210
F-9 O_2 , 41°C Data Plot Sample 1A	212
F-10 $\text{Log}(D_{eff})$ versus $1/T$ for all test results, Foam 2.	215
F-11 CO_2 , 80°C Data Plot Sample 2A.	216
F-12 CO_2 , 80°C (Test A) Data Plot Sample 2B.	218
F-13 CO_2 , 80°C (Test B) Data Plot Sample 2B.	220
F-14 CO_2 , 60°C Data Plot Sample 2B	222
F-15 CO_2 , 40°C Data Plot Sample 2B	224
F-16 O_2 , 80°C Data Plot Sample 2A.	226
F-17 N_2 , 80°C Data Plot Sample 2A.	228

F-18 CFC-11, 80°C Data Plot Sample 2B.	230
F-19 Log(D_{eff}) versus 1/ T for all test results, Foam 14.	233
F-20 CO ₂ , 80°C Data Plot Sample 14A.	234
F-21 CO ₂ , 80°C (Test A) Data Plot Sample 14B.	236
F-22 CO ₂ , 80°C (Test B) Data Plot Sample 14B.	238
F-23 CO ₂ 40°C Data Plot Sample 14A	240
F-24 CO ₂ 40°C Data Plot Sample 14B	242
F-25 O ₂ , 80°C Data Plot Sample 14A.	244
F-26 CFC-11, 80°C Data Plot Sample 14A.	246
F-27 Log(D_{eff}) versus 1/ T for all test results, Foam 15.	249
F-28 CO ₂ , 81°C Data Plot Sample 15B.	250
F-29 CO ₂ , 60°C Data Plot Sample 15B.	252
F-30 CO ₂ , 40°C Data Plot Sample 15A	254
F-31 Log(D_{eff}) versus 1/ T for all test results, Foam 16.	257
F-32 CO ₂ , 80°C Data Plot Sample 16A.	258
F-33 CO ₂ , 60°C Data Plot Sample 16A	260
F-34 CO ₂ , 40°C Data Plot Sample 16A	262
F-35 O ₂ , 60°C Data Plot Sample 16A	264
F-36 O ₂ , 40°C Data Plot Sample 16A	266
F-37 HCFC-123, 80°C Data Plot Sample 16A	268
F-38 HCFC-123, 60°C Data Plot Sample 16A	270
F-39 HCFC-123, 40°C Data Plot Sample 16A	272
F-40 Log(D_{eff}) versus 1/ T for all test results, Foam 17.	275
F-41 CO ₂ , 80°C Data Plot Sample 17A.	276
F-42 CO ₂ , 60°C (Test A) Data Plot Sample 17A	278
F-43 CO ₂ , 60°C (Test B) Data Plot Sample 17A	280
F-44 CO ₂ , 40°C Data Plot Sample 17A	282
F-45 O ₂ , 80°C Data Plot Sample 17A.	284

F-46 O ₂ , 60°C Data Plot Sample 17A	286
F-47 O ₂ , 40°C Data Plot Sample 17A	288
F-48 HCFC-123, 60°C Data Plot Sample 17A	290
F-49 HCFC-123, 40°C Data Plot Sample 17A	292
F-50 Log(D_{eff}) versus 1/ T for all test results, Foam 18.	295
F-51 CO ₂ , 80°C Data Plot Sample 18A.	296
F-52 CO ₂ , 61°C Data Plot Sample 18A	298
F-53 CO ₂ , 44°C Data Plot Sample 18A	300
F-54 CO ₂ , 38°C Data Plot Sample 18A	302
F-55 O ₂ , 79°C Data Plot Sample 18A.	304
F-56 O ₂ , 59°C Data Plot Sample 18A	306
F-57 O ₂ , 36°C Data Plot Sample 18A	308
F-58 N ₂ , 80°C Data Plot Sample 18A.	310
F-59 N ₂ , 60°C Data Plot Sample 18A	312
F-60 N ₂ , 40°C Data Plot Sample 18A	314
F-61 CFC-11, 80°C Data Plot Sample 18C	316
F-62 HCFC-123, 80°C Data Plot Sample 18B	318
F-63 HCFC-123, 40°C Data Plot Sample 18B	320
F-64 HCFC-141b, 80°C Data Plot Sample 18A	322
F-65 HCFC-141b, 60°C Data Plot Sample 18A	324

List of Tables

1.1	Comparison of Blowing Agent Characteristics.	27
3.1	Estimation of Heat of Solution for Test Gases.	58
4.1	Summary of Steps in Test Chamber Volume Measurement.	72
5.1	Repeatability of Chamber #4 Total Volume Measurements.	85
6.1	Summary of Test Results and Foam Characteristics.	102
6.2	E_D/R , for CO ₂ and O ₂ , Derived from Test Data.	105
6.3	Air Component Effective Diffusion Coefficient Ratios.	106
6.4	Characteristics of Foams: O.R.N.L, Bayer Igloo, and Ostrogorsky	108
6.5	Cell Wall Thicknesses and Corresponding Lengths for Foams 16 and 18. .	110
6.6	CO ₂ /Blowing Agent Effective Diffusion Coefficient Ratios.	112
6.7	Calculated and Measured k_R , k_S and k_{T_i} in [mW/m·K]	115
6.8	Igloo Aging Prediction at 15°C and Measured Values, After 27 Years. . .	122
A.1	Test Gas Properties.	138
D.1	Summary of Apparatus Hardware.	185
D.2	Summary of Measurements, Chamber Total Volume Without Foam. . .	187
F.1	Test Parameters for Mobay Samples Tested.	193
F.2	Test Sample Dimensions	194

Chapter 1

Introduction

Halogenated chlorofluorocarbons, CFCs, have been used since the late 1950s as blowing agents for rigid foams. CFC blown, closed cell, foam insulation has the lowest effective thermal conductivity of any non-vacuum insulation currently available. Since the early 1970s there has been concern that CFCs cause depletion of the ozone layer. Under recent international agreement CFC production will be phased-out.

With the phase out of CFC underway, there is an ongoing industry-wide search for viable replacements. Foams blown with these replacements will have to meet many requirements from environmental safety and energy standpoints. It is essential that these potential alternates have significantly lower impact on the ozone layer. Also, the thermal conductivity must be low enough to maintain foam's competitive advantage with other types of insulation.

Over the life of gas-filled closed-cell foam insulation, air gases permeate into the cells and the blowing agents diffuse out (see Figure 1-1) a process that changes the cell gas composition. As blowing agents have lower thermal conductivity than air, the net effect is an increase in effective foam thermal conductivity over time. This process is known as *aging*. Air permeates into the foam faster than the CFC's permeate out so the process is generally considered two staged, first the air in then the CFC out. Aging rates depend on permeation rates, efficacy of permeation barriers, installation techniques and

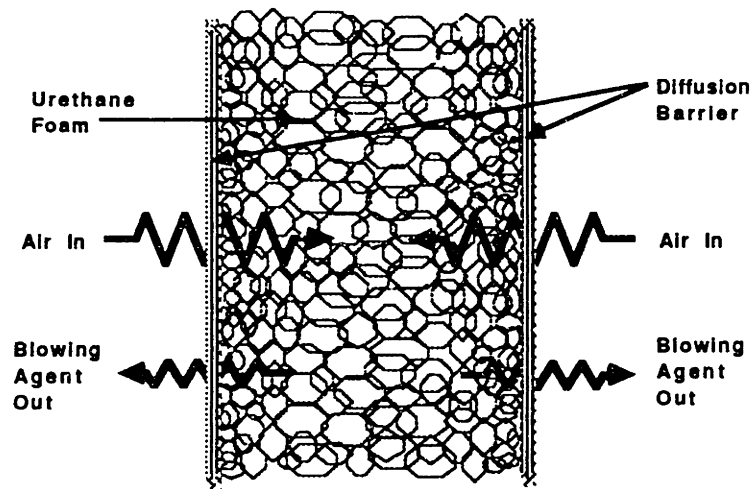


Figure 1-1: The Foam Aging Process.

environmental conditions.

Thus over the life of closed cell foam, its insulation capacity diminishes. Initially, a foam board blown with CFC-11, has approximately three times the insulating capacity of the same thickness of fiber glass batt. When it is fully aged, that is when the cell gas is only air which for a two inch thick foam board may take 50 to 100 years, the foam and fiber glass have approximately the same insulation capacity per unit thickness.

The aging rate of foam with any viable alternative blowing agent must be slow to maintain a low thermal conductivity over the life of the product. This research focuses on two alternate blowing agent candidates, HCFC-123 and HCFC-141b. Compared to CFC-11 these two gases should have a significantly lower impact on the ozone layer.

The next sections will give brief description of foams, the alternates and the focus of this research.

1.1 What is Foam Insulation?

There are many types of cellular plastic foams. They can be grouped into general categories. In terms of physical or structural properties they can be categorized as thermoset

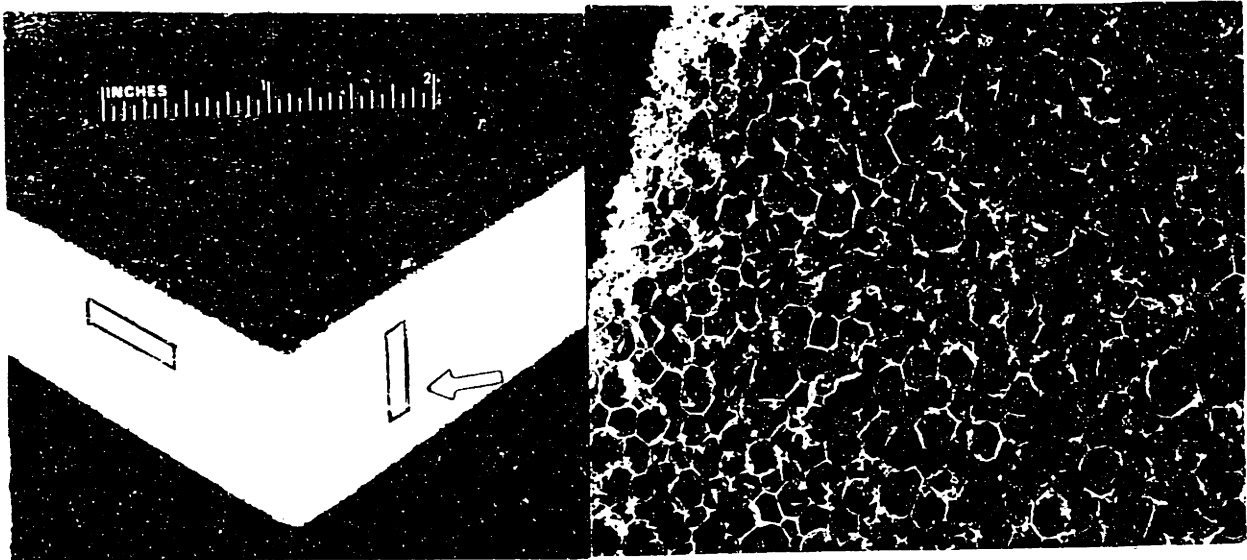


Figure 1-2: Closed Cell Foam Insulation.

or thermoplastic, flexible or rigid foams and they can be opened cell or closed cell. From a chemical standpoint these foams can be classified as polyurethane, polyisocyanurate, polystyrene or phenolic foams. The foaming method can also be used to categorize foams. They can be blown by phase change of the blowing agent or frothed by mixing. The manufacturing techniques, free rise bun stock, laminated or unlaminated board stock or poured or injection molding, can be used to categorize foams and can effect overall properties. Under consideration in this research are refrigerant blown closed cell rigid polyisocyanurate or polyurethane foams, particularly those used in insulation board stock and poured in to appliances such as refrigerators. These foams are thermosetting materials in that once the polymer is cured, it can not be remolded by reheating; it will decompose. These rigid foams provide not only thermal insulation but also can serve as structural members. A typical foam is show in Figure 1-2. A general description of the foaming process will facilitate a description of foam and the role of a blowing agent. One source of detailed descriptions is found in the handbooks published by leading polymer manufacturers [1, 2]

Foams are made by mixing two basic components, a polyol and an isocyanurate. A

polyol is a chemical compound with more than one reactive hydroxyl group attached to the molecule. They do not react with themselves but are hydrophilic. An isocyanate is a chemical compound with one or more NCO radicals attached to the main molecule. They are reactive towards any hydroxyl containing material (polyol or water). When they react with water, urea and CO_2 are produced. They also react with themselves. The combination of polyol and isocyanate forms a urethane. The degree to which molecular chains of these urethanes, polyurethanes, are chemically linked, cross-linked, determines the rigidity of the solid polymer material. If only these two components are mixed the results would be a solid plastic. Additives to the basic components are necessary to make a foam and to control its properties.

Three of the basic additives are the catalyst, surfactant, and blowing agent. The catalyst controls reaction rates and flow properties, the surfactant controls cell sizes and shapes. Although the blowing agent can effect the solid polymer chemistry and the foaming process in many ways, in general the blowing agent serves two purposes, both of which are directly related to the exothermic nature of the reaction that takes place when the two basic components are mixed.

The blowing agent can be a low boiling point chemical such as CFC-11 that is nonreactive and vaporizes from the heat of reaction, producing a solvent blown foam. The blowing agent is added to one of the basic components in liquid form. When the two components, polyol and isocyanate are mixed, the increase in temperature causes the liquid refrigerant to vaporize. At the beginning of the phase change, the refrigerant gas begins occupying the microscopic voids known as nucleation sites. As more gas is formed, the voids become larger. As the gas expands with the increasing temperature, the voids become even larger, in a process that expands the reacting polymer until the polymer has enough strength to resist the gas pressure. Another type of blowing agent is a chemical, such as water, that reacts with the isocyanate material to produce carbon dioxide, producing what is known as a water blown foam. In closed cell foams, the blowing agent gas is trapped in the cells, a "honey comb" like matrix of triangular

structural members called struts, that support thin membranes called cell walls. In opened cell foams, the expanding gas literally blows the cell walls open.

1.2 The CFC Issue

1.2.1 The Problem

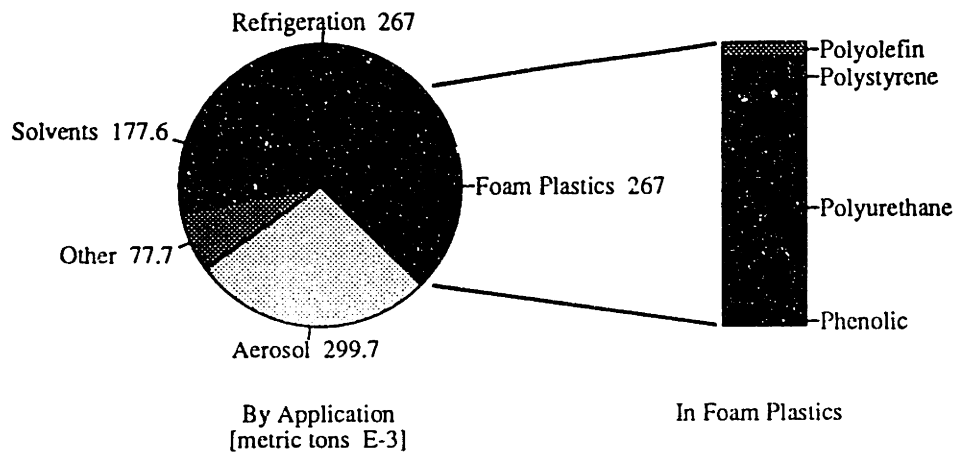
The history of the problem and the search for a solution are recent. Concern about the possible destruction of stratospheric ozone began in 1970. Emissions from high flying aircraft were blamed. In 1974 Rowland and Molina [3] produced a theory that compounds containing chlorine, such as CFCs, might contribute to the destruction.

CFCs are stable inert molecules that have an atmospheric life of approximately 65 years [4]. As concentrations of CFCs build up in the atmosphere they also migrate to the stratosphere, where the increased level of ultra violet (UV) radiation is enough to initiate the release of chlorine radicals from the fully halogenated CFCs. This chlorine catalytically converts ozone (O_3) to oxygen (O_2).

The ozone in the stratosphere acts as a filter for UV radiation. Increased levels of UV radiation in the atmosphere pose the threat of increasing the risk of skin cancer and unknown changes in crops and marine life. Increased levels of UV in the atmosphere will also accelerate the trend towards global warming. CFCs are considered greenhouse gases. They contribute to global warming because they are transparent to incoming radiation from the sun but are relatively opaque to, absorb, radiation emitted from the surface of the earth thereby trapping the energy in the earth's atmosphere.

To study the CFC problem, the Committee on Impacts of Stratospheric Change was formed by the NRC in 1975 [5]. As a response to these studies, CFCs were banned for use as aerosols in the U.S.A. in 1978. Although studies continued, the next major legislation was inspired by the discovery in 1986 of a hole in the ozone layer over the antarctic. CFCs, mostly CFC-11, CFC-12 and CFC-113, were blamed.

In 1987 the Montreal Protocol, an historically significant international environmen-



Source: Eliminating CFCs in Foam Plastic:
 SPI, 1989
 from United Nations Environment Programme

Figure 1-3: 1986 Global CFC Use.

tal agreement to limit the consumption of CFCs, was signed by a majority of the worlds leading manufacturers and consumers of CFCs. The goal was to reduce emissions 50% by 1998. Beginning in July 1989, production levels are to be reduced to 1986 levels and reduced an additional 20% by July 1993. The phaseout of production is the immanent next step. In addition to these measures, CFC's are now taxed in the U.S.

The worlds total production in 1986 was 1089 thousand metric tons. Figure 1-3 breaks down the global use of CFCs. The potential impact of reduced availability on the foam industry, which relies on CFCs as it's major blowing agent, has motivated an industry wide search for alternates.

1.2.2 The Options

The three types of options being considered are substitute materials, recovery methods and alternate blowing agents. These options are in various stages of research and implementation.

Expanded polystyrene foam, gypsum, fiberboard and fiberglass are existing materials that can be used in some applications as substitute materials. These materials have a higher thermal conductivity per unit thickness, so thicker layers of materials are required. Therefore, in many cases use of the substitutes would result in higher first cost or energy penalties. Other materials are in various stages of development. Use of composite materials that combined structural members and insulation may reduce first costs through labor and space savings. Other types of insulations are under development such as those that use vacuum technology.

Reduced production of CFCs naturally motivate an effort to be more economical with existing supplies. In this spirit, recovery recycling and reduction of amounts used are on the table. Recovery of CFCs previously lost during the production process requires efficient containment during production and development of effective carbon absorption techniques. Effective containment of production emissions is also important if destruction by thermal or catalytic incineration is attempted. Recycling of CFCs is more of an issue for uses in refrigeration and power applications.

The reduction of total amounts used can be approached in a number of ways. One currently implementable method is replacement of CFC-11 with water blown foams where appropriate. Blending CFC-11 with other chemicals is another method of reducing consumption. Some of the blends being considered include: CFC-11/CFC-22, CFC-11/ H_2O , CFC-11/HCFCs and CFC-11/Methyl Chloride. Research on the use of alternate chemical blowing agents is well under way. Currently the focus of research has narrowed to two major candidates: HCFC-123 and HCFC-141b. This work forms part of an investigation of these two most promising chemical alternates.

1.3 The Alternates

A blowing agent must meet a number of requirements; it must be environmentally acceptable, it must have low toxicity and it must have suitable physical and chemical

properties. Two of the most promising alternates being considered are the hydrogenated fluorocarbons, HCFC-123 and HCFC-141b. There is ongoing research to understand the basic properties of the HCFCs. Current material safety data sheets, MSDS, for HCFC-123 and HCFC-141b and summaries of their basic properties are in appendix A. Much of this research is organized and funded by industry in cooperation with government agencies.

The alternates potential to cause adverse environmental effects are currently being weighed in terms of the extent to which they will contribute to ozone layer destruction and act as greenhouse gases. The ozone depletion factor, a measure of capacity to destroy ozone in the stratosphere, is expressed in Table 1.1 relative CFC-11's. This factor accounts for the percentage of gas that will not reach the ozone layer due to reactions in the atmosphere (a function of atmospheric life of a substance) and the amount of chlorine radicals that will be available from the gas that reaches the layer (a function of the percent weight of chlorine in the molecule). Both HCFCs considered in this work are considerably less damaging to the ozone than CFC-11. The shorter atmospheric life of these products may, unfortunately, lead to another environmental problem, photochemical pollution in the lower atmosphere. The EPA is currently considering the volatile organic compound status of the HCFC's.

Toxicity is another issue of concern. This evaluation is still in progress. The Environmental Protection Agency and industry sponsored programs have initiated animal exposure testing. Short term testing has shown no adverse effects. Long term studies on HCFC-141b began in late 1989; results are expected in 1992. The industry sponsored program, Program for Alternative Fluorocarbon Toxicity (PAFT), has reported no adverse effects from HCFC-123 in long term vapor exposure tests. There have been notices [6], however, that under certain conditions HCFC-123 can react to form HCFC-133a, a known carcinogen. Current recommended exposure levels for the alternates are 500 ppm for HCFC-141b and 50-100 ppm for HCFC-123. Due to difference in boiling points, vapor pressures and production temperatures the exposure to vapor during

Cell Gas	Foam Effective Conductivity [BTU/hr · ft · °F]	Ozone Depletion Factor **	Greenhouse Potential **	Blowing Efficiency [%] ***	Atmospheric Life [Years] **
CFC-11 (CCL ₃ F)	* 0.0104	1	1	100	65
HCFC-123 (CF ₃ -CCL ₂ H)	0.0116	0.016	0.019	89	1.5
HCFC-141b (CH ₃ -CCL ₂ F)	0.0114	0.08	0.092	115	7.0
CO ₂	0.021	0	1	95	-
Air	0.032	-	-	-	-

* Baseline value given by Glicksman [7].

** Alternative Fluorocarbon Environmental Acceptability Study, Boulder, CO, May 1989.

*** Mobay Chemical Company [8].

Table 1.1: Comparison of Blowing Agent Characteristics.

the manufacturing process will vary with different blowing agents. Emission levels have been monitored in plant-scale manufacturing conditions [9]. These trials indicated that manufacturing within exposure limits is possible.

Another safety concern is flammability. CFC-11, HCFC-123 and HCFC-141b have no flash point. Of the three, HCFC-141b alone has a narrow range of vapor flame limits in air. This is not sufficient to present an obstacle to commercial use.

Their other effects on the foaming process and mechanical properties of foams are a major topic of papers presented at industry conferences. Appropriate chemical properties such as liquid solubility in foam system, proper boiling point and good blowing efficiency are important criteria. Blowing efficiency is measured relative to CFC-11 in terms of mass of liquid required to produce foam of the same density. Relative to CFC-11 more HCFC-123 and less HCFC-141b is required to produce similar foams, see Table 1.1. The relative amounts used will affect overall cost as well as total environmental emissions. In 1988, Dupont estimated that relative to CFC-11 the cost of HCFC-123 would be 2 to 4 times greater and HCFC-141b up to 3 times greater.

These alternates must also be noncorrosive. The refrigerant liquid, vapor and foams blown with them are used in conjunction with other materials, e.g. plastics or metals storage containers, ABS refrigerator liners and aluminum board stock facers. The effects of the alternates on other materials is therefore important to industry, especially when looking for “drop-in” replacements. It is also important in the design of testing equipment, such as that used in this research, especially the effects on gasket and container materials. Manufacturers reports on compatibility with some materials is in appendix A. A report by Dupont [10] indicates that in both wet and dry environments, HCFC-123 and HCFC-141b have corrosive effects on 1020 steel and aluminum similar to that of CFC-11. This same report examined elastomer and plastic compatibility in terms of the amount of linear swell. The results indicated that the effects of CFC-11, HCFC-123 and HCFC-141b were not comparable. The linear swell depended upon the gas and the elastomer or plastic tested. In general, both alternates showed higher percent linear swell in the elastomers compared to CFC-11. Thiokol FA was the only elastomer reported “probably suitable” for use with the HCFCs. Both HCFCs are considered strong solvents. This is evident in the results reported for plastics compatibility. Although nylon and epoxy were reported probably compatible with both HCFCs, HCFC-123 dissolved ABS and Lucite. The solubility is of importance not only when considering materials used in conjunction with the foams but also for it’s effects on the solid polymer material of the foam. The solubility plays an important role in the permeation process under study in this research.

Other properties of importance to this research are thermal conductivity and mass diffusivity. The alternates have slightly higher thermal conductivity than the CFCs (see the summary of properties in appendix A). The effect of this difference in gas thermal conductivity on initial foam thermal conductivity is shown on the first column in Table 1.1. These values use the model developed by Schuetz [11] to calculate the thermal conductivity of the foam. Heat transfer through foams is due to three mechanisms; conduction through the solid polymer lattice, conduction through the cell gas, and radiation. Foam cell sizes are generally small enough that convective heat transfer may be

ignored. The overall effective thermal conductivity can be predicted as the sum of the three mechanisms. The values calculated in Table 1.1 use a foam with 1.9 lb/ft³ density, 20% percent of solid polymer in the cell walls and 400 μm average cell diameter blown with CFC-11 as a base line. The thermal conductivity of the same foam with different cell gas was then calculated. These values are for foams with only blowing agent in the cells, ie. a freshly made foam.

It has been shown that even in CFC-11 blown foams, approximately 50% of the heat transfer is due to conduction through the cell gas [12]. This gas contribution to effective conductivity varies with cell gas composition. The cell gas composition varies with time as air permeates into the cells and the blowing agent permeates out. The overall effect is an increase in effective foam thermal conductivity. So, an understanding of gas transport and storage phenomena in polymer systems is essential in prediction of insulation aging rates. Central to this understanding are the diffusion coefficient, quantifying the transient transport process, and the solubility coefficient, quantifying the steady state storage capacity. The product of these two coefficients is called the permeability coefficient, which characterizes the steady state gas flow through a medium. The change over time of the thermal conductivity can be predicted if the change in cell gas composition over time can be modeled.

To understand what polymer formulations and process changes can be used to maintain and continue to improve insulation values with these alternates, industry needs effective methods of evaluating new developments. Methods that are effective need to be reasonably accurate and rapid. In response to industry's needs, methods have been developed at M.I.T. to measure diffusion and solubility of gas in a foam sample and predict mass fluxes of air and the blowing agent from the results.

1.4 Focus of this Research

The purpose of this work is to address some of industry's questions about the effects of alternate blowing agents on foam aging and to continue to develop methods that will lead to timely answers. Measurements of permeability of blowing agent and air components in foams are the basis of the analyses. The effect blowing agent has on the mass transport properties of the solid polymer will be examined through a comparison of permeability of foams of the same basic polymer chemistry blown with different blowing agents. The permeability of the solid polymers will be compared by factoring out effects of the physical structure, foam density and the amount of solid polymer in the cell walls. The permeability test results used in a model, developed at M.I.T. [13], to predict the foam's aging characteristics will be compared to measurement of the foam's thermal conductivity over time. First methods used to determine foam structure and test foam permeability are detailed. Then error inherent in the methods and results of work to date are discussed.

Chapter 2

Characterization of Foam Structure

Closed cell foam insulation is a three dimensional matrix composed of gas filled voids defined by solid polymer cell walls (membranes or windows) supported by a grid of solid polymer structural members, struts, (see Figure 2-1) found at the intersection of cell walls. The distribution of solid polymer through the matrix affects both the mass and heat transfer characteristics of a foam.

Most of the solid polymer, 60 to 90 %, is in the struts. They provide the primary path for heat conduction through the solid polymer in the foam. Heat conduction in the solid polymer is proportional to the concentration of mass in the struts [11]. Orientation of anisotropic cells can effect the magnitude.

Orientation of the cells also has important effects on radiative heat transfer [14]. Struts are considered opaque to thermal radiation. Radiation conduction through foam is a function of their surface to volume ratio and can also be effected by their degree of staggerdness. Window opacity, which may be a function of cell wall thickness as well as polymer chemistry, is a secondary factor in radiative thermal conductivity [15].

The cell walls, usually 0.5 to 1 micron thick, also provide the path of least resistance for gas diffusion. The higher the concentration of mass in the cell walls, the greater the resistance to mass transfer.

Foam effective diffusivity, D_{eff} , is inversely proportional to two physical parame-

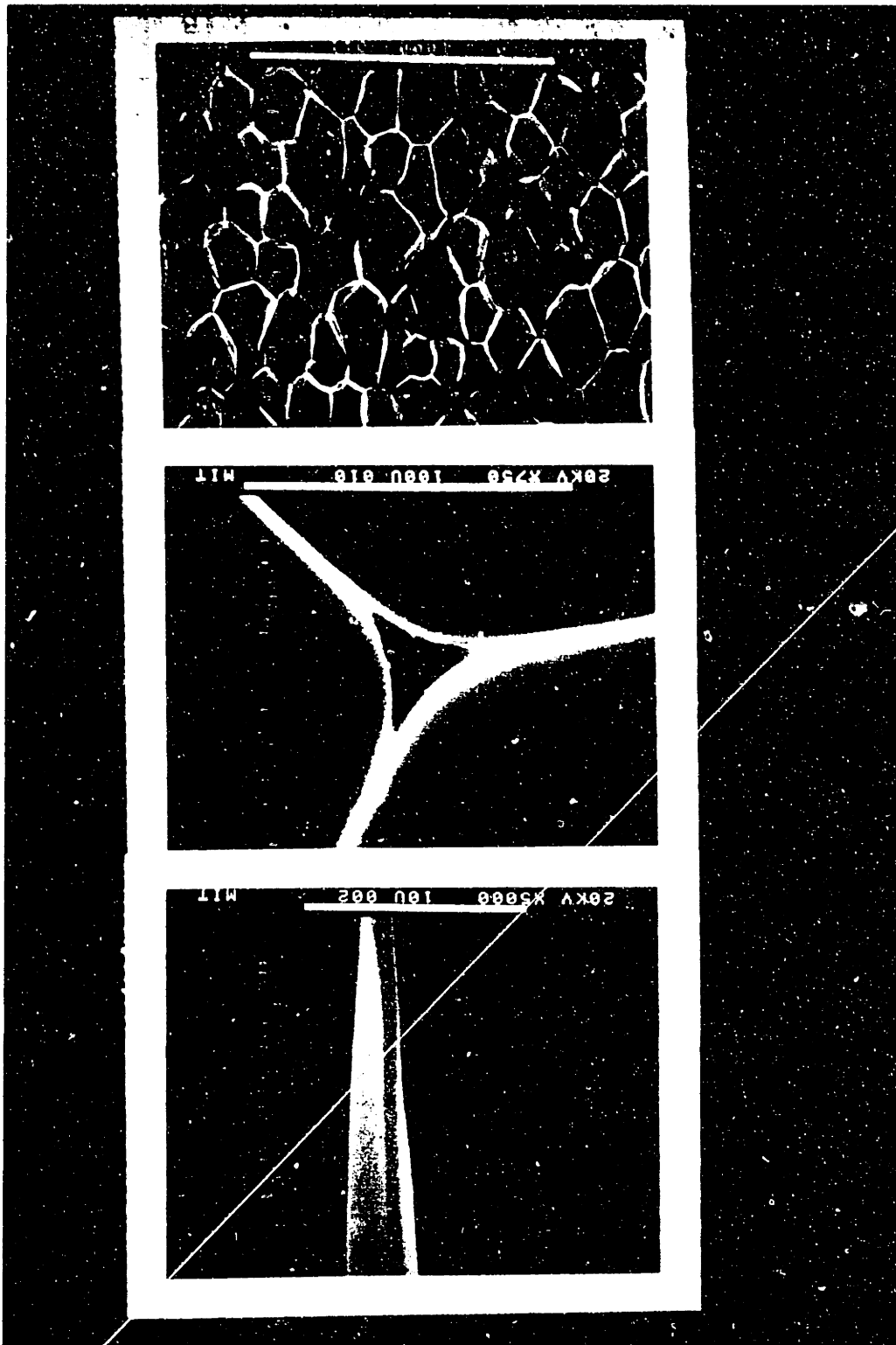


Figure 2-1: SEM Micrographs Showing from Top to Bottom: a Typical Foam Cell matrix; a Strut; a Cell Wall.

ters; the foam density, ρ_f , and the percent of solid polymer in the cell wall, P_{cw} , and directly proportional to the diffusivity of the solid polymer [13, 16]. In section 6.3 calculated values of ρ_f , P_{cw} and test results values for D_{eff} for each foam tested will be used to compare solid polymer diffusivity. The following sections detail methods used to measure and calculate foam physical parameters.

2.1 Determination of Percent Of Solid Polymer in Cell Walls

The amount of solid polymer in the cell walls can be expressed as a ratio of the measured cell wall thickness, t_{cw} , to the thickness a cell wall would have if all of the solid polymer were in the cell walls, $t_{100\%cw}$ [16].

$$P_{cw} = \frac{t_{cw}}{t_{100\%cw}} 100 \quad (2.1)$$

The method used to measure of t_{cw} is detailed in the following section. The $t_{100\%cw}$ is derived from a definition for the volume of solid polymer, V_{solid} , per unit volume of foam, V_{total} .

$$\frac{V_{solid}}{V_{total}} = (1 - \delta) = (t_{100\%cw})S_v \quad (2.2)$$

where, δ , the foam void fraction or porosity is defined as a ratio of solid polymer density, ρ_{sp} , foam effective density, ρ_f and the cell gas density, ρ_g

$$\delta = \frac{\rho_{sp} - \rho_f}{\rho_{sp} - \rho_g} \quad (2.3)$$

S_v , the surface area to volume ratio, is determined using lineal analysis, a metalography technique described in the next section. Combining equations (1.2) and (1.3), the percent

of material in the cell walls is calculated

$$P_{cw} = \frac{S_v t_{cw}}{(1 - \delta)} 100. \quad (2.4)$$

2.1.1 Determination of Surface to Volume Ratio

Stereology techniques used frequently in metallography to determine three dimensional characteristics of an object from projections of that object on a two dimensional plane, can be used to determine average foam surface to volume ratios [16]. A plane image from a random section, representative of the foam structure must be obtained. A series of random lines of known length are superimposed upon this image. The number of intersections of each line with a cell wall is counted and the average distance between line intersections (cell walls), $\langle l \rangle$, is calculated. An expression for the average surface to volume ratio of an isometric structure, developed using probability theory is given by Underwood [17] as

$$S_v = 2N_L \quad (2.5)$$

where

$$N_L = \frac{1}{\langle l \rangle} \quad (2.6)$$

assumes only that the cell wall thickness is negligible compared to the cell dimensions, and is valid regardless of structure geometry.

Most of the foams examined in this research were anisotropic. They tended to be linearly oriented, elongated along an axis parallel to the rise direction. To account for the degree of elongation or cell aspect ratio the surface to volume ratio is modified

$$S_v = 1.571N_{L\perp} + 0.429N_{L\parallel}. \quad (2.7)$$

Where $N_{L\perp}$ is determined from lines perpendicular to the rise direction and $N_{L\parallel}$ from lines parallel to the rise direction.

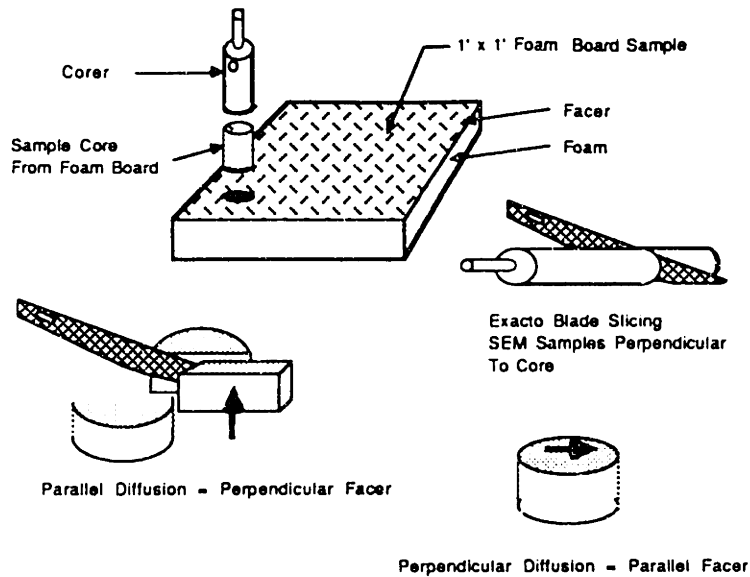


Figure 2-2: Technique used to obtain specimen for SEM.

Both expressions for S_v are stated by Underwood to be “statistically exact” within the limits of error of three requirements. The sample section must represent the foam as a whole. The sampling techniques must be executed in a random fashion. The resolution of the photo do not create uncertainty in the length of the test figure. One manifestation of error occurs when the test line-cell wall intersections are counted. There are three types of intersections; a cleanly defined pass through a wall; a pass of the test line tangent to a section of the cell wall; or a pass through a strut, a triple intersection. Underwood [17] suggests that a tangent hit count as 0.5 an intersection and a strut hit count as 1.5 intersections. He also suggests that the error in the measurement is proportional to the number of tangent hit counts.

Scanning Electron Microscope, SEM, photographs of the foams provided the two dimensional analysis planes. Samples for the SEM were cored with a 1 cm diameter cork borer from foam adjacent to permeability test sample cores (see Figure 2-2). Two specimens were cut from each foam; one each from two orthogonal planes, perpendicular and parallel to the face of the board stock sample. All specimen were taken from the

center of the board stock. Samples parallel to the board face were obtained by pushing the foam cylinder out of the cork borer to the desired sample thickness. Approximately parallel cuts were achieved by cutting flush to the borers edge. A fresh razor blade was used to cut the face to be viewed, giving cleanly cut cells that terminate on the cut edge. The SEM used for this work was a Cambridge Instruments Stereoscan 240 equipped with a Polaroid 4x5 camera and [50 mm] Nikon lens. Manufacturer specifications give a $\pm 5\%$ accuracy with a 2% repeatability for measurements of a $1\mu m$ line at a working distance of 12mm with an acceleration voltage of 1.5 kV. Photographs at approximately 30x magnification were used in the lineal analysis. All photographs are reproduced in appendix B.

A standardized method of drawing test lines was used to insure random measurement free from bias. Orthogonal sets of ten parallel lines were drawn on the transparent face of a plastic pocket. The photos fit snugly in the pocket. Each photo in the plane parallel to the foams rise direction was taken so that the elongated axis was approximately parallel to the long side of the photo, see Figure 2-3.

Obtaining a two dimensional view of the specimen where all of the points to be analyzed are in one plane, is important to the application of this technique. In the SEM photos the cutting plane was used as the analysis plane.

2.2 Determination of Cell Wall Thickness

From each specimen two cell walls were photographed at high magnification for determination of cell wall thickness. Figure 2-4 shows a typical photograph. These photographs were taken of sections of the cell wall after it tappers to a constant thickness from the strut. On each photograph the cell wall thickness was measured at 10 locations the average of these measurements is tabulated in the appendix C. It was noted that the thickness of the cell wall appeared to be a function of the wall length; that is, shorter walls appeared to be thicker than the longer walls. This will be the subject of future

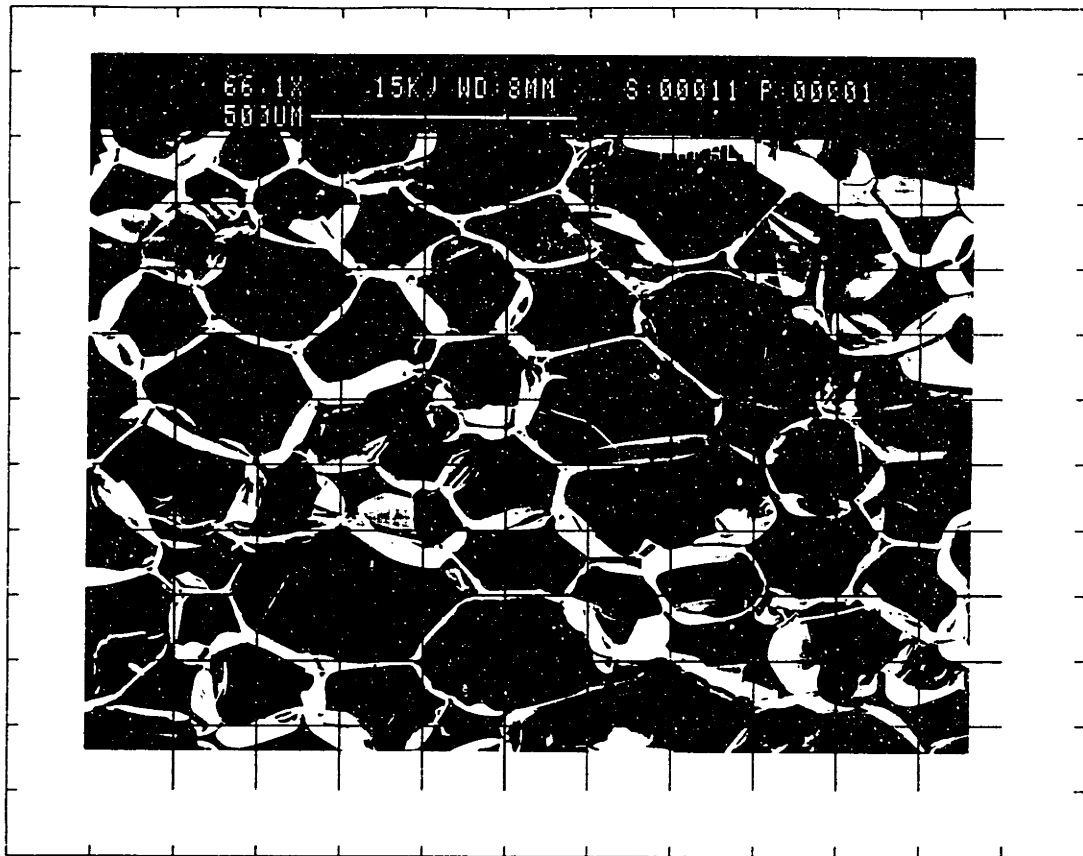


Figure 2-3: Typical SEM Photograph Used in Lineal Analysis.

research.

To determine the exact angle of the wall with respect to the photo plane is difficult. The measured thickness of a wall depends upon the angle of cut and view; a normal cut and view gives the correct thickness. A three dimensional view can be obtained in the SEM by rotating the specimen so a plane of cut through the wall that is approximately normal to the photo plane can be selected. It is also difficult to determine the distance from the plane of the cut through the cell wall and the strut below. Therefore there is uncertainty in whether the cell wall is still tapering down from the strut below. Measurements made in that case would result in measuring cell walls thicker than actual.

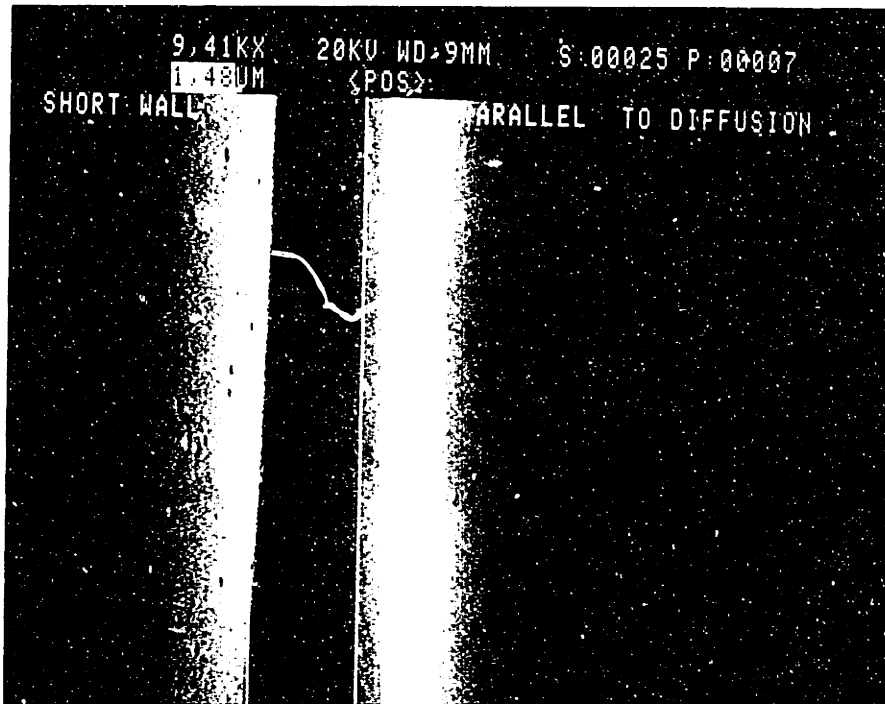


Figure 2-4: Typical SEM Photograph Used to Determine Cell Wall Thickness.

2.3 Determination of Average Cell Diameter

From the stereography technique described above, the calculated average surface to volume ratio can be used to calculate d_c , the average cell diameter, if an assumption about cell geometry made. Work by Reitz [16] indicates that truncated octahedron or pentagonal dodecahedron geometry can be used to model cell structure. From two dimensional projections he determined that the average numbers of sides per polygon and edges per face were 6 and 5 respectively. Both truncated octahedron and pentagonal dodecahedron have an average of 6 sides per face. To compare possible foam geometries to actual foam structure, Reitz use these models to predict actual foam densities for foams with known solid polymer densities. A cube model under predicted density for all foams , the

truncated octahedron and pentagonal dodecahedron both over predicted. The truncated octahedron was better for foams within the density range for these tests. The mean projected height of a truncated octahedron is

$$d_c = 3.55/S_v. \quad (2.8)$$

The direction of diffusion through the foam samples used in the permeability tests is perpendicular to the foam face therefore the SEM specimens cut in this plane show the cells as seen by the diffusing gas. Industry convention calls the plane perpendicular to the facer of a foam board, the rise direction. Counter to this standard and intuition, in most cases the foams rise direction is not perpendicular to the face of the foam. This is due to the lateral expansion that takes place between the facers after the rising foam has filled the space of the predetermined thickness (1 to 2 inches).

Cell diameter determinations were made from four photos per foam, two per specimen. A list of results of these measurements for the foams tested is in appendix E.

2.4 Density Measurements

Average foam density was calculated from cored samples that are later sliced into discs for the permeability measurements (see section 4.3.1). Local density was determined from a center section adjacent to the sample core. These two densities may differ due to the techniques used to produce the foam and differences of cell gas composition at the time of measurement. As exact cell gas composition at the time of measurement is not known the error in foam density determination includes variability of cell gas composition. In a foam with 1.9 lbs/ft³ density this would account for less than 4% change in density, assuming negligible mass of gas stored in the solid polymer. This difference is of the same order of magnitude as the differences encountered between density measurement of different cores cut from the same board stock. The fact that foams tested were produced on commercial lamination machines may explain these differences. Thin layers of solid

polymer forms at the foam/diffusion barrier and foam/foam interfaces. From these dense sheets of solid the density of the foam decreases towards the center of the foam.

A vernier with 0.001 inch precision was used to measure dimensions for volume determination. All samples were weighed on a Mettler H51AR balance with a precision of 0.01 mg. Results of foam densities calculations are tabulated in appendix E.

Chapter 3

Transient Sorption Method for Permeability Measurement

The basis of the technique is the measurement of the transient pressure in an isolated, constant-volume chamber containing the foam sample and the test gas, immediately after the test gas pressure surrounding the sample has been increased or decreased in a step fashion. The transient diffusion equation for the sample/chamber geometry is solved and a comparison between the solution and the transient pressure curve gives the effective diffusion and solubility coefficients of the test gas in the foam.

The time to perform any diffusion measurement is proportional to the square of the effective sample thickness. For a given physical sample thickness, the sorption technique cuts the effective thickness in half simply by allowing the gas to diffuse into both sides of the sample rather than through the sample from one side to the other. Thin samples may be used because the effect of open pathways through the sample is minor. The sample thickness in a sorption measurement is limited only by the need to adequately represent the foam as an idealized homogeneous continuum. To minimize test times, samples for this set of tests were approximately 10 to 15 cells thick.

This chapter describes the theoretical basis for the tests.

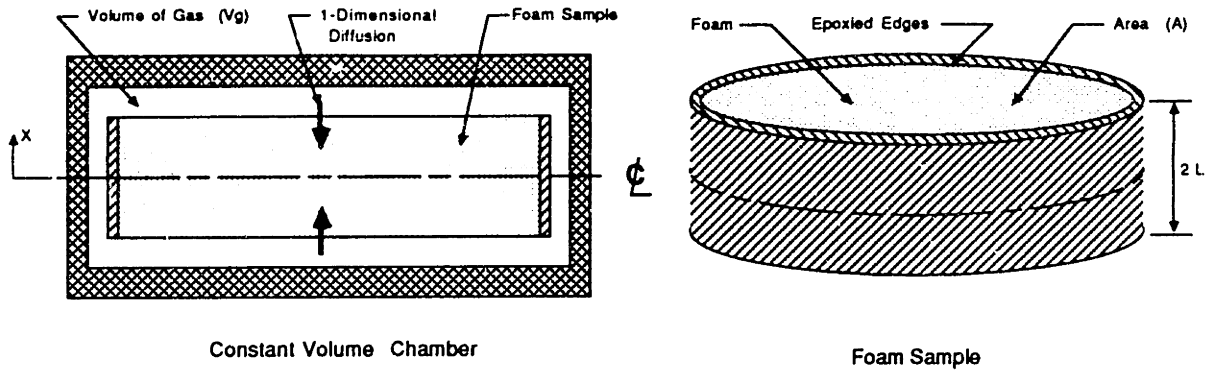


Figure 3-1: Conceptual Schematic of Transient Sorption Chamber and Sample.

3.1 Analysis of Physical Model

Fick's Law with constant diffusion coefficient and Henry's Law with constant solubility coefficient are used to model the gas transport in the foam. It is assumed that the sample is large enough to allow treatment as a homogeneous continuum. With sealed edges the sample may be treated as a plane sheet of cross-sectional area, A , and half-thickness, L , immersed in a fixed volume of test gas as shown in the Figure 3-1 schematic. In the time just before the beginning of a test there is a uniform pressure, P_1 , of the test gas throughout the entire test chamber (in the volume of gas surrounding the sample and in the sample) and no other gas is in the sample or chamber. To initiate a test, the pressure in the volume of gas surrounding the sample is changed by a pressure step, ΔP .

The method of solution for this geometry and these boundary conditions is given by Wilson [18] and the analysis was detailed for this experiment by Brehm [19]. In the following section Brehm's analysis will be outlined in tandem with a revised analysis from a different point of view.

3.1.1 Governing Laws

Fick's First Law of Diffusion

The phenomenological law that describes the diffusion process through a solid medium defines a constant of proportionality between the rate of mass transfer and the concentration gradient in the solid in the direction of flux. This equation is known as Fick's first law of diffusion. For the flux of a single species of gas it can be written as

$$D \equiv \frac{-J}{(\partial C / \partial x)}, \quad (3.1)$$

where J is the rate of transfer of the diffusant per unit area of section, C is the concentration of the gas in the solid, and x is the space coordinate normal to the section. If J and C are expressed in terms of the same mass unit then D is independent of this unit and has dimensions of $\text{length}^2 \text{time}^{-1}$, e.g. cm^2/sec .

When testing a single gas, the partial pressure, P , in the chamber is what is measured. It is therefore useful to write the governing equations in terms of gas pressure. Using the ideal gas law $C_g = \rho_g$, therefore

$$C_g = \frac{P}{RT} \quad (3.2)$$

where R is the gas constant of the gas species and T is the absolute temperature. In the analysis of the permeation process in foams C_g is the concentration in the cell interiors and the C used in equation 3.1 is the concentration of the gas in the polymer. The driving potential for diffusion is the chemical potential but in the absence of temperature gradients the driving potential is proportional to the concentration gradient in the solid (in our case the solid polymer). To express this driving potential in terms of pressure Henry's Law of solubility must be used.

Henry's Law of Solubility

The concentration of a single gas species in the solid polymer, C_{sp} , can be expressed in terms of the proportionality at equilibrium between the concentration of a gas species just *inside* the surface of the polymer and the partial pressure of that gas species just *outside* the surface. The constant of proportionality is called the solubility coefficient and is defined as follows

$$S_{sp} \equiv \frac{C_{sp}}{P}, \quad (3.3)$$

where C_{sp} and P are the concentration of the gas in the solid polymer and partial pressure of the gas at the foam surface, respectively. Equation 3.3 is known as Henry's law of solubility. For simple gases S_{sp} is usually expressed in units of $(\text{cm}^3_{STP}/\text{cm}^3 \cdot \text{atm})$, where the unit of mass is based on the Ideal Gas Law as follows,

$$1\text{cm}^3_{STP} = \left(\frac{P}{RT} \right)_{STP} (1\text{cm}^3) = (1\text{atm})(1\text{cm}^3) \frac{1}{RT_{STP}}, \quad (3.4)$$

where R is the gas constant and T_{STP} is the standard absolute temperature (298°K).

3.1.2 Mass Transfer in Foams

Fick's law as written above is for concentration gradients in the solid, but foam is a matrix of voids and solids. The question then is how to define the concentration gradient in the foam. A steady state concentration gradient across a thickness of foam can be expressed in three ways; the gradient of concentration in the gas phase on either side of the face of the foam and inside the voids of the foam cell; the concentration gradient in each solid polymer membrane; or the effective concentration gradient that is a volume weighted average of the concentrations in the foam's solid polymer and cells. Figure 3.1.2 is a visualization of the three.

In the analysis of their results both Brehm and Ostrogorsky defined the effective concentration gradient, C_{eff} , as the driving potential across the hypothetical homogeneous continuum of the foam sample with effective properties D_{eff} , effective diffusion

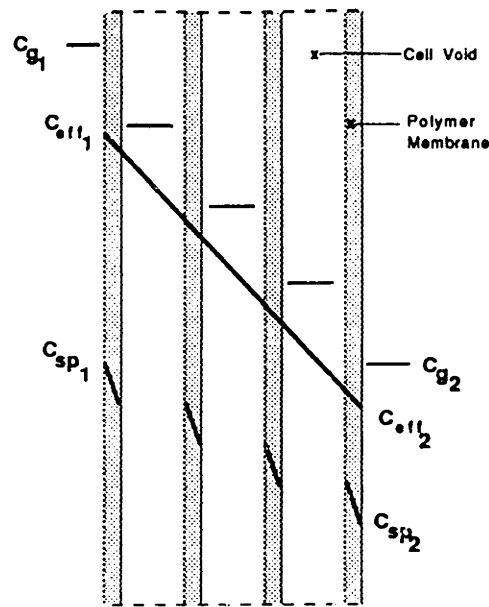


Figure 3-2: Visualization of Concentration Gradients in Foam Idealized as a Series of Successive Membranes.

coefficient, and S_{eff} , effective solubility coefficient. The effective concentration is defined as

$$C_{eff} = C_g \delta + (1 - \delta) C_{sp} \quad (3.5)$$

where δ is the foam void fraction (see section 2.1). In the same way foam effective diffusion coefficient is defined as

$$D_{eff} = D_g \delta + (1 - \delta) D_{sp} \quad (3.6)$$

where D_{sp} , the diffusion coefficient for the solid polymer is defined in Fick's First Law, equation 3.1 and in a similar manner the diffusion coefficient D_g is defined as the constant of proportionality between the rate of mass transfer and the concentration gradient in the gas phase in the direction of flux as shown in equation 3.12. The foam effective solubility coefficient is defined as

$$S_{eff} = S_g \delta + (1 - \delta) S_{sp}. \quad (3.7)$$

S_g , the solubility of the gas in the voids is defined by the Ideal Gas Law

$$S_g = \frac{C_g}{P} = \frac{1}{RT} = \frac{T_{STP}}{T}. \quad (3.8)$$

Another approach is to consider the gradient in concentration of the gas, C_g , in the gas phases only (ie. the gas in the cells and the gas outside the face of the foam) as the driving potential. The motivation for analysis on this basis is that it is most directly related to the transient sorption test's measured quantity, pressure. From equations 3.2 and 3.3, C_g can be related to C_{sp} the driving potential as defined by Fick's first law,

$$C_{sp} = S_{sp}(RT)C_g \quad (3.9)$$

The coefficient for C_g in this expression is the polymer solubility ratio (some times called the partition coefficient)

$$K_{sp} = \frac{S_{sp}}{(1/RT)} = \frac{S_{sp}}{S_g}. \quad (3.10)$$

Both approaches will be discussed in the analysis of the mathematical model. In the analysis of the test results presented in this paper the mathematical model based on effective foam properties will be used. Using this model will facilitate comparison with results from previous work.

Fick' first law expressed in term of these two gradients is

$$J = -D_{eff} \frac{\partial C_{eff}}{\partial x} \quad (3.11)$$

$$J = -D_g \frac{\partial C_g}{\partial x} \quad (3.12)$$

Assuming that the diffusion coefficient is independent of concentration and position, tests run at constant temperature the above equations and expressions for the mass flux can

be written in terms of the measured gas pressure as

$$J = -D_{eff} S_{eff} \frac{\partial P}{\partial x} \quad (3.13)$$

$$J = -\frac{D_g}{RT} \frac{\partial P}{\partial x}. \quad (3.14)$$

The equality of the right hand side of both these expressions leads to the relationship between the two diffusion coefficients. The ratio between the mass flux and the pressure gradient is the permeability. The foam effective permeability is

$$Pe_{eff} = D_{eff} S_{eff} = \frac{D_g}{RT} \quad (3.15)$$

In developing the model it will be useful to define the foam effective solubility (or concentration) ratio

$$K_{eff} = K_{sp}(1 - \delta) + \delta = \frac{C_{eff}}{C_g} = \frac{S_{eff}}{1/(RT)}. \quad (3.16)$$

As with the diffusion coefficient, we will assume that the solubility coefficients S_{eff} and S_{sp} , as well as the solubility ratios K_{eff} and K_{sp} , are independent of concentration in the range of pressures tested. According to Crank [20] and Van Krevelen [21], this assumption is good for pressures up to 1 or 2 atmospheres, which covers all measurements performed in this project. All of these assumptions break down if the gas condenses, this is possible with the refrigerants for tests at or below room temperature.

3.1.3 Fick's Second Law of Diffusion

To analyze one dimensional transient diffusion processes for a single gas species conservation of mass for an elemental control volume is applied to Fick's first law. The mass of gas per unit volume in the control volume of foam can be expressed as the sum of the

volume weighted concentrations of gas in the solid polymer and in the cells or in terms of pressure and effective solubility as

$$m_{c.v.} = C_g \delta + (1 - \delta) C_{sp} = P S_{eff} \quad (3.17)$$

In general the mass flux through the control volume is

$$\frac{\partial m_{c.v.}}{\partial t} = D \frac{\partial^2 C}{\partial x^2}. \quad (3.18)$$

This is Fick's Second Law, the governing equation for transient mass transport. Substituting the definitions from equations 3.3 and 3.17 into equation 3.18, this can be expressed in terms of the chamber gas pressure. For the analysis in terms of the effective concentration gradient this becomes,

$$\frac{\partial P}{\partial t} = D_{eff} \frac{\partial^2 P}{\partial x^2} \quad (3.19)$$

for the analysis in terms of the gas concentration gradient

$$\frac{\partial P}{\partial t} = \frac{D_g}{K_{eff}} \frac{\partial^2 P}{\partial x^2}. \quad (3.20)$$

3.1.4 Initial State of Sample and Chamber

Before a test begins a known initial condition must be established in the chamber and foam sample. Through a flushing process, described in section 4.3.3, the foam sample is conditioned so that the only gas species present in the foam or chamber is the test gas, the gas pressure is constant throughout the sample and the gas pressure inside the foam is the same as the pressure in the surrounding chamber. The test begins by disturbing the equilibrium with a step change in the chamber pressure, this can be thought of as an instantaneous change in pressure at the surface of the sample. Immediately after the pressure is changed the chamber is sealed. The mathematical statement of these initial

conditions is

$$P(x, 0^+) = \begin{cases} P_1 & x \neq \pm L \\ P_2 = (P_1 + \Delta P) & x = \pm L \end{cases} \quad (3.21)$$

where P_1 is the pressure in the chamber just before the test begins and ΔP is the imposed pressure change at $t = 0$. The foam sample extends from $-L$ to $+L$ in thickness and the other dimensions are large compared to this thickness.

Therefore the test begins with uniform concentration of the test gas in the solid polymer and uniform concentration of the same test gas in the void volume, V_g , surrounding the sample and in the cells.

3.1.5 Mass Conservation in Chamber

The mass in the chamber at the start of the test may be expressed in terms of concentrations as

$$m(0^+) = V_g C_g(L, 0^+) + V_f C_g(x, 0^-) K_{eff} \quad (3.22)$$

where V_f is the foam sample volume and V_g is the volume of the chamber less the volume of the foam sample. In terms of pressures equation 3.22 can be written as

$$m(0^+) = \frac{V_g}{RT} (P_1 + \Delta P) + \frac{2ALK_{eff}}{RT} P_1 \quad (3.23)$$

where the first term on the right hand side represents the mass of gas in the chamber surrounding the sample and the second term the mass of gas in the sample. This must equal the mass in the chamber at any time t

$$m(t) = \frac{V_g}{RT} P(L, t) + \frac{AK_{eff}}{RT} \int_{-L}^{+L} P(x, t) dx. \quad (3.24)$$

3.2 Analytical Solution

The solution to the governing equation with the given boundary conditions is most conveniently found and expressed in terms of four non-dimensional parameters. The non-dimensional pressure, \bar{P} , is scaled by the test pressure step, ΔP

$$\bar{P}(x, t) \equiv \frac{P(x, t) - P_1}{\Delta P} \quad (3.25)$$

and the non-dimensional length scale, z , is scaled by the test sample half-thickness.

$$z \equiv \frac{x}{L} \quad (3.26)$$

The variable τ represents the characteristic time scale of the diffusion process. Its expression depends upon the definition of the concentration used in the governing equation as follows

$$\tau_{eff} \equiv \frac{D_{eff}t}{L^2} \quad \tau_g \equiv \frac{D_g t}{L^2} \frac{1}{K_{eff}}. \quad (3.27)$$

where τ_{eff} corresponds to C_{eff} as τ_g to C_g . The equilibrium sorption parameter, G , represents the ratio of the gas storage capacity of the foam sample to that of the volume of gas surrounding the sample.

$$G \equiv \frac{V_f}{V_g} K_{eff}. \quad (3.28)$$

Both expressions of Fick's Second Law, equations 3.19 and 3.20, in terms of these non-dimensional parameters are the same so the subscripts will be temporarily abandoned

$$\frac{\partial \bar{P}}{\partial \tau} = \frac{\partial^2 \bar{P}}{\partial z^2}. \quad (3.29)$$

It is subject to the boundary conditions,

$$\frac{\partial \bar{P}}{\partial z} \Big|_{(0, \tau)} = 0, \quad (3.30)$$

due to symmetry at the center of the foam and from the mass balance

$$\bar{P}(1, \tau) + \frac{G}{2} \int_{-1}^{+1} P(z, \tau) dz = 1. \quad (3.31)$$

at the foam gas interface. The initial condition is

$$\bar{P}(z, 0) = \begin{cases} 0 & z \neq \pm 1 \\ 1 & z = \pm 1 \end{cases} \quad (3.32)$$

The expression for the equilibrium value of the non-dimensional pressure from the mass balance is

$$\bar{P}(z, \infty) = \frac{R_d}{1 + G} \quad (3.33)$$

where R_d is the ratio of equilibrium pressure if the sample is deformed by the initial pressure step to the equilibrium pressure with no sample deformation.

This system of equations, in non-dimensional form, is the starting point for the solutions in the next sections. Note that when derived in terms of C_{eff} or C_g the only difference between these equations is in the additional solubility term in the denominator of τ_g .

3.2.1 Solving the Governing Equation

The solution to the second order differential equation developed above is not straight forward due to the mass balance boundary condition at the foam gas interface. This becomes a homogeneous Dirichlet-type boundary condition and the equation is readily solved using a transformation first given by Wilson [18]. This method was adapted by Brehm for this experiment and is reviewed here in a slightly different form.

A variable $\phi(z, \tau)$ is defined as

$$\phi(z, \tau) \equiv \beta z + \int_0^z \bar{P}(z', \tau) dz', \quad (3.34)$$

where β is a constant to be determined. This definition implies the following equalities:

$$\frac{\partial \phi}{\partial z}(z, \tau) = \beta + \bar{P}(z, \tau) \quad (3.35)$$

$$\frac{\partial^2 \phi}{\partial z^2}(z, \tau) = \frac{\partial \bar{P}}{\partial z}(z, \tau). \quad (3.36)$$

Using these relations, the governing equation 3.29, the time derivative of $\phi(z, \tau)$ can be written as follows:

$$\frac{\partial \phi}{\partial \tau}(z, \tau) = \int_0^z \frac{\partial \bar{P}}{\partial \tau} dz' = \int_0^z \frac{\partial^2 \bar{P}}{\partial z'^2} dz' = \frac{\partial \bar{P}}{\partial z}(z, \tau) = \frac{\partial^2 \phi}{\partial z^2}(z, \tau), \quad (3.37)$$

where we have used the symmetry condition from Equation 3.30. $\phi(z, \tau)$ still satisfies the diffusion equation, so the new governing equation is simply

$$\frac{\partial \phi}{\partial \tau}(z, \tau) = \frac{\partial^2 \phi}{\partial z^2}(z, \tau). \quad (3.38)$$

The new boundary condition at $z = 1$ is found by writing Equation 3.31 in terms of $\phi(z, \tau)$

$$\frac{\partial \phi}{\partial z}|_{(1, \tau)} - \beta + G(\phi(1, \tau) - \beta) = 1. \quad (3.39)$$

Rearranging terms the final form is to get

$$\frac{\partial \phi}{\partial z}(1, \tau) + G\phi(1, \tau) = 1 + \beta(G + 1). \quad (3.40)$$

We define β to make this boundary condition homogeneous,

$$\beta = \frac{-1}{G + 1}, \quad (3.41)$$

completing the definition of $\phi(z, \tau)$. At $z = 0$ the boundary condition is taken from the definition $\phi(z, \tau)$ in which

$$\phi(0, \tau) = 0, \quad (3.42)$$

The initial condition in terms of $\phi(z, \tau)$ is

$$\phi(z, 0) = \beta z = \frac{-z}{G+1}. \quad (3.43)$$

The solution is obtained by separation of variables,

$$\phi(z, \tau) = \sum_{n=0}^{\infty} \frac{2G}{G(G+1) + \alpha_n^2} \frac{\sin \alpha_n z}{\alpha_n \cos \alpha_n} \exp(-\alpha_n^2 \tau) \quad (3.44)$$

where the α_n are the real, positive roots of the equation

$$\alpha_n + G \tan \alpha_n = 0. \quad (3.45)$$

To rewrite this result in terms of the non-dimensional pressure function $\bar{P}(z, \tau)$, Equation 3.35 is used as follows,

$$\bar{P}(z, \tau) = -\beta + \frac{\partial \phi}{\partial z}(z, \tau) = \frac{1}{G+1} + \sum_{n=0}^{\infty} \frac{2G}{G(G+1) + \alpha_n^2} \frac{\cos \alpha_n z}{\cos \alpha_n} \exp(-\alpha_n^2 \tau). \quad (3.46)$$

The non-dimensional pressure evaluated at the sample surface, $z = 1$, is equal to the non-dimensional pressure measured in the chamber. Therefore the desired expression for the non-dimensional pressure transient to be evaluated is

$$\bar{P}(\tau, G) = \frac{1}{G+1} + \sum_{n=0}^{\infty} \frac{2G}{G(G+1) + \alpha_n^2} \exp -\alpha_n^2 \tau. \quad (3.47)$$

The solution to both cases 3.19 and 3.20, is the same. There is a difference in the analysis due to the definitions of τ .

3.2.2 Determination of S_{sp} and D_{eff} (D_g)

A plot of \bar{P} for several values of G is shown in Figure 3-3. From the measured equilibrium pressure, $\bar{P}_{\infty} = 1/(G+1)$, the value of G for the test is calculated. Using the definition

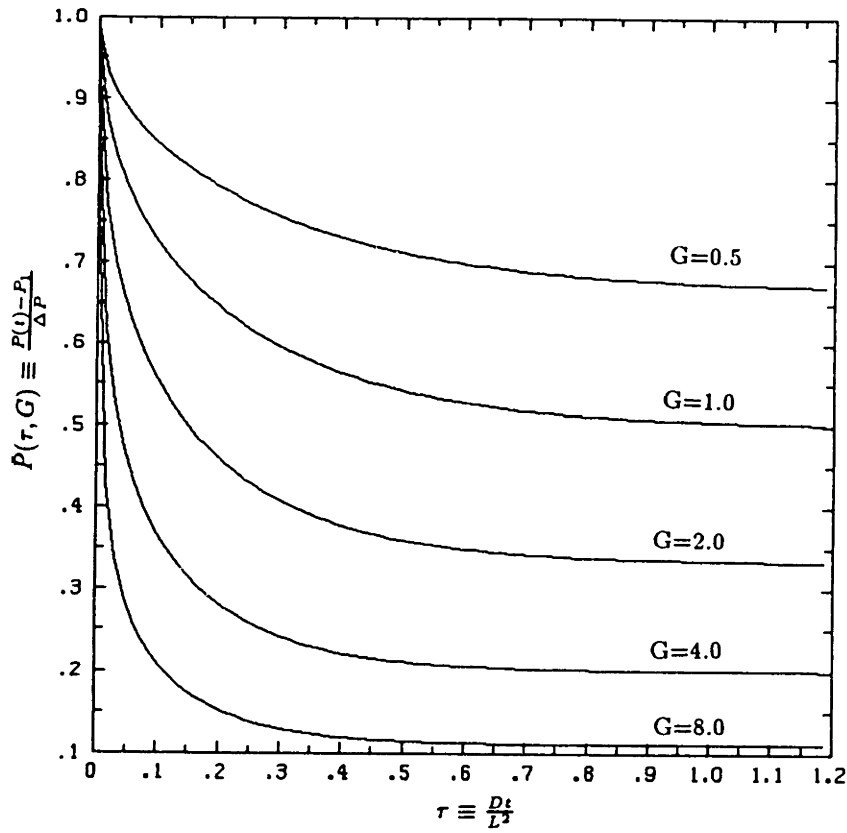


Figure 3-3: Plot of analytical solution showing $P(\tau, G)$ for a range of G .

of G , the solubility ratio is then calculated as

$$K_{eff} = \left(\frac{1}{\bar{P}_\infty} - 1 \right) \left(\frac{V_g/RT}{2AL} \right). \quad (3.48)$$

The value of G is used to generate a characteristic curve which is then matched with the transient data points to determine the diffusion coefficient. Figure 3-4 illustrates this matching process. For each measured pressure $\bar{P}(t)$ the predicted curve is consulted to find the value of τ which gives the same value of \bar{P} . By virtue of the definition of τ_{eff} (or τ_g), a plot of the (t, τ) pairs gives a straight line with slope $m = D_{eff}/L^2$ or ($m = D_g/K_{eff}L^2$), so the diffusion coefficient is found as

$$D_{eff} = mL^2. \quad (3.49)$$

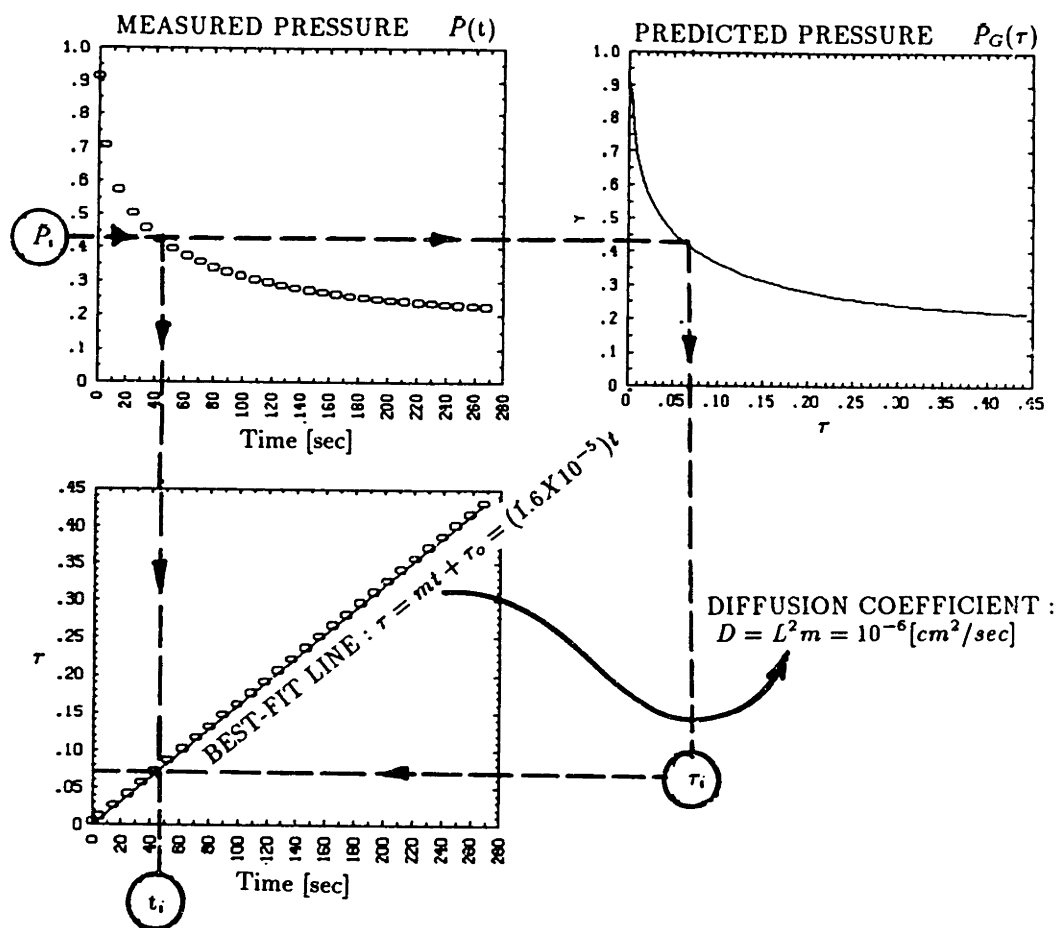


Figure 3-4: Diagram of mapping from $\bar{P}(t)$ and $\bar{P}_G(\tau)$ curves to the τ vs. t plane, as given by Brehm. The numbers correspond to an ideal case with $G=4.0$, $L=.025\text{cm}$, and $D_{eff} = 10^{-6}\text{cm}^2/\text{sec}$.

or

$$D_g = mK_{eff}L^2 \quad (3.50)$$

The uncertainty in D_{eff} obtained in this process is a function of the uncertainties in the pressure and volume measurements, the value of G for the test, the number of transient data points incorporated in the best fit plot of (t, τ) and the interval of τ considered. In the case of D_g the error in determining the solubility ratio is also a consideration. Single-sample uncertainty analysis [22] for fifty transient data points in the interval $0.05 < \tau < 0.25$ gives uncertainty in D_{eff} of approximately 10%. Although the analytically

determined uncertainty for D_g is higher, both methods will yield the same uncertainty in the prediction of the aging process.

From the value of K_{eff} and its definition, S_{eff} is found

$$S_{eff} = K_{eff}(1/RT) \quad (3.51)$$

and S_p can then be determined

$$S_p = \frac{S_{eff} - (\frac{1}{RT})\delta}{1 - \delta} \quad (3.52)$$

Accelerated Determination of D_{eff} (D_g)

When the foam solubility coefficient can be estimated in advance, either by extrapolating from a completed test at a different temperature or by some knowledge of the normal behavior of the gas this information may be used to determine D_{eff} (D_g) without waiting for the test to reach equilibrium. In this case, the value of G and the corresponding characteristic curve are generated in advance and D_{eff} (D_g) may be calculated from the transient data. A typical test like this need only continue to $\tau \approx 0.25$, providing a fourfold time savings over tests run to equilibrium.

Temperature Dependence of Solubility

Due to the large void volume, the effective solubility of the air components in the foam is dominated by the solubility of the gas in the cells, so it is expected to be inversely proportional to temperature, as follows,

$$S_{eff} \approx S_g(T) = \frac{1}{RT} \quad (3.53)$$

which may be written in terms of the effective foam solubility ratio as

$$K_{eff}(T) \equiv \frac{S_{eff}(T)}{S_g(T)} \approx 1. \quad (3.54)$$

In cases where the solubility of the solid polymer is high, however, the temperature dependence of the polymer solubility becomes important. The temperature dependence of solubility is not well understood. Van Krevelen [21] gives this temperature dependence for polymer-gas systems using the Clausius-Clapeyron equation as

$$\Delta H = -R \frac{d(\ln S_{sp})}{d(1/T)} \quad (3.55)$$

where ΔH is the heat of solution.

If the solubility ratio K_{eff} is measured at some temperature T_o , it's value at another temperature T is most conveniently given in terms of K_{eff} at T_o , and the ratio of the solid polymer solubilities at the two temperatures. The development of this expression comes from writing K_{sp} in terms of K_{eff} as

$$K_{sp} = \frac{K_{eff} - \delta}{1 - \delta}, \quad (3.56)$$

taking the ratio at two temperatures

$$\frac{K_{sp}(T)}{K_{sp}(T_o)} = \frac{K_{eff}(T) - \delta}{K_{eff}(T_o) - \delta}, \quad (3.57)$$

and multiplying both sides by the right hand side's denominator and dividing both sides by $K_{eff}(T_o)$. The resulting expression is

$$\frac{K_{eff}(T)}{K_{eff}(T_o)} = \frac{K_{sp}(T)}{K_{sp}(T_o)} \left(1 - \frac{\delta}{K_{eff}(T_o)} \right) + \frac{\delta}{K_{eff}(T_o)}. \quad (3.58)$$

Van Krevelen [21] also gives a correlation by Van Amerongen for ΔH for polymers in rubbery state with a correction by Meares for polymers in glassy state, based on the critical temperature or boiling point of the gas. In kJ/mol the expressions are

$$\Delta H \approx -0.104T_{cr} - 8.35 \quad (3.59)$$

GAS	T_{cr} [K]	T_b [K]	ΔH [kJ/mol]	$\Delta H/R$ [K]
N_2^{***}	126.2	77.4	-21.57	-72.65
O_2^{**}	154.6	90.2	-24.15	-92.93
CO_2^{***}	304.2	194.6	-40.91	-216.5
CCl_3F^{***}	471.2	297.0	-58.39	-964.9
$CF_3-CCl_2H^{**}$	456	301.7	-58.00	-1066.3
$CH_3-CCl_2F^*$	477.8	305	-59.4	-835.8

Table 3.1: Estimation of Heat of Solution for CO_2 , O_2 , N_2 CFC-11, HCFC-123 and HCFC-141b. Critical temperatures and boiling temperatures are given by ***Reynolds [23]; **ICI; *Allied Chemical.

$$\Delta H \approx -0.172T_b - 8.35 \quad (3.60)$$

The ratio of the solubilities in the solid polymer at the two temperatures can be estimated using these correlations as

$$\frac{K_{sp}(T)}{K_{sp}(T_o)} = \frac{S_{sp}(T)}{S_{sp}(T_o)} \approx \exp \left[\frac{\Delta H}{R} \left(\frac{1}{T_o} - \frac{1}{T} \right) \right] \quad (3.61)$$

The above approximations are, according to Van Krevelen, good for the polymers tested and with reservation applicable to other polymers. Although the polymer physics involved in these correlations is beyond the scope of this work a brief description may be helpful in understanding the reservations placed on the use of these approximations. The correlations are given for polymers that undergo a glass transition. Glass transition is defined as a range of temperatures where the polymer exhibits a radical change in specific volume (a pseudo second order transition), this is due to a change in the free volume of the polymer matrix. Below the glass transition temperature, T_g , the polymer is an amorphous, solid phase, above T_g the polymer is in a rubbery, liquid phase. Below and above T_g most temperature dependent polymer properties follow an Arrhenius relation. In the glass transition region the temperature dependent properties are strongly affected

by the changes in free volume and follow a different temperature dependence. This dependence is given by the WLF equation as

$$\ln(A_t) = \frac{C_1(T - T_o)}{C_2 + T - T_o} \quad (3.62)$$

where A_t is the ratio of the property at temperature T to the property at a reference temperature T_o and C_1 and C_2 are empirically determined constants. If the reference temperature $T_o = T_g$, then the constant $C_1 = -17.44$ and $C_2 = 51.6$. The polymers in foam insulation are crosslinked polymers that do not display a discrete glass transition temperature due to volume restrictions imposed by the crosslinks. Further consideration should be given when applying these correlations to crosslinked polymers, especially when the polymer is in the presence of a plasticizing solvent like HCFC-123.

3.2.3 Definition of Permeability

When analysing the steady flow of gas through a medium the diffusion and solubility coefficients always appears as product. This product has been defined as the permeability coefficient

$$Pe \equiv DS \quad (3.63)$$

and all processes of diffusion and sorption are referred to as permeation processes. Although still termed permeation, in the transient processes involved in the tests for this research and the aging process of foam, diffusion and solubility operate independently. The definition is given here for clarity as it is useful when comparing these results to results from steady state methods.

Temperature Dependence of Permeation Processes

The temperature dependence of the permeability coefficient follows from the temperature dependence of D and S .

Diffusion is considered to be a thermally activated process whose temperature de-

pendance can be described by an Arrhenius-type equation

$$D = D_o \exp\left(\frac{-E_D}{RT}\right) \quad (3.64)$$

where D_o and E_D are constants for a particular gas-foam combination. These constants can be evaluated if the diffusion coefficient is measured at two or more temperatures. This will be discussed later in chapter 6.

Combining the temperature dependence of both diffusion and solubility coefficients, the temperature dependence of permeability is

$$Pe(T) = D_o \exp\left(\frac{-E_D}{RT}\right) \left(\frac{1}{RT}\right) = Pe_o \exp(-E_P/RT), \quad (3.65)$$

where we have used the approximation of Equation 3.53 to express the temperature dependence of S and we have defined the new constants Pe_o and E_P for convenience in working with the temperature dependence of the permeability.

Chapter 4

Test Apparatus and Procedure

The nature of transient sorption method dictates the some basic prerequisites of the apparatus and test preparation. The test requires isolating a foam sample in a fixed volume of gas. The chamber must be well sealed and free from outgassing contaminants. Before a test begins the chamber and sample must be free of all gas but the test gas and the pressure of that test gas must be measured. The pressure in the test chamber must be monitored and recorded throughout the test. Tests for each test gas are run at least three different temperatures. Constant temperature must be maintained during each test. The test chamber was submerged in a temperature controlled water bath to this end. The corrosiveness of the refrigerants tested and the emersion in a water bath place restrictions on the materials of the components and associated piping. In the following sections the test apparatus individual components will be described, the procedure for preparing and running a test is outlined and data acquisition computer hardware and software is described.

4.1 Hardware

The configuration of the test apparatus components used in this research is shown in Figure 4-1. The test chamber, gas reservoir, gas supply, and valves will be discussed.

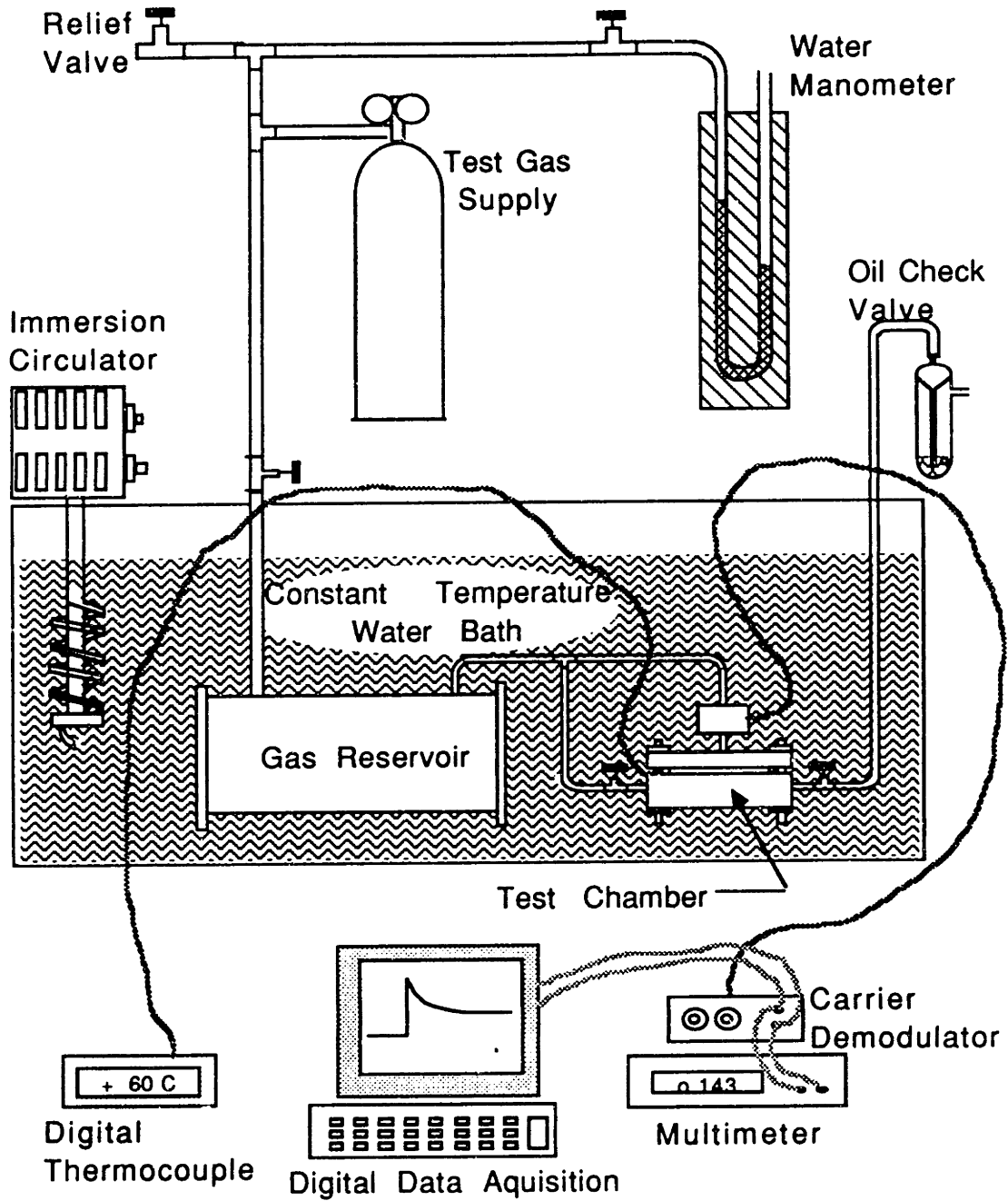


Figure 4-1: Schematic of the Test Apparatus.

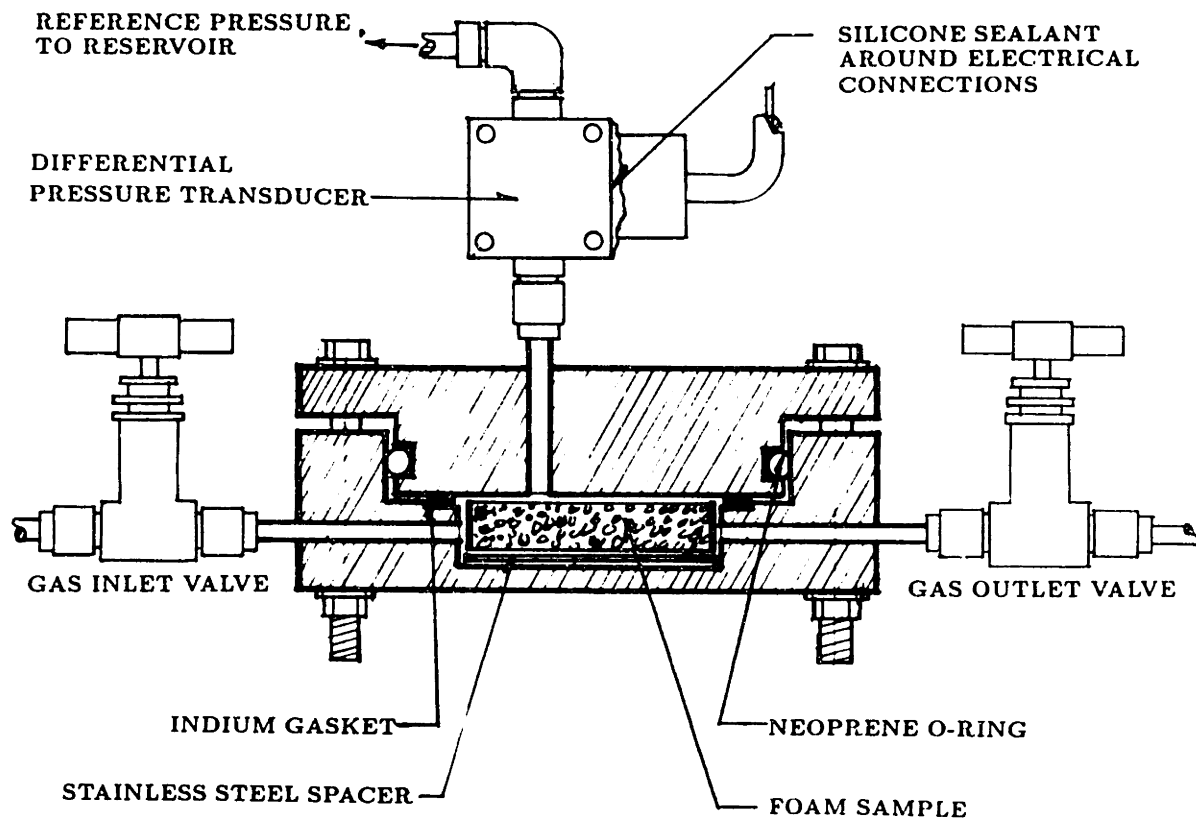


Figure 4-2: Cutaway View of Constant Volume Test Chamber.

4.1.1 Test Chamber

The central component of the system is the constant-volume test chamber, shown in Figure 4-2. The chamber allows a maximum sample thickness of approximately 0.5 cm. When thinner samples are used, solid stainless steel discs, 3.35 cm diameter, 0.99cm thick, are added to fill the chamber to maintain a low, V_g , volume of gas in the chamber surrounding the foam. The maximum sample diameter is approximately 4.0 cm. To maintain a low V_g with smaller diameter samples strips of stainless steel shim stock, 0.01 x 0.693 cm, were used as annular spacers. All actual chamber inner dimensions are tabulated in appendix D.

The main body of the chamber is machined from stainless steel stock, and the

stainless steel tubes are helium arc welded in place. All connections are made with Swagelok stainless steel fittings. All surfaces exposed to the test gas are cleaned thoroughly and baked to eliminate outgassing. The cleaning procedure for new parts was to swab or flush inaccessible areas with a series of solvents: trichloroethylene and/or R11, acetone and ethyl alcohol then bath in ultrasound with deionized water and finally bake at 110 °C for 12 hours. All subsequent cleaning was performed only with the series of solvents.

4.1.2 Chamber Seals

The chamber is completely sealed once the pressure step is imposed so that the total mass in the test chamber is assumed constant throughout the test. Maintaining a constant mass requires rigorous sealing. To achieve this, techniques developed for maintaining high vacuums have been used [13]. Chamber gasket and valves are the critical areas. The inlet and outlet valves have stainless steel bodies and stainless steel ball-joint stem tips for repeatable leak-tight closure. A highly-malleable indium gasket provides an essentially impermeable seal and establishes approximately the same total chamber volume on successive closures. See section 5.1.3 for effects of gasket on volume measurement error.

Gasket preparation is a multistage process. First indium slugs are melted and the molten indium is poured onto a cleaned surface. The indium lump is then pressed in a rolling mill between clean sheets of thin stainless shim stock until the indium is approximately twice as thick as the chamber gasket lip height (see Figure 4-2). The resulting disk of indium is then cut in a spiral into a long tape. The tape is cut to approximately one half of the chamber gasket lip width. A gasket is formed by cutting a piece of indium tape slightly longer than the diameter of the intended gasket. The tape is placed on the chamber gasket lip and the ends are overlapped to close the ring. A new gasket is used each time a new seal is made. Used gaskets were recycled by remelting them. During this remelting a solid layer of impurities forms on the top of the melt. This layer does not pour off with the purified indium.

4.1.3 Transducers

In this research two test apparatus rigs, built with the same materials and construction techniques, were used. The difference between these rigs is in the pressure transducer hardware. One rig, built by Brehm, uses absolute pressure transducers on each of three test chambers (see Figure 4-3). The other rig, built for this research, (shown in Figure 4-1, and in more detail in Figure 4-4) uses a differential pressure transducer on a single test cell.

Validyne AP-10 variable reluctance absolute pressure transducers with a range from 0 to 20 psia were used in the three chamber rig. These AP-10 have an output of approximately 1 volt per psi. The other rig uses a Validyne DP-15 variable reluctance differential pressure transducer with a replaceable diaphragm rated for a maximum pressure differential of 8 psi. The response of this transducer is approximately 2 volts per psi. Calibration curve for all transducers are in appendix D. Both transducers are of stainless steel. The AP-10 is all-welded construction. The replaceable diaphragm in the DP-15 is bolted between the electronics housing. Teflon o-rings replaced the standard, buna-n, used between the housings and the diaphragms. The signal cable from the transducer to the demodulator is shielded and contains two shielded pairs of wires. Different shielded pair must be used for the signal and carrier wire to avoid voltage drift due to induced magnetic fields. Some of the standard cable coatings become brittle and crack after long exposure to hot water, teflon coated cable was used to avoid this problem.

The transducer's electrical connections were sealed so that they could be submerged in a temperature-controlled bath of deionized water. In previous work, this sealing was provided by applying silicone sealant directly to the bare pin connectors on the transducer face and up the attached signal cable for a length of approximately 1.5 inches. This method proved ineffective after several months in water cycling from 25 to 80° C. Unavoidable movement of the signal cable also aggravated the situation. After numerous trial and error revisions, the following method that emphasizes meticulous care, cleanliness and stress relief has provided adequate moisture protection under test conditions

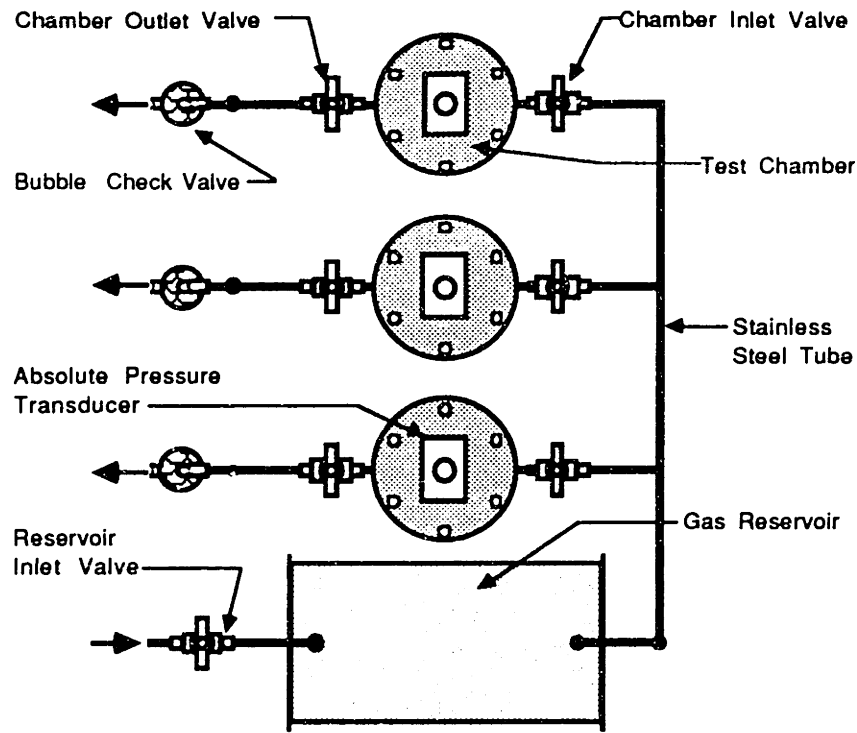


Figure 4-3: Apparatus with 3 Chambers Built by Brehm.

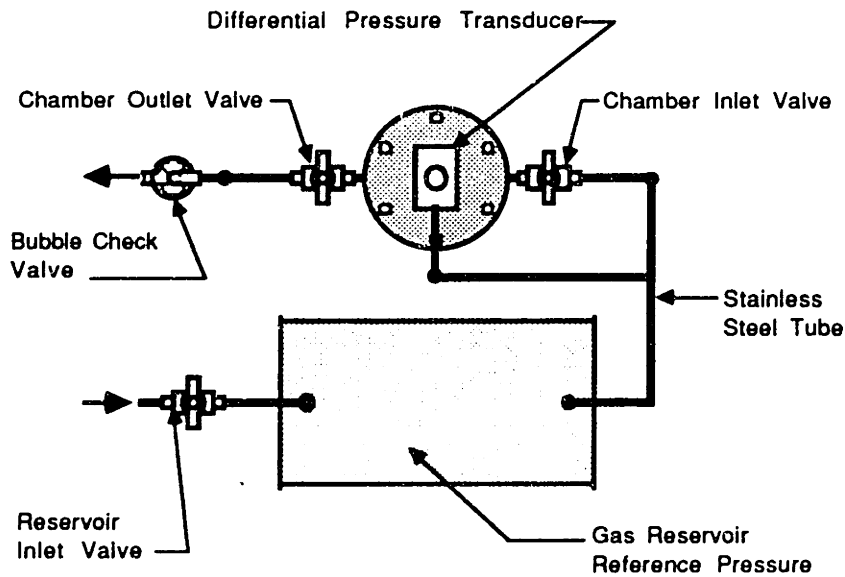


Figure 4-4: Apparatus Built for This Research.

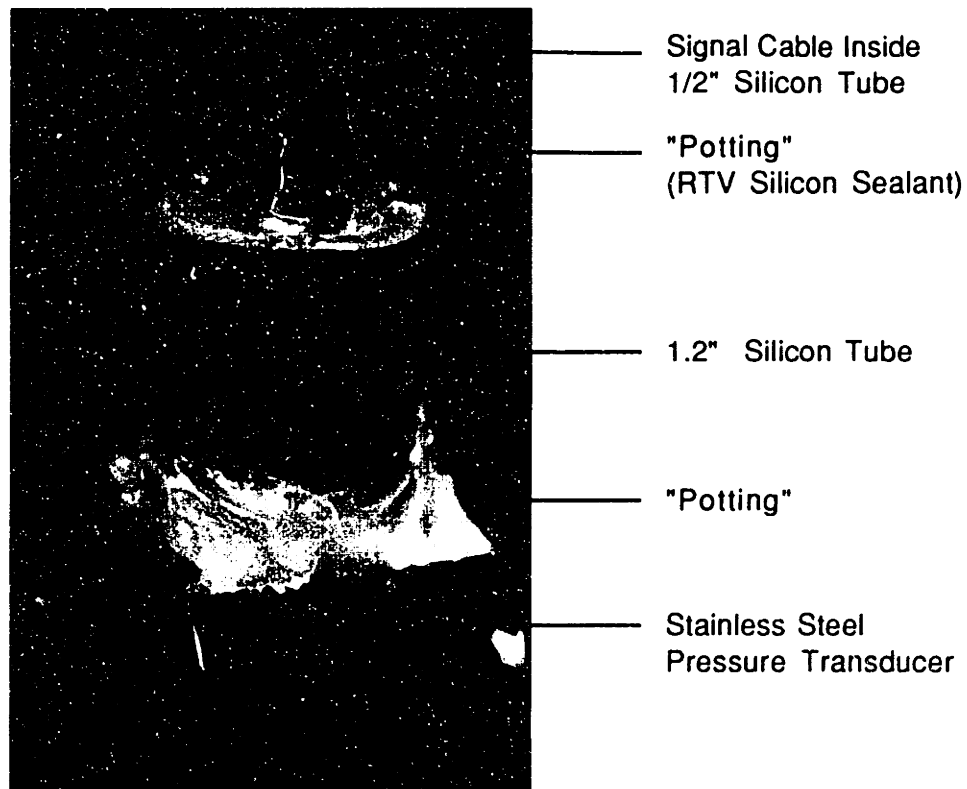


Figure 4-5: "Potting" on Transducer Electrical Connections.

for over one year for all but one transducer. The old sealant and cable were removed and the pin connectors and that face of the transducer were polished and cleaned with acetone. To insure stress relieved electrical connections, each signal cable wire was wound around it's pin connector before resoldering. Again, before applying silicon sealant, all surfaces to be coated were cleaned with acetone. To minimize total exposed surface area of the sealant, a one inch long, 1.2 inch diameter silicone tube was placed around the pin connectors, fixed with sealant flush to the face of the transducer and filled with sealant. For the same purpose, a half inch diameter silicone tube covers the entire length of signal wire exposed to the water bath. A detailed photo 4-5 shows a "potted" transducer.

The combined power supply and signal conditioner, a Validyne CD-280 carrier demodulator, in conjunction with the transducers provide a 0-10 VDC output with a

calibrated accuracy of approximately 1% over the test range of 0.0 to 105.5 cm H_2O (see section 5.1.1).

4.1.4 The Rest of the Assembly

Reservoir

The reservoirs are thin wall stainless steel pipe with helium arc welded stainless steel end caps, and inlet and outlet tubing. In both rigs the reservoir serves as preheater for the test gas. In the apparatus with a differential transducer shown in Figure 4-4 when all valves are closed it provides the reference pressure for the transducer during a test.

Water Bath

To achieve constant test temperatures, the rigs are submerged in a bath of deionized water. Temperature is maintained to within 0.02° C by a Fisher Scientific Immersion circulator. Temperature was monitored by type "T" thermocouple thermometers.

Test Gas

Test gas supply was piped to each chamber through 1/8th inch stainless steel tubing. The gas was not filtered. Regulated gas bottles provided air component (nitrogen, oxygen or carbon dioxide) supply. 500 ml stainless steel lecture bottles with stainless steel bellows valves were filled with the liquid refrigerants. The boiling points of the refrigerant gases are at or slightly above room temperature, therefore control of the gas temperature is required from the bottles to the water bath. To obtain the pressures required, the bottles were submerged in a warm water bath.

Check Valve

Vacuum pump oil was used in the check valves at the test chamber outlet, because of its low vapor pressure. However, all of the blowing agents tested were found to be miscible

in it at room temperature. This is unacceptable during the flushing procedure, because as the valve fills with the solution the pressure needed to keep even a slow flow increases, increasing the pressure in the test chamber. Silicone oil was also tried with the same results. To eliminate liquid buildup when flushing with refrigerants, the oil valve was partially immersed in warm water to keep the oil temperature above the boiling point of the test gas.

4.2 Data Acquisition

A digital data acquisition system was used to monitor and record transducer voltage output for the majority of the tests. The basic hardware was an IBM XT with 4.77 Mhz clock speed, 20 megabyte hardcard, math co-processor and AST clock. The analog to digital conversion was done by a 12 bit IBM DACA board with multiplexer. This configuration gives a combined resolution of 2.44 mv which corresponds, for the AP-10 (DP-15), to 0.12% (0.06%) of the maximum voltage excursion for a typical test with a 2 psi pressure step. Initial voltages and step pressure voltages were also recorded by hand from a Fluke digital multimeter. This provided a backup and check for any computer problems. The multimeter provided the main source of data for the longer tests (refrigerants at 40 and 60 °C).

Unkle-Scope software was used as a digital chart recorder to sample and store raw data. This software allows user programmable macros to sequence user defined data collection setups (formats) on a maximum of four channels. These setups establish sampling rates and number of data points to be stored, as well as axis ranges for real time data plotting to the computer screen.

A data sampling sequence was determined for each gas at each test temperature. These were saved as macros and used on each foam tested. How these sequences were determined is described in the next section.

4.3 Experimental Procedures

4.3.1 Sample Preparation

The first step in obtaining a test sample is coring a cylindrical plug from the foam to be tested. A coring tool was made from a section of thin wall pipe. One end of the pipe was filed to a tapered cutting edge. The other end was fit with a removable chuck designed to be held in the jaws of a drill press. All the foams tested for this research were supplied in rectangular sections of 1 or 2 inch thick board stock. Cored cylinders perpendicular to the face of the foams were achieved by placing the foam on a flat surface perpendicular to the drill axis. The cored foam plug is measured and weighed to obtain the average foam density.

The analysis of the test results assumes parallel faces on the test specimen. To this end the test specimen is sliced from the foam plug on an Buler Isomet Low-Speed Saw with a 5 inch diameter High Density Diamond-Edged Wafering Blade. The plug is held on the saw with a custom built chuck. The previously determined average distance between cell walls (see section 2.3) are used to select specimen thickness. Samples for this set of tests were sliced 10 to 15 cells thick to expedite the testing. The specimens were cut from the center of the cylindrical foam plug (see figure 4.3.1). Density measurements from

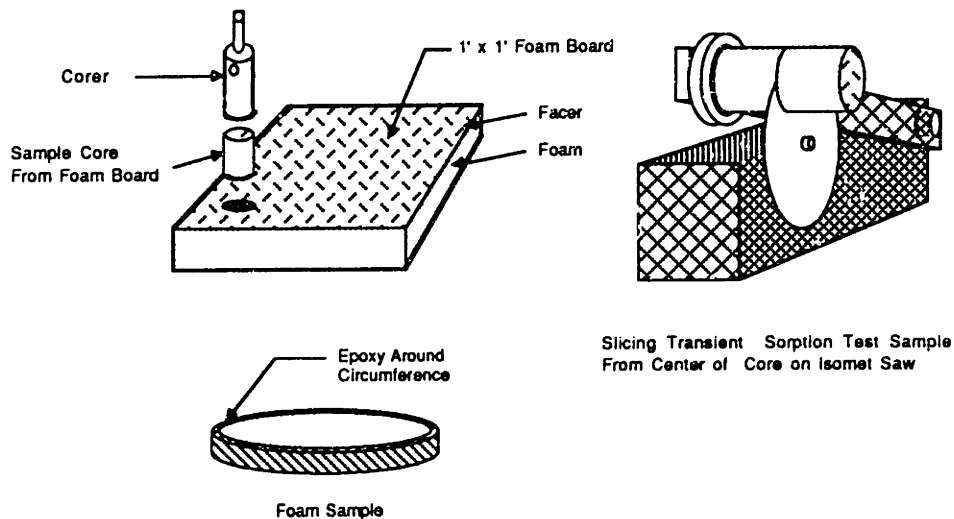


Figure 4-6: Transient Sorption Test Sample Preparation.

adjacent center sections were made. If core densities and average densities differ, this difference must be accounted for when predicting aging of board stock from permeability test results.

The circumference of the specimen is coated with a thin layer of DER 331 epoxy from Allied Resin Corporation. This epoxy, used by Ostrogorsky [13] and Brehm [19], forms an impermeable edge and therefore allows one dimensional analysis of the permeation test. It has been suggested that without epoxy, the edge effects would be minimal and could be accounted for analytically [24]. The edges were epoxied for this series of test to avoid added uncertainties.

4.3.2 Volume Measurements

For each sample tested, the volume of the test chamber is determined by using a pycnometer-type measurement. This method is described by Brehm [19]. The method uses the pressure volume relationship described by Boyles Law to measure the chamber volume

$$V = P_{ref} \frac{\Delta V}{\Delta P} \quad (4.1)$$

where P_{ref} in this case is the atmospheric pressure, P_{atm} . A capillary tube is connected to the test chamber's outlet valve. A schematic of the setup is shown in Figure 4-7. The valve designations in the figure are keyed to Table 4.1 to outline the steps in the measurement process.

In **step 1** the chamber side end of the slug is set to zero by raising and lowering the end of the capillary tube. The inlet to the chamber is open to atmospheric pressure.

In **step 2** the volume of the chamber and tube are set at the zero reference state by closing the inlet valve. Note that the outlet valve is in its full opened position.

In **step 3** closing the outlet valve moves the alcohol slug in the tubes the equivalent of the internal volume of valve V_o . This change in volume is the same as the change in volume due to reopening V_o to the same full open position in **step 6**.

Step	Valve V_G	Valve V_R	Valve V_I	Chamber Pressure	Valve V_O	Capillary Volume
1	Closed	Open	Open	P_{atm}	Opened	Zero Slug
2	Closed	Opened	Close	P_{atm}	Opened	0
3	Closed	Closed	Closed	P_{atm}	Close	$0 + Vol_{V_O}$
4	Open	Closed	Open	$P_{atm} + \Delta P$	Closed	$0 + Vol_{V_O}$
5	Opened	Closed	Close	$P_{atm} + \Delta P$	Closed	$0 + Vol_{V_O}$
6	Close	Closed	Closed	P_{atm}	Open slowly	ΔV

Table 4.1: Summary of Steps in Test Chamber Volume Measurement. Valve designations keyed to Figure 4-7.

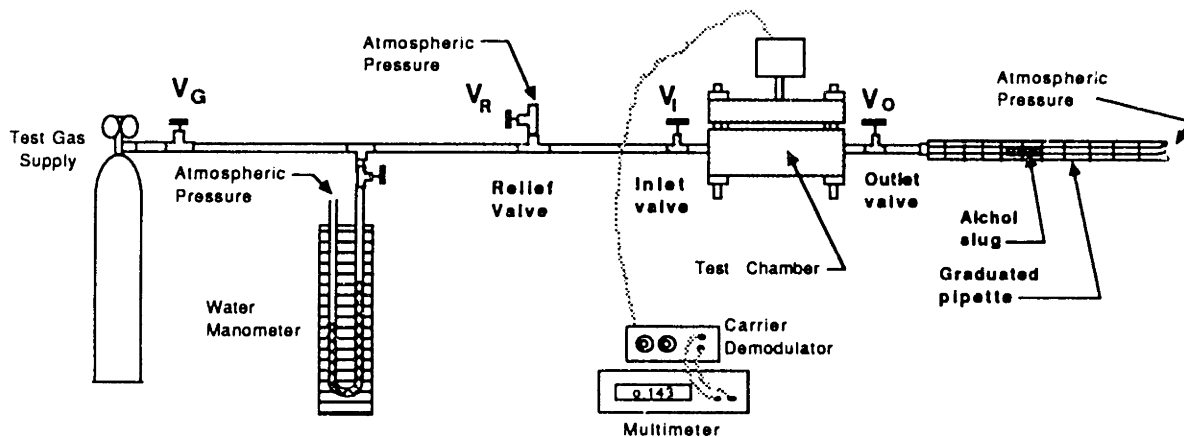


Figure 4-7: Schematic of Chamber Volume Measurement setup.

In **step 4** and **5** mass is added to the chamber by increasing the pressure by ΔP .

In **step 6** the outlet valve is opened and atmospheric pressure is established in the chamber/capillary tube volume. It is essential that V_o is opened slowly in this step so that momentum does not drive the slug. The outlet valve is turned to its full open position (as in **steps 1** and **2**) to reestablish the initial reference volume. If the valve is not reopened to the same position the difference in the volume in the valve will effect the measured of ΔV .

First the total volume, V_T , without the sample in place, is measured. The specimen is then placed in the clean chamber and sealed with a fresh gasket. The volume is measured again. This measures the volume of gas, V_g , in the chamber around the foam. The difference between the two measurements, V_T and V_g , gives the sample volume, from which an effective sample half-thickness, L_{eff} , can be calculated knowing the sample diameter. This means of determining L_{eff} factors out any open cells on the surface of the sample. The difference between the thickness determined in this manner and the thickness determined with caliper measurements, shows an average of 0.9 open cells at each cut surface. These measurements are tabulated in appendix F.

To maximize accuracy when measuring V_g it is important to use a gas with low permeability so that no significant amount of mass permeates the sample during the volume measurement process. The measurements in this work were made with N_2 and at room temperature.

4.3.3 Sample Conditioning (Flushing)

The rig is immersed in the bath of deionized water and slowly brought up to test temperature. Meanwhile the outlet valve is opened and the inlet valve is throttled to allow the test gas to flush through the chamber at atmospheric pressure. This process allows the test gas to fully permeate the sample and it allows any other gas species which may have been in the sample to diffuse out. The flow rate can be monitored through the bubble rate in the oil check valve. A rate of one bubble, approximately 0.2 inch diame-

ter, every two seconds was used for air gases. This gives a chamber with a 3 ml volume, approximately one volume change of gas every 88 seconds.

This flushing procedure establishes a known equilibrium state in the chamber, before a test begins. The flushing time required to reach equilibrium not only depends upon the temperature and the sample thickness, but also on the diffusion coefficients of the test gas and other gas to be flushed from the foam. If an educated guess can be made as to the order of magnitude of the diffusion coefficients, the equilibrium time can be estimated, either by solving the exact equation for transient pressure with constant pressure boundary conditions (available in the literature e.g. Carslaw and Jaeger [25]), or by using the Fourier number (characteristic time scale), equation 3.27 .

In order to determine when complete equilibrium has been achieved, the inlet and outlet valves are both closed and the chamber pressure is monitored. If the pressure remains steady, equilibrium has been established and the test may begin. If the pressure changes, non-equilibrium exists in the chamber, so flushing is resumed. At the beginning of a set of tests with a new sample, the amounts of nitrogen and refrigerant in the specimen are unknown. If the pressure remains constant for a length of time equal to the expected duration of the test then a test may begin. For slower gases at lower temperatures where tests may last weeks, this may not be convenient.

To minimize gas consumption, while flushing with refrigerants, a periodic flushing scheme was employed. The chamber is flushed with at least one volume change of gas, then the rest of the specimen's conditioning takes place in a large volume of stationary gas. This large volume, consisting of the chamber and the reservoir, is established in the following manner. The inlet valve to the reservoir is closed and the chamber flushed until both chamber and reservoir are at atmospheric pressure. The inlet valve to the chamber is then opened and the chamber outlet valve is closed.

The flushing process is time consuming especially when the test gas is nitrogen or a refrigerant. To free the test chamber for testing, another large vessel was used to precondition the samples. Design criteria for such a conditioning chamber is similar to

that of the test chamber itself. It must be made of material that is non corrosive and inert, especially when in the presents of the refrigerants. It should have a very low vapor pressure so that outgassing will not cause contamination at the flushing temperatures. The construction must allow ease of cleaning with no niches for residue collection. The rigorous seal required for the test chamber is not necessary for the flushing chamber. For economy's sake, the chamber designed and built by Ostrogorsky for the steady state permeability test was retrofit for this purpose. The stainless steel chamber, with a 10 cm id. and 6 cm chamber height, was built with the same technique as the test chambers described earlier. A teflon gasket was used.

Results from one series of preconditioning exemplifies an important issue with regard to foam cell gas pressures. A group of specimens with no epoxy on their edges were flushed with CO_2 at $80^\circ C$ for approximately four weeks. The specimens were removed from the flushing chamber and epoxy was applied to the edges. As the epoxy dried on one of the thicker samples the diameter began to shrink and acquire an hour glass profile at a rate visible to the naked eye. Figure 4-8 is a photograph of this sample. This was the first time that measurable changes in specimen diameter had been observed as the epoxy hardens. This results is a visual representation of difference in permeability of CO_2 , O_2 and N_2 . When the foam was removed from the chamber it experienced a step change in external partial pressures from one atmosphere of CO_2 in the chamber to roughly 0.7 atmosphere of N_2 and 0.2 atmosphere of O_2 in the air. After a few hours of exposure to these conditions, the total cell pressure at the center of the foam was well below that of the cells at the surface which were just beginning to experience partial pressures of oxygen. This is due to the rapid diffusion of CO_2 out of the cells. During the testing and flushing process care must be taken when changing from one test gas to another that no structural damage is done due to differences between cell gas and chamber total pressures.

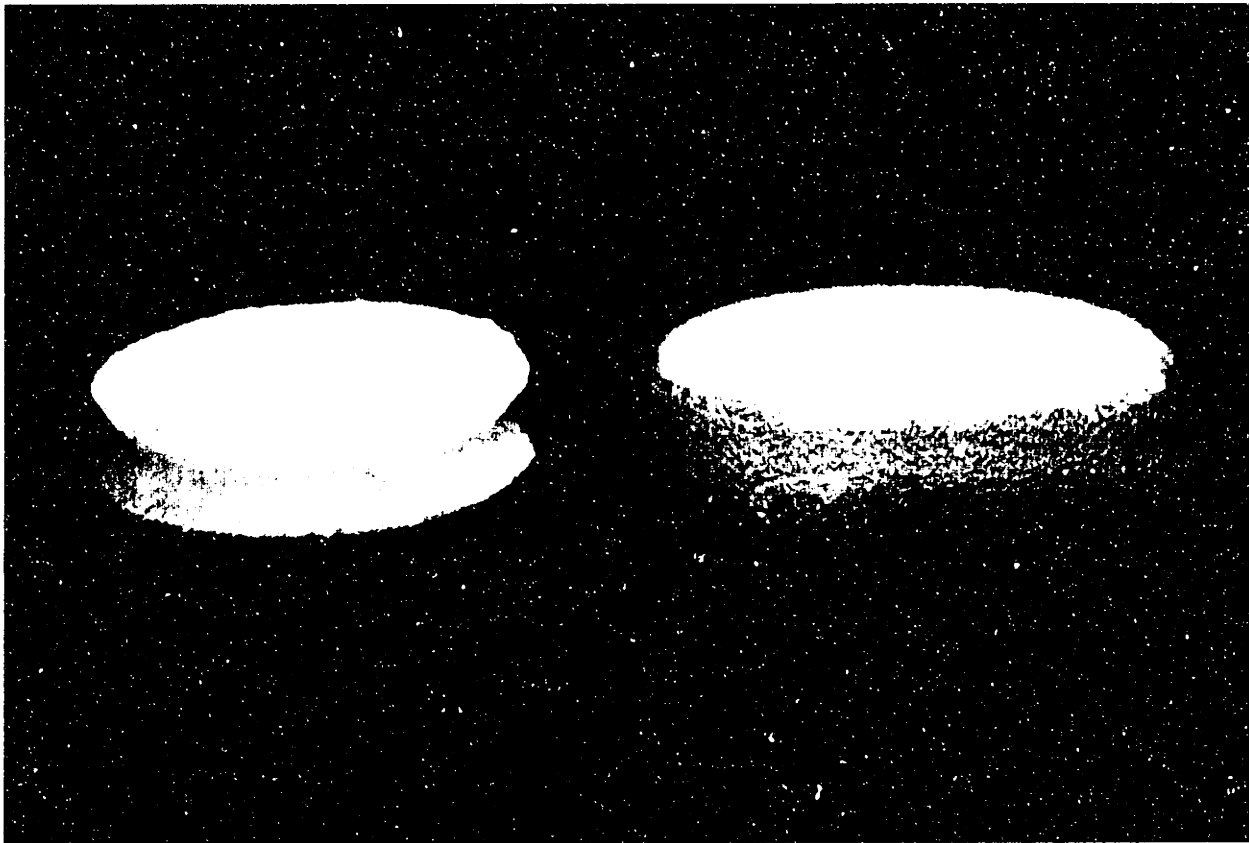


Figure 4-8: On Left, Preconditioned Sample Showing Deformation Due to Low Internal Pressures and Shrinking of Epoxy. On Right, Normal Sample.

4.3.4 Test Initiation

To initiate the sorption test, the outlet valve is closed and then the inlet valve is briefly opened to impose a step pressure change of ΔP at the surface of the sample. The inlet valve is quickly closed again, establishing the chamber constant volume. This opening and closing process takes approximately two seconds. The chamber pressure is recorded from the time just before the step pressure is imposed until the pressure returns to equilibrium or until a pressure has reached a predetermined level.

The following procedure has been suggested as a method to expedite a series of tests for one gas at a variety of temperatures. At the end of a test the valves are left closed and the temperature changed to the next temperature. Then a new test is initiated once

equilibrium has been established at the new temperature. This procedure may accelerate the procedure for fast gases with low solubilities. However, for slowly diffusing gases with high polymer solubilities (refrigerants) the temperature dependence of the solubility and the significant amount of mass stored in the solid polymer has the effect of creating a non-equilibrium condition between the concentration of gas in the solid polymer and the concentration of gas in the cells and chamber gas. Therefore once the new temperature has been achieved the pressure in the sealed chamber must be monitored before a new test begins, as it was after flushing. Note that for similar reasons a period of waiting for equilibrium must also occur before a test if the previous test at another temperature was not run to equilibrium.

4.3.5 Data Acquisition

The routines created to sample data as well as the format of the raw data collected was controlled by the structure of the off-the-shelf data acquisition software used in this project. Within the Unkle-Scope environment, a computer procedure like a batch file, a series of routines, was created for each gas temperature combination. The procedures are all alike in basic structure, the only difference being the sampling times and number of data points saved. A procedure consists of a series of calls to setup files containing a sampling rate, the total number of samples to be taken at that rate, which channel to sample as well as information needed to scale the real time computer screen plot of the data.

When the procedure is initiated the first in the list of setup files is called. The values read from this file establish the details of the first series of data. A voltage versus time axis appears on the screen and sampling begins. Time and corresponding voltage are held in RAM until the preset number of points have been taken. The procedure then writes the data to a file on the hard disk. The time required for this storage process, approximately 17 seconds, depends on the total number of data points and channels sampled. The next setup file is called read and the voltage vs. time axis reappears and

the next set of points are taken. This process repeats until all setup files in the procedure list have been called.

Ideally, the transducer voltage would be sampled at a constant rate throughout the test. A sampling rate no slower than twice per seconds would be sufficient. This slow sampling rate would allow data manipulation during the test, eg. the reduction of data points, conversion of voltage to dimensionless pressure and saving the data to files.

The strategy actually used for determining sampling rate and the number of data points for the initial set of data is the same for all tests. The first set of data for any test includes transducer voltages before the test begins, the pressure step and the initial voltage transient. The sampling rate needs to be fast enough to resolve the step change in pressure as the test begins. The maximum number of data points allowed by Unkle Scope per setup is 1024. A sampling rate of once each 0.5 seconds for 8.53 minutes (the maximum number of points possible) was used for all initial data sets to allow for: some data points before test initiation, adequate resolution of the pressure step and to maximize the number of data points taken at the beginning of a test before interrupting to store the data.

The total number of data points and the sampling rates for the remainder of the test depends upon the expected test duration. As an example, for the shortest test CO_2 at $80^\circ C$ there are a total of four setups in the procedure, the initial setup as described above and three setups with a 1 second sampling rate for 1024 points. As an example of the longest test, a refrigerant at $40^\circ C$, there are a total of six setups in the procedure, again the initial setup, then three setups sampling at 5 second intervals for a total of 1024 points each, and then two sets of data are taken by sampling at 500 seconds for a total of 512 points each. At the end of this 6.1 days the data is analyzed and depending upon the determined Fourier number reached at that point the test is either terminated or data collection is resumed.

To free the XT computer for data acquisition all data reduction and analysis was performed on a VAX. A Vax Fortran code was developed to combine Unkle Scope data

files for each test into one file, reformat the file to be compatible with the data analysis software [19] and reduce the total number of data points.

Blank Page

Chapter 5

Error and Uncertainty

Single sample uncertainty analysis is used in determining error in the results from this series of tests. Work by Kline and McClintock [22] still forms the basis for this type of analysis [26]. The analysis is based on the statistical theory that given enough samples and assuming that they are normal distributed, the uncertainty interval for 20 to 1 odds (that the true value lies within that range) will be equal to twice the standard deviation of the sample population, σ . This is equivalent to a 95% uncertainty interval. This uncertainty can also be expressed in terms of S_N , the standard deviation of a set of N measurements, as

$$\epsilon = \frac{t_S S_N}{N^{1/2}} \quad (5.1)$$

where t_S is the Student's multiplier for N samples.

In the present case the results, R , must be calculated from N independent variable inputs, (X_1, X_2, \dots, X_N) , the uncertainty in the results, ϵ_R , can be expressed as the root sum squared of the contribution of the individual uncertainties, ϵ_{X_i} , as follows.

$$\epsilon_R = \left[\sum_{i=1}^N \left(\frac{\partial R}{\partial X_i} \epsilon_{X_i} \right)^2 \right]^{1/2} \quad (5.2)$$

For convenience sake, the uncertainty is usually expressed as a percent of the actual

value.

$$\xi_R \equiv \frac{\epsilon_R}{R} = \left[\sum_{i=1}^N \left(\frac{X_i}{R} \frac{\partial R}{\partial X_i} \xi_{X_i} \right)^2 \right]^{1/2} \quad (5.3)$$

The combined uncertainty in the experimentally determined values of the effective diffusion and solubility coefficients gives the approximate error in their product, the effective foam permeability coefficient. This uncertainty combined with the errors associated with the determined values of foam density and percent of material in the cell walls is used to approximate error in the foam aging predictions. The next section will outline the uncertainty calculations for the basic measurements, in preparation for the following discussion of their combined effect on the uncertainty in the test results.

5.1 Estimation of Measurement Uncertainty

Some of the component errors described in this section are based on manufacturers specifications, which do not describe the statistical properties of the population of the instrument. In the following analysis the interpretation will be that there are 20 to 1 odds against the error being larger than the specified errors.

5.1.1 Pressure Measurements

Manufacturer specifications for the precision for both transducer and demodulator are expressed as a percent of the full scale pressure excursion which corresponds to ΔP in this case.

The entire pressure measurement system was calibrated to analyze the inaccuracy of the pressure measurement at a given time. The calibration system includes the transducer, the carrier demodulator, the computer data acquisition system and a water manometer. The manometer, graduated in steps of 0.1 cm, gives a precision of 0.14% over the test range. Manufacturer specified combined linearity, hysteresis and repeatability precision for the Validyne CD-280 carrier demodulator and DP-15 differential transducers

are 0.05% and 0.25% respectively. The data acquisition system gives a resolution of 2.44 mv which for the calibrated transducer output of the differential pressure transducer, 2.4 v/psi, corresponds to a $\xi_{P_{resolution}}$ of 0.1% for a test ΔP of 1 psi. For the output of the three absolute pressure transducer chambers this corresponds to a $\xi_{P_{resolution}}$ of approximately 0.24% of a test ΔP of 1 psi. This gives a theoretical calibration accuracy of

$$\xi_{P_{calibration}} = \left[(0.14\%)^2 + (0.05\%)^2 + (0.25\%)^2 + (\Delta P \xi_{P_{resolution}})^2 \right]^{1/2} \quad (5.4)$$

For the 1.5 psi ΔP of foam 18's CO₂ test at 80°C, $\xi_{P_{calibration}}$ is 0.33%.

Over the test range the manufacturer specifies a thermal zero shift results in a precision of 0.21 and 0.009% per °C for the transducer and demodulator respectively. Although the water bath temperature is controlled to within 0.03°C, Water temperature measurement with a type K thermocouple was measured to a precision of 0.5°C which results in a error of 0.1%°C for the transducer. The room temperature varies a maximum of 4°C giving a demodulator thermal zero shift error of 0.04%. Combining the calibrated and thermal uncertainties the total uncertainty in a given pressure measurement is

$$\xi_P = \left[(\xi_{P_{calibration}})^2 + (0.04\%)^2 + (0.1\%)^2 \right]^{1/2} \quad (5.5)$$

Again for foam 18's CO₂ test at 80°C, ξ_P is 0.34%.

5.1.2 Time Measurements

The time measurement for a test is executed by the computer which has a clock speed of 4.7 MHz. This gives a negligible machine error, a precision of 4.2E-5% of the smallest time step measurement, 0.5 seconds. The two limiting factors in the time measurement error become the sampling rate and the amount of time between the opening and closing of the valve at the beginning of a test, approximately 1 second. Both of these factors have their greatest impact on uncertainty during short tests and during periods of fastest transients, ie. at the beginning of a test.

In general, for the determination of D_{eff} values of τ less than 0.05 are not considered. To look at the maximum uncertainty caused by a precision in time of 1 second, consider a typical test of CO_2 at $80^\circ C$ where a test reaches $\tau=1$ in approximately $t=1/2$ hour. A typical D_{eff} determination would include an interval of $\tau=0.05$ to 0.3; the error in time would range from 1.1% to 0.2%. The test time for the other test gases are longer and the error in the time measurement is proportionally lower (approximately 0.3%, 0.05% and 0.001% for O_2 , N_2 and CFC-11 respectively.)

5.1.3 Chamber Volume

Analytical Determination of Uncertainty in Chamber Volume Measurement

The total chamber volume without a sample, V_T , and the volume of gas in the chamber surrounding a sample (the void volume), V_g are both determined using the picnometer method discussed in section 4.3.2. The equation used in determining the volume is

$$V = P_{atm} \left(\frac{\Delta V_{capillary}}{\Delta P_{manometer}} \right). \quad (5.6)$$

The atmospheric pressure, P_{atm} , is measured with a mercury barometer located near the test rig. The barometer has a precision of 0.1 mm Hg, or 0.013% of standard atmospheric pressure. The 1.0 cc capillary tube used to measure the change in volume, $\Delta V_{capillary}$, due to a change in pressure, $\Delta P_{manometer}$, is graduated in steps of 0.01 cc. This gives an uncertainty in the volume measurement of 0.005 cc which is 0.8% and 2.5% of a typical full scale ΔV for determination of V_T and V_g respectively. The pressure measurement is made with the same water manometer describe above. A typical ΔP for these measurements gives a pressure uncertainty of 0.14%. The percent uncertainty in the volume can be determined as

$$\xi_{V_{T,g}} = \left[(\xi_{P_{atm}})^2 + (\xi_{\Delta V_{capillary}})^2 + (\xi_{\Delta P_{manometer}})^2 \right]^{1/2} \quad (5.7)$$

This gives a total uncertainty of 0.8% for V_T and 2.5% for V_g . However, a higher uncertainty is calculated from the standard deviations of the sets of measurements used in the volume determinations. Using equations 5.1 and 5.3 the average uncertainty in these measurements for V_T is 2.3% and for V_g is 3.2% (see Tables D.2 and F.2 in appendix D). In this research the uncertainty analysis for each test uses the ξ_{V_T} and ξ_{V_g} calculated from the set of measurements for that test.

This calculated uncertainty does not account for the error due to changing gaskets between the measurement of V_T and V_g , which in turn would cause an error in the determination of the volume of the foam sample. The magnitude of this error is the subject of the next discussion.

Experimental Determination of V_T Measurement Uncertainty

A series of volume measurements, of rig number P4 with 4 stainless steel spacers in the chamber, were made to check gasket effect on volume measurements. In this series, the chamber was sealed and six volume measurements were made, the chamber was then opened and sealed with a new gasket and six new volume measurements made. This procedure was repeated so that four sets of six volume measurements can be compared, see Table 5.1.

Indium Gasket	N_s	V_T [ml]	$(S_N / V_T)100$ [%]	N	Date
A-1	4	6.263	1.4	6	4-22-90
A-2	4	6.248	2.2	6	4-22-90
B-1	4	6.138	1.38	6	4-22-90
B-2	4	6.176	0.86	6	4-22-90

Table 5.1: Repeatability of Puck 4 Chamber Total Volume Measurements. The gaskets for this set of measurements were cut from two different flat indium discs, A or B. N_s = Number of spacers in the chamber. S_N = Standard deviation of the set of N measurements

During the volume measurements made for permeability tests, the gaskets used for both V_T and V_g measurements were not always cut from the same indium disk. Two

indium disks, disks A and B, were prepared (see section 4.1.2) and two gaskets were cut from each disk so that the effects of deviations in disk thicknesses could be observed. The average of all 12 volume measurements made with gaskets from disk A is 6.255 cc. The same average from disk B is 6.157 cc. The difference between these averages falls between the standard deviations of the measurements from disk A, 0.11 cc, and disk B, 0.071 cc. The standard deviation of all 24 measurements is 1.67% of the average volume. For these measurements the effect of different gaskets from the same disk is negligible. Measured volume with gaskets from different disks show a 1.6% difference.

Determination of V_g Measurement Uncertainty

Although it is possible that the effects of the gasket on V_g may be significant since the volume of gas around a sample in the chamber is smaller than the total volume, a similar set of measurements was not made for the measurement of V_g . The V_g measurements are listed in Table F.2 in appendix F. For foam sample 18A ξ_{V_g} is 1.78%.

Uncertainty in V_f

The uncertainty in the foam sample volume, $V_f = V_T - V_g$, is

$$\xi_{V_f} = \frac{\left[(V_T \xi_{V_T})^2 + (V_g \xi_{V_g})^2 \right]^{1/2}}{V_f} \quad (5.8)$$

This uncertainty is different for each foam sample tested, depending upon the chamber used, the number of spacers and the foam sample thickness and diameter. The uncertainty in foam volume for sample 18A is 5.2%

Another source of error in V_f occurs during the permeability test. If a large enough pressure step is introduced into the test chamber the foam can be temporarily compressed. Tests run in this research had small enough ΔP that no measurable deflection occurred.

5.1.4 Temperature

The accuracy of the temperature control is 0.03°C per manufacturer specifications and is used in the determination of the uncertainty of the pressure measurement in section 5.1.1. Temperature was measured to a precision of $\pm 0.5^{\circ}\text{C}$ with a K-type thermocouple that was placed in contact with the submerged test chamber. The error in temperature measurement is calculated at each temperature as

$$\xi_T = \frac{0.5}{T^{\circ}\text{C} + 273} 100 \quad (5.9)$$

giving values of 0.16%, 0.15% and 0.14% for 40°C , 60°C and 80°C respectively.

Temperature fluctuations due to addition of water to the water bath, low water levels and unpredictable power-outages add uncertainty to these measurements. During the tests the temperature was monitored by visual inspection, once a day for the long tests. No temperature/time history was recorded. If temperature transients were detected during the steep pressure transient ($\tau < 0.5$) then the test was aborted. However, if a temperature transient occurred when the chamber pressure was near its equilibrium value ($\tau > 0.5$) then the original test temperature was reestablished and the test continued until equilibrium. The temperature transient in these tests is noticeable in the \bar{P} vs. time plots of the data, the O_2 test at 36°C on sample 18A is an example of such a test (see figure F-57).

The measured temperature is used in some tests to determine the foam effective solubility coefficient at one temperature from that at another temperature. The uncertainty in temperature measurement is also a factor when extrapolating permeability test results to lower temperatures and when determining constants and exponents in the Arrhenius equation for aging predictions.

5.1.5 Sample Dimensions

All length and thickness measurements were made with a vernier with 0.001 in increments. The uncertainty due to the precision of the vernier is then 0.0013 cm.

Brehm [19] found the uncertainty in the diameter of a transient sorption test sample due to sample non-uniformity to be, $\epsilon_{davg.}=0.003$ cm, if the average of eight measurements is used. The uncertainty due to the epoxy sealant is approximately, ϵ_{ep} 0.004 cm. The total uncertainty is then

$$\epsilon_d = \left[4(\epsilon_{davg.})^2 + (\epsilon_{ep})^2 \right]^{1/2} = 0.006cm. \quad (5.10)$$

For sample 18A the percent uncertainty is, $\xi_d=(0.006/3.3)100=0.18\%$.

The same vernier was used to measure all samples used to determine foam density.

5.1.6 Density

The three densities that are important to this work are the densities of the foam, the solid polymer and the cell gas. The density of the cell gas, a variable in the calculation of the foam void fraction, is of course a function of the cell gas composition, which is in turn a function of time. If the initial cell gas pressure and the thermal history of the foam are known and the permeability of air and blowing agent have been measured then a determination of the partial pressures of the cell gases can be made. It is interesting to note the error induced by making an assumption at either extreme. At 25°C and one atmosphere the density of *CFC* - 11 is approximately 0.00606 g/cm³. Assuming the ideal gas law at a typical initial pressure of one half an atmosphere the density would be 0.00303 g/cm³. In a fully aged foam at the same temperature with one atm of air, the cell gas density would be 0.00185 g/cm³. For a 1.9 lb/ft³ foam this would result in a 3.9% change in density over the life of the foam, assuming that no substantial mass of blowing agent initially solved in the solid polymer.

The worst case scenario for the uncertainty in ρ_g is the absence of data for either

cell gas composition or manufacturing date and foam thermal history. In this case a guess between the initial and final gas densities would have a 70% uncertainty in gas density.

The average side of a cube of foam used in the foam density determinations was approximately 3.8 cm. This gives an uncertainty in the length measurement of 0.03%. The faces of the cubes were not perfect squares. The length of one face typically had a maximum deviation of approximately 1.0%. The uncertainty in the volume measurement can be expressed as

$$\xi_V \approx 3\xi_L = 3.0\% \quad (5.11)$$

Determination of sample weight was made on a Mettler H51AR balance with a precision of 0.01 mg. The mass of the measured samples ranged from 0.8 to 1.3 grams and therefore have uncertainties from 1.2E-3 to 0.8E-3%.

The uncertainty in the foam density measurement

$$\xi_{\rho_f} = [(\xi_V)^2 + (\xi_M)^2]^{1/2} = 3.0\% \quad (5.12)$$

reflects only the error in the measurement and not the possibility that the cube of foam is not truly representative of either the foam in bulk or the small sample used in the permeability measurements.

To accurately predict the aging of foams the foam density gradients facer to facer as well as the density of the permeability test sample need to be determined so that measured permeability can be adjusted to account for bulk foam properties.

Typical solid polymer densities are in the range of 69.9 to 73.7 lb/ft³ [11]. The densities of the solid polymer of the tested foams were not measured. A solid polymer density of 71.8lb/ft³ will be assumed with an uncertainty of 2.6%.

5.1.7 Average Distance Between Cell Walls

Error in the determination of $\langle l \rangle$, the average distance between cell walls, has three potential sources. Error in measurement from the resolution and accuracy of the scaling of

the S.E.M. photograph and the resolution of the scale used to measure the lengths. Error inherent in the process bias of the photographs may have due to picking unrepresentative samples, human error in counting intercepts, as well as errors due to the difficulties in establishing a perfect planar foam surface.

5.1.8 Cell Wall Thickness

The S.E.M. Manufacturer specifications give a resolution of $0.05\mu m$ at high magnification. With most cell wall measuring between 0.5 and $1.5\mu m$ this gives an uncertainty between 3 and 10%. However it is difficult to find a wall that looks perpendicular to the photo plane or to measure it's degree of perpendicularity. An angle greater than 5.7 degrees from the photo plane will give an error greater than 10%. If a wall is found and a good image can be achieved on the screen and the wall has not begun to waver due to charging it is difficult, if not some times impossible, to tell how close to the wall section is to the strut behind it. If the plane of the wall cut is through a section still tapering down from the strut the measurement will exaggerate the average wall thickness.

5.2 Uncertainty in Permeability Test Results

The uncertainties in this section will be calculated from analysis of test results based on the effective concentration gradient, C_{eff} as the driving potential. This will facilitate comparison with uncertainties calculated by Brehm [19].

Permeability is defined as the product of the diffusion and solubility coefficients, which are determined separately. The error in the foam effective permeability is then

$$\xi_{P_{eff}} = \left[(\xi_{D_{eff}})^2 + (\xi_{S_{eff}})^2 \right]^{1/2} \quad (5.13)$$

In the next sections the determination of $\xi_{D_{eff}}$, $\xi_{S_{eff}}$ will be detailed.

5.2.1 Effective Diffusion Coefficient

The effective diffusion coefficient is determined from the slope, m , of the best fit line on a plot of test time versus the characteristic time constant, τ_{eff} . From equation 3.27 ($D_{eff} = mL_{eff}^2$), $\xi_{D_{eff}}$ will be determined as a function of $\xi_{L_{eff}}$ and ξ_m .

Effective Diffusion Length

The effective diffusion length is determined from the foam sample volume and diameter as, $L_{eff} = V_f/(2\pi d^2)$, so the uncertainty is

$$\xi_{L_{eff}} = \left[(\xi_{V_f})^2 + 4(\xi_d)^2 \right]^{1/2} \quad (5.14)$$

From the previously calculated uncertainties in sample 18A the uncertainty in the effective diffusion length is 5.2%.

Slope of Best Fit Line

The slope of the best fit line is a function of both τ_{eff} and time, t . The uncertainty in time has been established at less than 1.1%. The uncertainty in τ_{eff} , on the order of 10%, calculated analytically (later in this section), is large enough to validate the assumption that the uncertainty in the slope, m , can be approximated as a function of the uncertainty in τ_{eff} only. Errors in m are proportional to the errors in the points used in it's calculation and inversely proportional to the total number of points. First the standard deviation of τ is calculated from all of the points in the best fit range. This is then used as a weighing factor for the standard deviation of m .

The method described by Beers [27] to develop an expression for the root mean squared deviation of one variable (in our case tau) around the slope of the best fit is as follows. The standard deviation of the values of τ about the best fit line is defined as

$$S_\tau = \left[\frac{\sum (\delta\tau_n)^2}{N - 2} \right]^{1/2} \quad (5.15)$$

Where $\delta\tau_n$ is the difference between the point, τ_n , and its corresponding value, τ_o , on the best fit line, and N is the number of matched points used to determine the best fit line.

The standard deviation of m is found by taking the root sum squared of the contribution of each match point. The contribution of one point is found and summing over all j from 1 to N the population standard deviation of m , S_m , is

$$S_m = S_r \left[\frac{N}{N \sum t_n^2 - (\sum t_n)^2} \right]^{1/2} \quad (5.16)$$

An expression for ξ_m based on the above equations and equations 5.1 and 5.3 for the determination of slope from one set of test data is

$$\xi_m = \frac{t_s}{N^{1/2}m} \left[\frac{\sum (\delta\tau_n)^2}{N-2} \right]^{1/2} \left[\frac{N}{N \sum \tau^2 - (\sum \tau)^2} \right]^{1/2}. \quad (5.17)$$

The first bracketed term on the right hand side gives the uncertainty in the data relative to the best fit line. The second term scales the uncertainty as a function of N , the number of data points in best fit range, and the distribution of those points.

The uncertainty in the slope of the best fit line decreases with increasing number of points in the best fit range. For tests in this research the number of points ranged from about 10 to 300 depending on test gas, temperature and final value of τ . These values are included in the summary of test values for each test in Appendix F. For foam 18's CO₂ test at 80°C with 129 points in the best fit range and a ΔP of 1.51 psi, ξ_m is 0.6%. The ξ_m for the same foam tested with HCFC-141b at 80°C with 49 points in the best fit range and a ΔP of 1.57 psi is 1.2%.

Uncertainty in effective diffusion coefficient, D_{eff}

Now the uncertainty in D_{eff} can be determined as

$$\xi_{D_{eff}} = \left[4 \left(\xi_{L_{eff}} \right)^2 + \left(\xi_m \right)^2 \right]^{1/2}. \quad (5.18)$$

Again for foam 18, $\xi_{D,ff}$ for CO₂ at 80°C is 10.4% and for HCFC-141b at 80°C is 10.6%. Note that in the determination of $\xi_{D,ff}$, the contribution of ξ_m is negligible compared to $\xi_{L,ff}$.

Uncertainty in τ

The uncertainty in τ varies over the duration of a test. An estimate of the magnitude of ξ_τ is useful in understanding the impact of the choice of the range for the best fit line for t vs. τ in the uncertainty in the test results. The expression for the error in τ can be found as a function of the uncertainty in the measured dimensionless pressure. The analytical solution to the tests transient pressure, equation 3.47 is repeated here.

$$\bar{P} = \frac{1}{G+1} + \sum_{n=0}^{\infty} \frac{2G}{G(G+1) + \alpha_n^2} \exp(-\alpha_n^2 \tau) \quad (5.19)$$

The uncertainty in \bar{P} , ξ_P , is then

$$\xi_P = \left[\left(\frac{G}{\bar{P}} \frac{\partial \bar{P}}{\partial G} \xi_G \right)^2 + \left(\frac{\tau}{\bar{P}} \frac{\partial \bar{P}}{\partial \tau} \xi_\tau \right)^2 \right]^{1/2} \quad (5.20)$$

To find ξ_τ invert the above and write the uncertainty in G as a function of \bar{P} . To do this for tests run to equilibrium take equation 3.33 and find ξ_G

$$\xi_G = R_d \frac{G+1}{G} \xi_P \quad (5.21)$$

where R_d , the ratio of equilibrium pressure if the sample is deformed by the initial pressure step to the equilibrium pressure with no sample deformation, for all tests in this research is unity. So finally

$$\xi_\tau = \frac{\xi_P}{\tau} \left(\frac{\partial \bar{P}}{\partial \tau} \right)^{-1} \left[\bar{P}^2 + \left(R_d (G+1) \frac{\partial \bar{P}}{\partial G} \right)^2 \right]^{1/2} \quad (5.22)$$

where

$$\frac{\partial \bar{P}}{\partial \tau} = \sum \frac{-2G\alpha_n^2}{G(G+1) + \alpha_n^2} \exp -\alpha_n^2 \tau \quad (5.23)$$

and

$$\frac{\partial \bar{P}}{\partial G} = \frac{-1}{(G+1)^2} + \sum \frac{2(\alpha_n^2 - G^2)}{[G(G+1) + \alpha_n^2]^2} \exp -\alpha_n^2 \tau. \quad (5.24)$$

Dimensionless Pressure

The uncertainty in the pressure measurement is defined in terms of the full scale pressure excursion, so the expression for the uncertainty in dimensionless pressure

$$\bar{P}(t) = \frac{P(t) - P_1}{P_2 - P_1} = \frac{\Delta P(t)}{\Delta P} \quad (5.25)$$

is derived from consideration of the ΔP 's. The three pressures in the above expression can be considered independent variables. In this case both the uncertainty in $\Delta P(t)$ and ΔP are equal to the uncertainty in the pressure measurement, ξ_P . On the other hand when calculating $\xi_{P(t)}$ the uncertainties in the ΔP 's can be considered not totally independent. In this case a correlation coefficient, π_P , (see Beers [27]) defining the level of independence must be defined and the expression for $\xi_{P(t)}$ is

$$\xi_{P(t)} = \xi_P \left[\left(\frac{\Delta P}{\bar{P}(t)} \frac{\partial \bar{P}(t)}{\partial \Delta P} \right)^2 + \left(\frac{\Delta P(t)}{\bar{P}(t)} \frac{\partial \bar{P}(t)}{\partial \Delta P(t)} \right)^2 + \left(2\pi_P \frac{\Delta P \Delta P(t)}{\bar{P}(t)} \frac{\partial \bar{P}(t)}{\partial \Delta P} \frac{\partial \bar{P}(t)}{\partial \Delta P(t)} \right) \right]^{1/2}. \quad (5.26)$$

In the limit of totally correlated errors, π_P is unity. The resulting uncertainty assuming totally correlated errors is

$$\xi_{P(t)} = 2\xi_P \quad (5.27)$$

which is still a function of ΔP and varies with the transducer used.

Now ξ_τ can be determined. Figure 5-1 illustrates the effects of test time and equilibrium sorption parameter on the error in τ . This figure indicates that a best fit

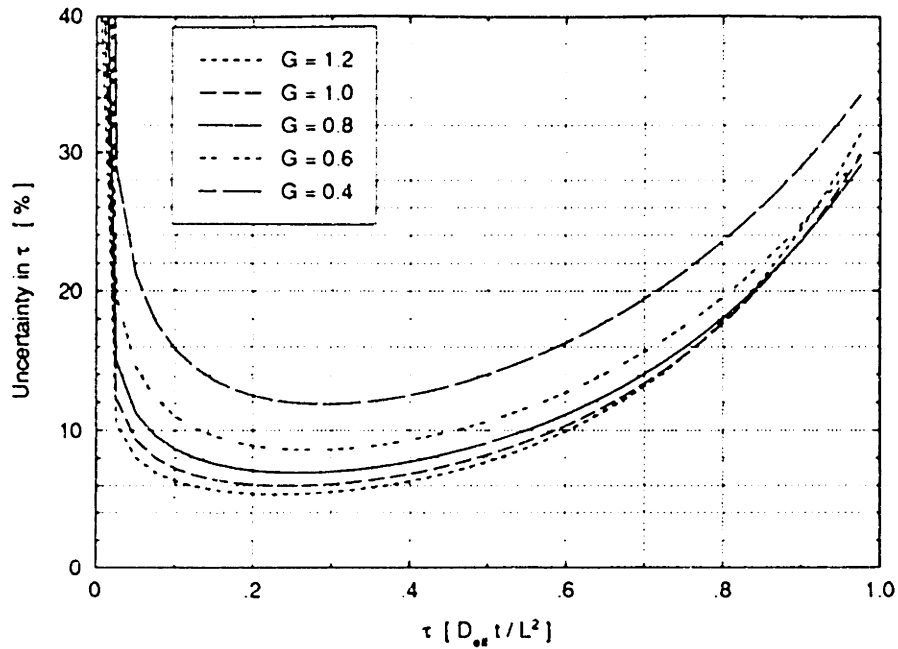


Figure 5-1: Uncertainty in τ as a Function of τ and G for $\xi_p = 1.0$.

range between $\tau = 0.1$ and $\tau = 0.4$ will minimize the uncertainty in the analysis. Since G is proportional to the sample volume to chamber volume ratio, this figure also emphasizes the importance of maximizing V_f/V_g to minimize uncertainty in the test results.

5.2.2 Solubility

The two methods used to determine S_{eff} and S_p generate different uncertainties. These methods, described in section 3.2.2, involve either calculating the solubility of the foam from a test's final equilibrium pressure or from extrapolation of results from one temperature to another.

Tests Run to Equilibrium

If a test is run to large values of τ ($\tau \geq 1.0$) then G is calculated from \bar{P}_∞ , equation 3.33, so ξ_G is calculated as in equation 5.21. The foam solubility is calculated as

$$K_{eff} = G \left(\frac{V_g}{V_f} \right), \quad (5.28)$$

therefore the uncertainty in the foam effective solubility ratio,

$$\xi_{K_{eff}} = \left[\xi_G^2 + \xi_{V_g}^2 + \xi_{V_f}^2 \right]^{1/2}, \quad (5.29)$$

for foam 18 tested with CO_2 at $80^\circ C$ is 6%.

The uncertainty in the calculation of the solubility of the solid polymer is a function of the uncertainties in the foam and solid polymer solubility ratios. From its' definition in equation 3.8, the uncertainty in S_g is equal to the uncertainty in temperature. From the definition of K_{eff} in equation 3.16, $\xi_{S_{eff}}$ is calculated

$$\xi_{S_{eff}} = \left[\xi_{K_{eff}}^2 + \xi_T^2 \right]^{1/2}. \quad (5.30)$$

So

$$\xi_{S_{eff}} \approx \xi_{K_{eff}} \quad (5.31)$$

since ξ_T (0.14% at $80^\circ C$) is negligible compared to $\xi_{K_{eff}}$. From another form of equation 3.16, $\xi_{K_{sp}}$ can be calculated

$$\xi_{K_{sp}} = \left(\frac{1}{K_{eff} - \delta} \right) \left[K_{eff}^2 \xi_{K_{eff}}^2 + \delta^2 \left(\frac{K_{eff} - 1}{1 - \delta} \right)^2 \xi_\delta^2 \right]^{1/2} \quad (5.32)$$

The uncertainty in δ is

$$\xi_\delta = \left[\left(\frac{\rho_f}{\rho_f - \rho_{sp}} \xi_{\rho_f} \right)^2 + \left(\left(\frac{\rho_{sp}}{\rho_g - \rho_{sp}} - \frac{\rho_{sp}}{\rho_f - \rho_{sp}} \right) \xi_{\rho_{sp}} \right)^2 + \left(\frac{\rho_g}{\rho_g - \rho_{sp}} \xi_{\rho_g} \right)^2 \right]^{1/2} \quad (5.33)$$

The uncertainty in calculated void fraction is approximately 0.2% for all foams. Now $\xi_{K,p}$ can be calculated for CO₂ at 80°C in foam 18; $\xi_{K,p} = 24\%$.

The uncertainty in the calculated solid polymer solubility is calculated as

$$\xi_{S,p} = [\xi_{K,p}^2 + \xi_T^2]^{1/2}, \quad (5.34)$$

however, compared to $\xi_{K,p}$, ξ_T is negligible, so $\xi_{S,p} \approx \xi_{K,p}$

Short Tests

If the solubilities determined at one temperature are extrapolated to another temperature, then uncertainties propagate in the opposite direction from those previously described, ultimately affecting the uncertainties in G. Since in this case the determination of G is by the relationship,

$$G = \frac{V_f}{V_g} K_{eff} \quad (5.35)$$

the uncertainty in G is a function of K_{eff} . This foam solubility ratio is determined from the value of K_{sp} at temperature T which is a function of the extrapolated value of S_{sp} .

When the solubility of the solid polymer has been determined at one temperature, $S_{sp}(T_o)$, the solubility at another temperature, $S_{sp}(T)$, is approximated using Van Krevlen's estimations of the heat of solution in the Clausius-Clapeyron equation shown in equation 3.61. The resulting uncertainty in $S_{sp}(T)$ is

$$\xi_{S,p}(T) = \left[\xi_{S,p}(T_o)^2 + \left(\frac{\Delta H}{R} \right)^2 \left[\left(\frac{1}{T} \right)^2 + \left(\frac{1}{T_o} \right)^2 \right] \xi_T^2 + \left[\left(\frac{1}{T_o} - \frac{1}{T} \right) \xi_{\Delta H} \right]^2 \right]^{1/2}. \quad (5.36)$$

Due to the large $\xi_{S,p}(T_o)$, the ξ_T term is insignificant. The contribution of the ξ_T term is largest for the largest values of $(\Delta H/R)^2$. Within the range of test temperatures it's maximum contribution to the sum of the squares of the $\xi_{S,p}(T_o)$, ξ_T and $\xi_{\Delta H}$ terms is 0.5% (remember, $\xi_{S,p}(T_o)$ is on the order of 24%).

The values of ΔH used to determine the temperature dependence of solubility of

the gases in the solid polymer, described in section 3.2.2, are only first approximations. The application of these approximations to foam polymers requires the assumptions that the polymer is below its glass transition temperature and that the approximation is valid for crosslinked polymers. This makes $\xi_{\Delta H}$ difficult to determine. However, the limit at which it becomes significant can be determined. The impact of uncertainty in ΔH on $\xi_{S_p(T)}$ is greatest for high values of $\Delta H/R$, i.e. for blowing agents. If $\xi_{S_p(T_0)}$ for HCFC-123 is 24%, and if $\xi_{\Delta H}=18\%$ then $\xi_{S_p(T_0)}$ would be 1% greater than $\xi_{S_p(T)}$. For air components, this 1% increase in $\xi_{S_p(T_0)}$ over $\xi_{S_p(T)}$ would occur for values of $\xi_{\Delta H}$ greater than 100%. Therefore for air components at least it may be safe to assume that the $\xi_{\Delta H}$ term is insignificant. So for the air components

$$\xi_{S_p(T)} \approx \xi_{S_p(T_0)}. \quad (5.37)$$

From the left hand side of equation 3.61, ξ_{S_p} is then used in the determination of ξ_{K_p}

$$\xi_{K_p(T)} = \left[(\xi_{K_p(T_0)})^2 + (\xi_{S_p(T_0)})^2 + (\xi_{S_p(T)})^2 \right]^{1/2}. \quad (5.38)$$

Equation 3.58 is the basis for the determination of $\xi_{K_{eff}}$.

$$\xi_{K_{eff}} = \frac{1}{K_{eff}} \left[(K_{sp}(1-\delta)\xi_{K_{sp}})^2 + (\delta(1-K_{sp})\xi_{\delta})^2 \right]^{1/2} \quad (5.39)$$

The value for $\xi_{K_{eff}}$, determined for foam 18 tested with HCFC - 123, calculated for 40°C from tests at 80°C is 23.6%. The resulting uncertainty in G is calculated as

$$\xi_G = \left[\xi_{V_g}^2 + \xi_{V_f}^2 + \xi_{K_{eff}}^2 \right]^{1/2} \quad (5.40)$$

For foam 18 tested with HCFC-123 at 40°C the uncertainty in the calculated value of G is 23.9%.

5.2.3 Permeability

The uncertainty in the effective permeability measurements are found for each test as

$$\xi_{P_{eff}} = \left[(\xi_{D_{eff}})^2 + (\xi_{S_{eff}})^2 \right]^{1/2}. \quad (5.41)$$

As shown above this calculation will be different for each test as a function of foam properties, sample dimensions, test gas, test temperature and whether the test has been run to equilibrium or not. The uncertainty in the permeability coefficient calculated in this manner for the test used throughout the above analysis, foam 18 tested with CO₂ at 80°C, is 12.1%.

Blank Page

Chapter 6

Results and Discussion

Tests were run on seven foams provided by the Mobay Chemical Company. Table 6.1 contains a description of these foams and a summary of the test results. Individual constant-volume transient sorption test data are presented in reduced form in appendix F. The seven foams tested are from four different solid polymer chemistries. Three of these foams have the same base polymer chemistry but were blown with different refrigerants. A different base polymer chemistry is shared by two other foams, one blown with HCFC-123 the other with HCFC-141b. Of the two remaining foams one has an industry standard chemistry blown with CFC-11, the other has a different base polymer chemistries blown with HCFC-123.

The composition of the group of foams tested allows a comparison between the effects of polymer chemistry and blowing agent on foam structure and solid polymer diffusivity. The product of the foam density and the percent of solid polymer in the cell walls characterizes the aspect of foam structure that affect foam aging. Weighing each foam for the differences in this product allows a comparison of the diffusivity of the solid polymer. This comparison is used to examine the set of CO₂ tests that was run on each of the seven foams.

The magnitudes and temperature dependence of the blowing agent diffusion coefficients will be compared. Results of the diffusion coefficient test will be used in an

Sample Number		1	2	14	15	16	17	18
Test Gas	Temp. [°C]	$D_{eff} \left[10^{-8} \frac{cm^3_{STP}}{cm \ sec \ atm} \right]$						
CO ₂	40	1326	1343	1875	3567	361.1	1470	(828)
	60	1908	2389	-	5349	159.6	(2190)	1880
	80	3256	(3678)	(3810)	7937	718.9	1900	2489
O ₂	40	234	-	-	-	16.9	168.2	(201)
	60	(396)	-	-	-	89.7	533.9	(400)
	80	2051	1139	2549	-	-	748.6	(724)
N ₂	40	-	-	-	-	-	-	34.16
	60	-	-	-	-	-	-	64.98
	80	-	609	-	-	-	-	282.1
CFC-11	40	-	-	-	-	-	-	-
	60	-	-	-	-	-	-	-
	80	-	76	36.4	-	-	-	6.3
HCFC-123	40	-	-	-	-	0.416	2.26	4.26
	60	-	-	-	-	0.768	1.51	-
	80	-	-	-	-	2.68	-	8.57
HCFC-141b	40	-	-	-	-	-	-	-
	60	-	-	-	-	-	-	3.5
	80	-	-	-	-	-	-	13.5
Isocyanate		MDI	MDI	MDI	MDI	MR200	MR	MR
† Polyol Base		A	S	S	S	S - PS	T	T
Blowing Agent		CFC-11	CFC-11	HCFC-141b	HCFC-123	HCFC-123	HCFC-123	HCFC-141b
ρ_f [lb/ft ³]		1.92	1.98	1.8	1.67	2.02	1.88	1.76
δ		0.978	0.978	0.98	0.982	0.977	0.979	0.981
$\langle l \rangle$ [μm]		342	314	417	500	145	166	235
	⊥	190	221	283	266	136	190	215
t_{cw} [μm]		0.45	0.51	1.23	0.47	0.77	0.56	0.75
P_{cw} [%]		16.3	16.2	33.3	14.1	41.0	23.8	28.7

() Values are interpolated or average values.

† Polyol chemistry: A = Aromatic Amine-Sucrose; S = Sucrose; S - PS = Stepan PS2852; T = Terate 203-Multranol 9171.

⊥ = Perpendicular facer; || = Parallel facer.

Table 6.1: Summary of Test Results and Foam Characteristics.

aging model to compare predicted aging with measured aging of full thickness samples.

The diffusion of gases is considered to be a thermally activated process. As discussed in section 3.2.2 it can be expressed by the following Arrhenius-type equation

$$D_{eff} = D_o \exp \left\{ -\frac{E_d}{R} \frac{1}{T} \right\}, \quad (6.1)$$

where D_o is a constant that scales the magnitude of the diffusion coefficient, E_d is the activation energy for diffusion and R is the specific gas constant. If the effective diffusion coefficient of a gas in a foam is measured at different temperatures, D_o and E_d/R can be evaluated. Values at other temperatures can then be calculated

$$D_{eff}(T) = D_{eff}(T_1) \exp \left\{ \left(\frac{E_d}{R} \right) \left(\frac{1}{T_1} - \frac{1}{T} \right) \right\}. \quad (6.2)$$

On a plot of $\log(D_{eff})$ vs. $1/T$, the equation for the best fit line is

$$\log(D_{eff}) = -m \frac{1}{T} + \log(D_o). \quad (6.3)$$

The slope of the best fit line, m , is proportional to E_d/R . Comparing the slopes of the best fit lines on these graphs is, in effect, comparing the temperature dependency. It has been noted in previous research [13] that there appears to be a constant ratio between diffusion coefficients of air components at a given temperature and that the slope of the best fit line for a gas is approximately the same, independent of the foam tested. This implies that there is a constant ratio between the slopes of these best fit lines for different gases. If this were found to be true for all foams then the number of tests could be limited to only a "fast" gas, CO_2 or O_2 at a high temperature, thereby significantly reducing total test times per sample. This observation will be discussed in light of the test results.

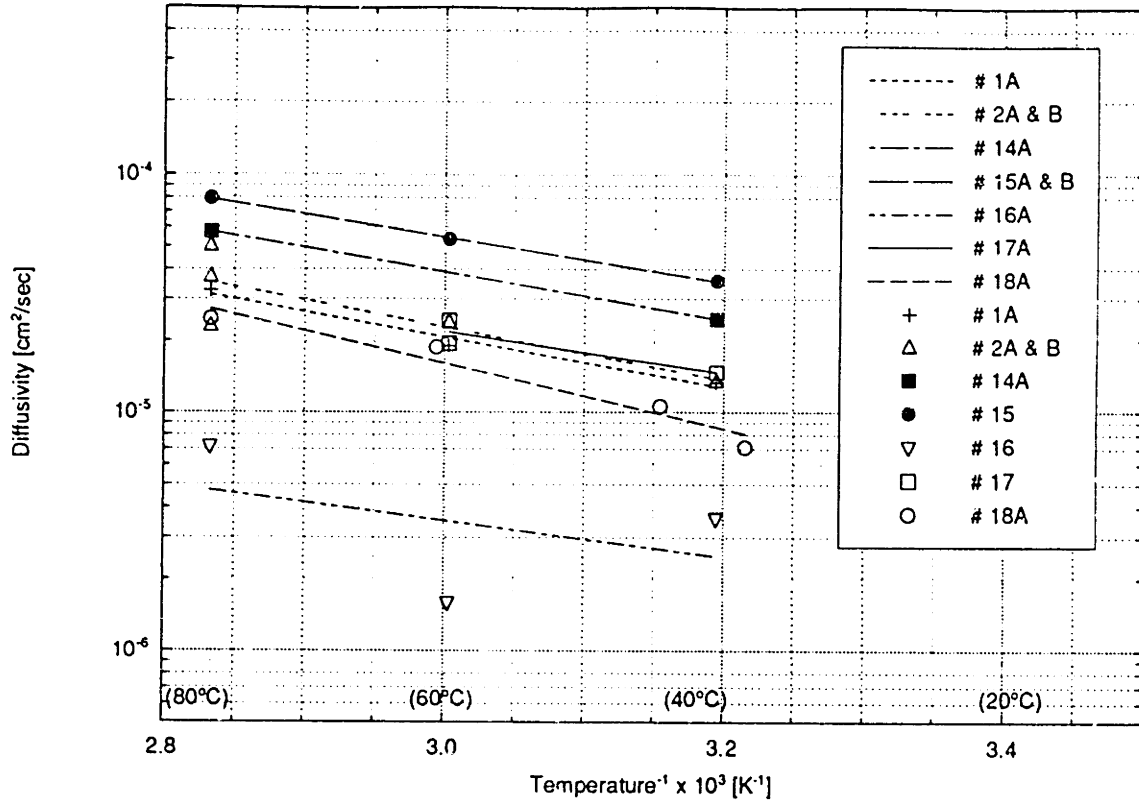


Figure 6-1: $\text{Log}(D_{eff})$ vs. $1/T$ Plot for Test Results All Foams, CO_2 Test Gas. Symbols = Data Points, Dashed Lines = Best Fit for Data.

6.1 Test Results for Air Components.

There is a similarity in temperature dependence (slope) of CO_2 diffusion coefficients that can be seen in Figure 6.1, a plot of $\text{log}(D_{eff})$ vs. $1/T$ for CO_2 test results for all seven foams. This is also in agreement with test results from research by Brehm [19] and Ostrogorsky [13]¹. E_d/R for CO_2 and O_2 for all of the foams tested in this research as well as those from Brehm and Ostrogorsky are listed in Table 6.2. The slight difference in slopes suggests that the activation energy for diffusion, E_d , is lightly dependent on the

¹Both of these results were from MDI foams. Foam densities were 1.57 lb/ft^3 [19] and 2.10 lb/ft^3 [13]

Foam	1	2	14	15	16	17	18	$B_{D_{eff}}$	$B_{P_{eff}}$	$O_{P_{eff}}$
Gas	E_d/R [K]									
			2051				† 3783 ‡ 3453		†2811	
CO ₂	2470	2605	2331	2207	1771	† 2046	3189	3181	*3532	4172
O ₂	† 2892	-	-	-	8698	4164	3347	4295	*3753	*2907
										4078

$B_{D_{eff}}$ = Brehm, E_D/R , Transient-Sorption Test.

$B_{P_{eff}}$ = Brehm, E_P/R , (†) = Transient-Sorption Test; (*) = Steady State Test [19].

$O_{P_{eff}}$ = Ostrogorsky [13], E_P/R , Steady State Test.

† excluding data at 80°C.

‡ Results from tests by Holometrix in "Permalizer".

Table 6.2: E_D/R , for CO₂ and O₂, Derived from Test Data.

polymer chemistry. With the exception of Foam 16, the slopes of O₂ are also similar, as shown in Table 6.2.

The ratio of CO₂ to O₂ diffusion coefficients at 80°C for the tested foams are between 4.6 and 2.3, as shown in Table 6.3. The ratio of CO₂ to N₂ was found in previous research to be approximately an order of magnitude higher (see Table 6.3). The results of tests with N₂ in this research are inconclusive in support of previous results.

The similarity of slopes and the ratio of the magnitudes would lend confidence in an order of magnitude estimate of short term aging, due to CO₂ and O₂ diffusion, based on CO₂ measurements and O₂ approximations. If this similarity holds for the blowing agents then tests of CO₂ permeability could also be used to estimate long term aging. This will be discussed in section 6.4.

Although the slopes are similar the magnitudes of the CO₂ diffusion coefficients vary not only from foam to foam but also for different samples of the same foam. To explain this variation, the properties that effect mass transfer in the foam were examined. They can be divided in two categories; foam macro structure and polymer chemistry. It

Foam		1	2	14	16	17	18	(1) $B_{D_{eff}}$	(2) $B_{P_{eff}}$	(3) $O_{P_{eff}}$
Gases	T [°C]	Effective Diffusion Coefficient Ratios								
$\frac{CO_2}{O_2}$	80		3.2					2.9	(t) 2.9	
	60	4.2	-	2.3	3.9	4.6	3.8	3.6	(s) 4.5	5.6
$\frac{CO_2}{N_2}$	80	-	6.0	-	-	-	8.8	28.8	(t) 27.9	23.6
	60						17.8	28.5	(s) 31.4	

(1) Brehm D_{eff} .

(2) Brehm P_{eff} . (t) = Transient-Sorption Test; (s) = Steady State Test [19].

(3) Ostrogorsky P_{eff} . Steady State Test [13].

Table 6.3: Air Component Effective Diffusion Coefficient Ratios.

has been shown that foam effective diffusivity is inversely proportional to two structural parameters; the foam density, and the percent of solid polymer and directly proportional to the diffusivity of the solid polymer [13, 16].

$$D_{eff} \propto \frac{D_{sp}}{\rho_f P_{cw}} \quad (6.4)$$

In different samples from the same foam there is a variation in the magnitude of the measured diffusion coefficients. The differences in foam density from sample to sample can partially explain this difference, even if the assumption is made that the diffusivity of the solid polymer and the percent of material in the cell walls is constant throughout the foam. Density differences as large as 11% have been measured in 3 inch diameter cores through 2 inch thick board stock. Although it is probable that P_{cw} varies throughout the foam, an explanation of the variation in foam effective diffusion coefficient due only to density differences may be useful. Results from foam 18 illustrate this point.

Tests were run on three different samples of foam 18. Two of these tests were run by Peggy Foreman at Holometrix in Cambridge, MA in a "Permalizer", a version of the apparatus used in this research under development for commercialization by Holometrix.

There is an 11% difference in D_{eff} at 80°C for these samples both taken from the same foam core. If one sample were taken from near the facer and the other from the lower density center then an 11% density gradient could be accountable. The Holometrix core was taken from the same board as the M.I.T. tested sample. The maximum difference in diffusion coefficient between the sample tested at M.I.T. and Holometrix is 20%. It is unlikely that density gradient alone is the source of the difference. Experimental apparatus variation, average core density are other possible sources.

6.2 Percent of Solid Polymer in Cell Wall, P_{cw}

The percent of material in the cell walls, as defined in equation 2.4, is proportional to the foam density and the ratio of cell wall thickness to the cell surface area/volume ratio. The greater percent of material in the cell walls the greater the resistance to mass transfer. Results from this research indicate that the percent of solid polymer in the cell walls for foams blown with the alternates was higher than that for foams blown with CFC - 11. This trend has been evident not only in the seven foams listed in table 6.1 but also at other foams measured at M.I.T. described in table 6.2. Samples of five foams, of the same polymer chemistry with different blowing agents, were provided by Dr. D.L. McElroy of the Oak Ridge National Laboratory as part of the Joint Government-Industry Research Project. The Igloo will be discussed in section 6.5.2

The P_{cw} for CFC-11 blown foams is 15-20% [16] where the P_{cw} for foams blown with the HCFC's is generally higher, as shown in Figure 6-2. For all chemistries, HCFC-141b blown foams appear to have approximately 50% higher concentration of solid polymer in the cell walls than CFC-11 blown foams. For HCFC-123 blown foams, P_{cw} seems to be more chemistry dependent. There also seems to be an increase in P_{cw} with decreased cell size, with the exception of foam 14.

In the calculations for the presented results, cell wall thickness is based on two SEM cell wall photographs per foam. The photographs and measurements for foams in

Sample Number	21	23	25	27	28	Igloo*	A**
Isocyanate	MDI	MDI	MDI	MDI	MDI	-	MDI
Polyol Base	†	†	†	†	†	-	-
Blowing Agent	CFC-11	HCFC-123	HCFC-141b	HCFC-(50/50) ‡	HCFC-(65/35) ‡	CFC-11	CFC-11
‡ ρ_f [lb/ft ³]	1.92	1.80	1.84	1.87	1.9	4.93	1.77
δ	0.977	0.978	0.978	0.977	0.977	0.936	0.979
$\langle l \rangle$ [μm]		238	196	247	-	-	-
	⊥	162	150	160	149	141	150
t_{cw} [μm]	0.38	0.4	0.5	0.53	0.01	0.55	0.37
P_{cw} [%]	16.5	29.5	36.5	33.8	8.5	12	10

*Igloo sample supplied by Dr. R. Weidemann of Bayer AG.

**A= Foam Measured by Ostrogorsky.

† Polymer chemistry from Joint Government-Industry Research Project described in reference [28].

‡ HCFC-123/HCFC-141b blends

Table 6.4: Characteristics of Foams: O.R.N.L, Bayer Igloo, and Ostrogorsky

this research are in appendices B and C. The thickness of cell walls in a one cm^2 sample of a foam varies by as much as a factor of three (0.5-1.5 μm). In an initial attempt to determine if the variation in wall thickness could be explained by a relationship between wall thickness and adjacent foam cell dimensions, five cell wall thicknesses and their lengths were measured in two samples of different foams. The results, presented in Table 6.5, although not conclusive indicate a trend for the shorter walls to be thicker.

This variation in cell wall thickness produces uncertainty in the calculated P_{cw} . This uncertainty may also be due to measurement error, as discussed in section 5.1.8. The cell wall thickness in the calculation of P_{cw} used in the comparison of foams and their aging predictions should represent the distribution of average foam cell characteristics. The calculations for this work are based on averages of all measurements. To accurately predict aging characteristics of foam boards from measurements on thin samples taken from the center of the board, the thin sample test results must be weighed for any deviation from foam average properties. Determining methods of quantifying effects of density gradients, cell size distribution and cell wall thickness distribution will be the

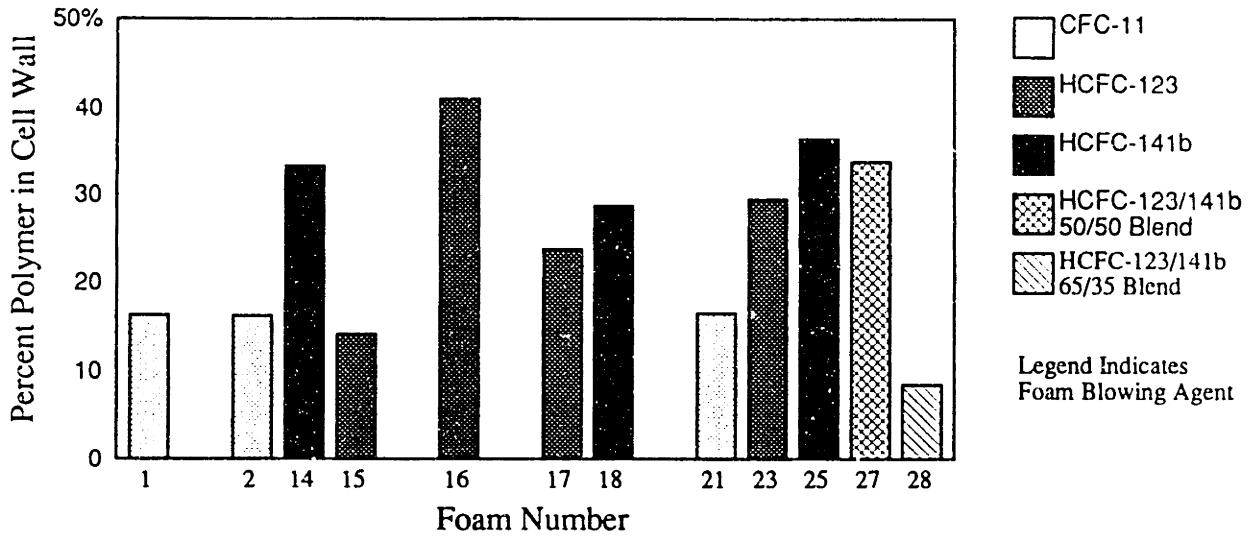


Figure 6-2: A comparison of P_{cw} . Bars are grouped by solid polymer chemistry.

subject of future work.

If two foams have the same solid polymer the foam with the higher P_{cw} should have a lower foam diffusion coefficient. Differences in solid polymer diffusivity will be the focus of the next section.

6.3 Solid Polymer Diffusion Coefficients, D_{sp}

Using the proportionality between D_{eff} , D_{sp} , ρ_f and P_{cw} from equation 6.4, we define a hypothetical foam that has the same solid polymer diffusivity, D_{sp} , as the test foam and foam structural parameters, $\hat{\rho}_f$ and \hat{P}_{cw} , so

$$\hat{D} = D_{eff} \frac{\rho_f P_{cw}}{\hat{\rho}_f \hat{P}_{cw}}. \quad (6.5)$$

A comparison of solid polymer diffusivities can be made by comparing the normalized diffusion coefficients, \hat{D} . The test foams were all normalized around a hypothetical foam with $\hat{\rho}_f = 1.9 \text{ lb/ft}^3$ and $\hat{P}_{cw} = 20\%$. A chart of the resulting \hat{D} and associated

Cell Wall			
Foam 16		Foam 18	
t_{cw}	l_{cw}	t_{cw}	l_{cw}
0.32	-	0.67	-
0.72	-	1.0	-
1.22	75	1.37	20
1.08	75	0.62	100
0.52	100	0.71	100
0.87	200	0.64	125
0.66	210	0.22	220

Table 6.5: Cell Wall Thickness, t_{cw} [μm] and Corresponding Cell Wall Length, l_{cw} [μm] for Foams 16 and 18.

D_{eff} for CO₂ at 80°C is shown in Figure 6-3. In this figure, to compare the magnitude of the crosshatched bars is to compare the solid polymer diffusion coefficients.

Two foams blown with CFC-11, foams 1 and 2, have the same isocyanate but different polyol. They are close in P_{cw} but foam 2 has a slightly higher density. In spite of this foam 1 has a lower D_{eff} . This would indicate that CFC-11 blown foams with aromatic amine polyols (foam 1) should have better k-factor retention than those based on the sucrose chemistry (foam 2). These results are in agreement with the work at Bayer AG by Wiedermann [29]. Figure 6-3 would seem to indicate that differences in D_{sp} is responsible.

Both alternate blowing agents appear to have a strong tendency to increase the diffusivity of MDI-Sucrose based foams. The measurements also indicate that HCFC-141b has stronger impact on the increase in D_{sp} than HCFC-123.

Foams 16, 17 and 18 all have structural properties that decrease their D_{eff} compared to the normalized values, but the low magnitudes, compared to the other foams tested, appears to be due to polymer chemistry. From the relative magnitudes of the diffusion coefficients of CO₂ at 80°C, the aging rates of these three foams would be: 16 < 17 < 18. In a series of studies by Baumann and Szabat [30] the thermal conductivity drift of these foams was measured. The results are presented in terms of percent change in thermal conductivity. The thickness of the foam samples tested varied from foam to

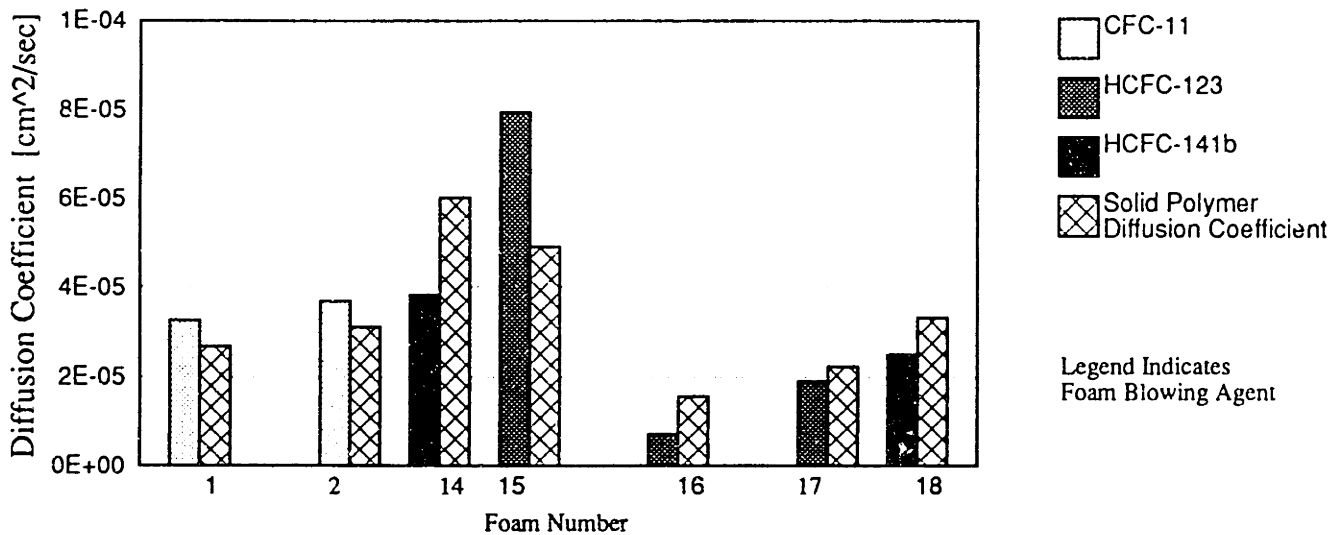


Figure 6-3: Comparison of CO₂ Solid Polymer Diffusivities at 80 °C. Measured Diffusion coefficients vs. Normalized Diffusion Coefficients.

foam. However, when the effects of the different thicknesses are included, the results of their 70°C aging is in agreement with the relative order of magnitude of the diffusion coefficients measurements.

6.4 Test Results: Blowing Agents

All results of tests with blowing agents as the test gas are plotted in Figure 6-4. The average ratios of CO₂/O₂ diffusion coefficient for the tested foams were found to be similar. The ratios of CO₂/blowing agents at 80°C are not of the same order of magnitude. This can be seen in Table 6.6. The ratio of CO₂/blowing agent diffusion coefficients and the values determined for E_d/R are not consistent enough to enable accurate estimation of aging characteristics from CO₂ results.

The uncertainty in the blowing agent data is higher than that of the CO₂ data in part due to the computation of solid polymer solubility at the test temperature from tests at higher temperatures. The uncertainty in the blowing agent data may be even higher than the analytical error analysis would indicate. The uncertainty of the measurements

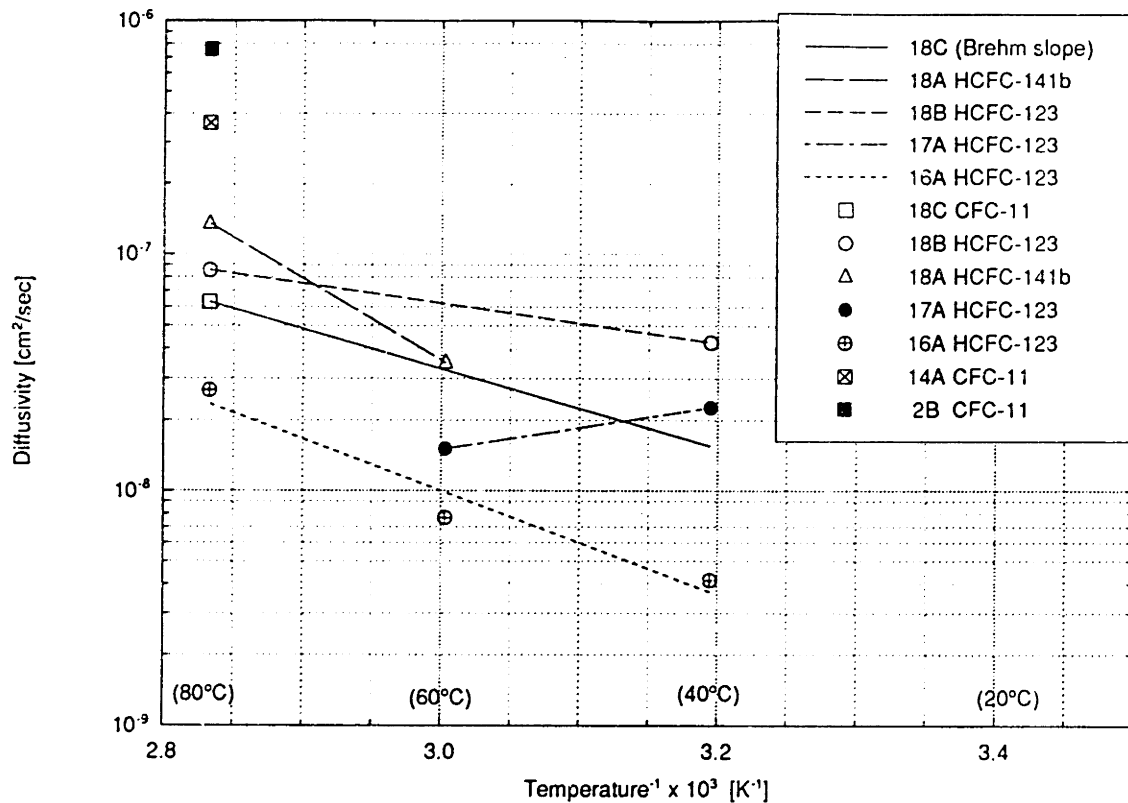


Figure 6-4: $\text{Log}(D_{eff})$ vs. $1/T$ Plot of Blowing Agent Test Results. Symbols are data points, dashed lines represent best fit for data. Solid line drawn with slope from Brehm's CFC-11 data fit to CFC-11 data for foam 18.

Foam		1	2	14	16	17	18	$B_{D_{eff}}$	$B_{P_{eff}}$	$O_{P_{eff}}$
Gases	T [°C]	Effective Diffusion Coefficient Ratios								
$\frac{CO_2}{CFC-11}$	80	-	48.4	78.1	-	-	394.9	260	^(t) 167	235
	60	-	-	-	-	-	-	376	^(t) 226	-
$\frac{CO_2}{HCFC-123}$	80	-	-	-	268	-	290	-	-	-
	60	-	-	-	358	1028	(258)	-	-	-
	40	-	-	-	-	650	-	-	-	-
$\frac{CO_2}{HCFC-141b}$	80	-	-	-	-	-	184	-	-	-

$B_{D_{eff}}$ = Brehm D_{eff} .

$B_{P_{eff}}$ Brehm P_{eff} . ^(t) = Transient-Sorption Test; ^(s) = Steady State Test [19].

$O_{P_{eff}}$ = Ostrogorsky P_{eff} . Steady State Test [13].

() = From interpolated values.

Table 6.6: CO_2 /Blowing Agent Effective Diffusion Coefficient Ratios.

for foam 17 is evident in the slope of the best fit line for HCFC-123. It is highly unlikely that the diffusion coefficient increases as temperature decreases. Refrigerant tests can last on the order of weeks (compared with a maximum of 1 to 2 hours for CO₂) so the effects of any temperature drift, electronic drift and any minute leaks are amplified. These effects increase with a decreases in test temperature due to the increase in test times. This error in the results is difficult to quantify. Therefore, confidence can only be placed in the order of magnitude of the blowing agent diffusion coefficients.

From the results of all three blowing agents on foam 18 the diffusion coefficients and therefore the implied aging rates (assuming that the solubility differences are negligible) compare with some other published results as follows:

Source	Relative Aging or D_{eff} Measurement Technique	Medium	Temp. [°C]
This Work	CFC-11 < HCFC-123 < HCFC-141b (See chapter 3)	PIR foam 18	80
Baumann [30]	HCFC-123 < CFC-11 < HCFC-141b Aged thermal conductivity	PIR foam	70
Cunningham [31]	CFC-11 < HCFC-141b < HCFC-123 Gas analysis	foam	70
Creazzo [10]	HCFC-123 < CFC-11 < HCFC-141b Gas transmission	film	20,60
Lund [4]	HCFC-123 < HCFC-141b < CFC-11 Constant pressure sorption balance	PUR film	25
Pikulin [32]	HCFC-123 < HCFC-141b \approx CFC-11 FTIR	PUR & PIR film	60
Molecular Weight	HCFC-141b < CFC-11 < HCFC-123		

In general significant uncertainties are associated with these results, and therefore, as in

this work, represent order of magnitude estimates. Although not in agreement as to the relative magnitudes, all the works sighted above, except Lund, do agree on the conclusion that the diffusion coefficients of all three blowing agents are of the same order of magnitude and therefore foams blown with them should have similar aging. In Lund's work the conclusion was that the diffusion coefficient of HCFC-123 was too low to measure. It is generally believed that HCFC-123 has the highest solubility of the three blowing agents. It is unlikely that no sorption occurred for HCFC-123 when CFC-11 sorption was measured. Either unusual polymer chemistry or experimental error may be the cause for the disagreement. The relative molecular weights are listed since the argument goes that larger molecules should diffuse slower. The molecular weight argument is not supported, this may be due to competing effects of solubility.

6.5 Aging Predictions

The aging model developed by Ostrogorsky [13] was originally verified by comparing predictions of thermal aging with long term thermal conductivity measurements. The basis for the aging model are measurements of gas permeability in the foam, foam density, cell size and cell wall thickness. Ostrogorsky's predictions were based on steady state measurements of foam permeability to air gases and CFC-11. The measurements were made at elevated temperatures and extrapolated to the temperature of the long term aging. In these comparisons there was agreement to within 6%.

The effective thermal conductivity of the foam is the sum of gas conduction, solid conduction and radiation. Changes in the effective conductivity with time (aging) are solely due to changes in the gas composition. The gas conduction is related to the cell gas composition which is computed using the measured gas diffusion coefficients and Fick's Law. The solid polymer and radiative thermal conductivity are calculated based on measured average foam properties using the equations developed by Schuetz [11]. The

expression for the solid polymer contribution to the thermal conductivity is

$$k_S = \left[\frac{2}{3} - \frac{(100 - P_{cw})}{300} \right] (1 - \delta) k_{sp} \quad (6.6)$$

where k_{sp} is the thermal conductivity of the solid polymer. The expression for the radiative component is

$$k_R = \frac{16}{3} \frac{d_c}{3.68} \frac{\sigma T^3}{(\rho_f / \rho_{sp})^{1/2}} \quad (6.7)$$

where σ is the Stefan-Boltzmann constant, ρ_{sp} is the density of the solid polymer and d_c is the average foam cell diameter. This expression is for transparent cell walls, although recent work [33] has found that cell wall opacity can be a factor in closed-cell foam radiative heat transfer. In this work assumptions will be made that; k_{sp} is 0.27 W/(m·K) and ρ_{sp} is 74 lb/ft³. The average cell diameter in the direction of heat transfer will be calculated for a truncated octahedron cell geometry. An initial cell gas pressure of 0.6 MPa will be assumed. In the simulations, any increase in the foam aging due to effects of open cells at the foam surface will be neglected. Using these values the k_S , k_R and initial foam total thermal conductivity, k_{T_i} , were calculated for some of the foams in this research and are compared to measured k_{T_i} in table 6.7.

Foam	k_R	k_{sp}	$k_{T_i}^C$	$k_{T_i}^M$
16	3.4	3.4	17.5	18.0
17	2.7	4.6	17.5	17.4
18	2.5	5.7	18.0	18.0

$k_{T_i}^C$ = Calculated initial foam thermal conductivity

$k_{T_i}^M$ = Measured initial foam thermal conductivity

Table 6.7: Calculated and Measured k_R , k_S and k_{T_i} in [mW/m·K].

6.5.1 Foam 18

Foam 18 is a HCFC-141b blown, MR-Terate 203-Multranol 9171 polyisocyanate foam from laminated board stock (see appendix E). Each of the test gases, air constituents and

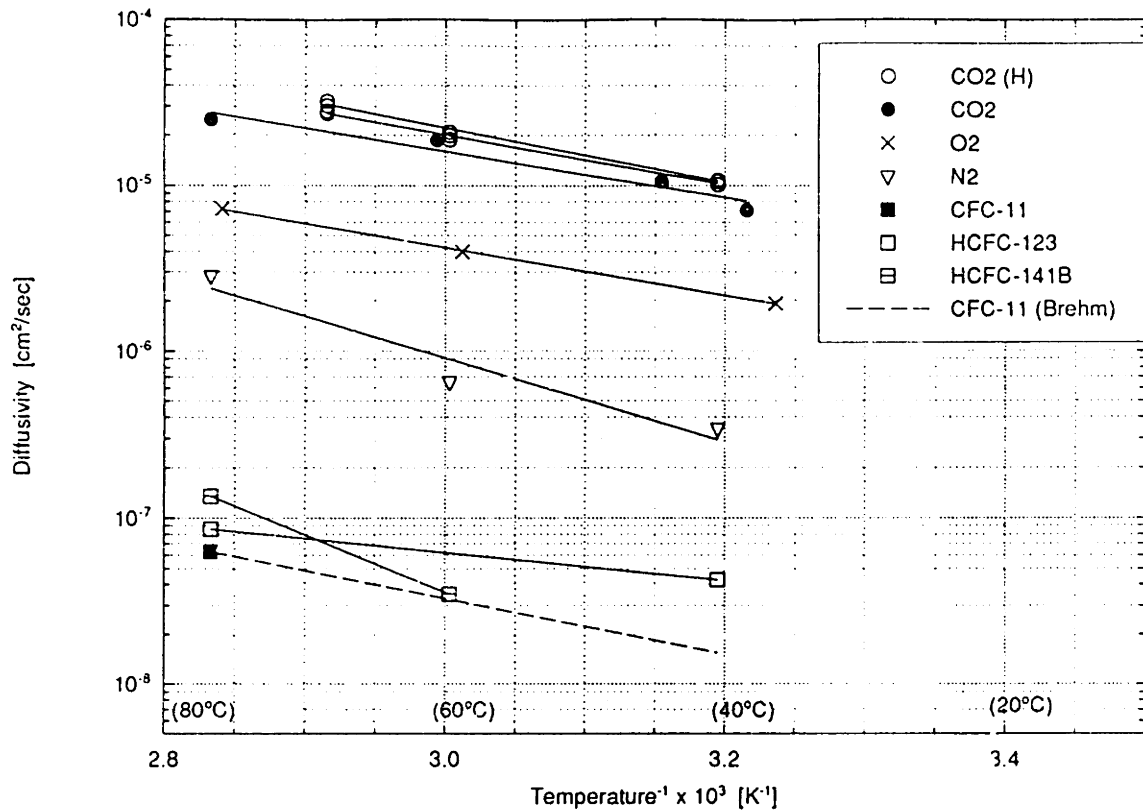


Figure 6-5: Test results for Foam 18, $\text{Log}(D_{eff})$ vs. $1/T$ for 6 test gases. Symbols are data points, solid lines represent best fit for data. Dashed line drawn with slope from Brehm's CFC-11 data fit to CFC-11 data for foam 18. $\text{CO}_2(\text{H})$ are results of CO_2 tests at Holometrix.

the three blowing agents, were individually tested in this foam. The results of the diffusion coefficient measurements is presented in a plot of $\log D_{eff}$ vs. $1/T$ in Figure 6-5. A comparison of the blowing agent diffusion coefficient measurements provides a measure of alternate and CFC-11 blown foams' long term aging characteristics.

Blowing agent diffusion coefficients measured in foam 18 for CFC-11, HCFC-123 and HCFC-141b at 80°C are within the same order of magnitude. The ratio of $\text{CO}_2/\text{CFC-11}$ diffusion coefficients for foam 18 at 80°C is 395. This ratio is consistent with results from previous research [12, 19] (see Table 6.6). This gives confidence in the order of magnitude of the D_{eff} measured for CFC-11 in foam 18. This order of magnitude agree-

ment is also seen for the alternate blowing agents. The ratio of diffusion coefficients for $\text{CO}_2/\text{HCFC-123}$ at 80°C is 290 and that of $\text{CO}_2/\text{HCFC-141}$ is 137.

The temperature dependence of D_{eff} of CO_2 as seen in Figure 6.1, appears to vary slightly with foam polymer chemistry and foam blowing agent. This evidence for predictable temperature dependence for the blowing agents can not be supported nor denied by the results for foam 18. The best fit of HCFC-123 and HCFC-141b is based on two data points. As there is only one data point for CFC-11, a dashed line representing the slope for CFC-11 from Brehm's foam, has been drawn through the CFC-11 data point at 80°C for reference.

Due to the temperature dependence uncertainty in the blowing agent results, the most accurate prediction of the aging characteristics should be made at elevated temperatures. The thermal conductivity of foam 18 was measured over time in two, 1.99 inch thick, unfaced foam board stock samples at Mobay [30]. One of these boards was aged at room temperature, the other at 70°C . The results of these measurements are plotted with the predicted aging based on diffusion coefficient measurements in Figure 6-7.

The predicted aging at 25°C is in reasonable agreement with the Mobay unfaced panel data point. The faced panel shows slower aging as expected. Contrary to expectations, the results at lower temperature match the Mobay results better than those at high temperature. This is not expected due to the added uncertainty in the extrapolation of high temperature diffusion coefficients measurement results to low temperature. Comparing the implied diffusion rates of gases in Mobay's 70°C data with the models predicted curve at 25°C both O_2 and N_2 diffusivities double. Ostrogorsky's data indicates a 6, 11.5, and 19 times increase in diffusion coefficients from 25 to 70°C for O_2 , N_2 , and CFC-11 respectively. Foam 18 data predicts a 4.4, 12.7 and 33.6 increase. This disagreement with the air data gives reason to doubt Mobay's high temperature aging values.

The aging at 25°C for this time span is dominated by the diffusion of air components into the foam, and the effect of HCFC-141b diffusion on foam thermal conductivity is

minimal, as shown in Figure 6-6. This is also illustrated in Figure 6.5.1. In this figure the arrows pointing to the left begin at $\tau=1$, the gas mean pressure across the foam at this time is within 93% of it's final value. At $\tau = 0.05$ the mean pressure of a gas is 80% of it's initial value, the arrows pointing to the right indicate the beginning of significant aging impact. Although still dominated by air component diffusion, the thermal conductivity of the foam sample aged at 70°C should reflect the change in partial pressure of blowing agent. After aging for 50 days the air components approach equilibrium, see Figure 6-6, after that all of the increase in foam thermal conductivity is due to HCFC-141b diffusion.

The comparison of the 25°C and 70°C results illustrate the difficulty encountered when using high temperature tests to represent accelerated aging at room temperature.

A number of factors other than error in the D_{eff} measurements could cause this disagreement. Some of the errors inherent in the modeling are as follows. As the initial cell gas pressures were not measured an assumption was made. Figure 6-7 plots the

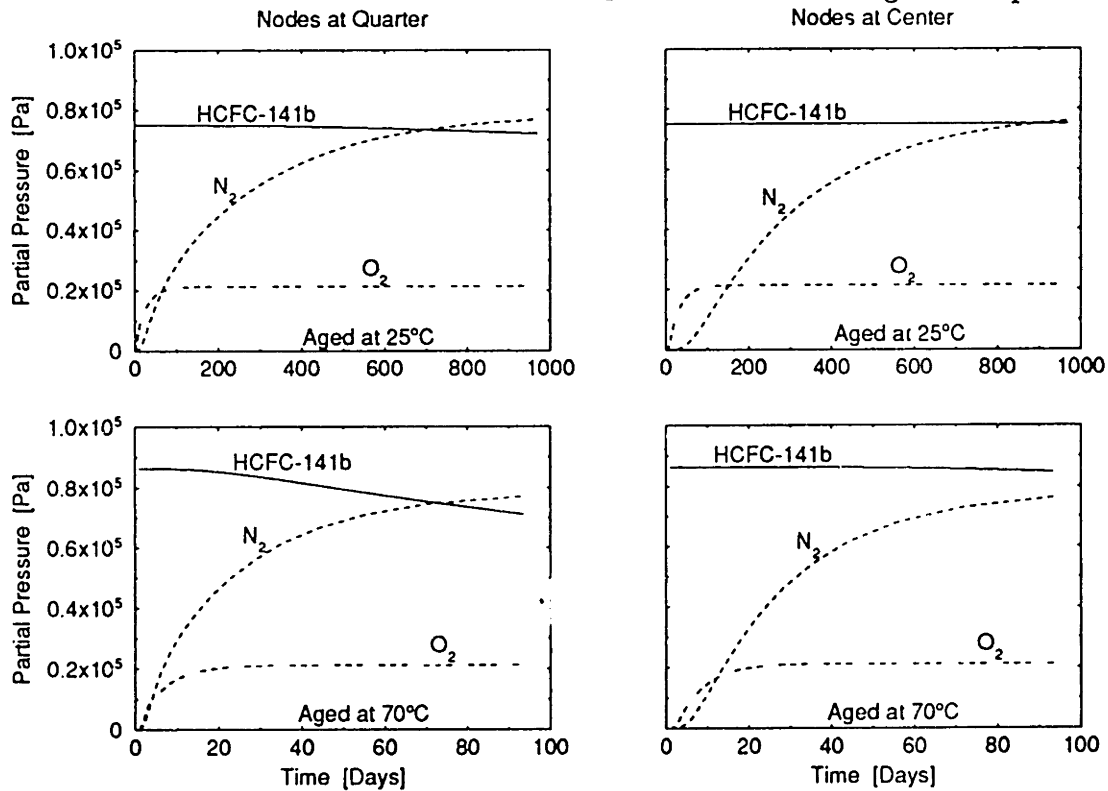


Figure 6-6: Foam 18, 1.99 inch thick sample, aging model cell gas pressures. Pressures at Aging Temperatures. Foam density: 1.83 lb/ft², Mobay (1.76 lb/ft², M.I.T.).

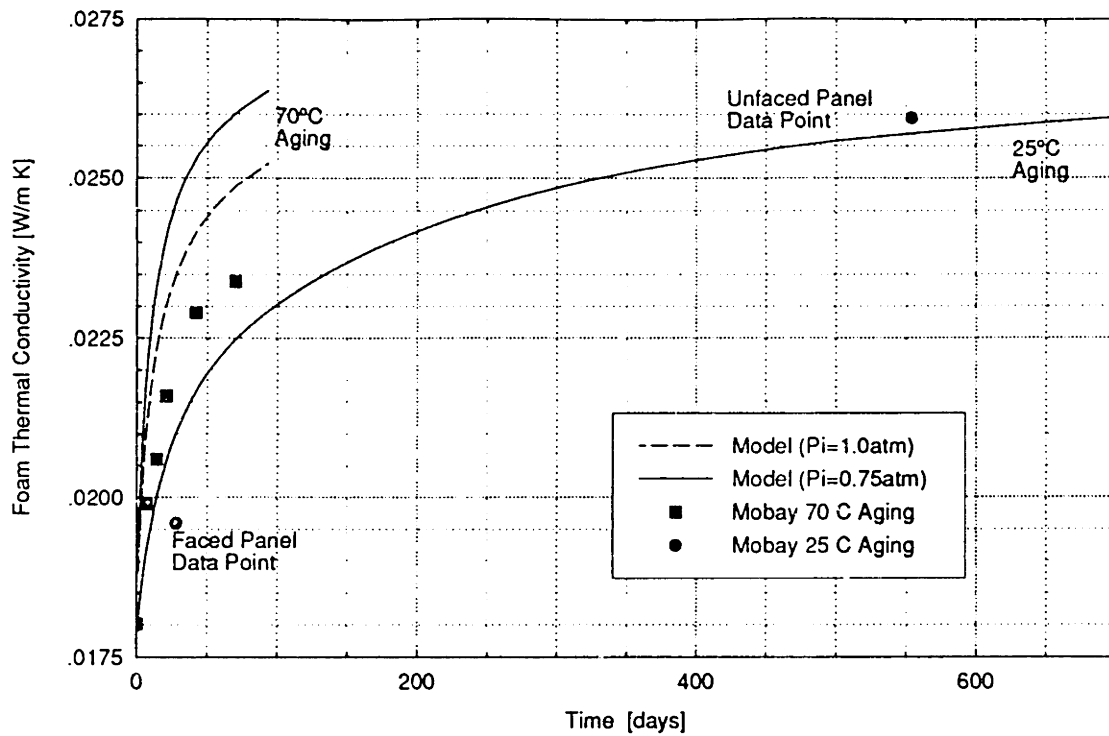


Figure 6-7: Foam 18, 1.99 inch thick sample, aging at 25°C and 70°C. Predicted and measured Thermal Conductivity vs. Time. Conductivity at 25°C. Foam density: 1.83 lb/ft², Mobay (1.76 lb/ft², M.I.T.).

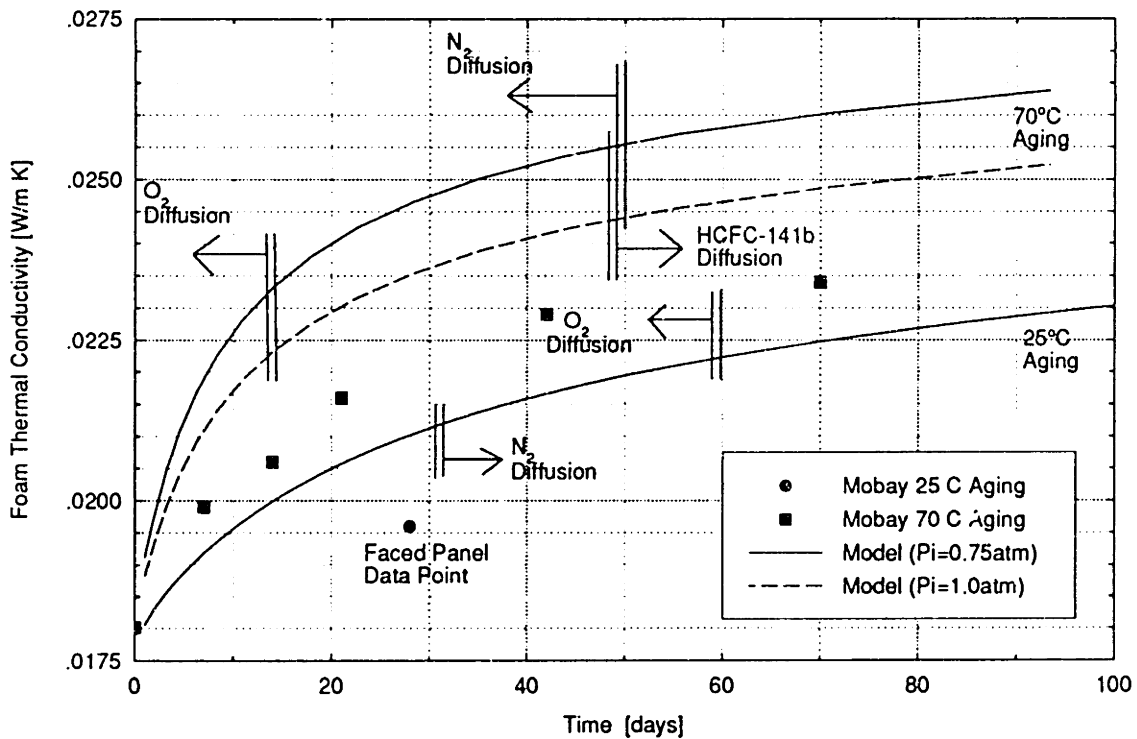


Figure 6-8: Foam 18 Initial Aging (Detail of Figure 6-7). Arrows pointing to left at $\tau=1.0$, arrows pointing to right at $\tau=0.05$.

results based on an assumption of 0.75 for the initial HCFC-141b and also shows the impact of increasing this value by 25%. The effect of test sample density lower than the foam bulk density would cause an error that would increase the aging rate. Using the methods described in section, 6.3, diffusion coefficients were calculated based on the assumption that the test sample density was 20% lower than the average foam density. This increase in density alone is not enough to account for the disagreement. Similarly gradients in P_{cw} through the foam may cause the test sample's P_{cw} to be lower than the average. Accounting for a combination of all of the above could bring the difference within the range of expected uncertainty. In the Mobay measurements there are numerous potential sources of error in the aging temperature alone, among them fluctuations in the oven average temperature, thermal gradients in the oven and temperature changes imposed on the sample while performing the thermal conductivity measurements. If the foam was aged at a temperature lower than reported this would also explain the discrepancy.

6.5.2 Igloo

Bayer AG in Leverkusen, Germany fabricated a CFC-11 blown foam igloo in 1961. It has shown unusually high k-factor retention. To determine if the aging characteristics are due to the structure of the foam or due to unusual polymer chemistry, the natural aging of this foam is compared to theoretically predicted values from the computer simulation.

This hemispherical structure with an approximate 2 meter radius of curvature was constructed by spraying foam in layers over a cardboard like form. A cross-section of the foam is composed of alternating layers of foam separated by film of solid polymer that forms at the surface after each layer is applied. A 7.25 cm thick sample of the igloo (see Figure 6.5.2), was provided by Dr. Wiedermann of Bayer AG. The average thickness of the wall varies from 6.5 to 10 cm depending upon location.

In the aging model the igloo foam was treated as a homogeneous material. The simulation also assumes; 0.6 bar CFC-11 as initial cell gas pressure and 15°C average

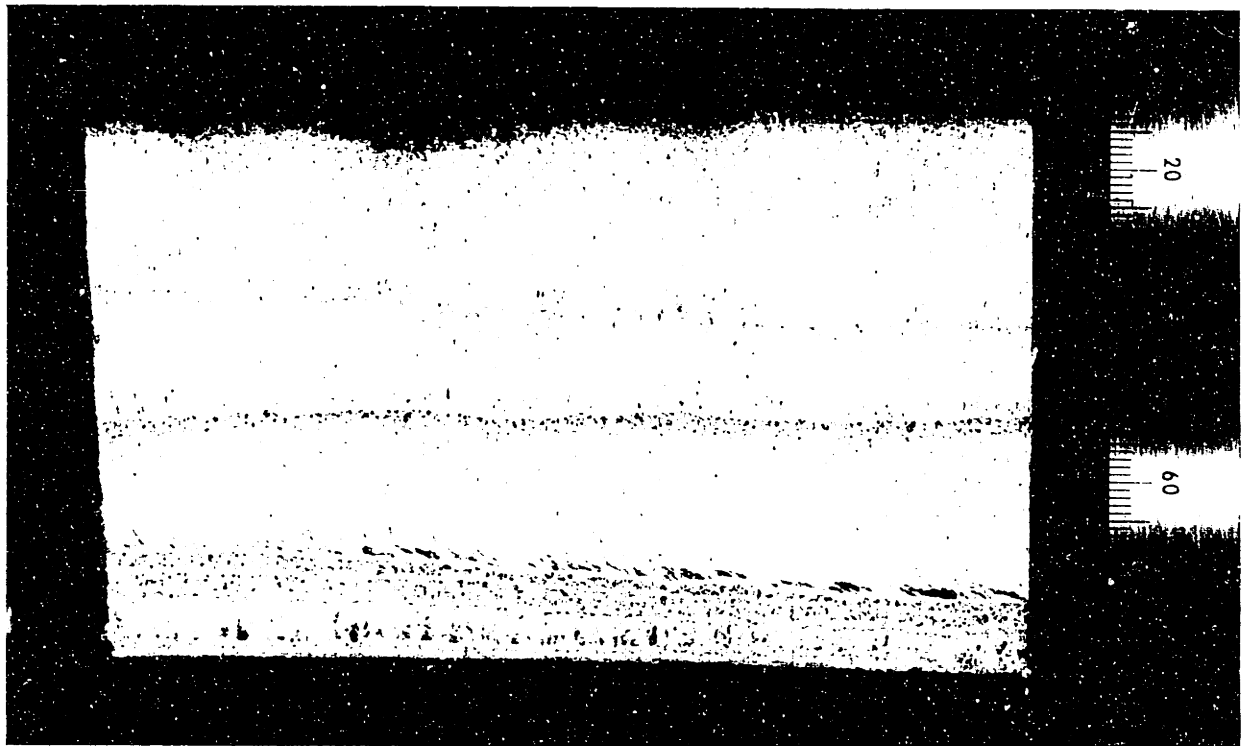


Figure 6-9: Cross Section of the Bayer Igloo.

temperature seen by the igloo over it's history. The D_{eff} of the igloo was not measured, as the intent was to see if solid polymer diffusivity of this foam is typical of those measured in commercially available board stock. The solid polymer diffusivity of the foam measured by Ostrogorsky was used. The effective diffusion coefficients for the igloo are calculated, as in equation 6.5

$$D_{effIgl\text{oo}} = D_{effA} \frac{(\rho_f P_{cw})_A}{(\rho_f P_{cw})_{Igl\text{oo}}}. \quad (6.8)$$

The measurements of foam cell wall thickness and average distance between cell walls used in the calculation of percent of material in the cell walls represent an approximation of the foam average properties. The sample has a high average density. Measured and calculated values are listed in Table 6.4.

In 1988 the thermal conductivity and cell gas pressure were measured at Bayer. Details of test procedures and results sent by Dr. Weidemann are summarized below.

The thermal conductivity measurements were performed on a $5 \times 80 \times 80$ cm panel cut from a sample of the hemispherical wall of the igloo. The actual thickness of the igloo wall in the location of the sample was not recorded. The thermal conductivity was measured at a number of temperatures and from the results of these tests the thermal conductivity at 10°C was reported. Wiedermann [34] claims a 1% uncertainty in the reported value. The simulation and measurements results in Table 6.8, and Figures 6-10 and 6-11 compare the simulation with these measurements.

The method used in the gas analysis as described by Wiedermann [29] involves analysis from three separate samples. One sample was burnt to determine the overall fluorine content and one sample was ground into a powder to determine the fluorine content in the solid polymer. Both of these samples were from the full thickness of the igloo and therefore represent average values; the exact thickness of the igloo at the location of these samples was not recorded. In the third sample a needle was inserted 3.0 cm into

Conductivity [$W/m \cdot K$]	Simulation Prediction		Bayer Measurements
k_S	0.0062		-
k_R	0.0023		-
k_{Foam}	0.0253		0.027
Foam Average			
Cell Gas	P	Pressure [mPa]	Composition
CFC-11	0.58		0.38 [mPa]
Air	<0.01		
3 cm From Surface			
Cell Gas	P	Pressure [mPa]	Composition
CFC-11	0.825	0.54	34.1%
Air	<0.01	1.035	65.3%

Table 6.8: Igloo Aging Prediction at 15°C and Measured Values, After 27 Years for Igloo Thickness ≈ 6.75 cm.

the foam, cell gas was extracted and gas-chromatography was used to determine the air to fluorine ratio. The reported values represent the average of five measurements. The samples were taken from a location where the igloo wall thickness is between 6.5 and 7.0 cm.

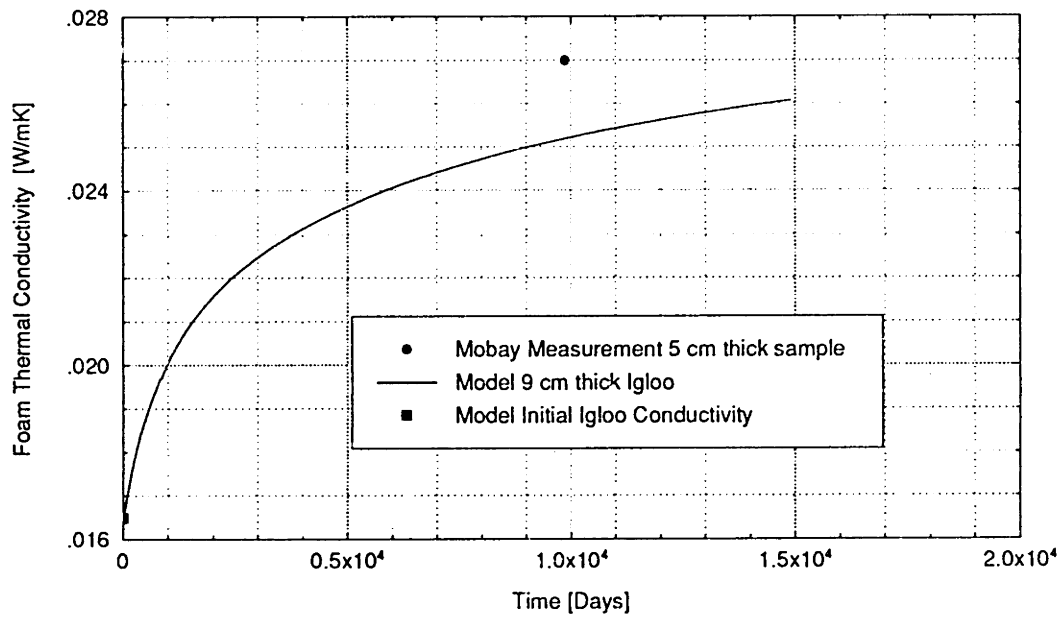


Figure 6-10: Simulation prediction of 9 cm thick Igloo Thermal Conductivity vs. Time Compared to Thermal Conductivity Measurement of 5 cm thick sample of Igloo Naturally Aged at 15°C.

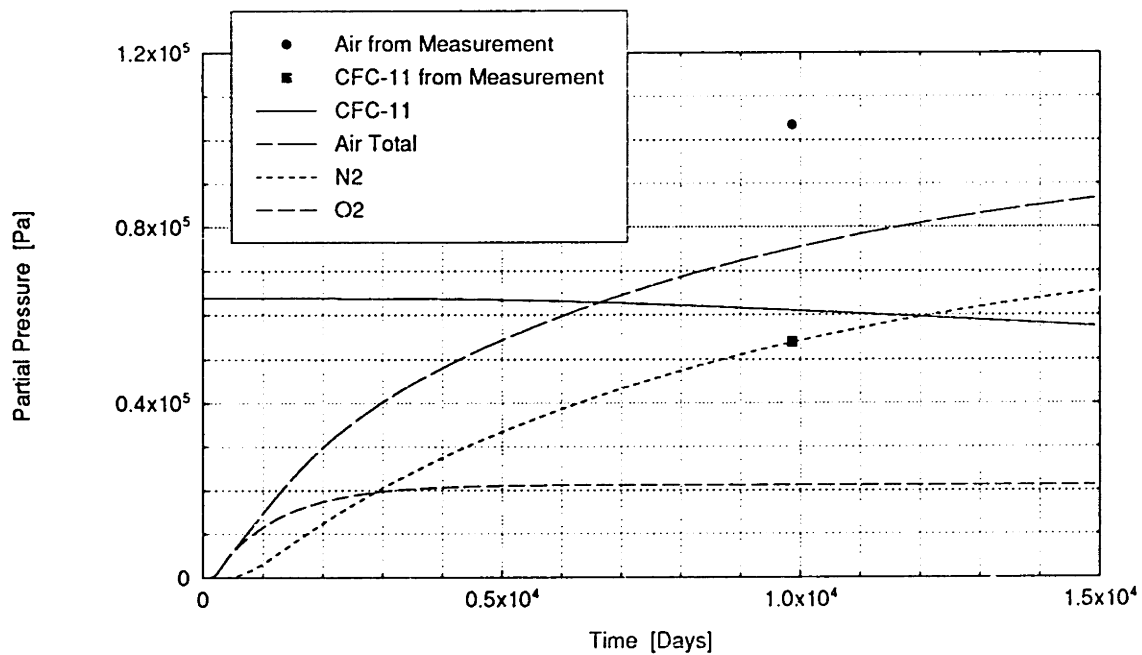


Figure 6-11: Model Prediction and Measured Values of Igloo Cell Gas Partial Pressure vs. Time at Node 3.0 cm Under Surface of Foam. Assumed, 0.66 bar, for initial partial pressure of CFC-11.

It is the first time that naturally aged foams this old have been compared to the aging model. The model and measured thermal conductivity of the Igloo show good agreement. Although results indicate that the slow aging of the igloo can be attributed to the structure of the foam, there are a number of difficulties in modeling the igloo's aging based on these measurements.

As mentioned in the discussion of foam 18 aging, using local measurements to calculate an average value of percent material in the cell walls may not give accurate results. The Igloo is obviously not a homogeneous continuum the average density may over simplify reality especially when comparing cell gas pressure measurements. If the needle sample were taken from the center of the Igloo in an area sandwiched between two of the dense skin layers then the measured air pressure would be lower and the fluorine content higher. Although a sample of cell gas taken 3 cm from the surface would fall in this region in the sample sent to M.I.T., it is not certain that this was the case for the air sample, since the thickness and location of each layer may vary.

The reported fluorine content represents an average for the full thickness of the Igloo. From this average value both the initial pressure and partial pressure at a given location can be calculated by solving Fick's second law for an infinite slab with constant pressure boundary conditions. The solution is analogous the Fourier law solution, found in the literature. Using the diffusion coefficients as calculated for the aging model and a sample thickness of 6.75 cm the initial CFC-11 partial pressure would be 0.66 bar. The CFC-11 pressure at 3 cm from the surface 27 years later, 0.54 bar. Calculation for the partial pressure of air gases at 27 years gives 1.035 bar, 3 cm from the surface.

The question of how to account for the effect of basing igloo conductivity on measurements from a rectangular slab cut from the hemispherical wall is another difficulty. Figure 6-12 illustrates the situation. The geometry will lead to partial pressure distributions across the sample due to depth profile across the face of the rectangular slab. This means that there is a gradient in gas contribution to thermal conductivity of the foam across the face of the sample. In the measurement of thermal conductivity of the foam

sample any assumption of one dimensional heat transfer would be erroneous.

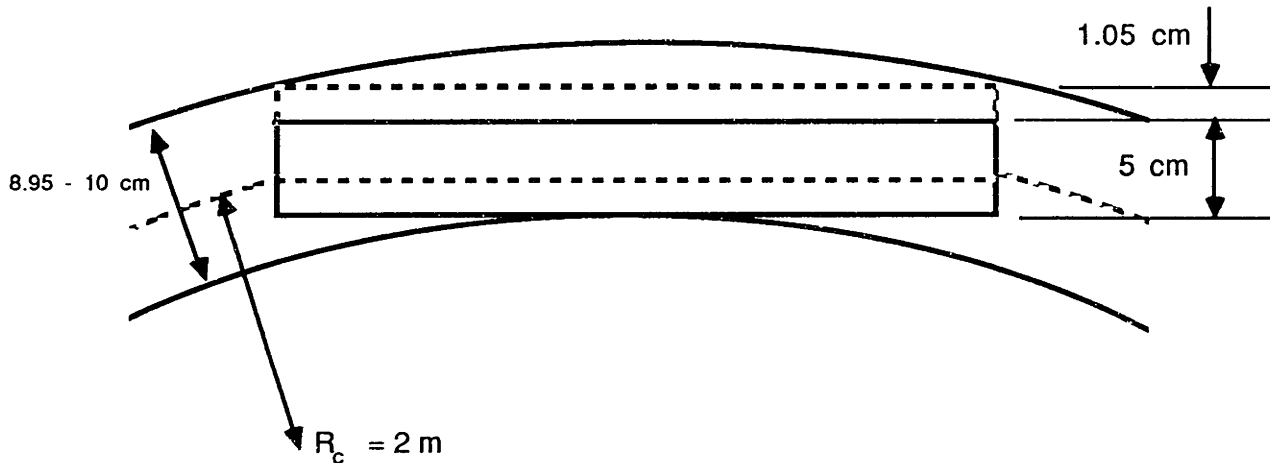


Figure 6-12: Possible Locations of Igloo K-Factor Measurement Sample.

These areas of uncertainty are typical of questions raised when aging is modeled or when the aged values of foam insulation is interpreted. Careful documentation of all parameters is essential for meaningful interpretation.

Blank Page

Chapter 7

Conclusions and Recommendations

7.1 Conclusions

Results from tests at an elevated temperature indicate that the magnitudes of the diffusion coefficients of CFC-11, HCFC-123 and HCFC-141b are the same. The ratio of diffusion coefficients of CO₂/blowing agents at 80°C have the same order of magnitude. If the temperature dependence of the diffusion coefficients, as characterized by the slope to a best fit line on a log D_{eff} vs. $1/T$, is the same, then the results extrapolated to room temperature indicate that the long term aging characteristics of foams blown with these alternates should be similar to those foams blown with CFC-11.

Initial results show that the percent of material in the cell walls, P_{cw} , is a function of blowing agent. Approximately 40% of the material is in the cell walls for HCFC-141b blown foams versus approximately 20% for CFC-11 blown foams. The higher P_{cw} seen in the HCFC-123 and HCFC-141b blown foams is offset in some chemistries by higher solid polymer permeability. The magnitude of both these effects is highly chemistry dependent. More testing is needed to determine if the ratios between diffusivities of different gases are constants.

7.2 Recommendations

Two categories of recommendations are in order. The first deals directly with suggestions for the test method used in this research. The second is a comment about other areas for improvement of aging characteristics for future commercial closed cell foam insulation.

7.2.1 Test Method

The first recommendation relates to the accuracy and speed of the test method. The tests in this research knowingly sacrificed accuracy for speed by using thin test samples. The resolution of foam solubility suffered the most. An accurate method for rapidly measuring solubility separately is recommended. Results of these tests can be used in the analytical solution of the transient permeability tests, thereby reducing the error in the determination of the diffusion coefficient.

Foam solubility can be measured in the apparatus used in this research by taking larger samples than those currently being tested, and crushing or slicing them into very thin (less than two cell diameters thick) so that all cells are open. By placing a larger volume of solid polymer in the test cell the resolution of the measurement increases. The resulting test effective half thickness, inherent in the foams micro structure, seen by the permeating gas would be on the order of microns. This would result in very short test times. The process would involve flushing, inducing a step change in pressure and waiting for equilibrium. The analysis would involve a mass balance based on initial and final pressures.

Other areas that effect the models accuracy include accounting for gradients of density, cell size and cell wall thickness that occur in foam panels. Improved methods of measuring cell wall thicknesses would be essential in any attempt to characterize it's distribution in the foam.

7.2.2 Foam Insulation

Among the list of potential alternate blowing agents along with the hydrogenated chlorofluorocarbons, HCFCs, is water. Water reacts during the foaming process leaving carbon dioxide, CO_2 , as the cell gas. CO_2 has two orders of magnitude higher permeability and approximately two times higher thermal conductivity than refrigerants and is a greenhouse gas but has the advantage of not depleting ozone. Aging rates in CO_2 foams could be improved if a diffusion barrier is well attached to the face of the foam. An aging simulation [12] was run to compare the aging rates of two one inch thick foam panels. One panel is an unfaced CFC-11 foam, the other a four foot wide CO_2 filled foam with an ideal diffusion barrier, ie. an impermeable sheet that is perfectly bound to the foam surface. The one inch edges of the panel are left exposed to the atmosphere, see Figure 7-1. The simulation assumes one dimensional mass and heat transfer. The superior long term performance of the CO_2 foam panel with impermeable surface barrier is shown in Figure 7-2. Even though a two dimensional diffusion model considering a more realistic 4 x 8 foot CO_2 foam panel would exhibit slightly faster aging, the current model should serve as incentive to improve diffusion barriers as another approach to replacing *CFCs* with minimum energy penalties. As pointed out by Ostrogorsky and Glicksman, improved diffusion barriers require an impermeable seal between the barrier and the foam. The effectiveness of a good barrier has been documented by Baumann [30]. He cites a foam enclosed between steel panels in an entry door, that has shown only a $0.5 \text{ mW/m}\cdot\text{K}$ drop after 10 years.

7.3 Future Work

The results of the aging comparisons in this research highlight the difficulties in the industry standard of predicting long term aging from thermal conductivity tests on board stock that has been aged in high temperature ovens for short periods of time. This difficulty arising mainly from the variation in gas permeability temperature dependence.

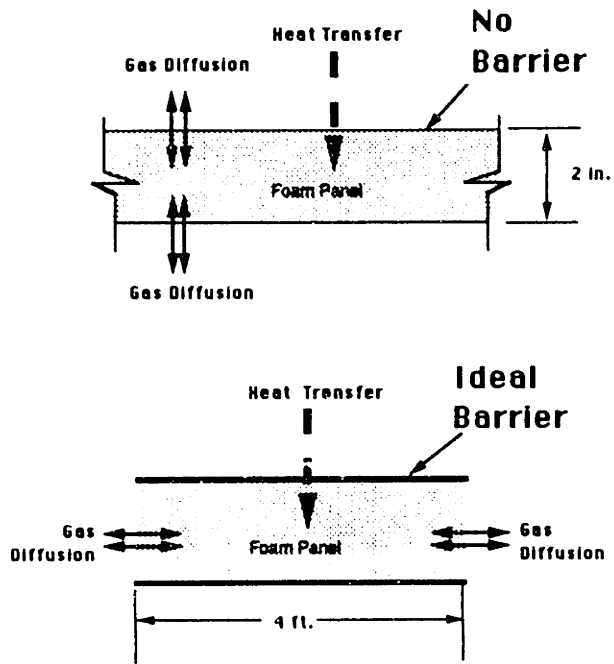


Figure 7-1: Foam Panel Schematic.

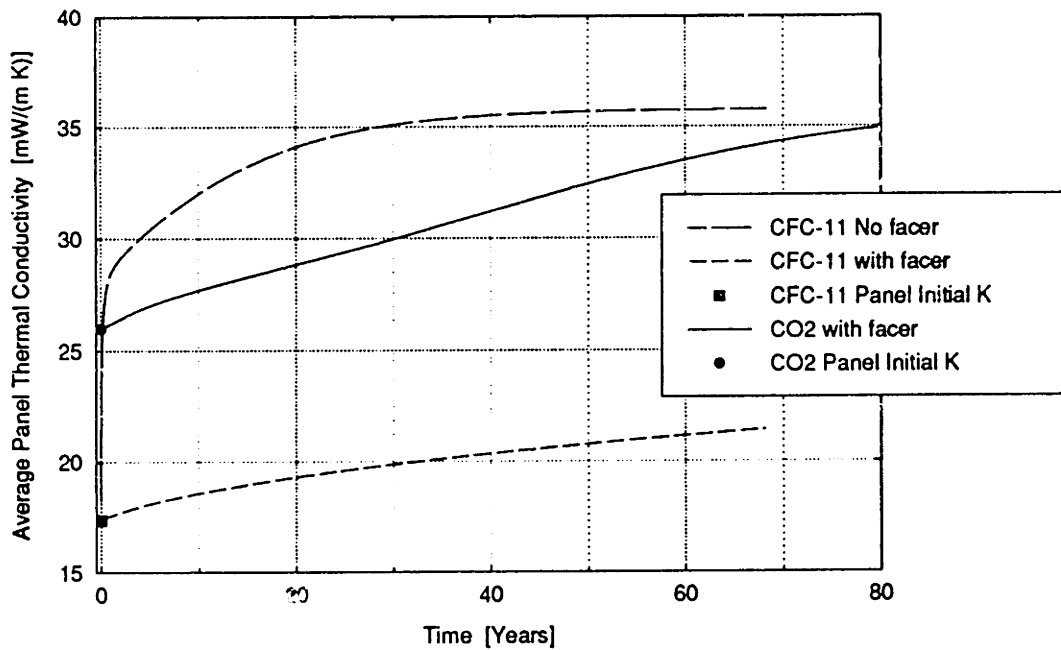


Figure 7-2: Aging of CFC-11 blown foam with and without barrier vs. CO₂ blown foam with ideal barrier. (simulation at 25°C)

The comparison of aging predictions to the natural aging of foams whose initial conditions (manufacture date and initial cell gas pressures) and thermal histories are well documented is essential in verifying our ability to predict aging.

A set of tests similar to those presented in this work is being run on foam supplied by Oak Ridge National Laboratory. Permeability of air gases as well as blowing agents will be measured for a matrix of laminated board stock of the same basic polymer chemistries but blown with different refrigerants. Each of the five foams are blown with one of the following: CFC-11, HCFC-123, HCFC-141b, a 50/50 blend of HCFC-123 and HCFC-141 or a 65/35 blend of HCFC-123 and HCFC-141. The aging predictions of these tests will be compared with thermal conductivity measurements of naturally aged full scale board stock of the same foams. The careful documentation of the history of these foams and the comparison of results from a consortium of independent laboratories will provide a unique and valuable opportunity to verify and improve the model for predicting thermal drift in closed-cell foam insulation.

Blank Page

Bibliography

- [1] Bayer AG, Polyurethane Application Research Department, **Bayer Polyurethanes Handbook**, Germany, 1979.
- [2] Woods, G., **The ICI Polyurethanes Book**, ICI Polyurethanes and John Wiley & Sons, 1987.
- [3] Rowland, F.S., Molina, M.J., *Nature*, 249: 8-10 (1974).
- [4] Lund, E.A.E., Richard, R.G., Shankland, I.R., "A Performance Evaluation of Environmentally Acceptable Foam Blowing Agents ", *SPI 31st Technical/Marketing Conference*, 290 (1988).
- [5] Committee on Impacts of Stratospheric change, National Research Council, **Protection Against Depletion of Stratospheric Ozone by Chlorofluorocarbons**, National Academy of Sciences, Washington, D.C. (1979).
- [6] Allied-Signal Inc., Health, Safety & Environmental Sciences., Letter to Mr. David Williams (TS-778) Coordinator, U.S. Environmental Protection Agency, Office of Toxic Substances (May 10, 1990).
- [7] Glicksman, L.R., "Methods to Enhance Insulation Values of Closed Cell Foams", Massachusetts Institute of Technology, 1988.
- [8] Conversations with John Szabat, Mobay Chemical Company, Pittsburgh, PA, 1989-1990

- [9] Dwyer, F.J., Knopeck, G.M. and Zwolinski, L.M., "CFC Alternates Emissions in Thermoset Foam Production ", *SPI 33rd Technical/Marketing Conference*, 141 (1990).
- [10] Creazzo, J.A., "The duPont Program on Alternative Blowing Agents for Polyurethane Foams - Recent Developments". E. I. duPont de Nemours and Company. Internal Bulletin. 1988
- [11] Schuetz, M.A., "Heat Transfer in Foam Insulation, M.S. Thesis, Department of Mechanical Engineering, Massachusetts Institute of Technology, 1982.
- [12] Ostrogorsky, A.G. and Glicksman, L.R., "Rapid, Steady-State Measurement of the Effective Diffusion Coefficient of Gases in Closed-Cell Foams", *Transactions of the ASME*, 110, 500 (1988).
- [13] Ostrogorsky, A.G., "Aging of Polyurethane Foams", Ph.D. Thesis, Department of Mechanical Engineering, Massachusetts Institute of Technology, 1985.
- [14] Cunningham, Rosbotham, Sparrow, Brown, Galbraith, "The Effects of Water as a Partial Blowing Agent for Rigid PUR and PUR/PIR Foams", *Journal of Cellular Plastics*, 164-170 (1989?).
- [15] Mozgoweic, M., "The Use of Small Cells to Reduce Radiation Heat Transfer in Foam Insulation", M.S. Thesis, Department of Mechanical Engineering, Massachusetts Institute of Technology, 1990.
- [16] Reitz, W.R., "A Basic Study of Gas Diffusion in Foam Insulation", M.S. Thesis, Department of Mechanical Engineering, Massachusetts Institute of Technology, 1983.
- [17] Underwood, E. E., **Quantitative Stereology**, Addison-Wesley Publishing Co., Reading, MA, 1970.
- [18] Wilson, A.H., "A Diffusion Problem in which the Amount of Diffusing Substance is Finite", *Philosophical Magazine*, vol. 39, 1948, p.48.

- [19] Brehm, T.R., "Transient Measurement of Gas Permeability in Closed-Cell Foam Insulation", M.S. Thesis, Department of Mechanical Engineering, Massachusetts Institute of Technology, 1989.
- [20] Crank, J., Park, G.S., eds., **Diffusion in Polymers**, Academic Press, London, UK, 1962.
- [21] Van Krevelen, D.W., **Properties of Polymers : Their Estimation and Correlation with Chemical Structure**, Elsevier Scientific Publishing Co., New York, 1976.
- [22] Kline, S.J, McClintock, F.A., "Describing Uncertainties in Single Sample Experiments", *Mechanical Engineering*, 75, 3 (1953).
- [23] Reynolds, W.C., **Thermodynamic Properties in SI**, Department of Mechanical Engineering, Stanford University, Stanford, CA, 1979.
- [24] Brehm, T.R., L.R., Glicksman "Implementation of a Constant-Volume Sorption Technique for Rapid Measurement of Gas Diffusion and Solubility in Closed-Cell Foam Insulation", *SPI Conference Proceedings 32nd SPI Conference*, San Francisco, CA, Oct. 1989
- [25] Carslaw, H.S., Jaeger, J.S., **The Conduction of Heat in Solids**, Oxford University Press, Oxford, England, 1959.
- [26] Moffat, R.J., "Describing the Uncertainties in Experimental Results", *Experimental Thermal and Fluid Science*, 1, 3-17 (1988).
- [27] Beers, Y., **Introduction to the Theory of Error**, Addison-Wesley Publishing Co., Reading, MA, 1957.
- [28] Blanpied, R.H., Knis, S.A., "Technical Viability of Alternate Blowing Agents in Polyisocyanate Roof Insulation. Part 1: Processing and Physical Properties", *SPI Conference Proceedings 33rd SPI Conference*, Orlando, Fla. Oct. 1990

- [29] Wiedermann, R.E., Adams, N. and Kaufung, R., "Flame- Retarded, Rigid PUR Foams with a Low Thermal Conductivity", *Journal of Thermal Insulation*, 11, 242 (1988).
- [30] Baumann, G.F., Szabat, J.F., "Alternate Blowing Agent Options in Polyisocyanate Laminate Foams", *SPI Conference Proceedings 32nd SPI Conference*, San Francisco, CA, Oct. 1989
- [31] Cunningham, A., Sparrow, D.J., Rosbotham, I.D., Du Cauze De Nazelle, G.M.R., "a Fundamental Study of the Thermal Conductivity Ageing of Rigid PUR Foam Blown with HFA-141b/Carbon Dioxide and HFA-123/Carbon Dioxide Mixtures", *SPI Conference Proceedings 32nd SPI Conference*, San Francisco, CA, Oct. 1989
- [32] Pikulin, S., Bhattacharjee, D., "Measurement of Blowing Agent Diffusion through Polymer Film", *SPI Conference Proceedings 32nd SPI Conference*, San Francisco, CA, Oct. 1989
- [33] Glicksman, L.R., Mozgowiec, M., Torpey, M., " Radiation Heat Transfer in Foam Insulation", *Proceedings of the Ninth International Heat Transfer Conference*, Jerusalem, Israel, (1990).
- [34] Wiedermann, R.E., Bayer AG, Leverkusen, Germany. Personal communications (May, 1991).
- [35] Lienhard, J.H., **A Heat Transfer Textbook**, Prentice-Hall, Inc., Englewood Cliffs, New Jersey, 1987.
- [36] Shanklin, I., Personal communication April 1991.
- [37] Dietrich, W.K., Doerge, H.P., "Performance of Alternative Chlorofluorocarbons in Rigid Urethane Appliance Foams ", *SPI 31st Technical/Marketing Conference*, 141 (1988).

Appendix A

Alternate Blowing Agent Information

Summary of Test Gas Properties

Test Gas		CCl ₃ F HCFC-11	CF ₃ -CCl ₂ H HCFC-123	CH ₃ -CCl ₂ F HCFC-141b	CO ₂	O ₂	N ₂
Molecular Weight [g/mol]		137.4	152.9	116.9	44.1	32	28
% Weight Chlorine		77.4	46.3	30.3	0	0	0
† R_{gas} [$\frac{kJ}{kg K}$]		0.0605	0.0544	0.0711	0.1889	0.2598	0.2929
Liquid Density [lb/ft ³] at 21°C		92.72	88.98	77.5	-	-	-
Vapor Density [lb/ft ³] at 25°C		0.378		0.4	0.125	0.0812	0.0911
Latent Heat [Btu/lb] at T _b		77.5	74.9	96.6			
Vapor Conductivity [W/m K]	10°C	³ 0.0075	³ 0.0091	³ 0.0089	⁴ 0.0191	⁴ 0.0253	⁴ 0.0246
	25°C	³ 0.0082	³ 0.0104	³ 0.010	⁴ 0.0166	⁴ 0.0268	⁴ 0.0259
	60°C	³ 0.010	³ 0.0135	³ 0.0127	⁴ 0.0276	⁴ 0.0253	⁴ 0.0281
Critical Temp [K]		471.2	456	⁵ 477.8			
Boiling Point [K] at 1 atm.		296.8	300.9	305.9	194.5	90.04	77.2
P _{Vapor} [psia]	21°C	13.3		10.			
	25 °C		14.		-	3.07	11.5

† Assuming perfect Gas.

¹Dupont [10]; ²Penwalt; ³ICI [4]; ⁴Lienhard [35]; ⁵Allied Chemical [36].

Table A.1: Test Gas Properties.

A.1 HCFC-123

Property Summary by Allied Signal

Chemical Formula		CF ₃ CHCl ₂
Molecular Weight		152.9
Boiling Point at 1 atm	°C °F	27.9 82.2
Freezing Point	°C °F	-107 -161
Critical Temperature	°C °F	185 365
Critical Pressure	atm psia	37.40 549.6
Vapor Pressure at 25 °C	psia	14
Liquid Density at 25 °C	g/cc lbs/cu ft	1.46 91.15
Liquid Specific Heat at 25 °C	cal / g °C	0.243
Vapor Specific Heat at 25 °C	cal / g °C	0.172
Heat of Vaporization at B.P.	cal/g BTU/lb	41.6 74.9
Liquid Thermal Conductivity at 25 °C	BTU/hr ft °F	0.0388 @ 60 °C
Vapor Thermal Conductivity at 25 °C	BTU/hr ft °F	0.00734 @ 60 °C
Solubility of FC in Water at 25 °C and 1 atm	wt%	0.39
Solubility of Water in FC 25 °C, autogenous pressure	wt%	0.08
Liquid Viscosity at 25 °C	centipoise	0.449
Vapor Viscosity at 25 °C	centipoise	0.0136 @ 60 °C

* Denotes calculated values

PRODUCT SAFETY DATA SHEETTRADE NAME: HCFC-123CAS.NO.: 306-83-2CHEMICAL NAME: 1,1 Dichloro,2,2,2 TrifluoroethaneFORMULA: CHCl_2CF_3 ADDRESS: Allied-Signal Inc.
Engineered Materials Sector
P. O. Box 1139R
Morristown, NJ 07960CONTACT: Director, Product Safety Phone: 201-455-2052DATE OF CURRENT ISSUE: June 1990

24-Hour Emergency Number: 201-455-2000

FIRST AID MEASURES:

INHALATION: Immediately remove to fresh air. If breathing has stopped give artificial respiration. Use oxygen as required, provided a qualified operator is available. Call a physician. Do not give epinephrine (adrenaline).

EYES: Immediately flush eyes with large amounts of water for at least 15 minutes [in case of frostbite, water should be lukewarm (not hot)], lifting eyelids occasionally to facilitate irrigation. Get medical attention if symptoms persist.

SKIN: Promptly flush skin with water until all chemical is removed. If there is evidence of frostbite, bathe (do not rub) with lukewarm (not hot) water. In the absence of water, cover with soft wool or similar covering. Call a physician.

INGESTION: If conscious, immediately give 2 to 4 glasses of water and induce vomiting by touching finger to back of throat. Call a physician.

HAZARDS INFORMATION:

PERMISSIBLE CONCENTRATION: AIR. No OSHA/PEL or ACGIH/TLV established.

Based on currently available data, Allied-Signal would estimate that when established the TWA for HCFC-123 will be in the 50-100 ppm range.

HCFC-123 toxicity is still relatively low order of to animal tests. Care needs to

140

Results to date suggest a acute and repeated exposure maintain exposures in the

HAZARDS INFORMATION

50-100 ppm range to avoid the depression of the central nervous system with the accompanying anesthetic effects. These effects, though transient, raise the question of alertness when working around machinery.

INHALATION: HCFC-123 is a weak anesthetic. When oxygen levels in air are reduced to 15-17%, symptoms of asphyxiation, loss of coordination, increased pulse rate and deeper respiration will also occur. It should be noted that at concentrations which cause these symptoms there will be deep anesthesia.

Many refrigerant gases have been demonstrated to induce cardiac sensitization to epinephrine and to induce cardiac arrhythmias. HCFC-123 may produce these effects at high exposures or in the presence of injected epinephrine. HCFC-123 has the potential to produce arrhythmia at concentrations of 2% or above.

INGESTION: Discomfort in the gastrointestinal tract would result from the rapid evaporation (perhaps boiling) of the material, as liquid, and consequent evolution of gas. In addition, some of the effects of inhalation might be expected.

SKIN: Irritation could result from a defatting action on tissue.

EYES: Liquid contact can cause irritation, which may be severe. Mist may irritate. Tests indicate HCFC-123 to be a mild irritant, causing temporary corneal opacity.

ADDITIONAL INFORMATION:

- (1) LCLo (mouse): 14% (140,000 ppm)/4 minutes
- (2) Toxicity testing (various sources) indicate HCFC-123 to be neither mutagenic nor teratogenic.
- (3) Reported LC50 (rat); 3.2% (32,000)/4 hours. 30 min LC50 (mice) = 7.4% (74000 ppm)
- (4) Median anesthetic concentration (mice) indicate prostration at 20,000 ppm, reduced response to noise at 5000; NOEL @ 1000 ppm.
- (5) In a 90-day study (rats) at 1000 ppm weight loss was observed and, at higher levels, mild liver enlargement has been reported in rats and dogs.
- (6) Cardiac Sensitization - EC50 = 19000 ppm
Dermal LD50 > 2000 mg/Kg

FIRE AND EXPLOSION: FLASH POINT: N.A - No flash point.

AUTO IGNITION: Unknown, probably not applicable.

FLAME LIMITS: (In air (% by vol.)) None

PERSONAL PROTECTIVE EQUIPMENT

OTHER CLOTHING AND EQUIPMENT:

Wear impervious boots in case of spillage or leakage, or if there is the probability of repeated or prolonged contact with liquid product. High dose-level warning signs are recommended for areas of potential exposure. Provide eyewash stations and quick-drench shower facilities at convenient locations. For tank cleaning operations, see OSHA regulations.

PHYSICAL DATA

HCFC-123 is a liquid at normal temperatures.

Appearance: Clear colorless liquid and vapor with a faint ethereal odor

Boiling Point: 27.9°C (82.2°F) @ 760 MM HG

Freezing Point: -107°C (-160.6°F)

Vapor Pressure: 11 psia (20°C) (68°F)

Vapor Density: (Air = 1) 3.6

% Volatiles by volume @ 20°C (68°F) = 100

Solubility in Water : 0.21% (wt) @ 70°F

REACTIVITY DATA

In storage the product is stable. However, in some applications, particularly when HCFC-123 is heated to high temperature in presence of some refrigeration lubricants, polyols and metals, toxic by-products may develop. Care must be taken to maintain exposure to HCFC-123 in the 50 - 100 ppm (v/v) in air to avoid exposure to these by-products.

CONDITIONS TO AVOID

Sources of high temperature such as lighted cigarettes, flames welding, cutting torches or unit heaters should be avoided to prevent formation of toxic and/or corrosive by-products. By analogy with other HCFC's, welding or burning on equipment containing HCFC-123 may result in explosion.

INCOMPATIBILITY (MATERIALS TO AVOID)

(Under specific conditions: e.g., very high temperatures and/or appropriate pressures.)

Freshly abraded aluminum surfaces (may cause strong exothermic reaction).

Chemically active metals for example, sodium, potassium, calcium
Powdered aluminum, magnesium and zinc.

Plastics: "Freon-123" has a greater effect on plastics than does "Freon-113". Comparative data of effects of "Freon-123" and "Freon-113" on various plastics are given in Table VI.

Table VI. EFFECT OF "FREON-113" AND "FREON-123" ON VARIOUS PLASTICS

Plastic	"Freon-113"		"Freon-123"	
	A	B	A	B
"Alathon" 7050 linear polyethylene resin	0	1	0	1
"Alathon" 9140 polypropylene resin	0	2	0	2
"Delrin" acetal resin	0	0	0	1
Epoxy resin	0	0	0	0
Ethyl cellulose	-	-	4	4
"Kralastic" ABS polymer	0	0	4	4
"Lexan" polycarbonate resin	0	0	4	4
"Lucite" methyl-methacrylate resin (cast)	0	0	4	4
Polyvinyl alcohol	-	-	1	2
Polyvinyl chloride, unplasticized	0	1	0	1
"Styron" 475 polystyrene	2	4	4	4
"Teflon" TFE resin	0	0	0	2
"Zytel" 101 nylon resin	0	0	0	0

A - 4 hours at 75°F, B - 100 hours at 130°F

- 0 - Suitable for use in contact with the fluorocarbon.
 1 - Probably suitable for use.
 2 - Probably not suitable for use.
 3 - Not suitable for use.
 4 - Plastic disintegrated or dissolved in liquid.

Wire Coatings: "Freon-123" has a greater effect on wire coatings than does "Freon-113". Comparative data of effects of "Freon-123" and "Freon-113" on various wire coatings are given in Table VII.

Table VII. EFFECT OF "FREON-113" AND "FREON-123" ON WIRE COATINGS

Coating	"Freon-113"	"Freon-123"
Polyvinyl formal	0	0
Isocyanate-modified	0	0
Polyvinyl formal		
Nylon-coated	0	3
Polyvinyl formal		
Acrylic	0	1
Solderable acrylic	0	0
Terephthalate polyester	0	0
Polyurethane	0	1
Polyimide	0	0
Epoxy	0	0
Oleoresinous	0	4

Table V Ratings are:

- 0 - No crazing, stress cracking, or softening. No change in appearance of liquid.
- 1 - Very slight coating effect but coating cannot be scraped off. Very slight change in appearance of liquid.
- 2 - Slight effect on coating and coating can be removed with difficulty. Slight change in appearance of liquid.
- 3 - Moderate effect on coating and coating can be scraped off easily.
- 4 - Severe effect on coating with very easy removal of coating.

Ratings assigned on the basis of observations made immediately after removal from the solvent at end of test and after 4 days of air drying at 75°F under 10X magnification.


The coated wires (4 per test, 17 to 19 A.W.G. size) were tested by putting them in two ml of the indicated solvent in a sealed Pyrex tube and heating the tube to 130°F for 100 hours.

Metals: "Freon-123" under anhydrous conditions does not undergo decomposition at 130°F after 100 days exposure to steel 1020CR, SS 304, nickel, monel, copper, Al-25, zinc, and Mg. alloy FS-1. Under wet conditions, 1 volume percent water, "Freon-123" appeared suitable for use with SS 304, copper and Al-2S for 100 hours at the boiling point and only with SS 304 if used at 130°F for 100 days.

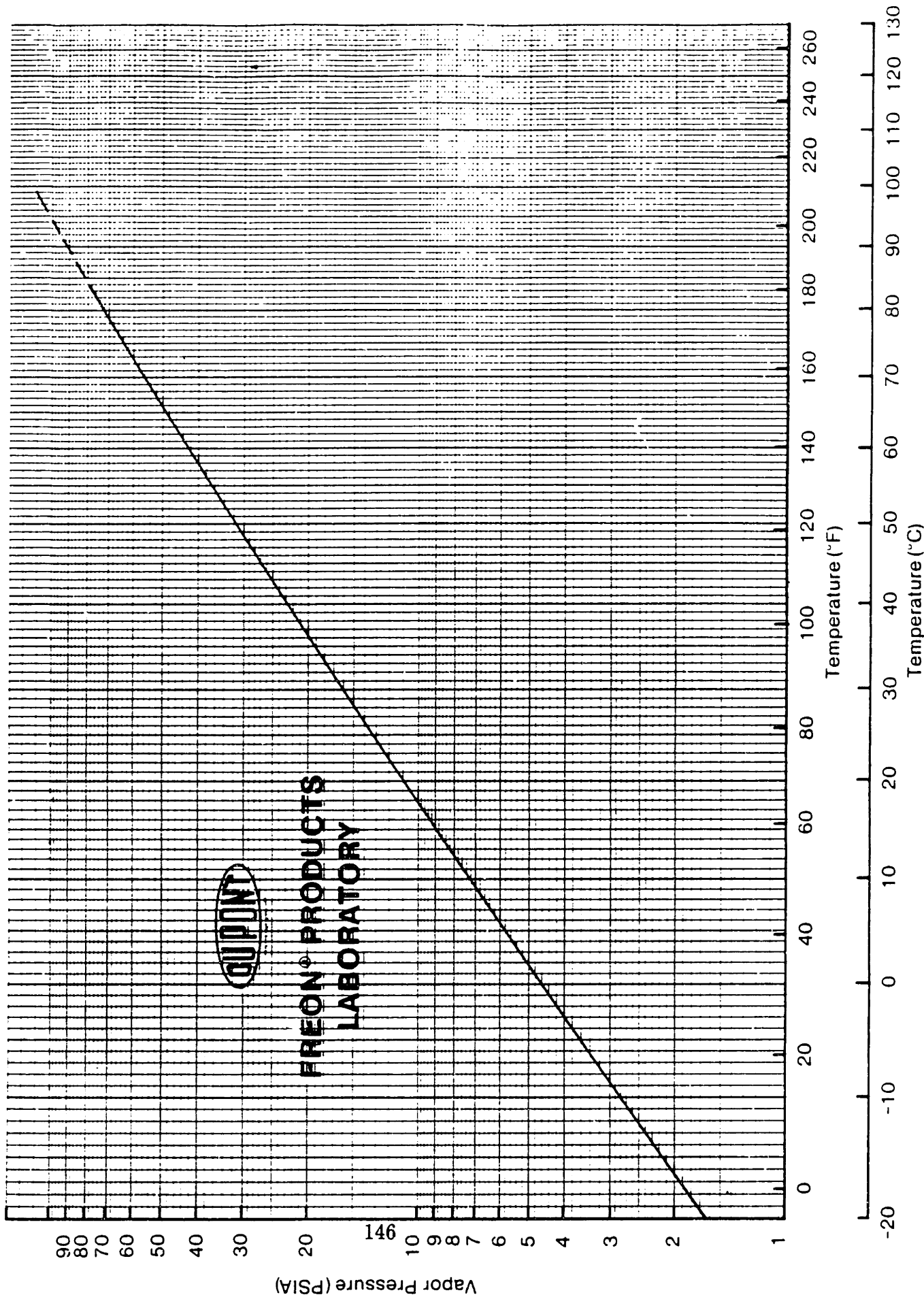
E. J. Bennett

SW

October 11, 1966



SATURATED VAPOR PRESSURE OF HCFC-123



Blank Page

A.2 HCFC-141b

Property Summary by Penwalt 1988

COMPARISON OF ISOTRON BLOWING AGENTS

1.	ISOTRON Blowing Agent	141b	11	142b	22
2.	Chemical Formula	CH ₃ CCl ₂ F	CCl ₃ F	CH ₃ CClF ₂	CHClF ₂
3.	Produced in Commercial Quantities	no	yes	yes	yes
4.	Suggested Replacements for:	R-11	-	R-12	R-12
5.	Molecular Weight	117	137.4	100.5	86.5
6.	Boiling Point(°F), 1 atm	89.6	74.9	14.4	-41.4
7.	Vapor Pressure (psia @ 70°F)	10	13.3	43.5	136.1
8.	Vapor, Specific Gravity ¹ air=1	4.0	4.7	3.5	3.0
9.	Liquid Density (lb/ft ³ @ 70°F)	77.5	92.72	69.93	75.47
10.	Thermal Conductivity (BTU/hr.ft°F) at 70°	0.0053 ²	0.0045	0.0064 ²	0.0062
11.	Toxicity	incomplete	low	low	low
12.	Ozone Depletion Potential ⁴	≤0.05	1.0	≤0.05	0.05
13.	Greenhouse Potential ⁴	≤0.1	0.4	≤0.2	0.07
14.	Flash Point	none	none	none	none
15.	Flammable Limits (LEL/UEL, vol.%)	7/16	Non-flammable	6.9/15.5	Non-flammable
16.	Flammability Index ⁵	+3	-11	+3.2	-6
17.	%22 to give Nonflammable ⁶ Mixture	33 ⁷	--	35	-
18.	Diffusivity Through Polymer	low ²	low	low ⁷	low ⁷
19.	Reactivity with Ingredients	148 none ²	none	none ⁷	none
20.	Stability	stable ²	stable	stable	stable

MATERIAL SAFETY DATA SHEET

PENNWALT CORPORATION
THREE PARKWAY
PHILADELPHIA, PA 19102

EMERGENCY PHONE NUMBERS
BUSINESS EAST: 215-587-7779
BUSINESS WEST:
OTHER: #1: 502-395-7121

PRODUCT IDENTIFICATION

PRODUCT NAME: ISOTRON (R) 141b
CAS NO. 1717-00-6
CHEMICAL NAME: 1,1 DICHLORO-1-FLUOROETHANE
MOLECULAR FORMULA: CH3CC12F
SYNONYMS: CFC 141b
CHEMICAL FAMILY: HALOGENATED HYDROCARBONS

INGREDIENTS ----HAZARD CLASSIFICATIONS

COMPONENTS:	CAS NO.:	%	OSHA:	NFPA:
1,1 DICHLORO-1-FLUOROETHANE	1717-00-6	99.6	N/A	2-4-0

RESEARCH CHEMICAL - FOR USE ONLY BY OR UNDER DIRECT SUPERVISION OF
TECHNICALLY QUALIFIED PERSONS (AS DEFINED IN 40 CFR 710.2 (aa))

SHIPPING INFORMATION

NOT REGULATED WHEN SHIPPED BY LAND OR WATER. IF SHIPPED BY AIR: ORMA, NOS;
ORMA; NA 1693.

SHIPPING DESCRIPTION: REFRIGERANTS, N.O.I., LIQUID OR GAS.

PHYSICAL PROPERTIES

BOILING POINT/RANGE: 89.6°F/32°C
MELTING POINT: -103.5°C
FREEZING POINT: NE

MOLECULAR WEIGHT: 117
SPECIFY GRAVITY (H2O=1): 1.25 at 50F/10C
VAPOR PRESSURE: PSIA: 10 @ 68 F

VAPOR DENSITY (AIR=1): 4.0
SOLUBILITY IN H2O: SLIGHT
% VOLATILES BY VOLUME: 100

APPEARANCE AND ODOR:
COLORLESS LIQUID AND VAPOR WITH FAINT, ETHEREAL ODOR.

FIRE AND EXPLOSION DATA

FLASH POINT: NONE
FLAMMABLE LIMITS: LOWER: 7 UPPER: 16
AUTOIGNITION TEMP: NE

NA - NOT APPLICABLE
NE - NOT ESTABLISHED
(R) - INDICATES REGISTERED TRADEMARK OF PENNWALT CORPORATION

SPILL MANAGEMENT

KEEP UPWIND, EVACUATE ENCLOSED SPACE

EXHAUST VAPORS OUTDOORS OR BLANKET SPILL AREA WITH AN INERTING ATMOSPHERE. DISPERSE VAPORS WITH FLOOR LEVEL FORCED AIR VENTILATION OR WATER SPRAY. DO NOT ALLOW VAPORS TO ACCUMULATE IN LOW AREAS. DO NOT SMOKE. REMOVE FLAMES, HEATING ELEMENTS, GAS ENGINES, ETC.

DISPOSAL PROCEDURES

BEST TO RECYCLE OR RECLAIM, IF POSSIBLE. MAY BE INCINERATED IN OIL-FIRED FURNACE BUT TOXIC AND CORROSIVE COMBUSTION GASES MUST BE HANDLED.

CONSULT FEDERAL, STATE, OR LOCAL AUTHORITIES FOR PROPER DISPOSAL PROCEDURES.

MSDS PREPARED BY TOM DOYLE

THE ABOVE INFORMATION IS ACCURATE TO THE BEST OF OUR KNOWLEDGE. HOWEVER, SINCE DATA, SAFETY STANDARDS, AND GOVERNMENT REGULATIONS ARE SUBJECT TO CHANGE AND THE CONDITIONS OF HANDLING AND USE, OR MISUSE ARE BEYOND OUR CONTROL, PENNWALT MAKES NO WARRANTY, EITHER EXPRESS OR IMPLIED, WITH RESPECT TO THE COMPLETENESS OR CONTINUING ACCURACY OF THE INFORMATION CONTAINED HEREIN AND DISCLAIMS ALL LIABILITY FOR RELIANCE THEREON. USER SHOULD SATISFY HIMSELF THAT HE HAS ALL CURRENT DATA RELEVANT TO HIS PARTICULAR USE.

NA - NOT APPLICABLE

NE - NOT ESTABLISHED

(R) - INDICTES REGISTERED TRADEMARK OF PENNWALT CORPORATION

PRODUCT DATA



PENNWALT BUILDING THREE PARKWAY, PHILADELPHIA PENNSYLVANIA 19102

ISOTRON DEPARTMENT

ISOTRON 141b Foam Blowing Agent: Material Compatibility

Foam blowing agents come in contact with a variety of materials in the processing equipment as well as the finished foam. As new blowing agents are introduced as alternatives to CFC 11, material compatibility testing must be performed to determine any detrimental effects on plastics and elastomers in existing equipment, or on the final product itself.

ISOTRON 141b was compared to CFC 11 for the effect on common elastomers and plastics, refrigerator liner materials, and roofing membrane materials.

Procedure

- Select an appropriate pressure container (4 Oz. aerosol bottle)
- Cut sample pieces to uniform dimensions (plastics - 10 X 70 mm)
- Weigh samples (elastomers - 10 X 50 mm)
- For elastomers, clamp sample pieces to a wooden stick 70 mm long.
- Place pieces into bottles, cover with liquid (or add small amount of liquid for vapor contact), cap, and age at constant temperature for 2 wks
- Observe condition, open bottles, and measure sample pieces

<u>Material</u>	<u>CFC-11</u>			<u>ISOTRON 141b</u>		
	<u>% swell</u>	<u>% weight</u>	<u>appearance</u>	<u>% swell</u>	<u>% weight</u>	<u>appearance</u>
	(1)	(2)		(1)	(2)	
<u>Thermoplastics</u>						
Polystyrene	--	--	Dissolved	--	--	Dissolved
Polyethylene (Low)	7	37	Slight swell	4	17	No effect
Polypropylene	6	32	Slight swell	3	15	Sl. swell
PTFE	0	3	No effect	0	2	No effect
FEP	0	0	No effect	0	0	No effect
KYNAR PVDF	0	0	No effect	0	0	No effect
PVC	0	6	No effect	2	13	Slight curl
<u>Elastomers</u>						
Neoprene	17	65	Slight swell	17	55	Sl. swell
Butyl	33	186	Swelled	22	93	Swelled
Buna N	10	48	Slight swell	24	100	Swelled
Viton	5	13	Slight swell	16	44	Sl. swell
<u>Refrig. Liner (liq. + vapor)</u>						
High Impact Polystyrene	--	--	Dissolved	--	--	Dissolved
High gloss ABS	0	12	No effect	10	160	Very soft
<u>Roofing Membranes (vapor)</u>						
Bitumen	--	--	Dissolved on liquid contact	--	--	Dissolved liq. contact
PVC based	--	--	Twisted, brittle	--	--	Twisted, brittle
CPM based	0	--	Softened	0	--	Softened
EDPM based	5	--	Slight swell	5	--	Sl. swell
<u>Miscellaneous</u>						
Epoxy - 5 min	1	0	No effect	1	0	No effect
Epoxy - 2 hr	20	0	15% light curl	16	0	Sl. curl
Polyurethane coating		Removed				otherwise no effect

1 X swell = Percent increase in length of test piece
2 X weight = Percent increase in weight of test piece

Blank Page

Appendix B

Scanning Electron Microscope Photographs

Note: In the following figures
Parallel Diffusion = Perpendicular Facers.

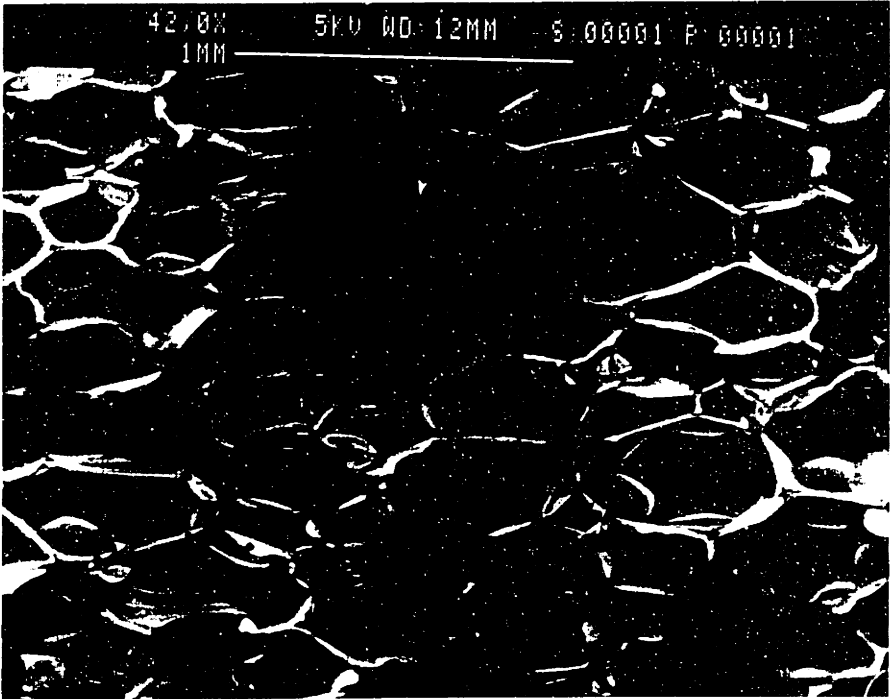
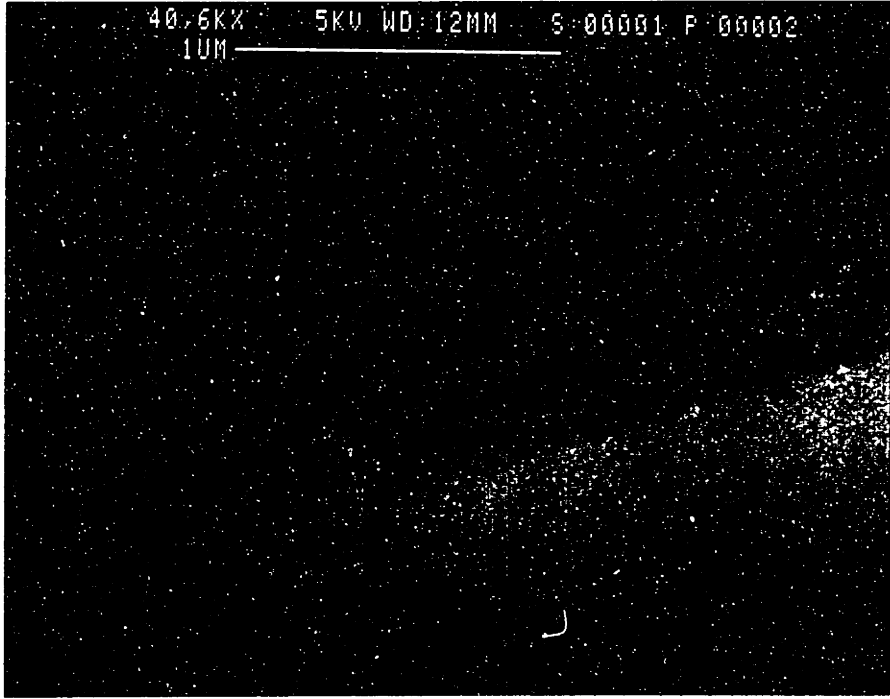


Figure B-1: S.E.M. Photographs Foam No. 1 Parallel Diffusion.

37.2KX 5KV WD:12MM S:00001 P:00004
1UM PERPENDICULAR

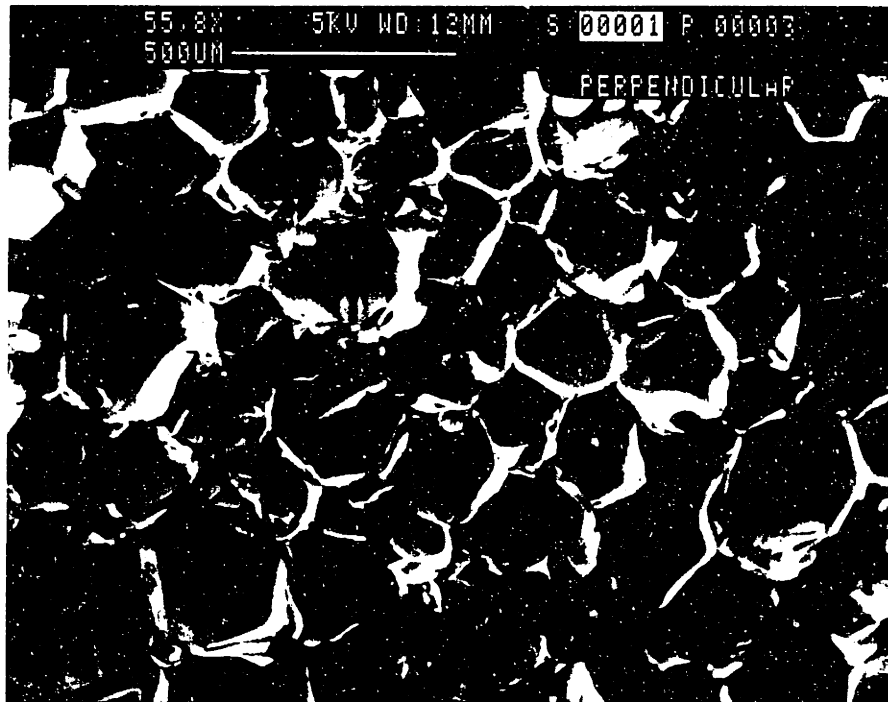
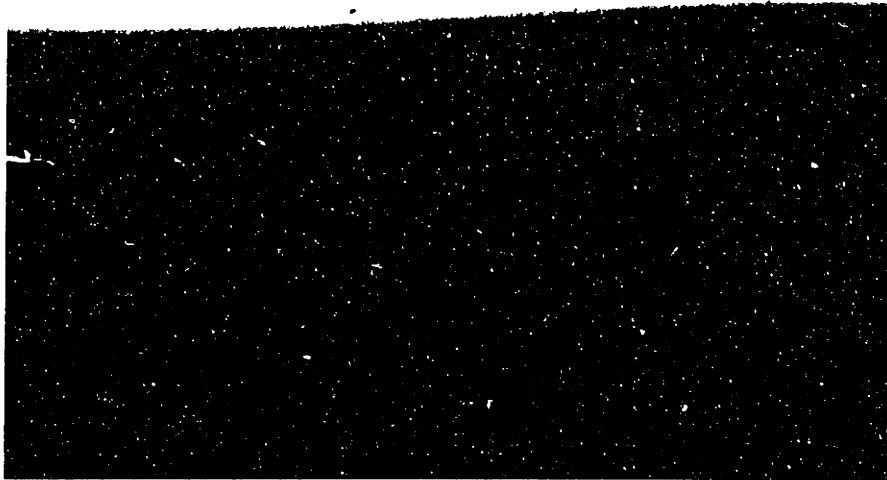


Figure B-2: S.E.M. Photographs Foam No. 1 Perpendicular Diffusion.

44.1KV 5KV WD 12MM S 00002 P 00002
1UM PARALLEL

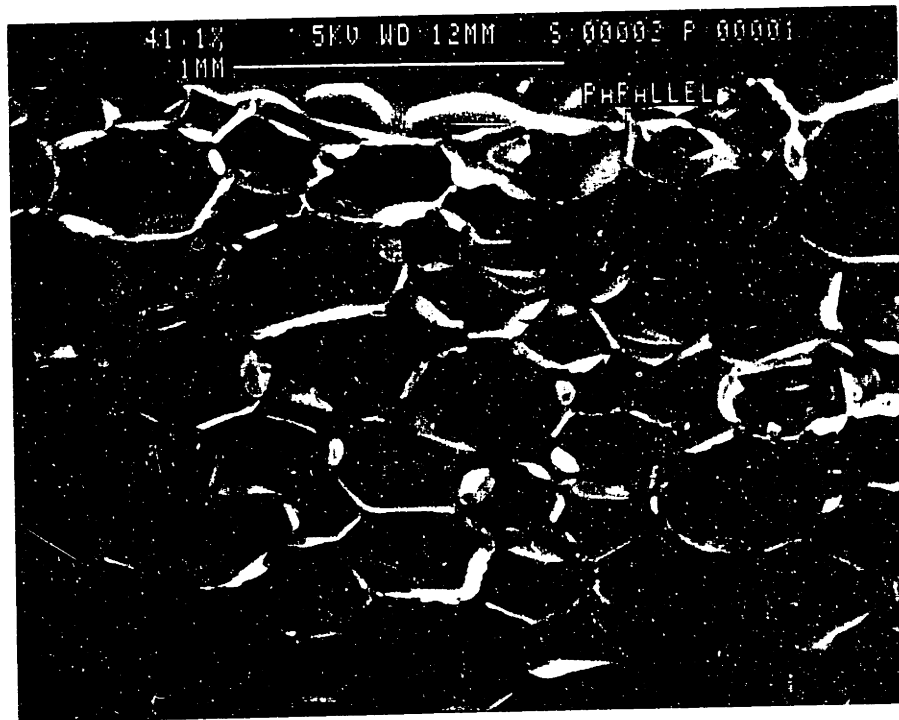
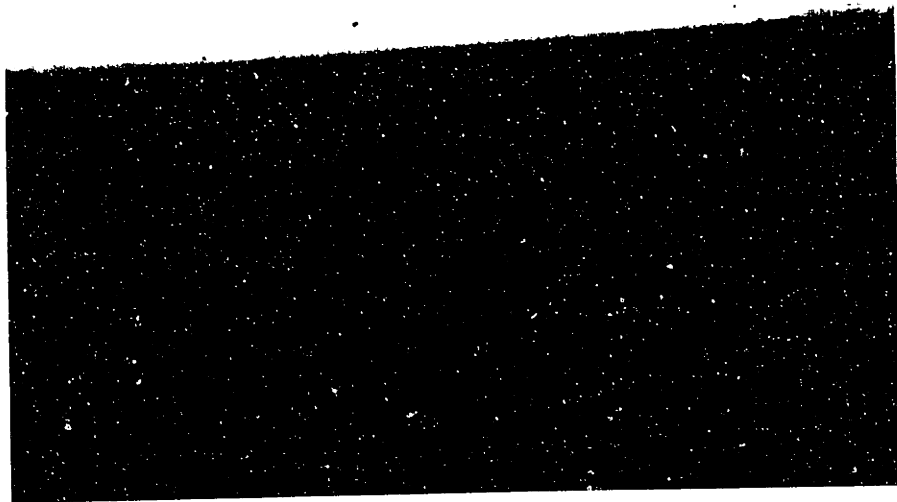


Figure B-3: S.E.M. Photographs Foam No. 2 Parallel Diffusion.

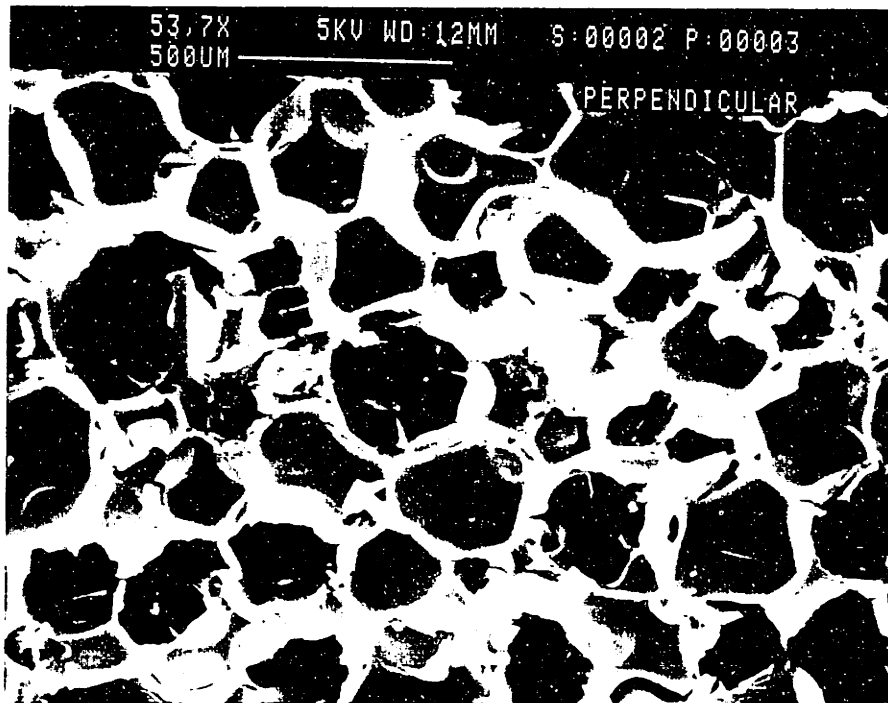
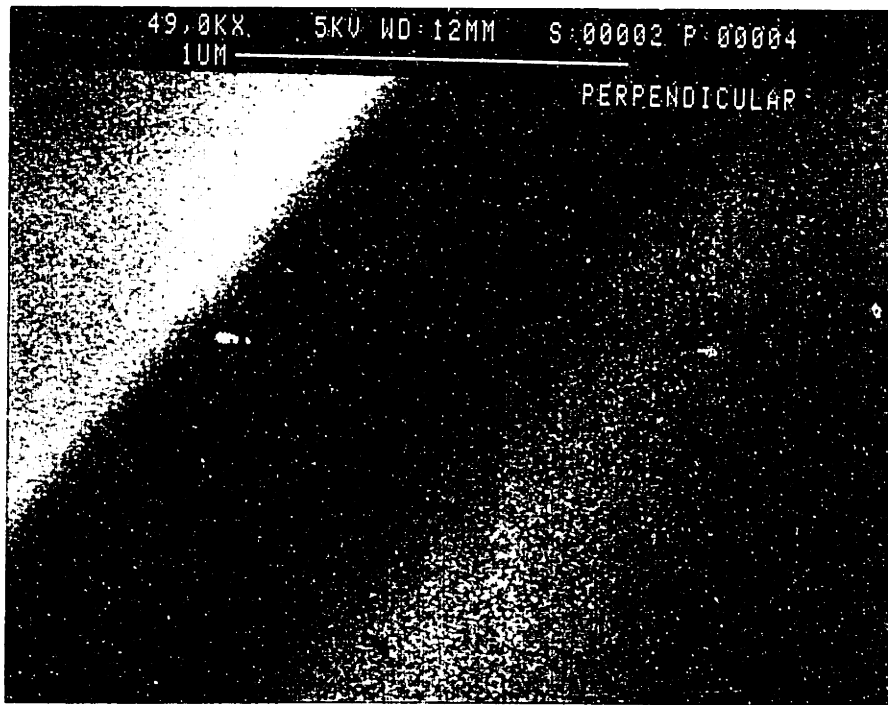


Figure B-4: S.E.M. Photographs Foam No. 2 Perpendicular Diffusion.

24.1KX * 5KV WD:11MM S:00014 P:00002
2UM

PARALLEL



30.9X 5KV WD:11MM S:00014 P:00001
1MM

PARALLEL



Figure B-5: S.E.M. Photographs Foam No. 14 Parallel Diffusion.

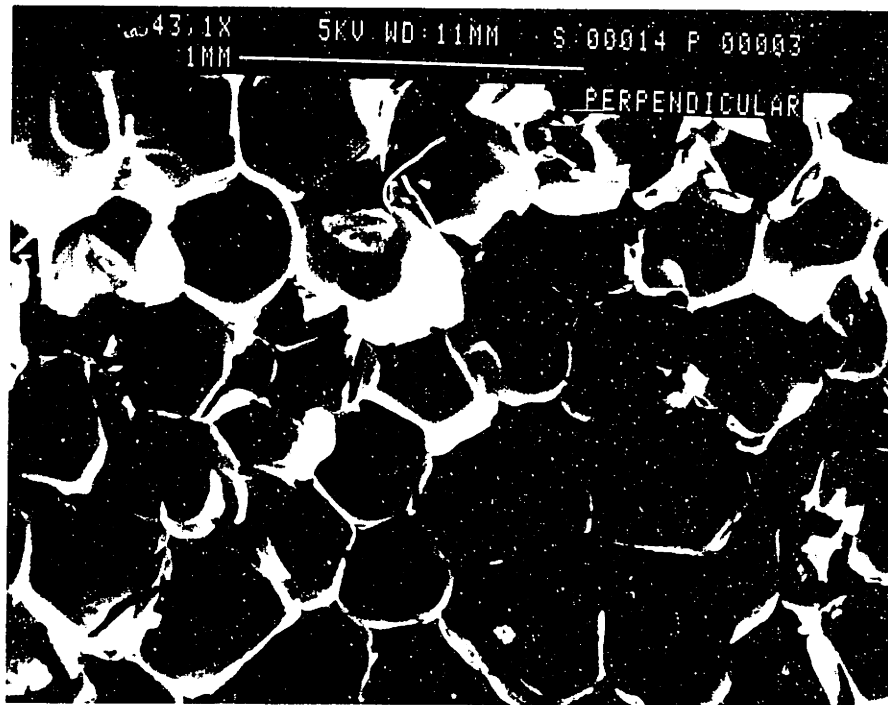
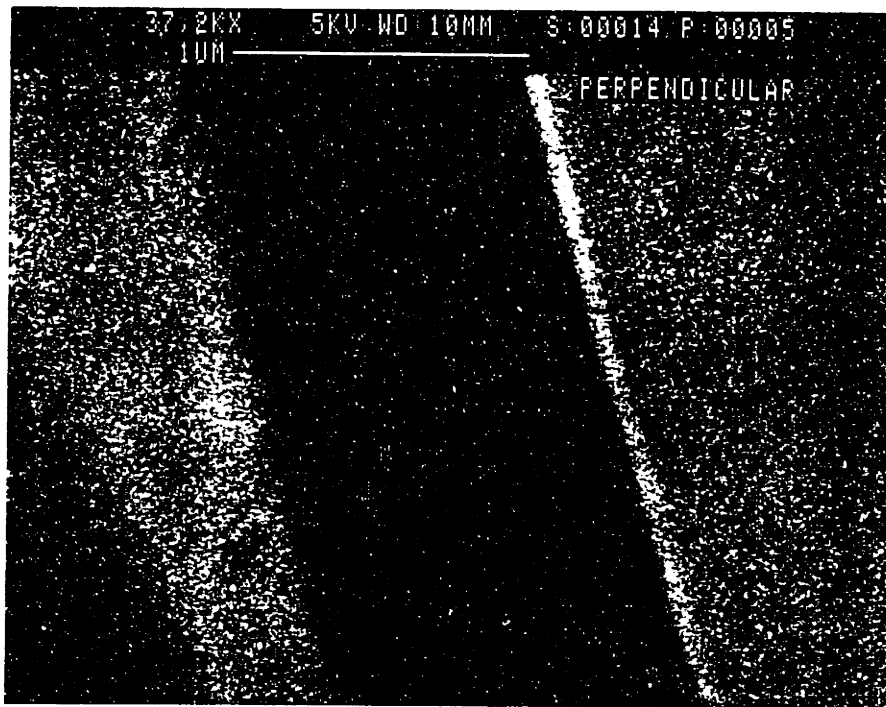


Figure B-6: S.E.M. Photographs Foam No. 14 Perpendicular Diffusion.

51.3KX 5KV WD:1.1MM 9:00015 P:00002
1UM PARALLEL

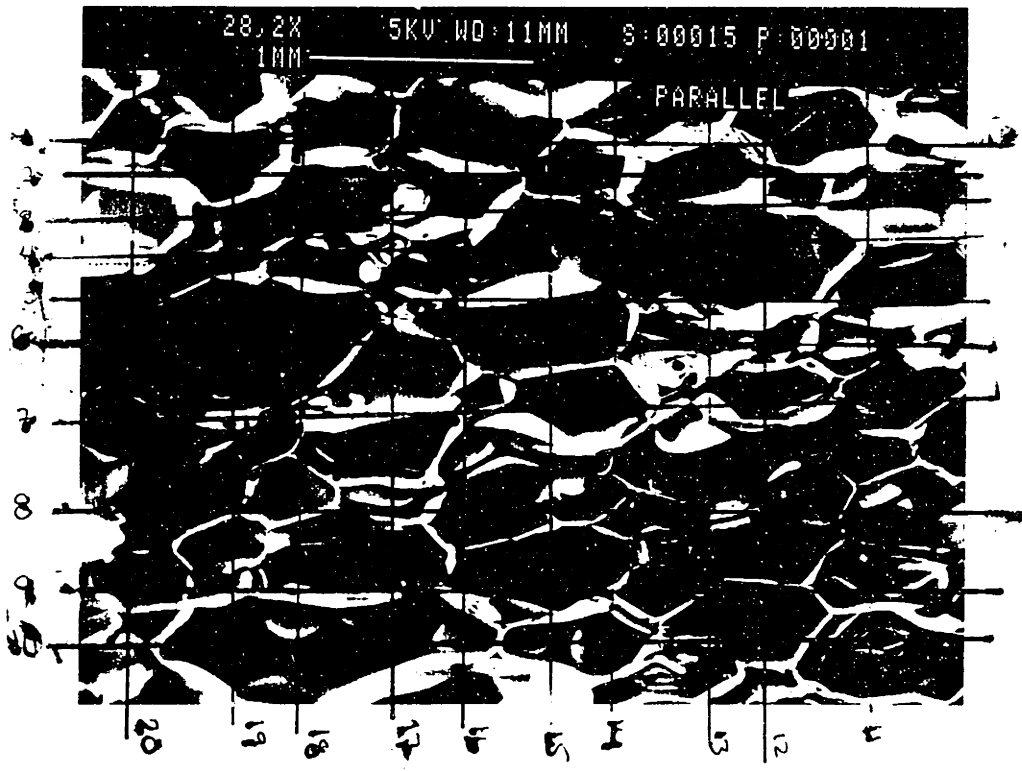


Figure B-7: S.E.M. Photographs Foam No. 15 Parallel Diffusion.

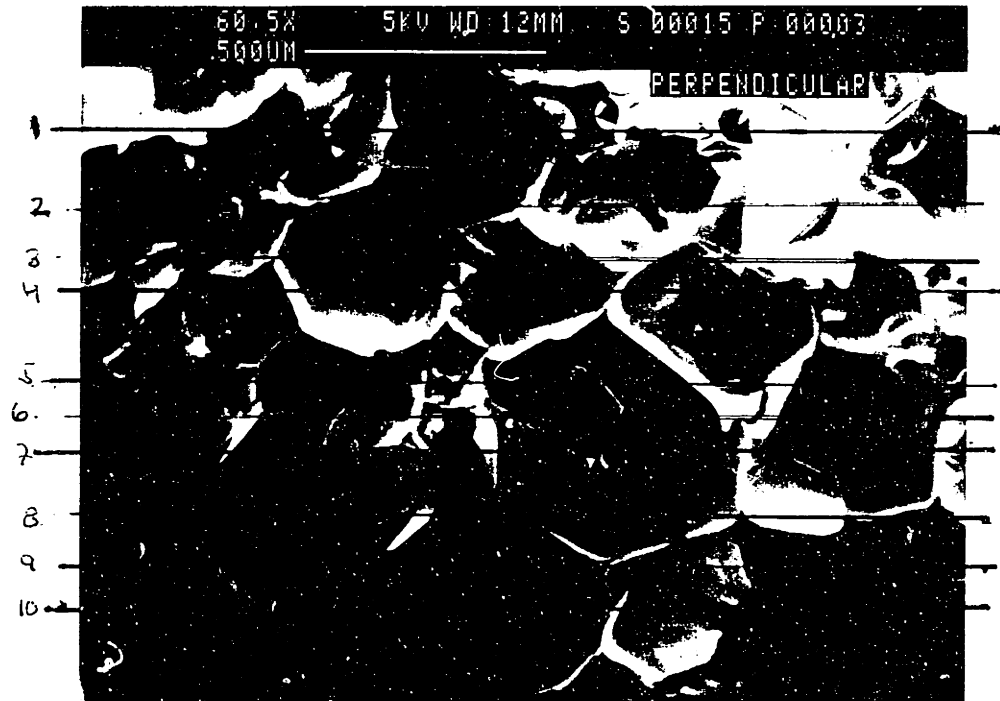
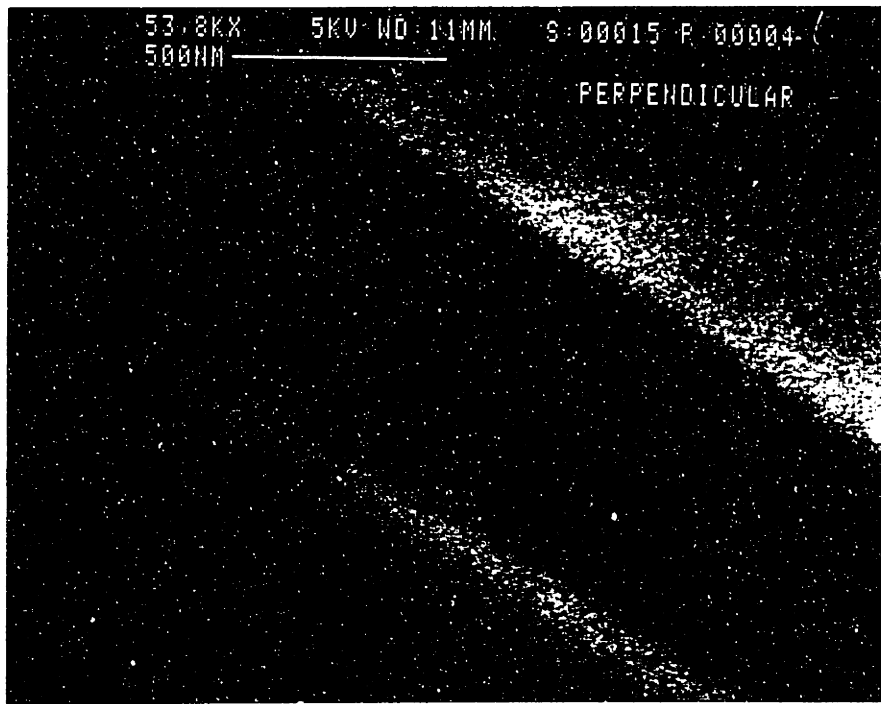


Figure B-8: S.E.M. Photographs Foam No. 15 Perpendicular Diffusion.

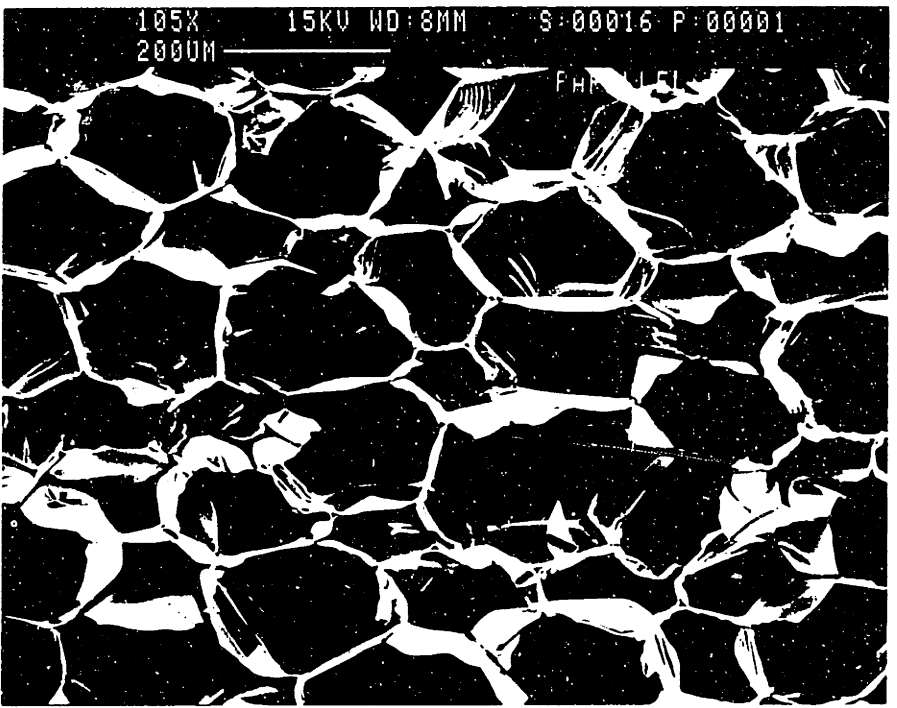
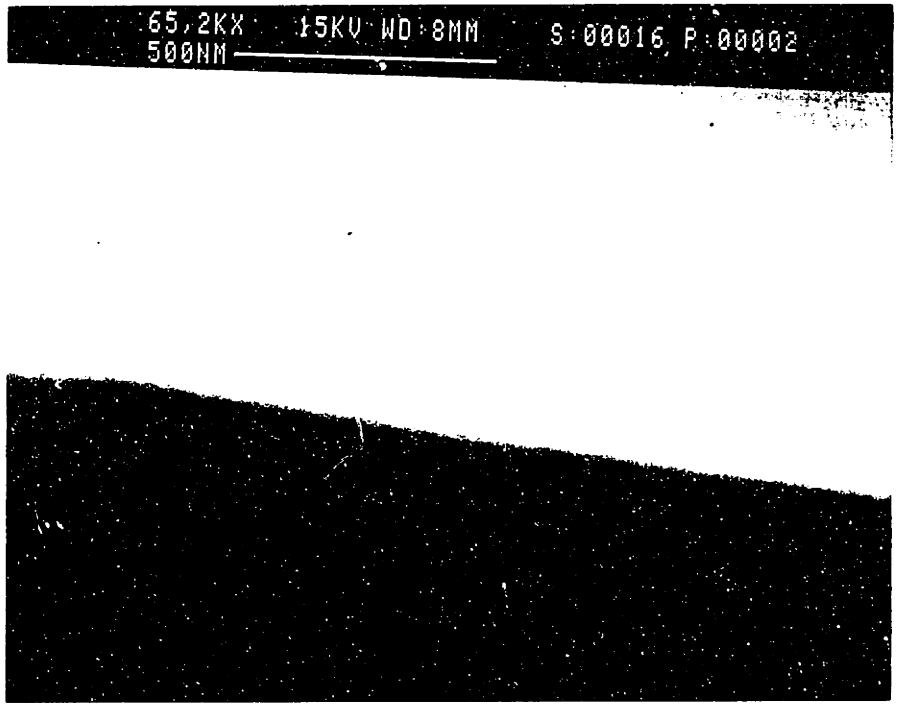


Figure B-9: S.E.M. Photographs Foam No. 16 Parallel Diffusion.

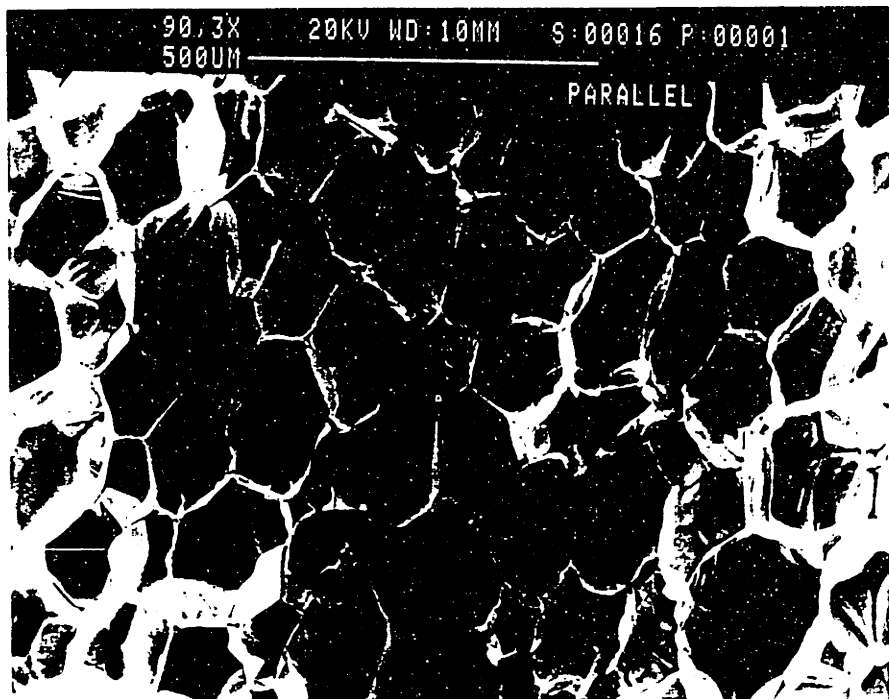


Figure B-10: S.E.M. Photographs Foam No. 16 Parallel Diffusion.

47.9KX 15KV WD:8MM S:00016 P:00004
1UM

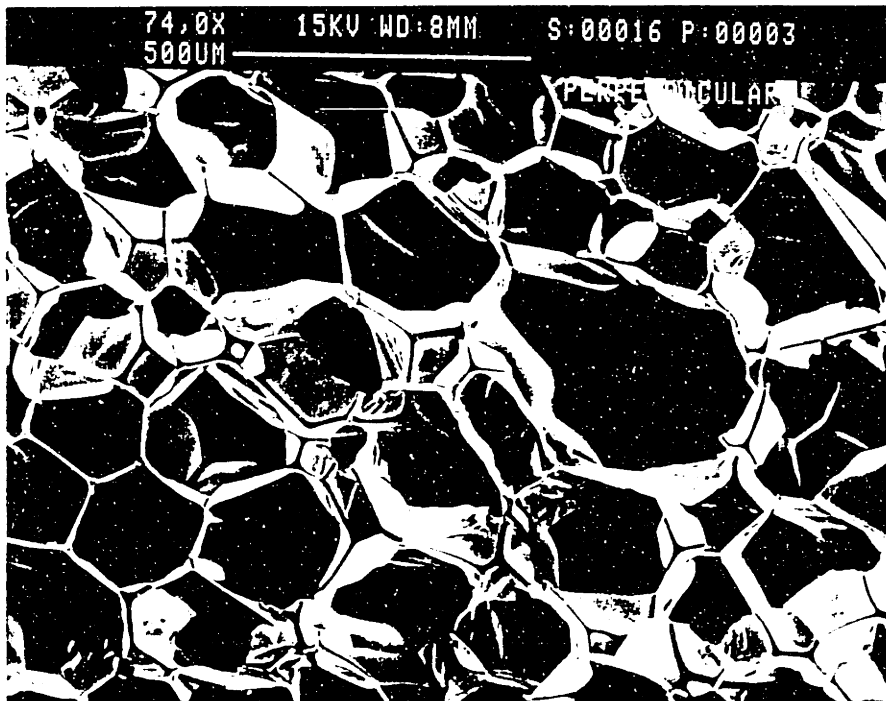


Figure B-11: S.E.M. Photographs Foam No. 16 Perpendicular Diffusion.

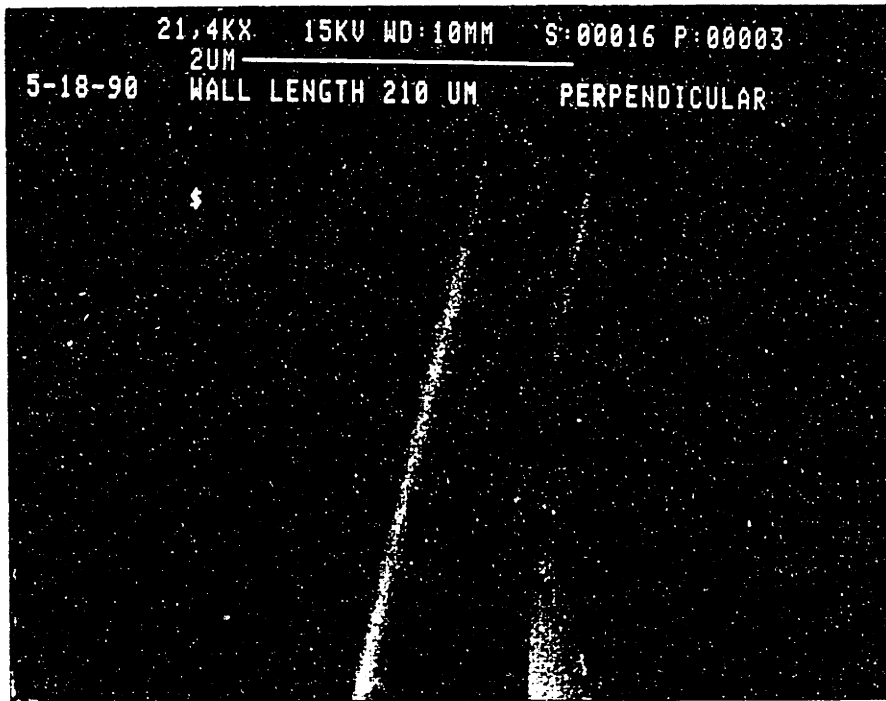


Figure B-12: S.E.M. Photographs Foam No. 16 Perpendicular Diffusion.

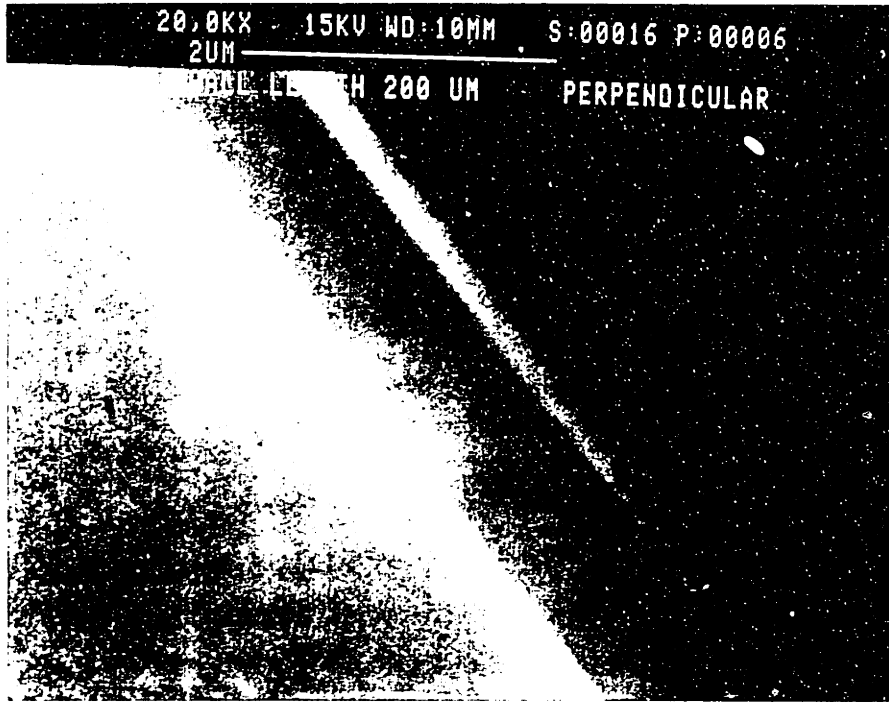


Figure B-13: S.E.M. Photographs Foam No. 16 Perpendicular Diffusion.

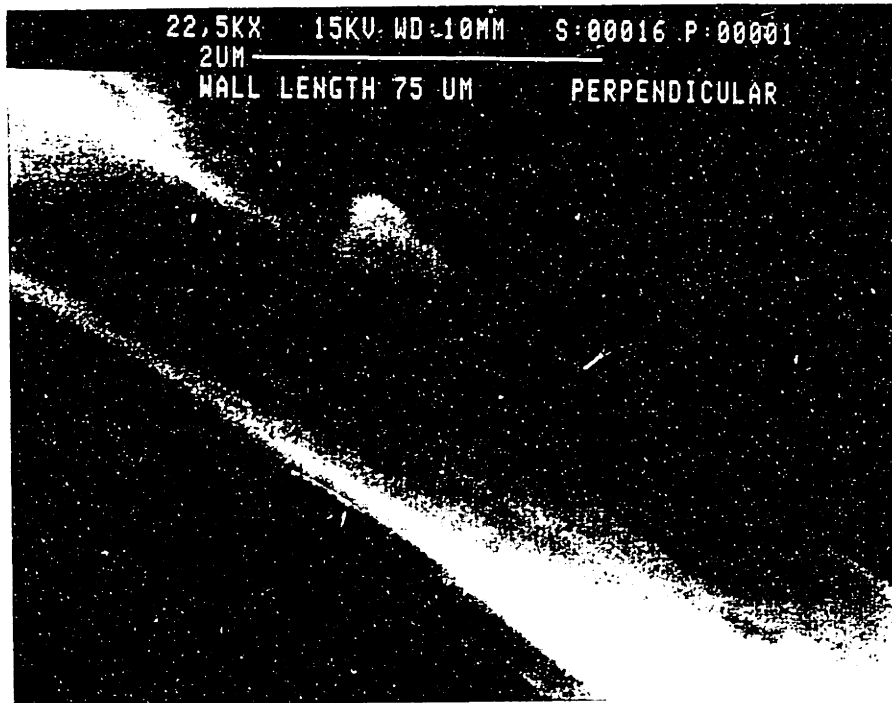


Figure B-14: S.E.M. Photographs Foam No. 16 Perpendicular Diffusion.

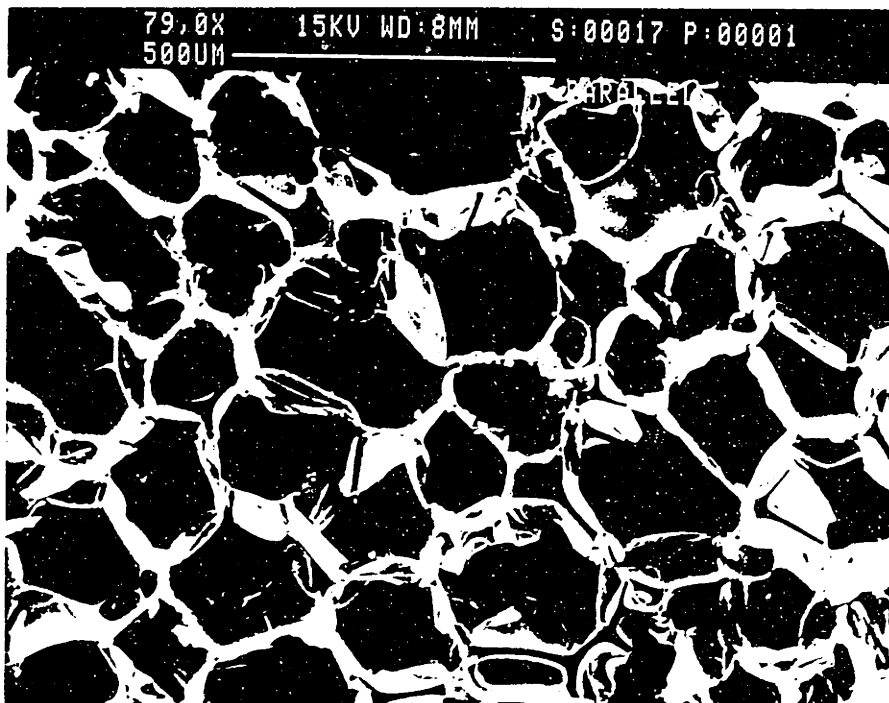
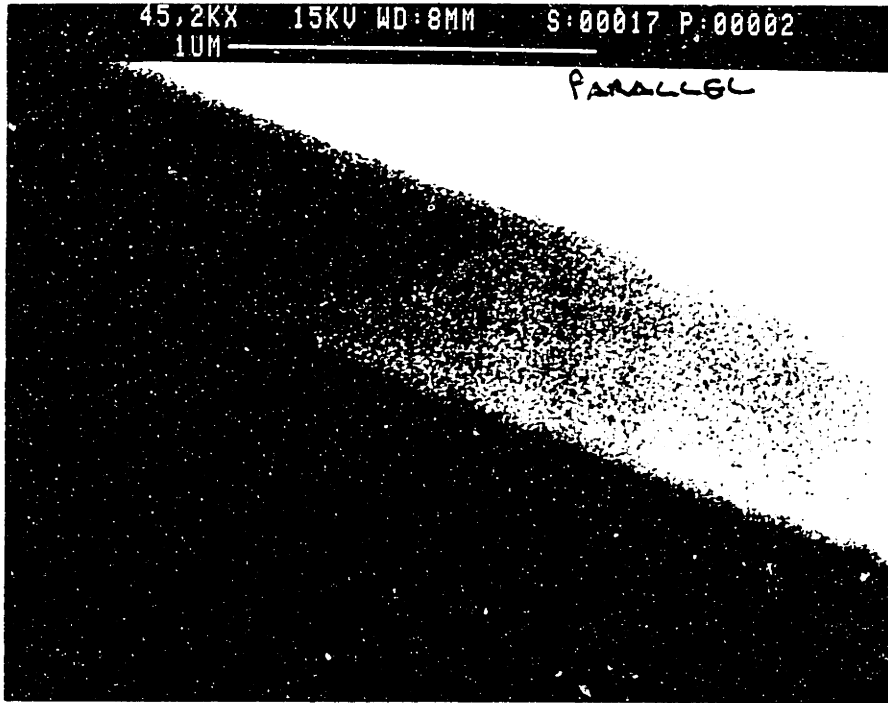


Figure B-15: S.E.M. Photographs Foam No. 17 Parallel Diffusion.

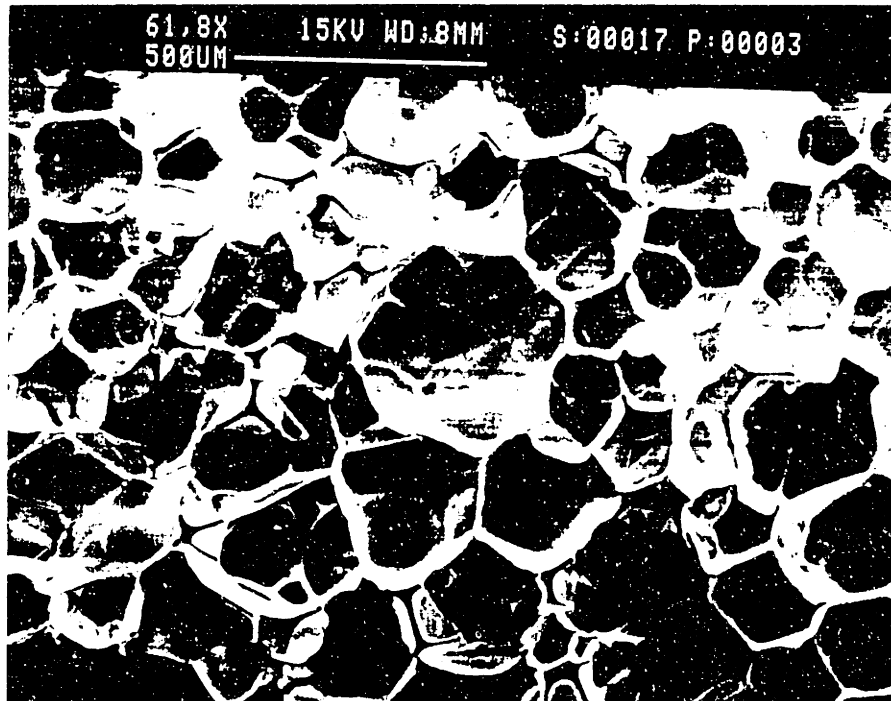
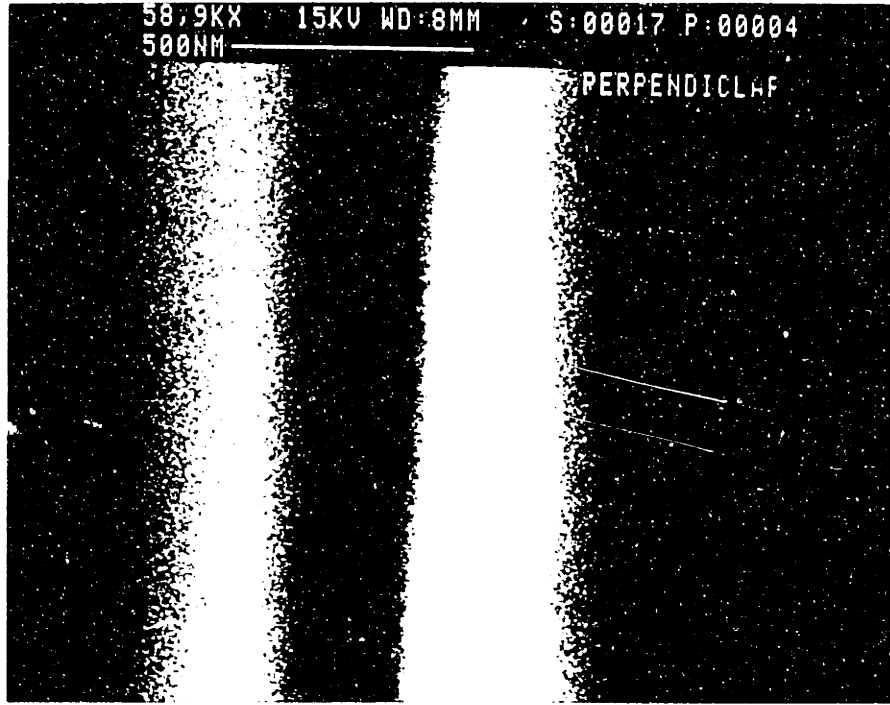


Figure B-16: S.E.M. Photographs Foam No. 17 Perpendicular Diffusion.

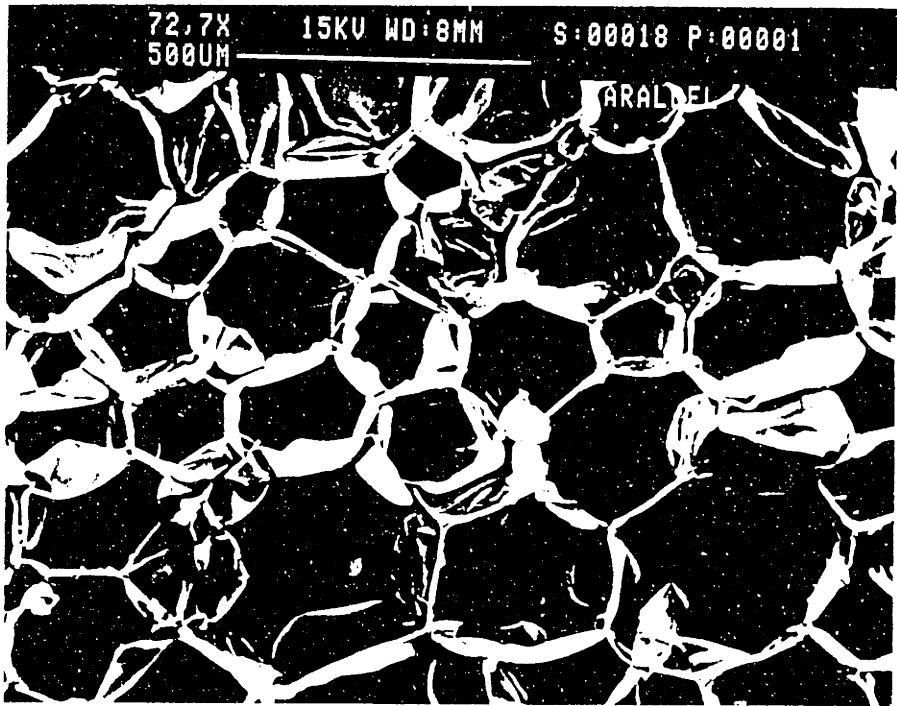
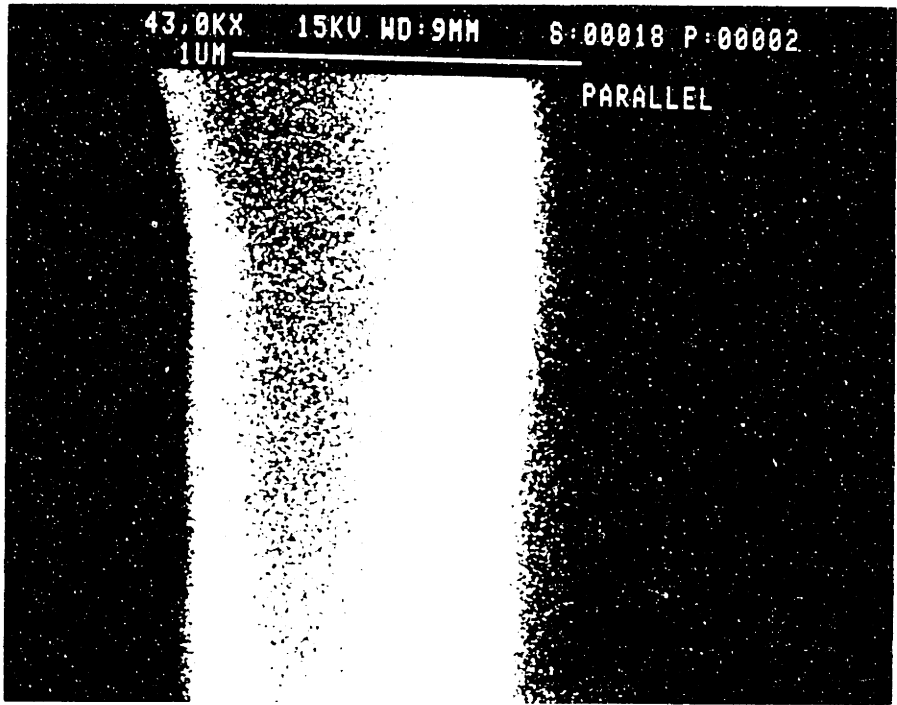


Figure B-17: S.E.M. Photographs Foam No. 18 Parallel Diffusion.

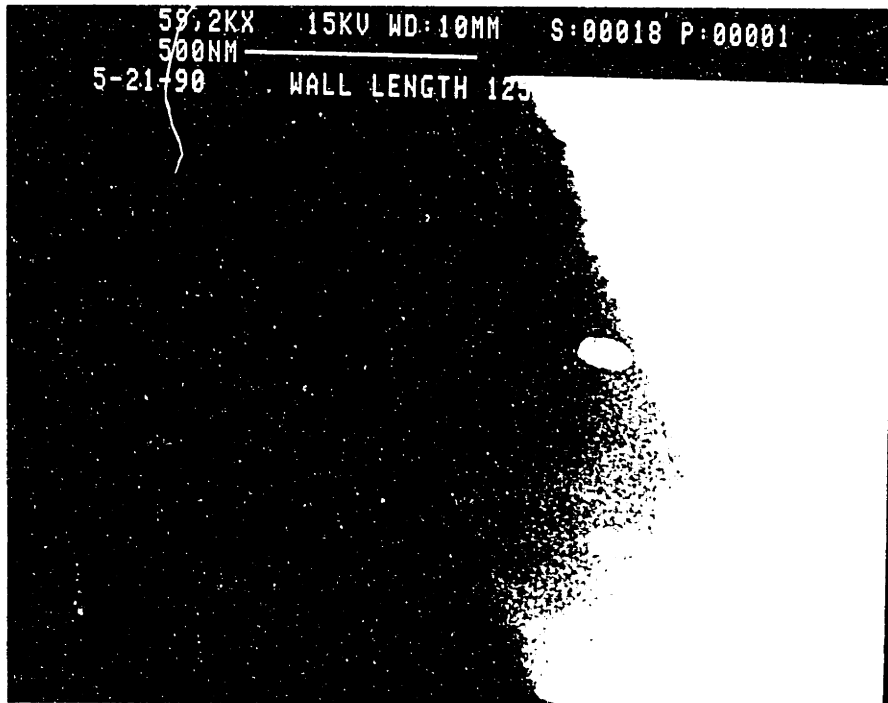
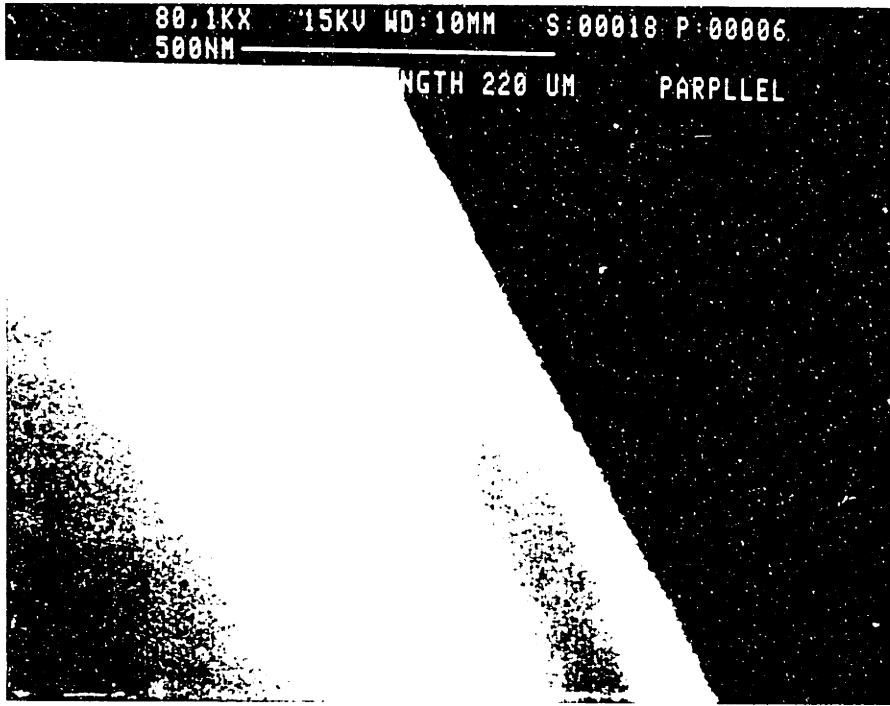


Figure B-18: S.E.M. Photographs Foam No. 18 Parallel Diffusion.

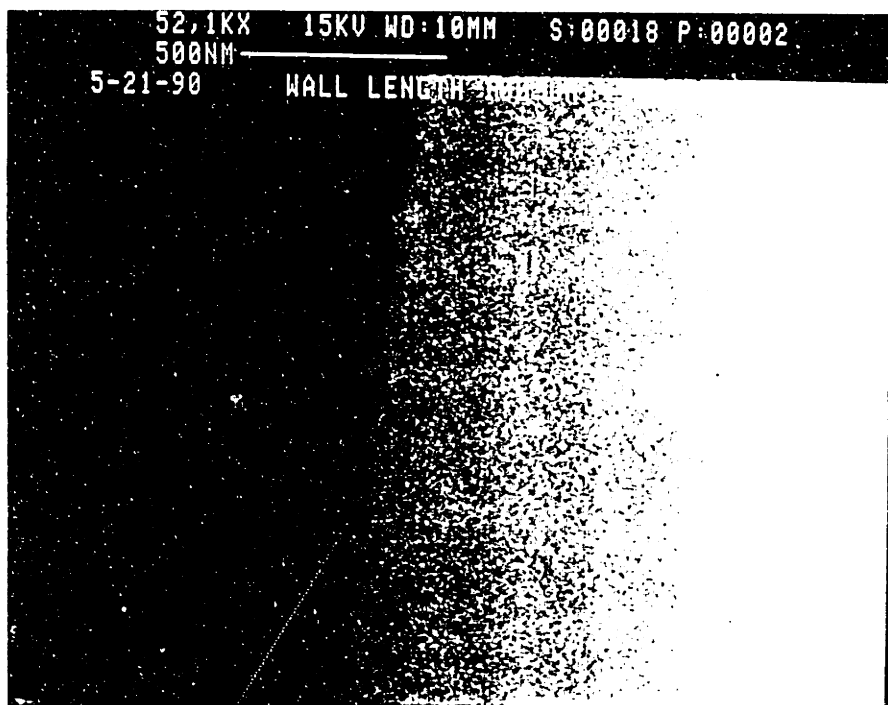
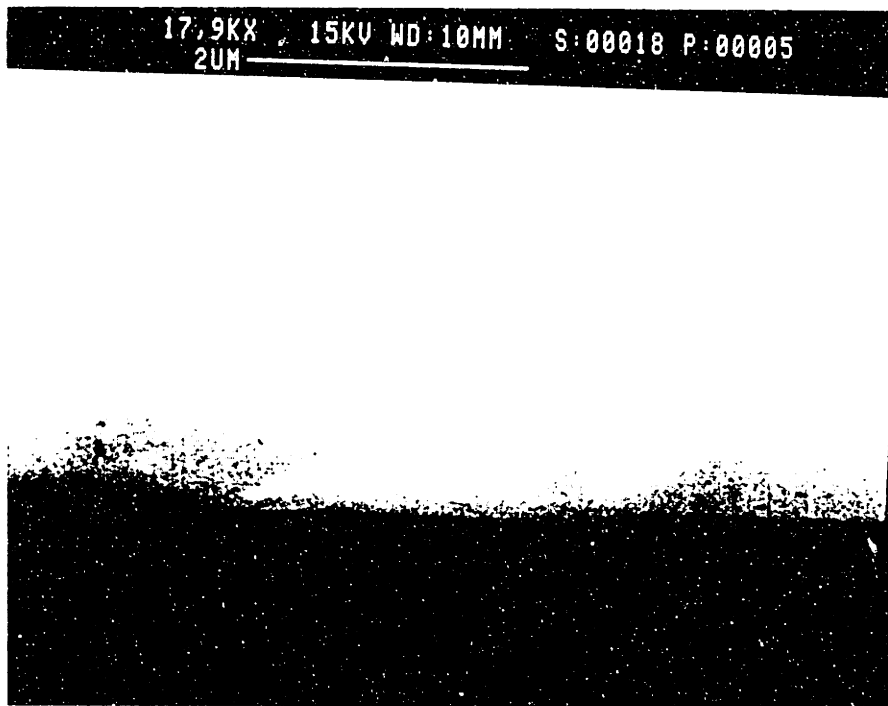


Figure B-19. S.E.M. Photographs Foam No. 18 Parallel Diffusion.

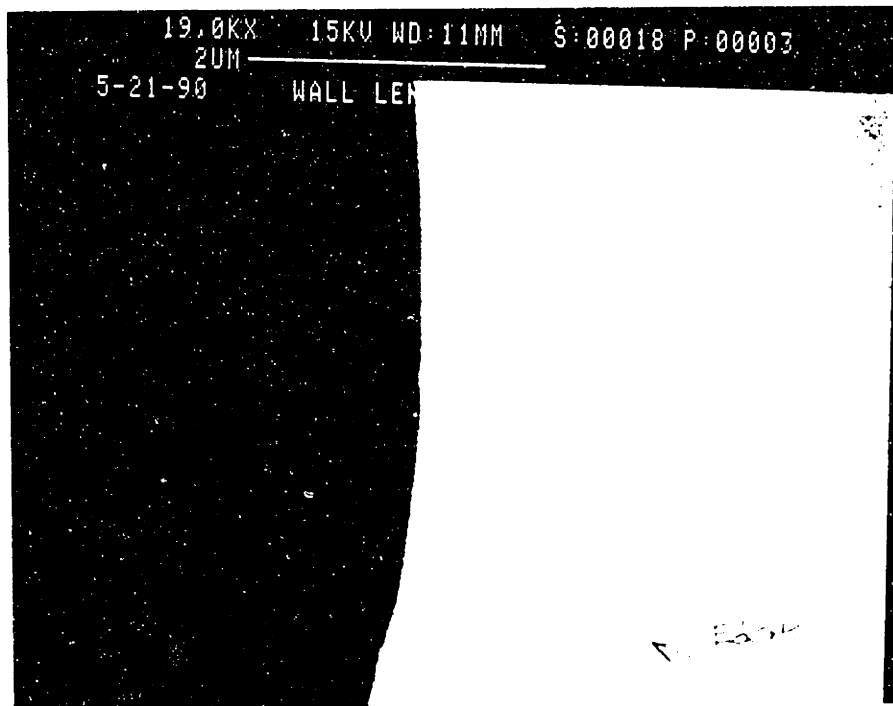


Figure B-20: S.E.M. Photographs Foam No. 18 Parallel Diffusion.

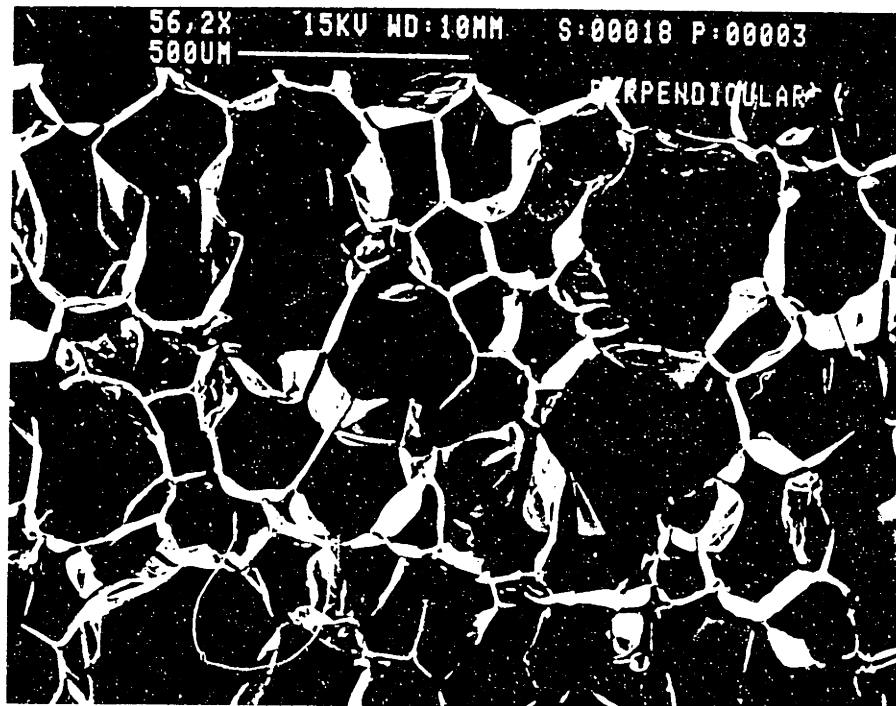
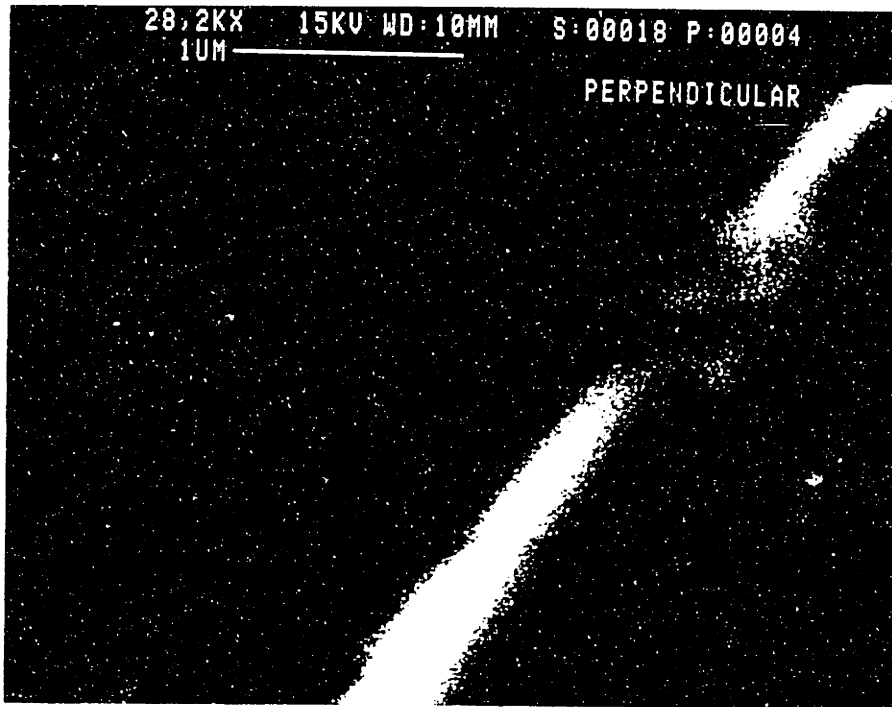


Figure B-21: S.E.M. Photographs Foam No. 18 Perpendicular Diffusion.

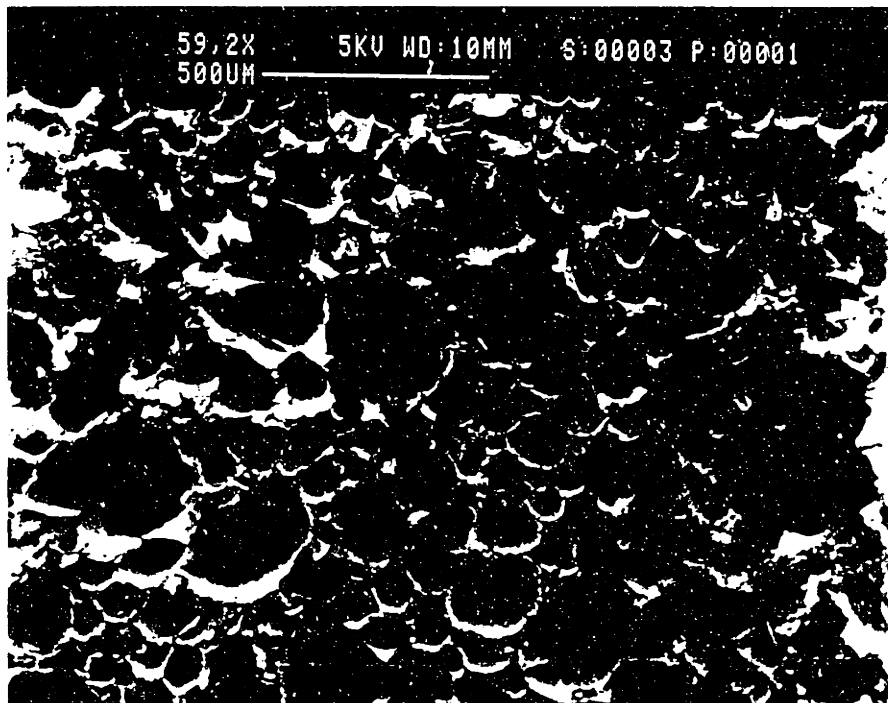
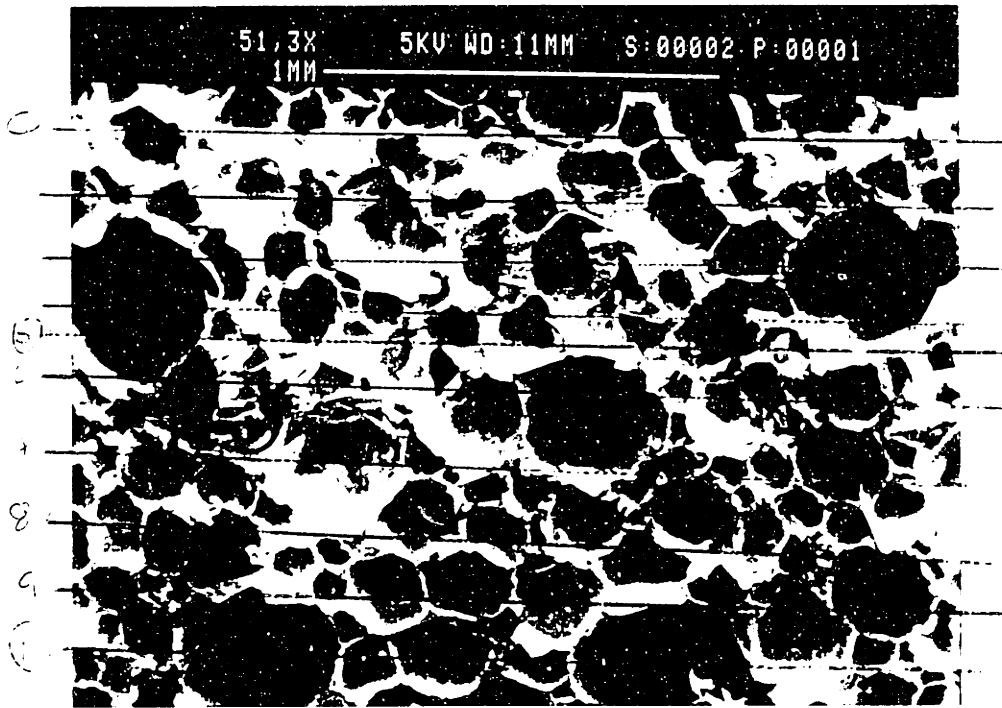


Figure B-22: S.E.M. Photographs Igloo Foam Parallel Diffusion.

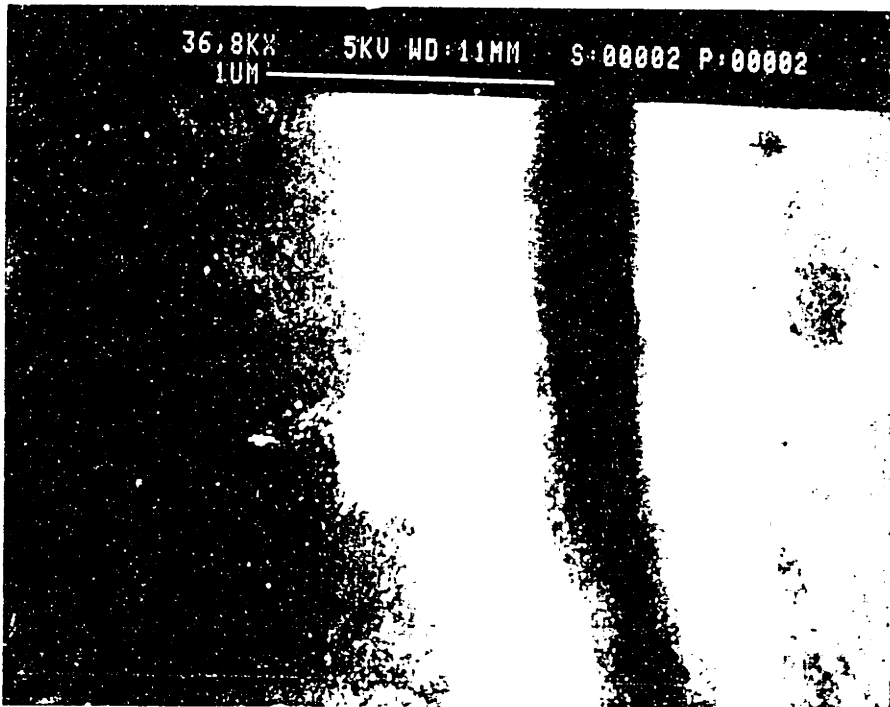
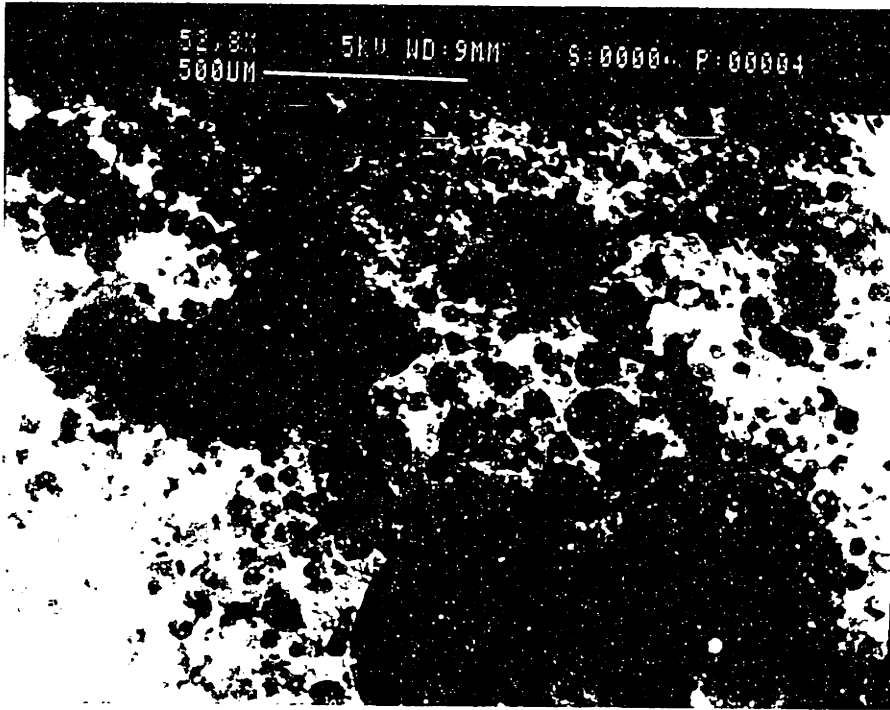


Figure B-23: S.E.M. Photographs Igloo Foam. Igloo Surface and Cell Wall

Appendix C

Foam Geometry Calculations

```

*****
*****
Foam Number 1
*****
Blowing Agent CFC-11
Density 1.920000 [lbs/ft^3]
Average cell wall thickness = 4.4500001E-04 [mm]
Void fraction = 0.9740541
*****
Photo # 1
parallel diffusion
parallel rise
*****
<l> avg.(parallel rise) = 0.3424653 [mm]
<l> avg.(perpendicular rise) = 0.1923628 [mm]
d (oct. parallel rise)= 0.6078759 [mm]
d (oct. perpendicular rise)= 0.3414440 [mm]
* * * * *
Sv = 9.419540 [mm** -1]
Ps = 16.15552 %
* * * * *
*****
Photo # 2
perpendicular diffusion
perpendicular rise
*****
<l> avg.(perpendicular rise) = 0.1883124 [mm]
d (oct. perpendicular rise)= 0.3342546 [mm]
* * * * *
Sv = 10.62065 [mm** -1]
Ps = 18.21555 %
* * * * *
** * * * *
Average for all photos
<l> avg.(parallel rise) = 0.3424653 [mm]
<l> avg.(perpendicular rise) = 0.1903376 [mm]
Sv = 9.506435 [mm** -1]
Ps = 16.30455 %
** ** * * * *

```


Foam Number 2

Blowing Agent CFC-11
Density 1.980000 [lbs/ft^3]
Average cell wall thickness = 5.0999998E-04 [mm]
Void fraction = 0.9732432

Photo # 1
parallel diffusion
parallel rise

<l> avg.(parallel rise) = 0.3137683 [mm]
<l> avg.(perpendicular rise) = 0.2037243 [mm]
d (oct. parallel rise) = 0.5569388 [mm]
d (oct. perpendicular rise) = 0.3616107 [mm]

Sv = 9.078651 [mm** -1]
Ps = 17.30442 %

Photo # 2
perpendicular diffusion
perpendicular rise

<l> avg.(perpendicular rise) = 0.2383858 [mm]
d (oct. perpendicular rise) = 0.4231347 [mm]

Sv = 8.389763 [mm** -1]
Ps = 15.99136 %

Average for all photos

<l> avg.(parallel rise) = 0.3137683 [mm]
<l> avg.(perpendicular rise) = 0.2210551 [mm]
Sv = 8.474077 [mm** -1]
Ps = 16.15206 %

Foam Number 15

Blowing Agent HCFC-123

Density 1.670000 [lbs/ft^3]

Average cell wall thickness = 4.7000000E-04 [mm]

Void fraction = 0.9774324

Photo # 1

parallel diffusion

parallel rise

<l> avg.(parallel rise) = 0.4999590 [mm]

<l> avg.(perpendicular rise) = 0.2719610 [mm]

d (oct. parallel rise)= 0.8874272 [mm]

d (oct. perpendicular rise)= 0.4827308 [mm]

Sv = 6.634634 [mm** -1]

Ps = 13.81752 %

Photo # 2

perpendicular diffusion

perpendicular rise

<l> avg.(perpendicular rise) = 0.2596083 [mm]

d (oct. perpendicular rise)= 0.4608047 [mm]

Sv = 7.703914 [mm** -1]

Ps = 16.04444 %

Average for all photos

<l> avg.(parallel rise) = 0.4999590 [mm]

<l> avg.(perpendicular rise) = 0.2657847 [mm]

Sv = 6.768871 [mm** -1]

Ps = 14.09708 %

Foam Number 16

Blowing Agent HCFC-123
Density 2.020000 [lbs/ft^3]
Average cell wall thickness = 7.6999998E-04 [mm]
Void fraction = 0.9727027

Photo # 1
parallel diffusion
parallel rise

<l> avg.(parallel rise) = 0.1542208 [mm]
<l> avg.(perpendicular rise) = 0.1021645 [mm]
d (oct. parallel rise)= 0.2737419 [mm]
d (oct. perpendicular rise)= 0.1813420 [mm]

Sv = 18.15889 [mm** -1]
Ps = 51.22251 %

Photo # 2
parallel diffusion
parallel rise

<l> avg.(parallel rise) = 0.1354222 [mm]
<l> avg.(perpendicular rise) = 9.7945660E-02 [mm]
d (oct. parallel rise)= 0.2403744 [mm]
d (oct. perpendicular rise)= 0.1738535 [mm]

Sv = 19.20738 [mm** -1]
Ps = 54.18010 %

Photo # 3
perpendicular diffusion
perpendicular rise

<l> avg.(perpendicular rise) = 0.1719102 [mm]
d (oct. perpendicular rise)= 0.3051406 [mm]

Sv = 11.63398 [mm** -1]
Ps = 32.81710 %

Photo # 4
perpendicular diffusion
perpendicular rise

<l> avg.(perpendicular rise) = 0.1704621 [mm]
d (oct. perpendicular rise)= 0.3025703 [mm]

Sv = 11.73281 [mm** -1]
Ps = 33.09587 %

Average for all photos

<l> avg.(parallel rise) = 0.1448215 [mm]
<l> avg.(perpendicular rise) = 0.1356206 [mm]

Sv = 14.54605 [mm** -1]
Ps = 41.03145 %

```

*****
*****
Foam Number 17
*****
Blowing Agent HCFC-123
Density 1.880000 [lbs/ft^3]
Average cell wall thickness = 5.5800000E-04 [mm]
Void fraction = 0.9745947
*****
Photo # 1
parallel diffusion
parallel rise
*****
<l> avg.(parallel rise) = 0.1660018 [mm]
<l> avg.(perpendicular rise) = 0.1635308 [mm]
d (oct. parallel rise)= 0.2946531 [mm]
d (oct. perpendicular rise)= 0.2902671 [mm]
* * * * *
Sv = 12.19106 [mm** -1]
Ps = 26.77631 %
* * * * *
*****
Photo # 2
perpendicular diffusion
perpendicular rise
*****
<l> avg.(perpendicular rise) = 0.2164360 [mm]
d (oct. perpendicular rise)= 0.3841739 [mm]
* * * * *
Sv = 9.240606 [mm** -1]
Ps = 20.29596 %
* * * * *
*****
Average for all photos
<l> avg.(parallel rise) = 0.1660018 [mm]
<l> avg.(perpendicular rise) = 0.1899834 [mm]
Sv = 10.85345 [mm** -1]
Ps = 23.83840 %
* * * * *

```

```

*****
*****
Foam Number 18
*****
Blowing Agent HCFC-141b
Density 1.760000 [lbs/ft^3]
Average cell wall thickness = 7.4699998E-04[mm]
Void fraction = 0.9762162
*****
Photo # 1
parallel diffusion
parallel rise
*****
<l> avg.(parallel rise) = 0.2346268 [mm]
<l> avg.(perpendicular rise) = 0.2100386 [mm]
d (oct. parallel rise)= 0.4164625 [mm]
d (oct. perpendicular rise)= 0.3728186 [mm]
* * * * *
Sv = 9.308012 [mm**(-1)]
Ps = 29.23454 %
* * * * *
*****
Photo # 2
perpendicular diffusion
perpendicular rise
*****
<l> avg.(perpendicular rise) = 0.2194827 [mm]
d (oct. perpendicular rise)= 0.3895819 [mm]
* * * * *
Sv = 9.112333 [mm**(-1)]
Ps = 28.61995 %
* * * * *
*****
Average for all photos
<l> avg.(parallel rise) = 0.2346268 [mm]
<l> avg.(perpendicular rise) = 0.2147607 [mm]
Sv = 9.143555 [mm**(-1)]
Ps = 28.71801 %
* * * * *

```

Appendix D

Apparatus Information and Calibrations

Puck Number	1	2	3	4
Transducer Type	Absolute	Absolute	Absolute	Differential
Mfr. Id. #	224227	224234	21659	
†	194488			
Chamber Height [cm]	0.72	0.777	0.742	0.732
Chamber Diameter [cm]	3.55	3.53	3.54	3.57
Reservoir Length [cm]	30.48			40
Reservoir Diameter [cm]	10.16			10.16
Typical Calibration				
Volts/psi	0.986	0.954	1.022	1.68
Temp. [°C]	80	80	80	21
Date	8-25-88	8-25-88	8-25-88	1-3-89

† Transducer changed in February 89.

Table D.1: Summary of Apparatus Hardware.

Blank Page

Puck Number	$N_{spacers}$	V_T [ml]	$(S_N / V_T)100$ [%]	N_m	Date
1	4	6.1	2.1	5	9-25-89
1	3 (Al)	6.507	2.25	3	7-6-89
1	3	6.38	1.7	3	8-7-89
1	0	8.25	1.7	9	3-27-90
2	5	5.26	0.8	4	9-25-89
2	1 (Al)	9.34	2.3	3	5-31-89
2	1	7.89	1.4	4	8-7-89
2	0	8.27	1.1	10	3-27-90
3	3	5.54	4.5	5	9-25-89
3	0	10.17	1.8	2	
3	0	8.69	0.54	9	3-27-90
4	4+shim [†]	5.19	1.3	4	11-30-89
4	4+shim [†]	5.8	1.46	5	1-23-90
4	4+shim [†]	5.99	3.	5	1-24-90
4 ^{††}	0	10.028	8.07	12	11-15-88
4	0	9.24	3.82	5	7-27-89
4	0	9.05	1.5	10	4-23-90
4	4	6.385	1.67	4	7-27-89

$N_{spacers}$ = Number of spacers in chamber.

S_N = Standard deviation of N_m number of measurements.

(Al) = aluminum spacers. Stainless steel spacers were used in the remainder of the tests.

Volumes: aluminum spacers= 0.623 cc; stainless steel spacers= 0.728 cc.

[†]Shims not measured.

[‡]Shims measured by volume displacement of alcohol in 0.5 ml graduated cylinder (0.1 ml divisions).

^{††} Measurement before volume reduction by shortening tubes.

Table D.2: Summary of Measurements, Chamber Total Volume Without Foam.

Blank Page

Appendix E

Supplementary Information on Tested Foams

Information in this section reproduced from Baumann and Szabat [30]
with the author's permission.

FOAM
16

Table 5 Comparative properties of PIR laminates blown with CFC-11, HCFC-123, and HCFC-141b

<u>FORMULATION, PPM</u>				
Stepanpol PS-2852	95	95	95	95
Pluracol 975	5	5	5	5
Silicone surfactant DC-193	3	3	3	3
Potassium Hex-Cem 977	2.8	2.8	2.8	2.8
CFC-11	43	43	--	--
HCFC-123	--	--	53	--
HCFC-141b	--	--	--	35
Mondur MR	177	--	--	177
Mondur MR200	--	179	179	--
Isocyanate Index	(250)	(250)	(250)	(250)
% CFC or HCFC in total system	(13.2)	(13.1)	(15.7)	(11.0)
<u>PHYSICAL PROPERTIES</u>				
Type of Facer	Alum. foil	Alum. foil	Alum. foil	Alum. foil
Laminate nominal thickness	2	2	2	2
Density, pcf				
In-place	1.90	1.85	1.85	1.86
Core	1.67	1.77	1.77	1.75
Closed cells, %	90	90	90	89
Compressive strength (parallel) at 10% deflection, psi				
Product	14.7	13.8	6.6	12.6
Core	17.3	17.7	9.7	14.9
Moisture vapor transmission, perm-in.	3.0	--	--	2.91
Dimensional Stability, % Vol. Change				
28 days at 70°C/100% R.H.	6.3	6.9	12.4	7.5
28 days at 100°C/amb. R.H.	3.4	4.5	8.5	5.2
28 days at -30°C/amb. R.H.	0.2	1.1	-0.4	-0.3
K-factor, BTU-in/hr. ft. ² °F				
@ R.T./amb. R.H., faced boardstock	<u>01.90°</u>	<u>01.85°</u>	<u>01.65°</u>	<u>01.82°</u>
Initial	0.119	0.116	0.118	0.113
12 months	--	0.142	0.122	0.131
18 months	<u>0.134</u>	--	--	--
Δ K, %	+ 12.60	+ 22.40	+ 3.40	+ 15.9
@ R.T./amb. R.H., unfaced boardstock	<u>01.90°</u>	<u>01.85°</u>	<u>01.63°</u>	<u>01.61°</u>
Initial	0.115	0.105	0.112	0.114
12 months	--	0.144	0.168	0.145
18 months	<u>0.142</u>	--	--	--
Δ K, %	+ 23.5	+ 37.1	+ 50.0	+ 27.2
@ 70°C/dry heat, unfaced specimens	<u>01.90°</u>	<u>01.85°</u>	<u>01.48°</u>	<u>1.82°</u>
Initial	0.115	0.103	0.125	0.113
1 week	0.120	0.124	0.155	0.120
2 weeks	0.124	0.122	0.157	0.124
3 weeks	0.126	0.128	0.163	0.126
6 weeks	0.132	0.133	0.167	0.126
10 weeks	<u>0.138</u>	<u>0.139</u>	<u>0.173</u>	<u>0.135</u>
Δ K, %	+ 20.0	+ 35.0	+ 38.4	+ 19.5
Fire Performance (4-foot tunnel)				
FSC ⁴⁸	28 (25) ^a	28	29	32
Max. flamespread, in.	37 (34)	39	40	42
Time to max. F.S., secs.	14 (13)	7	8	18
Smoke	115 (200)	132	137	115
Predicted E-84 performance	Class I	Class I	Class I	Class I

^a This numerical flamespread rating is not intended to reflect hazards presented by this or any other material under actual fire conditions. Values in closed parenthesis are for the control Class I material standard.

FOAM FOAM
17 18
↓ ↓

Table 4 Comparative properties of PIR laminates blown with CFC-11, HCFC-123 and HCFC-141b

FORMULATION, PHW		↓	↓
Terate 203	40	40	40
Multranol E-9171	36	36	36
Arcoi M-103	4	4	4
Fyrol PCF	20	20	20
Silicone Surfactant B-8421	2.5	2.5	2.5
Igepal CO-630	3	3	3
Potassium Hex-Cem 977	3	3	3
Catalyst OMP-30	1	1	1
CFC-11	40	--	--
HCFC-123	--	46	--
HCFC-141b	--	--	35
Mondur MR	149.5	149.5	149.5
Isocyanate Index	(220)	(220)	(220)
% CFC or HCFC in total system	(13.4)	(15.1)	(11.9)
PHYSICAL PROPERTIES			
Type of Facer	Alum. foil	Alum. foil	Alum. foil
Laminate nominal thickness, in.	2	2	2
Density, pcf			
In-place	1.80	1.84	1.83
Core	1.62	1.77	1.63
Closed cells, %	88	90	90
Compressive strength (parallel) at 10% deflection, psi			
Product	11	12	12.6
Core	14.6	14.4	12.4
Moisture vapor transmission, perm-in.	7.25	8.23	6.12
Dimensional Stability, % Vol. Change			
28 days at 70°C/100% R.H.	4.5	5.2	7.9
28 days at 100°C/amb. R.H.	3.9	1.7	3.8
28 days at -30°C/amb. R.H.	1.0	- 0.5	- 3.4
K-factor, BTU-in/hr. ft. ² °F			
@ R.T./amb. R.H., faced boardstock	<u>01.89°</u>	<u>01.78°</u>	<u>01.99°</u>
Initial	0.117	0.121	0.127
18 months	<u>0.165</u>	<u>0.159</u>	<u>0.177</u>
Δ K, %	+ 41.0	+ 31.4	+ 39.4
@ R.T./amb. R.H., unfaced boardstock	<u>01.87°</u>	<u>01.79°</u>	<u>01.99°</u>
Initial	0.117	0.121	0.125
18 months	<u>0.169</u>	<u>0.178</u>	<u>0.180</u>
Δ K, %	+ 44.4	+ 47.0	+ 41.7
@ 70°C/dry heat, unfaced specimens	<u>01.87°</u>	<u>01.79°</u>	<u>01.99°</u>
Initial	0.119	0.121	0.125
1 week	0.124	0.132	0.138
2 weeks	0.131	0.139	0.143
3 weeks	0.138	0.150	0.150
6 weeks	0.154	0.159	0.159
10 weeks	<u>0.157</u>	<u>0.163</u>	<u>0.162</u>
Δ K, %	+ 31.9	+ 34.7	+ 29.6
Fire Performance (4-foot tunnel)			
FSC ⁴⁸	26 (25)*	29	28
Max. flamespread, in.	34 (33)	36	37
Time to max. F.S., secs.	11 (25)	9	11
Smoke	135 (200)	137	115
Predicted E-84 performance	Class I	Class I	Class I

* This numerical flamespread rating is not intended to reflect hazards presented by this or any other material under actual fire conditions. Values in closed parenthesis are for the control Class I material standard.

Blank Page

Appendix F

Transient Sorption Test Data

Summary of Test Parameters

SAMPLE ID	D_s [cm]	V_t [ml]	V_g [ml]	L_{eff} [cm]	δ	$\frac{V_t}{V_g}$
1A	3.36	9.24	5.98	0.185	0.978	0.55
2A	3.256	6.49	3.73	0.166	0.978	0.74
2B	3.17	6.4	4.06	0.148	0.978	0.58
14A	3.25	9.13	4.6	0.273	0.98	0.49
14B	3.38	7.19	3.56	0.202	0.98	1.02
15A	3.258	10.17	3.59	0.395	0.982	1.8
15B	3.16	10.17	5.03	0.328	0.982	1.022
16A	3.47	5.26	3.73	0.081	0.977	0.41
17A	3.47	5.54	3.657	0.0996	0.979	0.52
18A	3.3	6.385	3.81	0.19	0.981	0.68
18B	3.344	5.1895	2.655	0.1446	0.981	0.96
18C	3.315	5.85	3.3	0.148	0.981	0.77

D_s = Sample diameter.

V_t = Total volume of test chamber with no foam.

V_g = Volume of gas surrounding sample in test chamber.

L_{eff} = Effective half thickness of foam sample.

δ = Foam void fraction.

G = Equilibrium sorption parameter.

Table F.1: Test Parameters for Mobay Samples Tested.

Summary of Foam Sample Measurements

Sample Number	Date	Temp. °[C]	V_g [ml]	$(\sigma/V_g)100$ [%]	N_m	D_s [cm]	L_{eff} [cm]	L_{cal} [cm]	d_c [cm]	N_{cell}
1-A	5-2-89	25	5.968	12	3	3.36	0.185	0.23	0.038	0.6
2-A	-	-	3.73	2.25	7	3.26	0.166	0.219	0.042	1.3
2-B	8-8-89	25	4.06	2.42	4	3.175	0.148	0.207	0.042	1.41
14-A	-	-	4.61	2.39	6	3.25	0.273	0.301	0.054	0.5
14-B	8-8-89	25	3.56	1.13	4	3.38	0.202	0.26	0.054	1.06
15-A	-	-	3.608	1.76	5	3.258	0.395	0.37	0.052	0.48
15-B	8-8-89	25	5.03	2.17	4	3.157	0.328	0.32	0.052	0.23
16-A	9-28-89	22	3.73	2.97	5	3.48	0.081	0.099	0.027	0.67
16-A	3-26-90	22	3.16	6.9	9	3.48	0.11	0.099	0.027	1.1
17-A	9-2-89	22	3.657	2.1	4	3.47	0.1	0.11	0.03	0.3
17-A	3-26-90	22	2.89	4.7	8	3.47	0.14	0.11	0.03	1
18-A	9-28-89	27	3.81	1.98	5	3.3	0.19	0.17	0.040	0.51
18-B	12-2-89	23	2.655	1.75	5	3.44	0.144	0.166	0.04	0.56
18-B	3-26-90	22	2.27	4.	8	3.44	0.157	0.166	0.04	0.22
18-C	1-27-90	25	3.26	0.92	5	3.315	0.147	0.1778	0.040	0.81
18-C	4-23-90	26	3.34	2.5	5	3.315	0.145	0.1788	0.04	0.82

V_g = Volume of Cell Gas around foam samples.

N_{cell} = Number of open cells at foam sample surface.

N_m = Number of measurements in V_g determination.

σ = standard deviation.

D_s = Sample diameter.

L_{eff} = Foam sample effective half thickness.

L_{cal} = Foam sample half thickness measured with calipers.

d_c = Average foam cell diameter parallel diffusion.

Table F.2: Test Sample Dimensions, with calculation of number of open cells at sample surface.

Summary of Test Pressure Steps

Chamber #	Foam Test	(P2-P1) [psi]	Chamber #	Foam Test	(P2-P1) [psi]
P4	1A - CO2		P2	16A - CO2	
2.4 v/psi	80	1.96	1.048 v/psi	81	-0.65
	60	1.97		60	-1.32
	40	1.92		40	-1.30
P4	1A - O2		P2	16A - O2	
2.4 v/psi	80	1.58	1.048 v/psi	80	-0.66
	61 a	1.54		60	-0.37
	61 b	1.20		40	-1.22
	61 c	1.11	P2	16A - HCFC-123	
	40	1.54	1.048 v/psi	80	-1.78
				60	-1.70
				40	-1.50
P1	2 - CO2				
1.014 v/psi	2A - 80	2.27	P3	17A - CO2	
	2B - 80 a	2.37	0.998 v/psi	80	-1.29
	2B - 80 b	-2.23		60a	-1.88
	2B - 60	-3.51		60b	-1.45
	2B - 40	-2.81		40	-1.63
	2A - O2		P3	17A - O2	
	80	2.47	0.998 v/psi	80	-0.69
P1	2A - N2			60a	-0.85
1.014 v/psi	80	-1.80		60b	-1.44
P1	2B - CFC-11			40	-1.78
1.014 v/psi	80	-1.30	P3	17A - HCFC-123	
			0.998 v/psi	60	-2.47
				40	-4.11
P2	14 - CO2				
1.048 v/psi	A - 80	1.63	P4	18A - CO2	
	B - 80a	1.26	2.4 v/psi	80	1.51
	B - 80b	-1.90		61	2.55
	B - 60	-1.47		44	2.28
	A - 40	1.52		38	1.66
	B - 40	-2.14	P4	18A - O2	
P2	14A - O2			79	2.06
1.048 v/psi	80	1.97		59	2.00
P2	14A - CFC-11			36	1.56
1.048 v/psi	80	-1.26	P4	18A - N2	
				80	1.54
P3	15 - CO2			60	-2.72
0.998 v/psi	B - 80	-1.28		40	0.40
	B - 60	-3.49	P4	18C - CFC-11	
	B - 40	2.12		80	-1.60
			P1	18B - HCFC-123	
			1.014 v/psi	80	-2.33
				40	-3.83
			P4	18A - HCFC-141b	
				80	1.57
				60	1.77

Blank Page

F.1 Foam No. 1

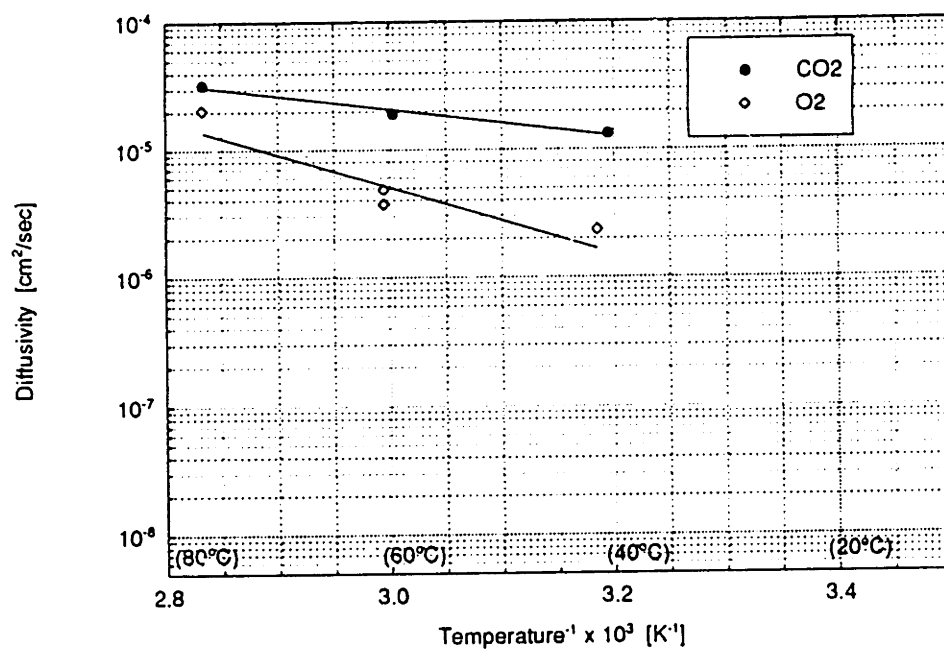


Figure F-1: $\log(D_{eff})$ versus $1/T$ for all test results, Foam 1.

Plotting frame

3

META OPTION :

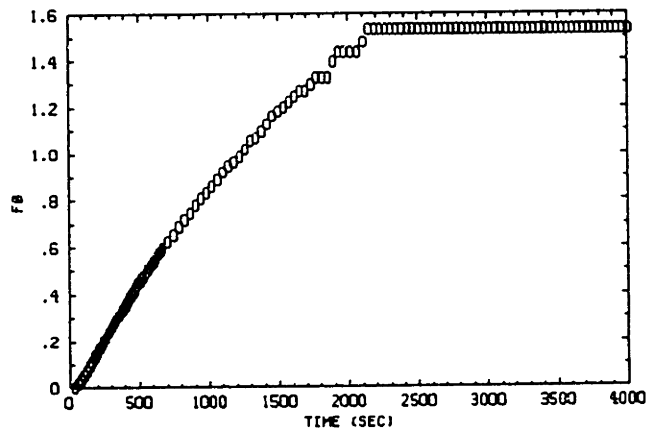
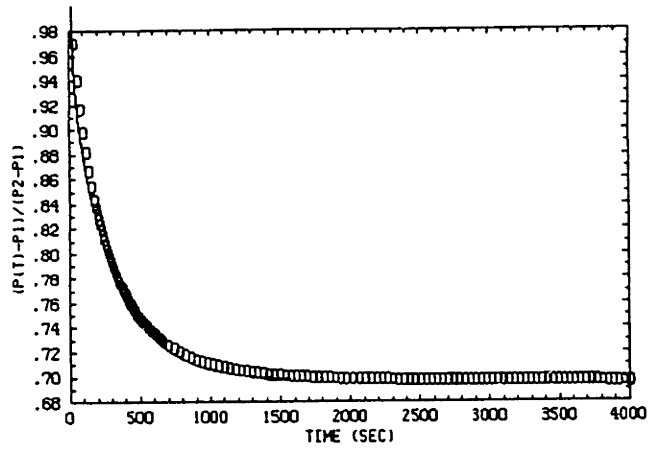


Figure F-2: CO₂, 80°C Data Plot Sample 1A.

SAMPLE # 1A-P4
GAS TESTED: CO2
TEST DATE: 3-20-89

*** INPUT PARAMETERS ***

SAMPLE DIAMETER (IN CM):	3.360
TOTAL CHAMBER VOLUME (IN CM**3):	9.240
CHAMBER GAS VOLUME, ZERO DEF. (IN CM**3):	5.968
CHAMBER GAS VOLUME, MAX. DEF. (IN CM**3):	5.968
FOAM VOID FRACTION:	0.978
START FO FOR BEST-FIT:	0.150
END FO FOR BEST-FIT:	0.550
TEMPERATURE (DEGREES C):	80.000

*** CALCULATED VALUES ***

BEST FIT : FO= 95.653E-5*T + -0.009

SAMPLE AREA (IN CM**2):	8.867
SAMPLE EFF. HALF-THICKNESS (IN CM):	0.185
EQUILIBRIUM SORPTION PARAMETER, G:	0.436
EQUILIBRIUM PRESSURE	0.697
FOAM SOLUBILITY RATIO	0.795
FOAM SOLUBILITY COEFFICIENT	0.671
POLYMER SOLUBILITY RATIO	-8.337
POLYMER SOLUBILITY	-7.038
DIFFUSION COEFFICIENT (x10**8)	3256.343
PERMEABILITY COEFFICIENT (x10**8)	2184.311

*** TRANSIENT PRESSURE DATA ***

TIME (SEC)	(P(T)-P1)/(P2-P1)
21.	0.970
120.	0.867
189.	0.828
238.	0.807
288.	0.790
337.	0.777
387.	0.765
436.	0.755
485.	0.747
535.	0.740
584.	0.735
634.	0.730
802.	0.718
1000.	0.710
1197.	0.705
1395.	0.702
1593.	0.700
1790.	0.700
1995.	0.699
2205.	0.698
2403.	0.698
2601.	0.697
2798.	0.697
2996.	0.697
3194.	0.697
3392.	0.697
3589.	0.697
3787.	0.697
3985.	0.697

Plotting frame

2

META OPTION :

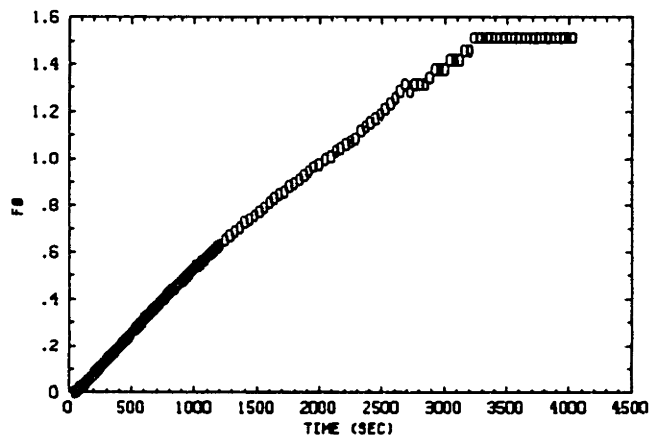
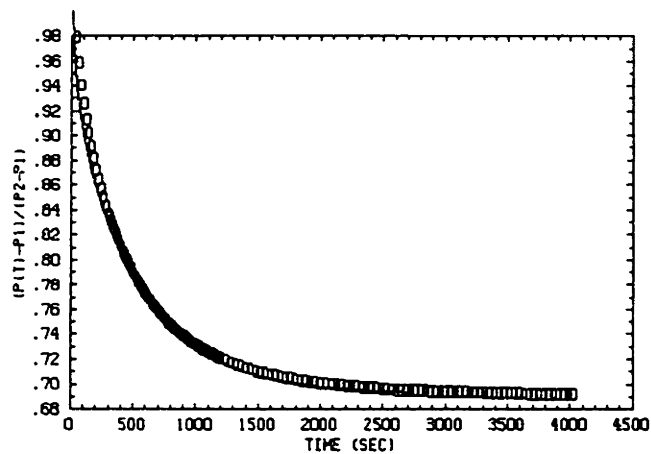


Figure F-3: CO₂, 60°C Data Plot Sample 1A

SAMPLE # 1A-P4
GAS TESTED: CO2
TEST DATE: 4-14-89

*** INPUT PARAMETERS ***

SAMPLE DIAMETER (IN CM):	3.360
TOTAL CHAMBER VOLUME (IN CM**3):	9.240
CHAMBER GAS VOLUME, ZERO DEF. (IN CM**3):	5.968
CHAMBER GAS VOLUME, MAX. DEF. (IN CM**3):	5.968
FOAM VOID FRACTION:	0.978
START FO FOR BEST-FIT:	0.150
END FO FOR BEST-FIT:	0.550
TEMPERATURE (DEGREES C):	60.000

*** CALCULATED VALUES ***

BEST FIT : $FO = 56.038E-5 * T + -0.010$

SAMPLE AREA (IN CM**2):	8.867
SAMPLE EFF. HALF-THICKNESS (IN CM):	0.185
EQUILIBRIUM SORPTION PARAMETER, G:	0.445
EQUILIBRIUM PRESSURE	0.692
FOAM SOLUBILITY RATIO	0.813
FOAM SOLUBILITY COEFFICIENT	0.727
POLYMER SOLUBILITY RATIO	-7.521
POLYMER SOLUBILITY	-6.730
DIFFUSION COEFFICIENT (x10**8)	1907.703
PERMEABILITY COEFFICIENT (x10**8)	1387.174

*** TRANSIENT PRESSURE DATA ***

TIME (SEC)	(P(T)-P1)/(P2-P1)
21.	0.979
120.	0.902
218.	0.857
298.	0.831
347.	0.818
396.	0.806
446.	0.795
495.	0.786
545.	0.778
594.	0.769
644.	0.763
693.	0.756
742.	0.752
792.	0.746
841.	0.742
891.	0.738
940.	0.734
990.	0.730
1089.	0.724
1138.	0.722
1217.	0.719
1415.	0.712
1613.	0.707
1810.	0.703
2017.	0.700
2222.	0.699
2420.	0.697
2617.	0.695
2815.	0.695
3013.	0.694
3211.	0.693
3804.	0.692
4002.	0.692

plotting frame

1

META OPTION :

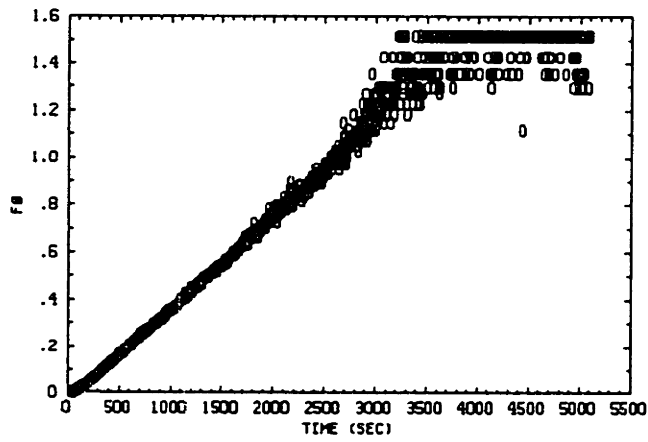
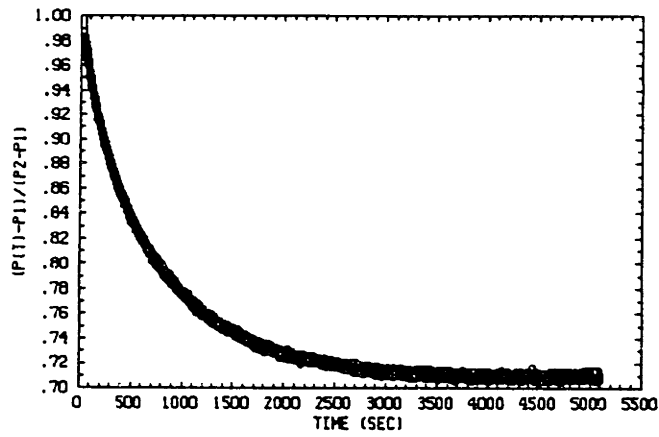


Figure F-4: CO₂, 40°C Data Plot Sample 1A

SAMPLE # 1A-P4
 GAS TESTED: CO2
 TEST DATE: 4-16-89

*** INPUT PARAMETERS ***

SAMPLE DIAMETER (IN CM): 3.360
 TOTAL CHAMBER VOLUME (IN CM**3): 9.240
 CHAMBER GAS VOLUME, ZERO DEF. (IN CM**3): 5.968
 CHAMBER GAS VOLUME, MAX. DEF. (IN CM**3): 5.968
 FOAM VOID FRACTION: 0.978
 START FO FOR BEST-FIT: 0.100
 END FO FOR BEST-FIT: 0.500
 TEMPERATURE (DEGREES C): 40.000

*** CALCULATED VALUES ***

BEST FIT : FO= 38.941E-5*T + -0.020
 SAMPLE AREA (IN CM**2): 8.867
 SAMPLE EFF. HALF-THICKNESS (IN CM): 0.185
 EQUILIBRIUM SORPTION PARAMETER, G: 0.411
 EQUILIBRIUM PRESSURE 0.708
 FOAM SOLUBILITY RATIO 0.751
 FOAM SOLUBILITY COEFFICIENT 0.715
 POLYMER SOLUBILITY RATIO -10.339
 POLYMER SOLUBILITY -9.843
 DIFFUSION COEFFICIENT (x10**8) 1325.684
 PERMEABILITY COEFFICIENT (x10**8) 947.307

*** TRANSIENT PRESSURE DATA ***

TIME (SEC)	(P(T)-P1)/(P2-P1)	TIME (SEC)	(P(T)-P1)/(P2-P1)
5.	0.975	905.	0.783
30.	0.971	980.	0.776
55.	0.957	1005.	0.774
80.	0.944	1105.	0.767
105.	0.933	1205.	0.759
130.	0.923	1305.	0.752
155.	0.913	1405.	0.748
180.	0.906	1529.	0.742
205.	0.897	1629.	0.738
230.	0.891	1729.	0.734
255.	0.883	1829.	0.731
280.	0.877	1929.	0.728
305.	0.870	2029.	0.727
330.	0.864	2129.	0.722
355.	0.860	2229.	0.722
380.	0.853	2329.	0.721
405.	0.848	2429.	0.720
430.	0.844	2529.	0.717
455.	0.839	2729.	0.716
480.	0.836	2904.	0.714
530.	0.828	3129.	0.711
555.	0.823	3429.	0.711
580.	0.820	3729.	0.711
605.	0.818	4029.	0.710
680.	0.804	4428.	0.709
755.	0.798	4928.	0.710
855.	0.789	5053.	0.709

plotting frame

5

META OPTION :

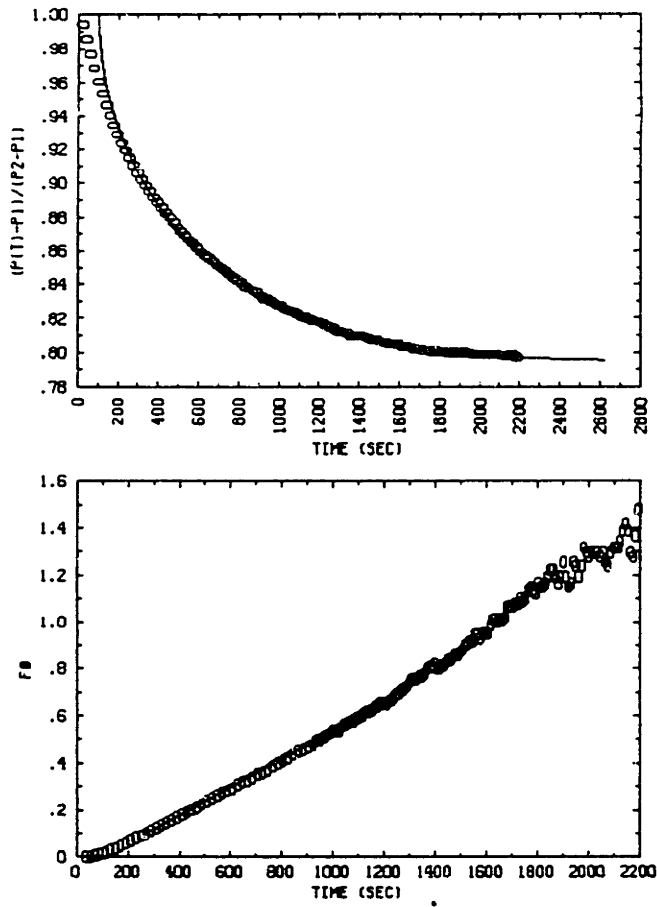


Figure F-5: O₂, 80°C Data Plot Sample 1A.

SAMPLE # 1A-P4
GAS TESTED: O2
TEST DATE: 3-22-89

*** INPUT PARAMETERS ***

SAMPLE DIAMETER (IN CM):	3.360
TOTAL CHAMBER VOLUME (IN CM**3):	9.240
CHAMBER GAS VOLUME, ZERO DEF. (IN CM**3):	5.968
CHAMBER GAS VOLUME, MAX. DEF. (IN CM**3):	5.968
FOAM VOID FRACTION:	0.978
START FO FOR BEST-FIT:	0.100
END FO FOR BEST-FIT:	0.700
TEMPERATURE (DEGREES C):	80.000

*** CALCULATED VALUES ***

BEST FIT : FO= 60.234E-5*T + -0.062

SAMPLE AREA (IN CM**2):	8.867
SAMPLE EFF. HALF-THICKNESS (IN CM):	0.185
EQUILIBRIUM SORPTION PARAMETER, G:	0.260
EQUILIBRIUM PRESSURE	0.793
FOAM SOLUBILITY RATIO	0.475
FOAM SOLUBILITY COEFFICIENT	0.401
POLYMER SOLUBILITY RATIO	-22.864
POLYMER SOLUBILITY	-19.301
DIFFUSION COEFFICIENT (x10**8)	2050.570
PERMEABILITY COEFFICIENT (x10**8)	822.261

*** TRANSIENT PRESSURE DATA ***

TIME (SEC)	(P(T)-P1)/(P2-P1)
21.	0.992
120.	0.951
218.	0.922
317.	0.901
416.	0.884
515.	0.870
614.	0.858
713.	0.848
812.	0.839
911.	0.831
960.	0.828
1059.	0.822
1158.	0.817
1257.	0.813
1355.	0.808
1454.	0.806
1553.	0.803
1652.	0.801
1751.	0.799
1850.	0.798
2000.	0.797
2162.	0.797

Plotting frame

2

META OPTION :

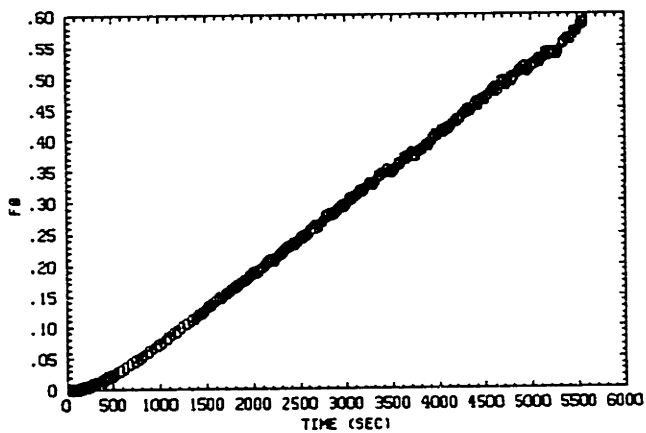
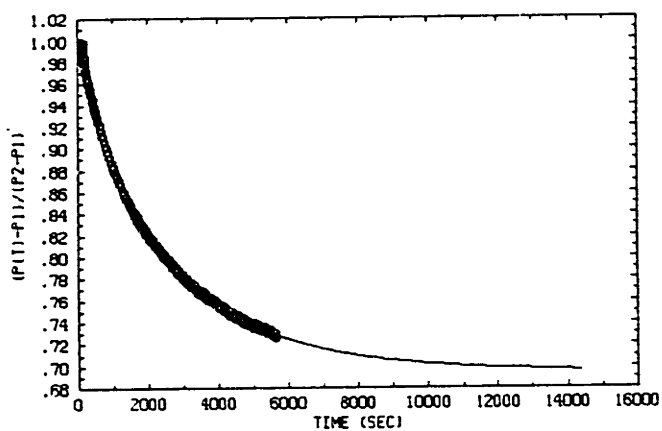


Figure F-6: O₂, 61°C (Test A) Data Plot Sample 1A

SAMPLE # 1A-P4
 GAS TESTED: O2 (61A)
 TEST DATE: 6-5-89

*** INPUT PARAMETERS ***

SAMPLE DIAMETER (IN CM):	3.360
TOTAL CHAMBER VOLUME (IN CM**3):	9.240
CHAMBER GAS VOLUME, ZERO DEF. (IN CM**3):	5.968
CHAMBER GAS VOLUME, MAX. DEF. (IN CM**3):	5.968
FOAM VOID FRACTION:	0.978
START FO FOR BEST-FIT:	0.050
END FO FOR BEST-FIT:	0.100
TEMPERATURE (DEGREES C):	61.000

*** CALCULATED VALUES ***

BEST FIT : FO= 10.853E-5*T + -0.031	
SAMPLE AREA (IN CM**2):	8.867
SAMPLE EFF. HALF-THICKNESS (IN CM):	0.185
EQUILIBRIUM SORPTION PARAMETER, G:	0.439
EQUILIBRIUM PRESSURE	0.695
FOAM SOLUBILITY RATIO	0.800
FOAM SOLUBILITY COEFFICIENT	0.714
POLYMER SOLUBILITY RATIO	-8.091
POLYMER SOLUBILITY	-7.219
DIFFUSION COEFFICIENT (x10**8)	369.458
PERMEABILITY COEFFICIENT (x10**8)	263.709

*** TRANSIENT PRESSURE DATA ***

TIME (SEC)	(P(T)-P1)/(P2-P1)
5.	0.994
30.	0.995
55.	0.989
79.	0.984
104.	0.980
129.	0.975
178.	0.967
228.	0.960
277.	0.953
302.	0.949
327.	0.946
376.	0.940
490.	0.926
744.	0.899
994.	0.877
1244.	0.858
1544.	0.839
1794.	0.826
2044.	0.815
2294.	0.804
2543.	0.795
2793.	0.785
3043.	0.777
3293.	0.770
3543.	0.764
3793.	0.759
4043.	0.753
4293.	0.748
4543.	207 0.742
4793.	0.739
5043.	0.735
5292.	0.732
5542.	0.728

Plotting frame

3

META OPTION :

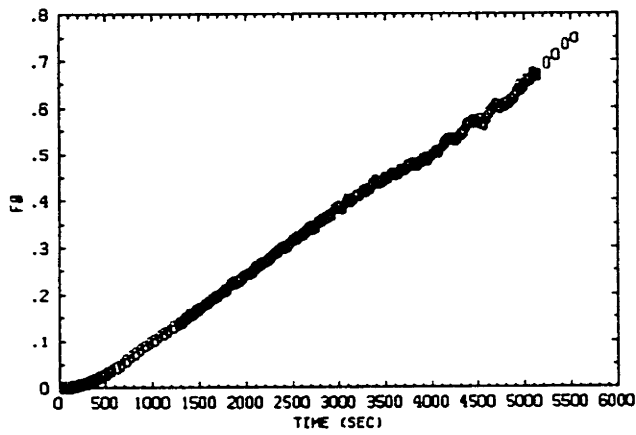
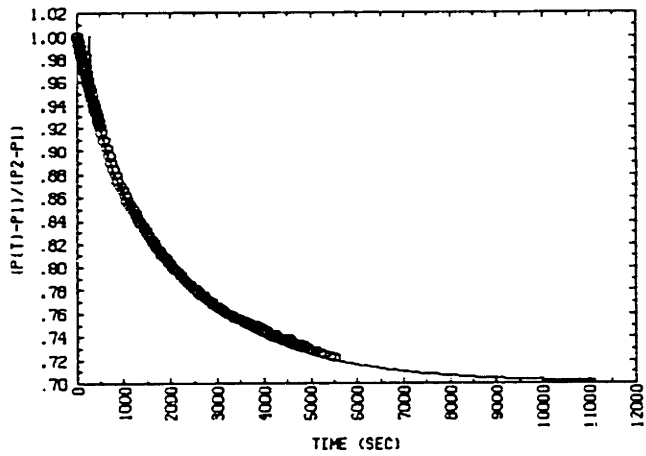


Figure F-7: O₂, 61°C (Test B) Data Plot Sample 1A

SAMPLE # 1A-P4
GAS TESTED: O2 (61B)
TEST DATE: 6-5-89

*** INPUT PARAMETERS ***

SAMPLE DIAMETER (IN CM):	3.360
TOTAL CHAMBER VOLUME (IN CM**3):	9.240
CHAMBER GAS VOLUME, ZERO DEF. (IN CM**3):	5.968
CHAMBER GAS VOLUME, MAX. DEF. (IN CM**3):	5.968
FOAM VOID FRACTION:	0.978
START FO FOR BEST-FIT:	0.050
END FO FOR BEST-FIT:	0.400
TEMPERATURE (DEGREES C):	61.000

*** CALCULATED VALUES ***

BEST FIT : FO=	14.261E-5*T +	-0.039	
SAMPLE AREA (IN CM**2):			8.867
SAMPLE EFF. HALF-THICKNESS (IN CM):			0.185
EQUILIBRIUM SORPTION PARAMETER, G:			0.428
EQUILIBRIUM PRESSURE			0.700
FOAM SOLUBILITY RATIO			0.780
FOAM SOLUBILITY COEFFICIENT			0.696
POLYMER SOLUBILITY RATIO			-9.000
POLYMER SOLUBILITY			-8.030
DIFFUSION COEFFICIENT (x10**8)			485.480
PERMEABILITY COEFFICIENT (x10**8)			337.859

*** TRANSIENT PRESSURE DATA ***

TIME (SEC)	(P(T)-P1)/(P2-P1)
5.	0.995
30.	0.993
55.	0.989
79.	0.984
104.	0.979
129.	0.975
153.	0.971
178.	0.967
203.	0.963
228.	0.959
252.	0.955
277.	0.951
302.	0.947
327.	0.943
351.	0.939
376.	0.936
401.	0.932
425.	0.929
834.	0.877
1284.	0.841
1534.	0.825
1909.	0.805
2159.	0.793
2408.	0.783
2908.	0.765
3408.	0.754
3908.	0.745
4158.	0.740
4908.	0.727
5307.	0.722

Plotting frame

4

META OPTION :

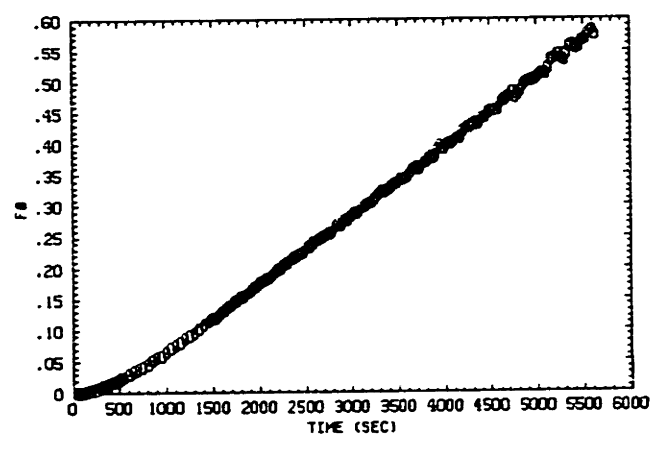
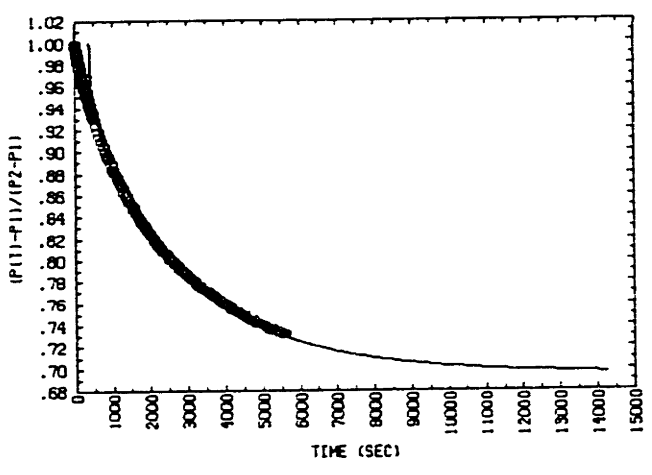


Figure F-8: O₂, 61°C (Test C) Data Plot Sample 1A

SAMPLE # 1A-P4
GAS TESTED: O2 (61C)
TEST DATE: 6-6-89

*** INPUT PARAMETERS ***

SAMPLE DIAMETER (IN CM):	3.360
TOTAL CHAMBER VOLUME (IN CM**3):	9.240
CHAMBER GAS VOLUME, ZERO DEF. (IN CM**3):	5.968
CHAMBER GAS VOLUME, MAX. DEF. (IN CM**3):	5.968
FOAM VOID FRACTION:	0.978
START FO FOR BEST-FIT:	0.100
END FO FOR BEST-FIT:	0.450
TEMPERATURE (DEGREES C):	61.000

*** CALCULATED VALUES ***

BEST FIT : FO=	$11.001E-5 * T + -0.042$	
SAMPLE AREA (IN CM**2):		8.867
SAMPLE EFF. HALF-THICKNESS (IN CM):		0.185
EQUILIBRIUM SORPTION PARAMETER, G:		0.439
EQUILIBRIUM PRESSURE		0.695
FOAM SOLUBILITY RATIO		0.800
FOAM SOLUBILITY COEFFICIENT		0.714
POLYMER SOLUBILITY RATIO		-8.091
POLYMER SOLUBILITY		-7.219
DIFFUSION COEFFICIENT (x10**8)		374.504
PERMEABILITY COEFFICIENT (x10**8)		267.311

*** TRANSIENT PRESSURE DATA ***

TIME (SEC)	(P(T)-P1) / (P2-P1)
5.	0.993
30.	0.991
55.	0.987
79.	0.982
104.	0.979
129.	0.974
153.	0.970
178.	0.968
203.	0.963
228.	0.960
252.	0.957
277.	0.955
302.	0.951
327.	0.948
351.	0.945
376.	0.942
401.	0.939
450.	0.934
615.	0.916
1114.	0.874
1514.	0.849
1764.	0.832
2014.	0.821
2389.	0.805
2639.	0.795
2889.	0.786
3264.	0.774
3764.	0.762
4263.	0.750
4763.	0.742
5513.	0.730

plotting frame

1

META OPTION :

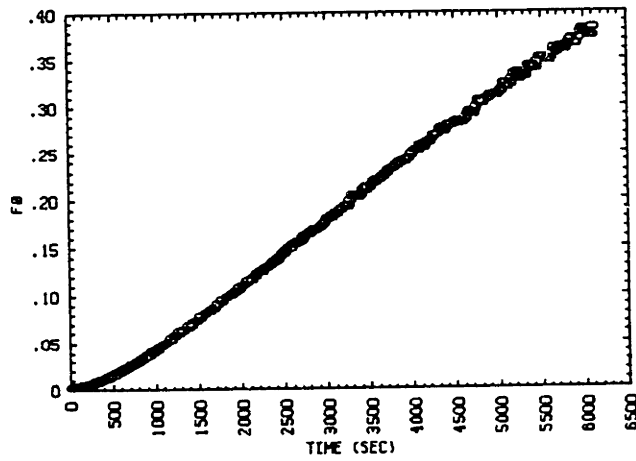
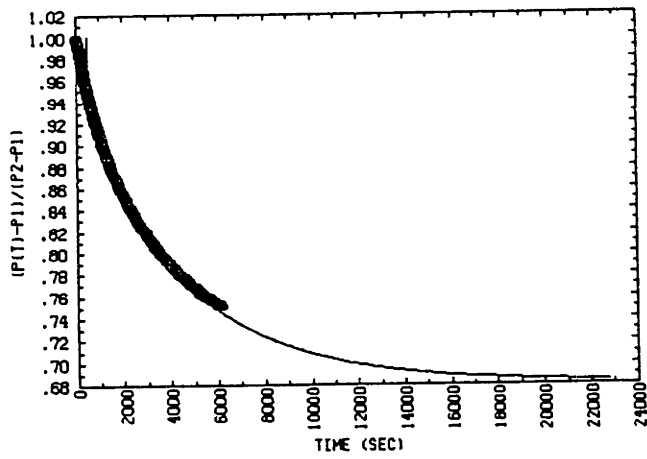


Figure F-9: O₂, 41°C Data Plot Sample 1A

SAMPLE # 1A-P4
 GAS TESTED: O2
 TEST DATE: 6-1-89

*** INPUT PARAMETERS ***

SAMPLE DIAMETER (IN CM):	3.360
TOTAL CHAMBER VOLUME (IN CM**3):	9.240
CHAMBER GAS VOLUME, ZERO DEF. (IN CM**3):	5.968
CHAMBER GAS VOLUME, MAX. DEF. (IN CM**3):	5.968
FOAM VOID FRACTION:	0.978
START FO FOR BEST-FIT:	0.050
END FO FOR BEST-FIT:	0.300
TEMPERATURE (DEGREES C):	41.000

*** CALCULATED VALUES ***

BEST FIT : FO= 6.880E-5*T + -0.030	
SAMPLE AREA (IN CM**2):	8.867
SAMPLE EFF. HALF-THICKNESS (IN CM):	0.185
EQUILIBRIUM SORPTION PARAMETER, G:	0.466
EQUILIBRIUM PRESSURE	0.682
FOAM SOLUBILITY RATIO	0.850
FOAM SOLUBILITY COEFFICIENT	0.807
POLYMER SOLUBILITY RATIO	-5.818
POLYMER SOLUBILITY	-5.522
DIFFUSION COEFFICIENT (x10**8)	234.231
PERMEABILITY COEFFICIENT (x10**8)	188.952

*** TRANSIENT PRESSURE DATA ***

TIME (SEC)	(P(T)-P1)/(P2-P1)
10.	0.994
60.	0.992
109.	0.987
159.	0.981
208.	0.975
258.	0.969
307.	0.963
356.	0.958
406.	0.953
455.	0.948
505.	0.943
554.	0.939
604.	0.934
653.	0.930
702.	0.926
752.	0.922
801.	0.918
851.	0.915
950.	0.907
1270.	0.886
1770.	0.859
2219.	0.840
2469.	0.830
2719.	0.821
2969.	0.814
3219.	0.806
3719.	0.792
4344.	0.776
4594.	0.774
5093.	0.763
5593.	0.756
6093.	0.750

Blank Page

F.2 Foam No. 2

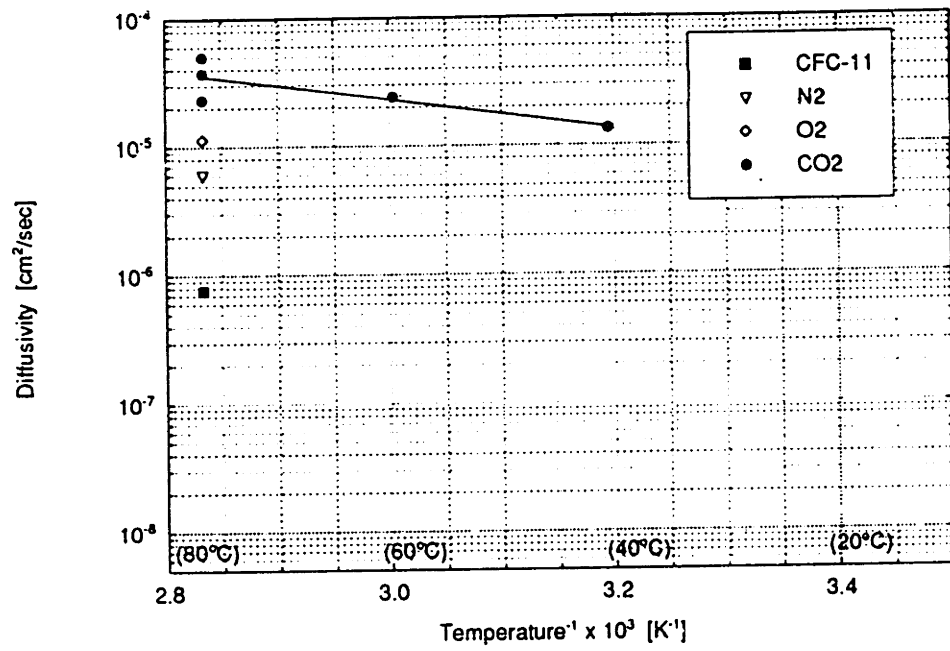


Figure F-10: $\text{Log}(D_{eff})$ versus $1/T$ for all test results, Foam 2.

Plotting frame

5

META OPTION :

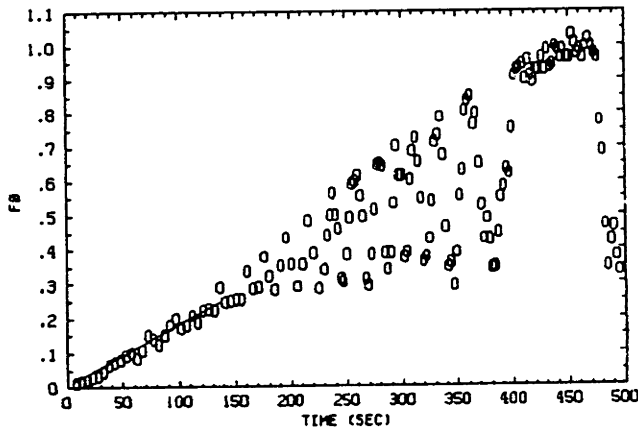
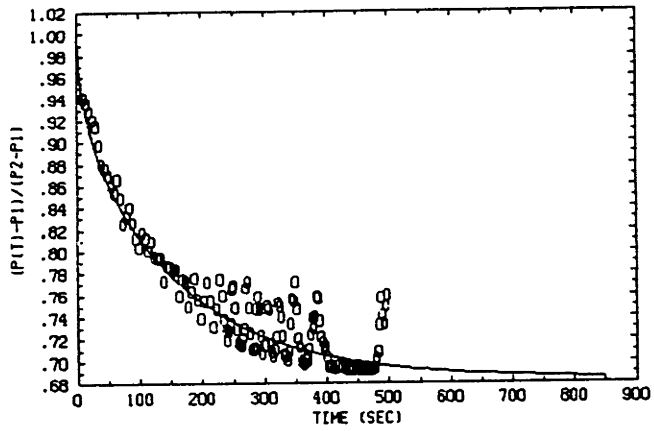


Figure F-11: CO₂, 80°C Data Plot Sample 2A.

SAMPLE # 2A-P1
 GAS TESTED: CO2
 TEST DATE: 7-12-89

*** INPUT PARAMETERS ***

SAMPLE DIAMETER (IN CM):	3.256
TOTAL CHAMBER VOLUME (IN CM**3):	6.490
CHAMBER GAS VOLUME, ZERO DEF. (IN CM**3):	3.730
CHAMBER GAS VOLUME, MAX. DEF. (IN CM**3):	3.730
FOAM VOID FRACTION:	0.978
START FO FOR BEST-FIT:	0.010
END FO FOR BEST-FIT:	0.250
TEMPERATURE (DEGREES C):	80.000

*** CALCULATED VALUES ***

BEST FIT : FO= 182.097E-5*T + -0.002	
SAMPLE AREA (IN CM**2):	8.326
NUMBER OF DATA POINTS IN BEST-FIT RANGE	28
SAMPLE EFF. HALF-THICKNESS (IN CM):	0.166
EQUILIBRIUM SORPTION PARAMETER, G:	0.462
EQUILIBRIUM PRESSURE	0.684
FOAM SOLUBILITY RATIO	0.625
FOAM SOLUBILITY COEFFICIENT	0.528
POLYMER SOLUBILITY RATIO	-16.045
POLYMER SOLUBILITY	-13.545
DIFFUSION COEFFICIENT (x10**8)	5001.992
PERMEABILITY COEFFICIENT (x10**8)	2639.153

*** TRANSIENT PRESSURE DATA ***

TIME (SEC)	(P(T)-P1)/(P2-P1)
5.	0.941
30.	0.898
55.	0.854
79.	0.840
104.	0.812
129.	0.794
153.	0.783
178.	0.763
203.	0.772
228.	0.759
240.	0.735
252.	0.717
265.	0.766
277.	0.711
289.	0.723
302.	0.747
314.	0.721
327.	0.706
339.	0.756
351.	0.712
364.	0.700
376.	0.740
388.	0.717
401.	0.694
413.	0.695
425.	0.694
438.	0.693
450.	0.691
462.	0.692
475.	0.702
487.	0.733

plotting frame

3

META OPTION :

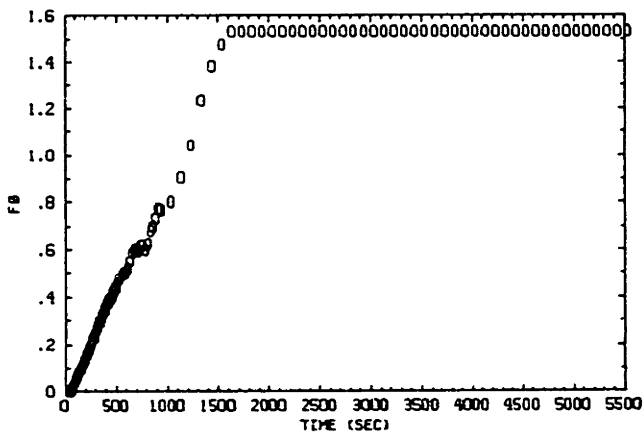
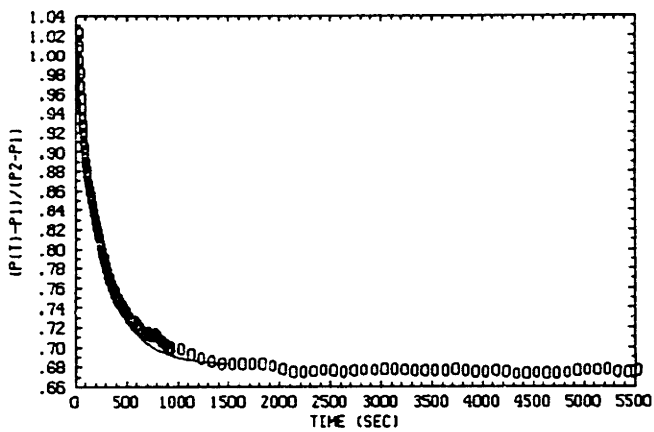


Figure F-12: CO₂, 80°C (Test A) Data Plot Sample 2B.

SAMPLE # 2B-P1
 GAS TESTED: CO2 (80A)
 TEST DATE: 8-16-89

*** INPUT PARAMETERS ***

SAMPLE DIAMETER (IN CM):	3.170
TOTAL CHAMBER VOLUME (IN CM**3):	6.400
CHAMBER GAS VOLUME, ZERO DEF. (IN CM**3):	4.060
CHAMBER GAS VOLUME, MAX. DEF. (IN CM**3):	4.060
FOAM VOID FRACTION:	0.978
START FO FOR BEST-FIT:	0.050
END FO FOR BEST-FIT:	0.400
TEMPERATURE (DEGREES C):	80.000

*** CALCULATED VALUES ***

BEST FIT : FO= 105.161E-5*T + -0.028	
SAMPLE AREA (IN CM**2):	7.892
NUMBER OF DATA POINTS IN BEST-FIT RANGE	110
SAMPLE EFF. HALF-THICKNESS (IN CM):	0.148
EQUILIBRIUM SORPTION PARAMETER, G:	0.467
EQUILIBRIUM PRESSURE	0.682
FOAM SOLUBILITY RATIO	0.810
FOAM SOLUBILITY COEFFICIENT	0.684
POLYMER SOLUBILITY RATIO	-7.636
POLYMER SOLUBILITY	-6.447
DIFFUSION COEFFICIENT (x10**8)	2311.046
PERMEABILITY COEFFICIENT (x10**8)	1580.284

*** TRANSIENT PRESSURE DATA ***

TIME (SEC)	(P(T)-P1)/(P2-P1)
5.	1.023
30.	0.955
55.	0.911
79.	0.885
104.	0.866
129.	0.852
153.	0.837
178.	0.823
203.	0.810
228.	0.797
240.	0.796
252.	0.791
265.	0.783
277.	0.779
289.	0.773
302.	0.768
314.	0.769
327.	0.762
339.	0.760
364.	0.755
388.	0.746
413.	0.745
438.	0.738
462.	0.736
626.	0.715
876.	0.700
1800.	0.683
2800.	0.677
3800.	0.677
4799.	0.674
5299.	0.676

plotting frame

4

META OPTION :

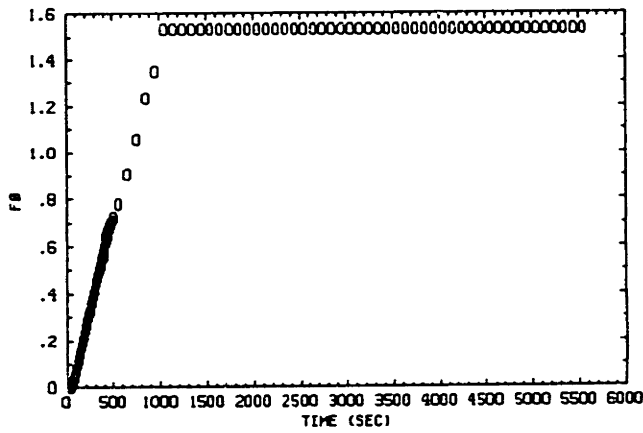
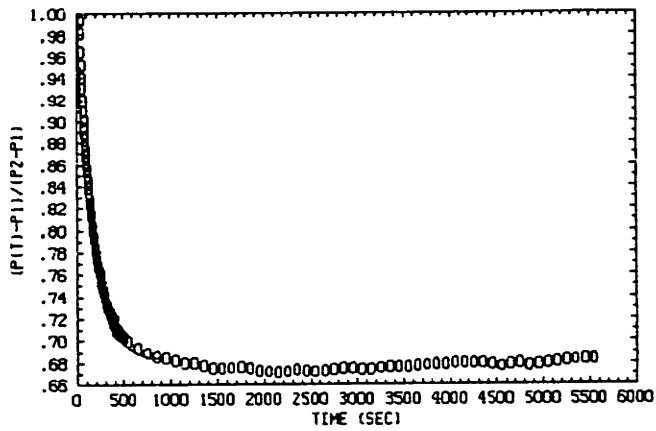


Figure F-13: CO₂, 80°C (Test B) Data Plot Sample 2B.

SAMPLE # 2B-P1
 GAS TESTED: CO2 (80B)
 TEST DATE: 8-30-89

*** INPUT PARAMETERS ***

SAMPLE DIAMETER (IN CM):	3.170
TOTAL CHAMBER VOLUME (IN CM**3):	6.400
CHAMBER GAS VOLUME, ZERO DEF. (IN CM**3):	4.060
CHAMBER GAS VOLUME, MAX. DEF. (IN CM**3):	4.060
FOAM VOID FRACTION:	0.978
START FO FOR BEST-FIT:	0.000
END FO FOR BEST-FIT:	0.500
TEMPERATURE (DEGREES C):	30.000

*** CALCULATED VALUES ***

BEST FIT : FO= 169.317E-5*T + -0.030	
SAMPLE AREA (IN CM**2):	7.892
NUMBER OF DATA POINTS IN BEST-FIT RANGE	107
SAMPLE EFF. HALF-THICKNESS (IN CM):	0.148
EQUILIBRIUM SORPTION PARAMETER, G:	0.467
EQUILIBRIUM PRESSURE	0.682
FOAM SOLUBILITY RATIO	0.810
FOAM SOLUBILITY COEFFICIENT	0.684
POLYMER SOLUBILITY RATIO	-7.636
POLYMER SOLUBILITY	-6.447
DIFFUSION COEFFICIENT (x10**8)	3720.960
PERMEABILITY COEFFICIENT (x10**8)	2544.378

*** TRANSIENT PRESSURE DATA ***

TIME (SEC)	(P(T)-P1)/(P2-P1)
5.	0.993
30.	0.930
55.	0.886
79.	0.856
104.	0.828
119.	0.815
131.	0.808
144.	0.797
156.	0.790
168.	0.782
181.	0.775
193.	0.768
205.	0.761
218.	0.761
230.	0.754
242.	0.750
255.	0.745
267.	0.740
292.	0.730
317.	0.727
341.	0.720
366.	0.714
391.	0.708
415.	0.706
448.	0.705
1215.	0.680
2214.	0.672
3214.	0.675
4214.	0.680

plotting frame

2

META OPTION :

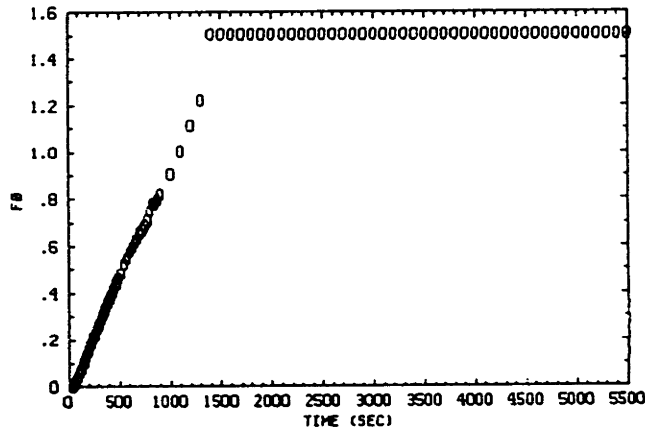
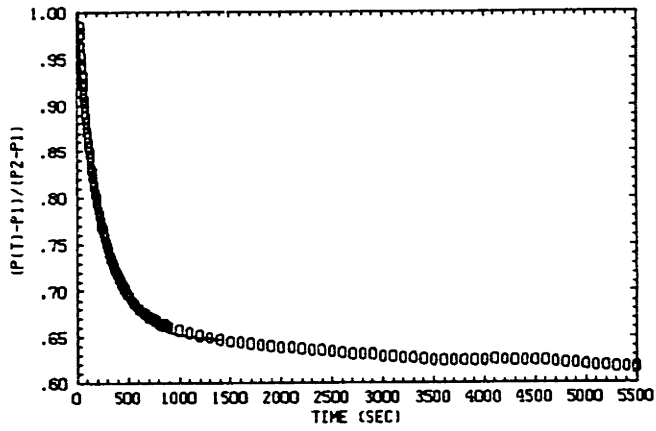


Figure F-14: CO₂, 60°C Data Plot Sample 2B

SAMPLE # 2B-P1
GAS TESTED: CO2
TEST DATE: 8-30-89

*** INPUT PARAMETERS ***

SAMPLE DIAMETER (IN CM):	3.170
TOTAL CHAMBER VOLUME (IN CM**3):	6.400
CHAMBER GAS VOLUME, ZERO DEF. (IN CM**3):	4.060
CHAMBER GAS VOLUME, MAX. DEF. (IN CM**3):	4.060
FOAM VOID FRACTION:	0.978
START FO FOR BEST-FIT:	0.050
END FO FOR BEST-FIT:	0.350
TEMPERATURE (DEGREES C):	60.000

*** CALCULATED VALUES ***

BEST FIT : FO= 108.712E-5*T + -0.024	
SAMPLE AREA (IN CM**2):	7.892
NUMBER OF DATA POINTS IN BEST-FIT RANGE	82
SAMPLE EFF. HALF-THICKNESS (IN CM):	0.148
EQUILIBRIUM SORPTION PARAMETER, G:	0.548
EQUILIBRIUM PRESSURE	0.646
FOAM SOLUBILITY RATIO	0.950
FOAM SOLUBILITY COEFFICIENT	0.850
POLYMER SOLUBILITY RATIO	-1.273
POLYMER SOLUBILITY	-1.139
DIFFUSION COEFFICIENT (x10**8)	2389.094
PERMEABILITY COEFFICIENT (x10**8)	2031.089

*** TRANSIENT PRESSURE DATA ***

TIME (SEC)	(P(T)-P1)/(P2-P1)
5.	0.984
30.	0.931
55.	0.893
79.	0.865
104.	0.842
129.	0.823
153.	0.804
178.	0.786
203.	0.775
223.	0.765
235.	0.759
247.	0.756
260.	0.750
272.	0.746
284.	0.741
297.	0.737
309.	0.732
322.	0.729
346.	0.722
359.	0.718
371.	0.715
408.	0.708
568.	0.681
693.	0.671
818.	0.664
1168.	0.652
2667.	0.632
3667.	0.624
5166.	0.618

plotting frame

1

META OPTION :

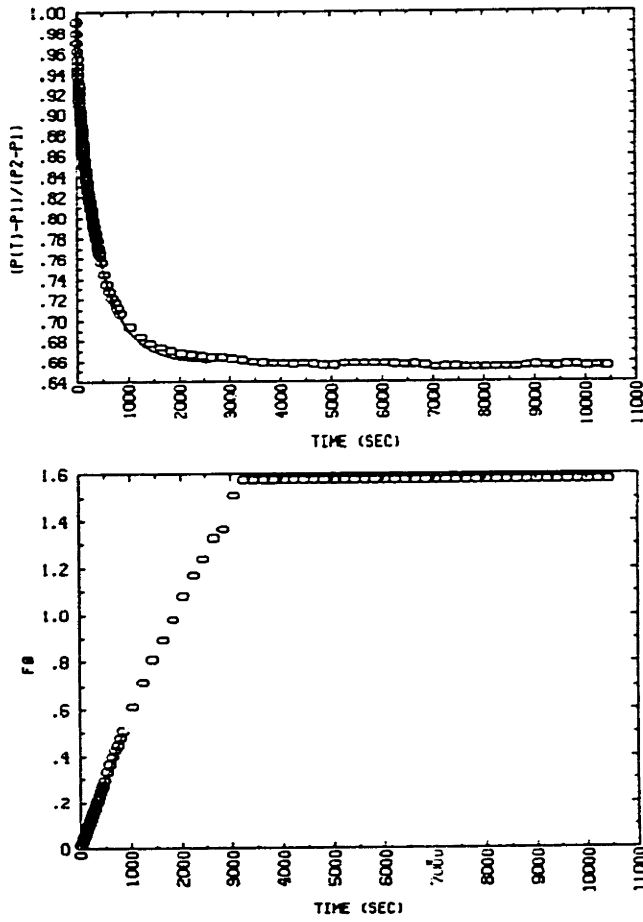


Figure F-15: CO₂, 40°C Data Plot Sample 2B

SAMPLE # 2B-P1
 GAS TESTED: CO2
 TEST DATE: 8-31-89

*** INPUT PARAMETERS ***

SAMPLE DIAMETER (IN CM):	3.170
TOTAL CHAMBER VOLUME (IN CM**3):	6.400
CHAMBER GAS VOLUME, ZERO DEF. (IN CM**3):	4.060
CHAMBER GAS VOLUME, MAX. DEF. (IN CM**3):	4.060
FOAM VOID FRACTION:	0.978
START FO FOR BEST-FIT:	0.050
END FO FOR BEST-FIT:	0.500
TEMPERATURE (DEGREES C):	40.000

*** CALCULATED VALUES ***

BEST FIT : FO= 61.145E-5*T + -0.015	
SAMPLE AREA (IN CM**2):	7.892
NUMBER OF DATA POINTS IN BEST-FIT RANGE	128
SAMPLE EFF. HALF-THICKNESS (IN CM):	0.148
EQUILIBRIUM SORPTION PARAMETER, G:	0.519
EQUILIBRIUM PRESSURE	0.658
FOAM SOLUBILITY RATIO	0.900
FOAM SOLUBILITY COEFFICIENT	0.857
POLYMER SOLUBILITY RATIO	-3.545
POLYMER SOLUBILITY	-3.376
DIFFUSION COEFFICIENT (x10**8)	1343.753
PERMEABILITY COEFFICIENT (x10**8)	1151.420

*** TRANSIENT PRESSURE DATA ***

TIME (SEC)	(P(T)-P1)/(P2-P1)
5.	0.988
30.	0.945
55.	0.921
79.	0.900
104.	0.883
129.	0.868
153.	0.855
178.	0.843
203.	0.833
223.	0.824
235.	0.822
247.	0.816
260.	0.812
272.	0.808
284.	0.806
297.	0.800
309.	0.797
322.	0.793
334.	0.789
346.	0.788
359.	0.783
371.	0.780
396.	0.773
408.	0.770
433.	0.766
481.	0.754
738.	0.715
1438.	0.675
3437.	0.656
5437.	0.655
7436.	0.652
8436.	0.651
10435.	0.652

Plotting frame

1

META OPTION :

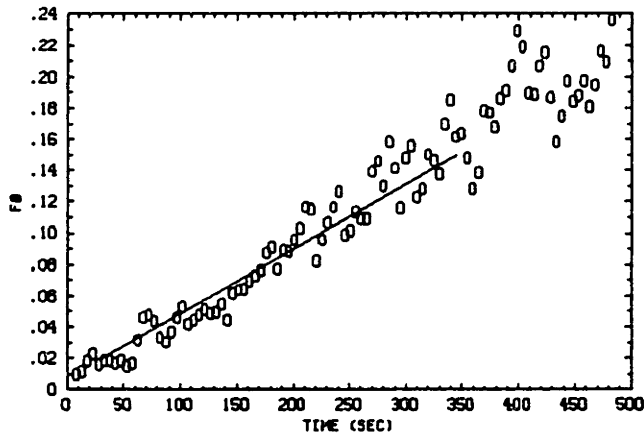
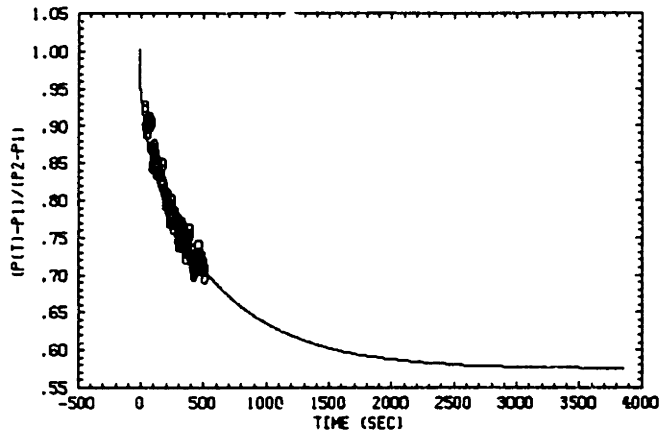


Figure F-16: O₂, 80°C Data Plot Sample 2A.

SAMPLE # 2A-P1
GAS TESTED: O2
TEST DATE: 7-17-89

*** INPUT PARAMETERS ***

SAMPLE DIAMETER (IN CM):	3.256
TOTAL CHAMBER VOLUME (IN CM**3):	6.490
CHAMBER GAS VOLUME, ZERO DEF. (IN CM**3):	3.730
CHAMBER GAS VOLUME, MAX. DEF. (IN CM**3):	3.730
FOAM VOID FRACTION:	0.978
START FO FOR BEST-FIT:	0.020
END FO FOR BEST-FIT:	0.150
TEMPERATURE (DEGREES C):	80.000

*** CALCULATED VALUES ***

BEST FIT : FO=	41.462E-5*T +	0.007	
SAMPLE AREA (IN CM**2):			8.326
NUMBER OF DATA POINTS IN BEST-FIT RANGE			56
SAMPLE EFF. HALF-THICKNESS (IN CM):			0.166
EQUILIBRIUM SORPTION PARAMETER, G:			0.740
EQUILIBRIUM PRESSURE			0.575
FOAM SOLUBILITY RATIO			1.000
FOAM SOLUBILITY COEFFICIENT			0.844
POLYMER SOLUBILITY RATIO			1.000
POLYMER SOLUBILITY			0.844
DIFFUSION COEFFICIENT (x10**8)			1138.923
PERMEABILITY COEFFICIENT (x10**8)			961.470

*** TRANSIENT PRESSURE DATA ***

TIME (SEC)	(P(T)-P1)/(P2-P1)
5.	0.926
30.	0.900
55.	0.905
79.	0.868
104.	0.852
129.	0.841
153.	0.821
178.	0.792
203.	0.781
228.	0.778
252.	0.772
277.	0.759
302.	0.741
327.	0.753
351.	0.746
376.	0.733
401.	0.705
425.	0.722
450.	0.721
475.	0.709

Plotting frame

1

META OPTION :

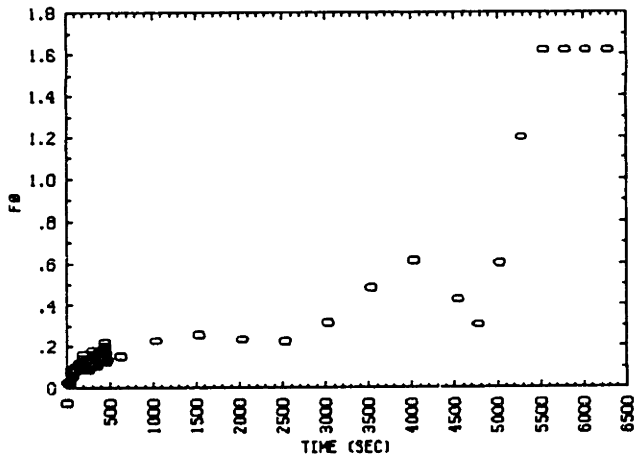
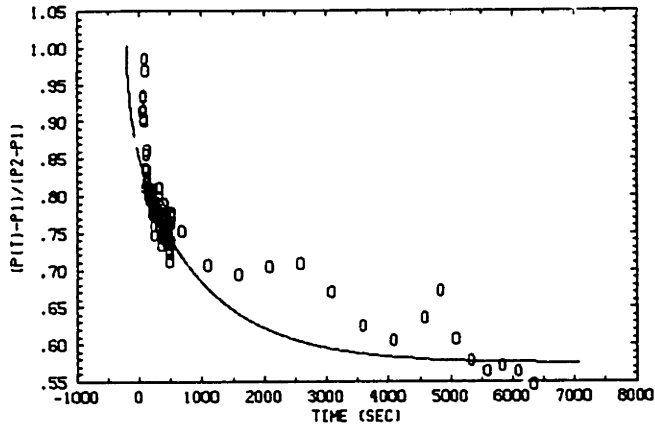


Figure F-17: N₂, 80°C Data Plot Sample 2A.

SAMPLE # 2A-P1
 GAS TESTED: N2
 TEST DATE: 7-30-89

*** INPUT PARAMETERS ***

SAMPLE DIAMETER (IN CM):	3.256
TOTAL CHAMBER VOLUME (IN CM**3):	6.490
CHAMBER GAS VOLUME, ZERO DEF. (IN CM**3):	3.730
CHAMBER GAS VOLUME, MAX. DEF. (IN CM**3):	3.730
FOAM VOID FRACTION:	0.978
START FO FOR BEST-FIT:	0.010
END FO FOR BEST-FIT:	0.100
TEMPERATURE (DEGREES C):	80.000

*** CALCULATED VALUES ***

BEST FIT : FO=	22.171E-5*T +	0.043	
SAMPLE AREA (IN CM**2):			8.326
NUMBER OF DATA POINTS IN BEST-FIT RANGE			38
SAMPLE EFF. HALF-THICKNESS (IN CM):			0.166
EQUILIBRIUM SORPTION PARAMETER, G:			0.740
EQUILIBRIUM PRESSURE			0.575
FOAM SOLUBILITY RATIO			1.000
FOAM SOLUBILITY COEFFICIENT			0.844
POLYMER SOLUBILITY RATIO			1.000
POLYMER SOLUBILITY			0.844
DIFFUSION COEFFICIENT (x10**8)			609.001
PERMEABILITY COEFFICIENT (x10**8)			514.114

*** TRANSIENT PRESSURE DATA ***

TIME (SEC)	(P(T)-P1)/(P2-P1)
5.	0.914
30.	0.901
55.	0.819
79.	0.825
104.	0.806
129.	0.799
153.	0.805
178.	0.773
203.	0.792
228.	0.789
252.	0.761
277.	0.776
302.	0.733
327.	0.764
351.	0.755
376.	0.736
401.	0.756
425.	0.750
450.	0.740
1033.	0.707
3532.	0.625
5281.	0.578

plotting frame

1

META OPTION :

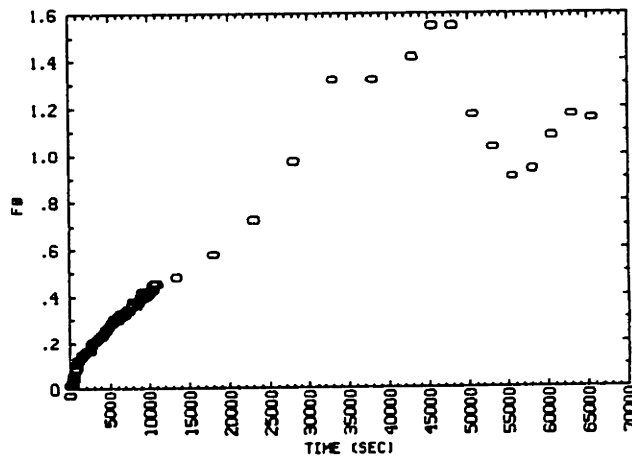
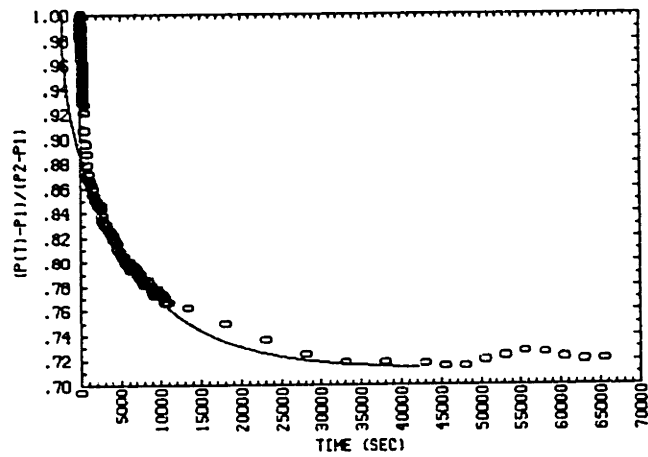


Figure F-18: CFC-11, 80°C Data Plot Sample 2B.

SAMPLE # 2B-P1
GAS TESTED: CFC-11
TEST DATE: 9-20-89

*** INPUT PARAMETERS ***

SAMPLE DIAMETER (IN CM):	3.170
TOTAL CHAMBER VOLUME (IN CM**3):	6.400
CHAMBER GAS VOLUME, ZERO DEF. (IN CM**3):	4.060
CHAMBER GAS VOLUME, MAX. DEF. (IN CM**3):	4.060
FOAM VOID FRACTION:	0.978
START FO FOR BEST-FIT:	0.050
END FO FOR BEST-FIT:	0.400
TEMPERATURE (DEGREES C):	80.000

*** CALCULATED VALUES ***

BEST FIT : FO=	3.460E-5*T +	0.077	
SAMPLE AREA (IN CM**2):			7.892
NUMBER OF DATA POINTS IN BEST-FIT RANGE			91
SAMPLE EFF. HALF-THICKNESS (IN CM):			0.148
EQUILIBRIUM SORPTION PARAMETER, G:			0.403
EQUILIBRIUM PRESSURE			0.713
FOAM SOLUBILITY RATIO			0.700
FOAM SOLUBILITY COEFFICIENT			0.591
POLYMER SOLUBILITY RATIO			-12.636
POLYMER SOLUBILITY			-10.668
DIFFUSION COEFFICIENT (x10**8)			76.029
PERMEABILITY COEFFICIENT (x10**8)			44.928

*** TRANSIENT PRESSURE DATA ***

TIME (SEC)	(P(T)-P1) / (P2-P1)
5.	0.987
30.	0.985
55.	0.985
79.	0.995
104.	0.997
129.	0.999
153.	0.994
178.	0.985
203.	0.978
228.	0.974
252.	0.968
277.	0.962
302.	0.958
327.	0.956
351.	0.949
376.	0.944
401.	0.941
425.	0.935
450.	0.930
475.	0.927
703.	0.893
1203.	0.863
1703.	0.852
2202.	0.845
3202.	0.828
5201.	0.802
6201.	0.795
7201.	0.786
8200.	0.780
9200.	0.772
10200.	0.769
33033.	0.716
63032.	0.718

Blank Page

F.3 Foam No. 14

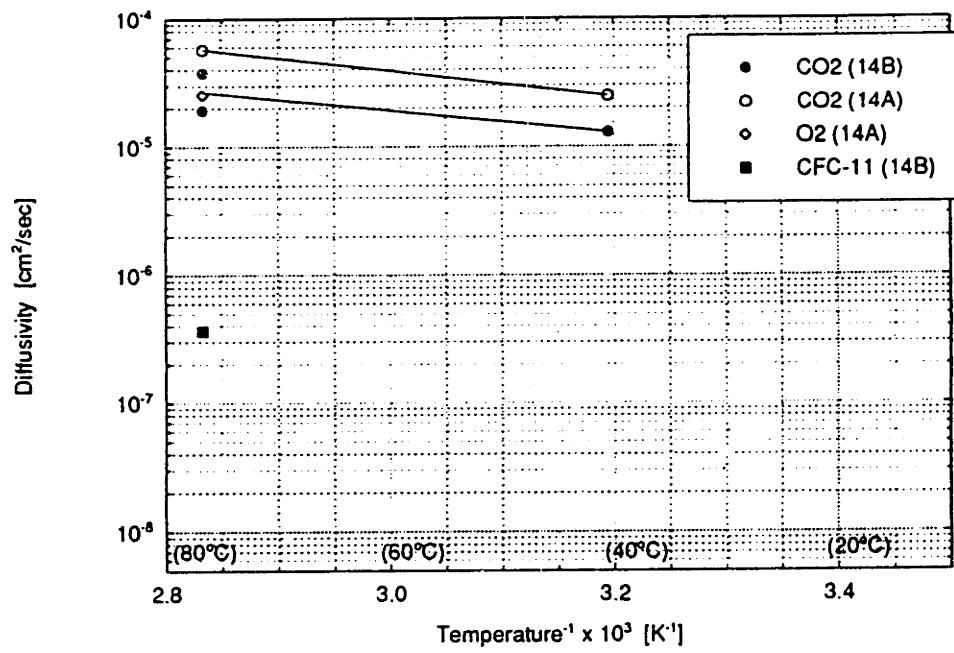


Figure F-19: $\text{Log}(D_{eff})$ versus $1/T$ for all test results, Foam 14.

Plotting frame

2

META OPTION :

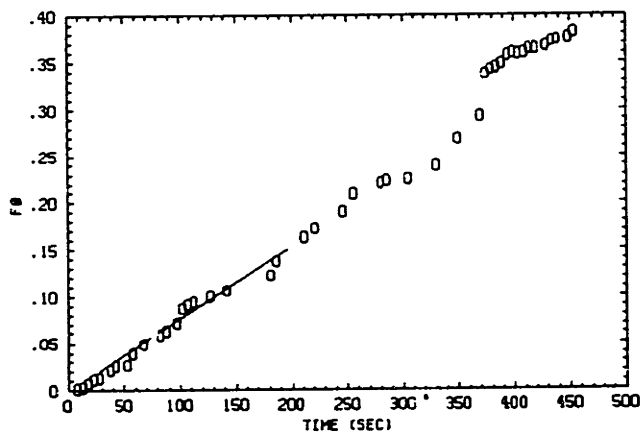
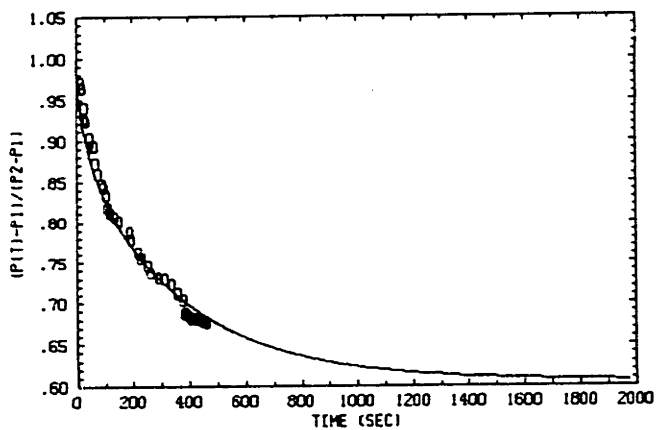


Figure F-20: CO₂, 80°C Data Plot Sample 14A.

SAMPLE # 14A-P2
 GAS TESTED: CO2
 TEST DATE: 6-12-89

*** INPUT PARAMETERS ***

SAMPLE DIAMETER (IN CM):	3.250
TOTAL CHAMBER VOLUME (IN CM**3):	9.130
CHAMBER GAS VOLUME, ZERO DEF. (IN CM**3):	4.600
CHAMBER GAS VOLUME, MAX. DEF. (IN CM**3):	4.600
FOAM VOID FRACTION:	0.980
START FO FOR BEST-FIT:	0.020
END FO FOR BEST-FIT:	0.150
TEMPERATURE (DEGREES C):	80.000

*** CALCULATED VALUES ***

BEST FIT : FO= 77.099E-5*T + -0.001	
SAMPLE AREA (IN CM**2):	8.296
NUMBER OF DATA POINTS IN BEST-FIT RANGE	15
SAMPLE EFF. HALF-THICKNESS (IN CM):	0.273
EQUILIBRIUM SORPTION PARAMETER, G:	0.650
EQUILIBRIUM PRESSURE	0.606
FOAM SOLUBILITY RATIO	0.660
FOAM SOLUBILITY COEFFICIENT	0.557
POLYMER SOLUBILITY RATIO	-16.000
POLYMER SOLUBILITY	-13.507
DIFFUSION COEFFICIENT (x10**8)	5747.382
PERMEABILITY COEFFICIENT (x10**8)	3202.253

*** TRANSIENT PRESSURE DATA ***

TIME (SEC)	(P(T)-P1)/(P2-P1)
5.	0.971
35.	0.902
79.	0.847
109.	0.810
208.	0.762
282.	0.730
371.	0.688
396.	0.682
425.	0.680

plotting frame

5

META OPTION :

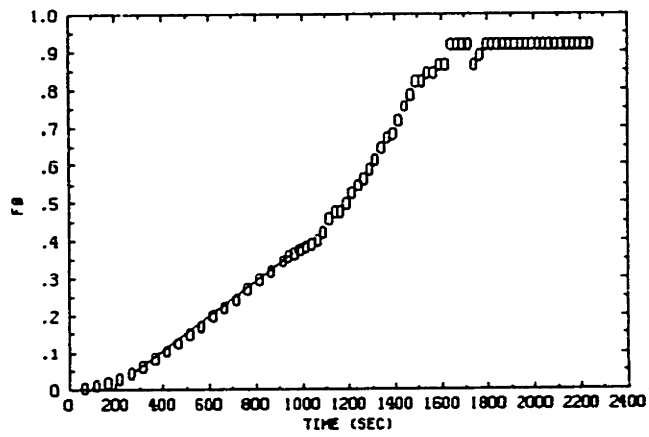
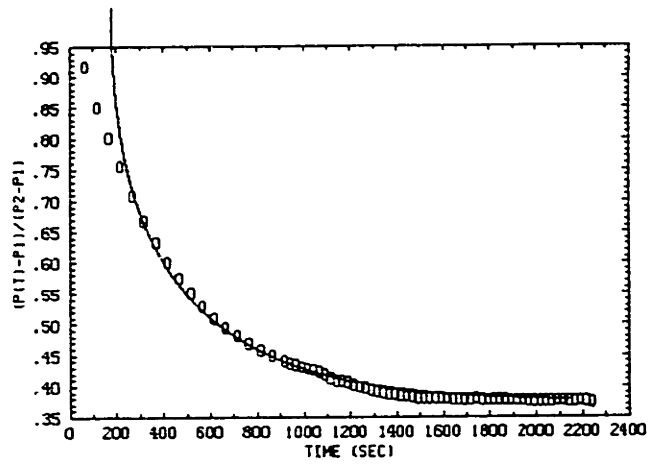


Figure F-21: CO₂, 80°C (Test A) Data Plot Sample 14B.

SAMPLE # 14B-P2
GAS TESTED: CO2 (80A)
TEST DATE: 8-16-89

*** INPUT PARAMETERS ***

SAMPLE DIAMETER (IN CM):	3.380
TOTAL CHAMBER VOLUME (IN CM**3):	7.190
CHAMBER GAS VOLUME, ZERO DEF. (IN CM**3):	3.560
CHAMBER GAS VOLUME, MAX. DEF. (IN CM**3):	3.560
FOAM VOID FRACTION:	0.980
START FO FOR BEST-FIT:	0.050
END FO FOR BEST-FIT:	0.400
TEMPERATURE (DEGREES C):	80.000

*** CALCULATED VALUES ***

BEST FIT : FO= 46.877E-5*T + -0.084

SAMPLE AREA (IN CM**2):	8.973
NUMBER OF DATA POINTS IN BEST-FIT RANGE	18
SAMPLE EFF. HALF-THICKNESS (IN CM):	0.202
EQUILIBRIUM SORPTION PARAMETER, G:	1.671
EQUILIBRIUM PRESSURE	0.374
FOAM SOLUBILITY RATIO	1.639
FOAM SOLUBILITY COEFFICIENT	1.384
POLYMER SOLUBILITY RATIO	32.953
POLYMER SOLUBILITY	27.818
DIFFUSION COEFFICIENT (x10**8)	1918.089
PERMEABILITY COEFFICIENT (x10**8)	2654.010

*** TRANSIENT PRESSURE DATA ***

TIME (SEC)	(P(T)-P1)/(P2-P1)
52.	0.917
302.	0.667
552.	0.530
802.	0.458
977.	0.431
1102.	0.412
1227.	0.399
1352.	0.387
1477.	0.381
1602.	0.379
1727.	0.380
1852.	0.378
1977.	0.376
2102.	0.377
2227.	0.374

Plotting frame

6

META OPTION :

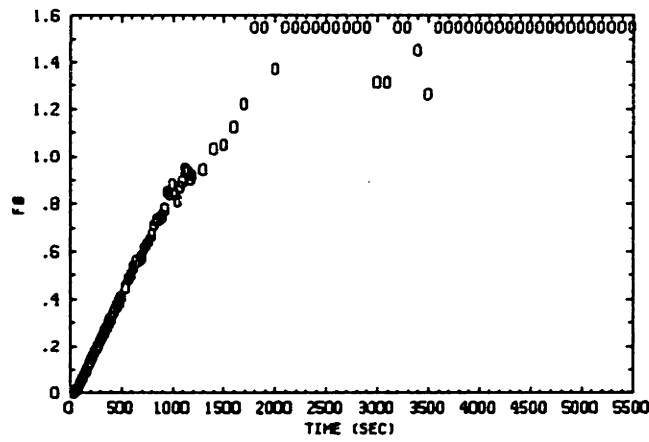
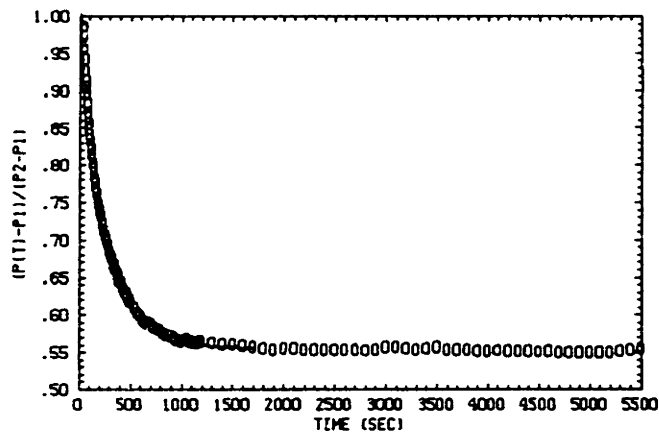


Figure F-22: CO₂, 80°C (Test B) Data Plot Sample 14B.

SAMPLE # 14B-P2
 GAS TESTED: CO2 (80B)
 TEST DATE: 8-30-89

*** INPUT PARAMETERS ***

SAMPLE DIAMETER (IN CM):	3.380
TOTAL CHAMBER VOLUME (IN CM**3):	7.190
CHAMBER GAS VOLUME, ZERO DEF. (IN CM**3):	3.560
CHAMBER GAS VOLUME, MAX. DEF. (IN CM**3):	3.560
FOAM VOID FRACTION:	0.980
START FO FOR BEST-FIT:	0.100
END FO FOR BEST-FIT:	0.600
TEMPERATURE (DEGREES C):	80.000

*** CALCULATED VALUES ***

BEST FIT : FO=	91.999E-5*T + -0.018	
SAMPLE AREA (IN CM**2):		8.973
NUMBER OF DATA POINTS IN BEST-FIT RANGE		110
SAMPLE EFF. HALF-THICKNESS (IN CM):		0.202
EQUILIBRIUM SORPTION PARAMETER, G:		0.801
EQUILIBRIUM PRESSURE		0.555
FOAM SOLUBILITY RATIO		0.786
FOAM SOLUBILITY COEFFICIENT		0.664
POLYMER SOLUBILITY RATIO		-9.698
POLYMER SOLUBILITY		-8.187
DIFFUSION COEFFICIENT (x10**8)		3764.329
PERMEABILITY COEFFICIENT (x10**8)		2497.889

*** TRANSIENT PRESSURE DATA ***

TIME (SEC)	(P(T)-P1)/(P2-P1)
5.	0.987
30.	0.914
55.	0.865
79.	0.827
104.	0.797
129.	0.771
153.	0.749
178.	0.732
203.	0.714
228.	0.701
252.	0.687
277.	0.677
294.	0.671
307.	0.668
319.	0.660
331.	0.658
344.	0.655
356.	0.644
369.	0.644
381.	0.641
406.	0.633
430.	0.626
455.	0.621
661.	0.588
911.	0.567
1161.	0.564
2161.	0.553
3161.	239 0.556
4160.	0.553
5160.	0.550

plotting frame 1

META OPTION :

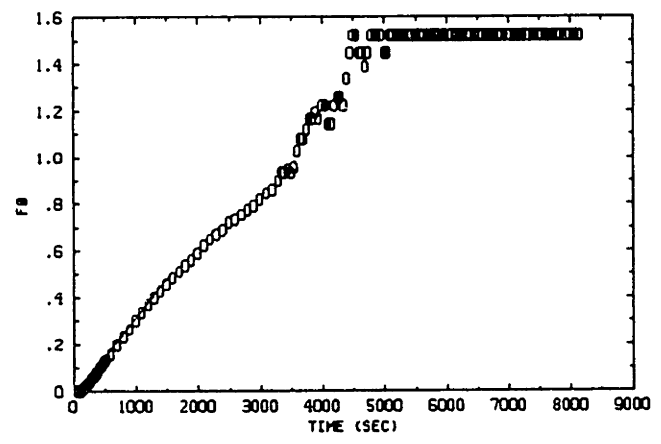
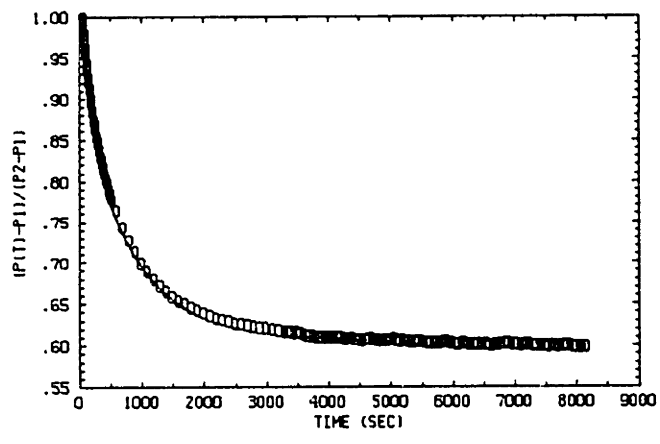


Figure F-23: CO₂ 40°C Data Plot Sample 14A

SAMPLE # 14A-P2
GAS TESTED: CO2
TEST DATE: 6-30-89

*** INPUT PARAMETERS ***

SAMPLE DIAMETER (IN CM): 3.250
TOTAL CHAMBER VOLUME (IN CM**3): 9.130
CHAMBER GAS VOLUME, ZERO DEF. (IN CM**3): 4.600
CHAMBER GAS VOLUME, MAX. DEF. (IN CM**3): 4.600
FOAM VOID FRACTION: 0.980
START FO FOR BEST-FIT: 0.000
END FO FOR BEST-FIT: 0.500
TEMPERATURE (DEGREES C): 40.000

*** CALCULATED VALUES ***

BEST FIT : FO= 33.156E-5*T + -0.019
SAMPLE AREA (IN CM**2): 8.296
NUMBER OF DATA POINTS IN BEST-FIT RANGE 103
SAMPLE EFF. HALF-THICKNESS (IN CM): 0.273
EQUILIBRIUM SORPTION PARAMETER, G: 0.650
EQUILIBRIUM PRESSURE 0.606
FOAM SOLUBILITY RATIO 0.660
FOAM SOLUBILITY COEFFICIENT 0.628
POLYMER SOLUBILITY RATIO -16.000
POLYMER SOLUBILITY -15.233
DIFFUSION COEFFICIENT (x10**8) 2471.621
PERMEABILITY COEFFICIENT (x10**8) 1553.094

*** TRANSIENT PRESSURE DATA ***

TIME (SEC)	(P(T)-P1)/(P2-P1)
5.	0.997
30.	0.979
55.	0.956
79.	0.935
104.	0.921
129.	0.903
153.	0.889
178.	0.876
203.	0.868
228.	0.853
252.	0.846
277.	0.834
302.	0.826
327.	0.819
351.	0.810
376.	0.802
401.	0.797
425.	0.788
450.	0.782
838.	0.713
1338.	0.666
1838.	0.643
2838.	0.622
3537.	0.613
4037.	0.610
4537.	0.607
5037.	0.606
5537.	0.604
6036.	241 0.602
6536.	0.601
7036.	0.601
7536.	0.600
8036.	0.598

plotting frame

3

META OPTION :

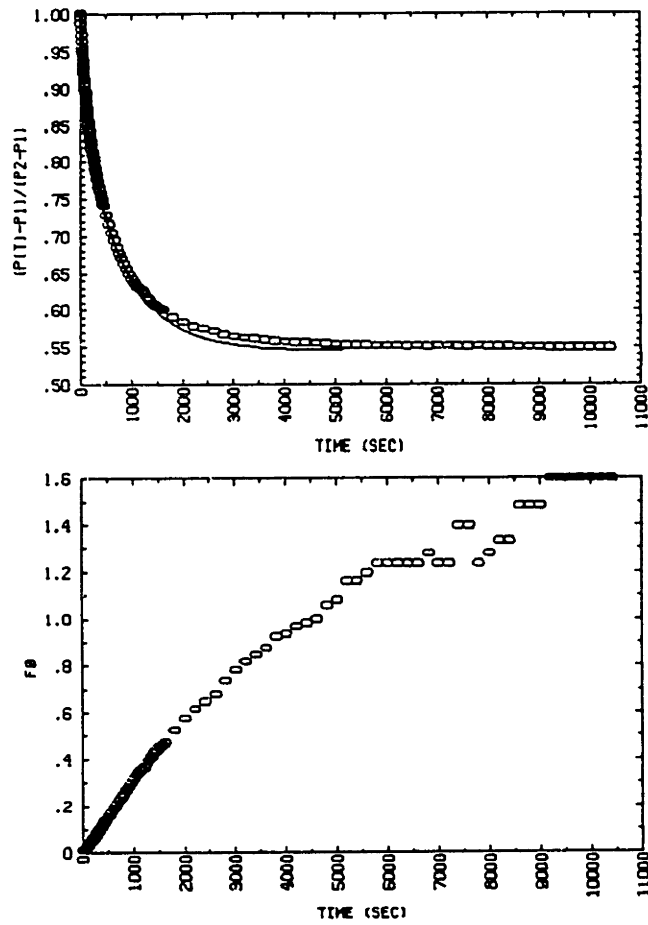


Figure F-24: CO₂ 40°C Data Plot Sample 14B

SAMPLE # 143-P2
 GAS TESTED: CO2
 TEST DATE: 8-31-89

*** INPUT PARAMETERS ***

SAMPLE DIAMETER (IN CM):	3.380
TOTAL CHAMBER VOLUME (IN CM**3):	7.190
CHAMBER GAS VOLUME, ZERO DEF. (IN CM**3):	3.560
CHAMBER GAS VOLUME, MAX. DEF. (IN CM**3):	3.560
FOAM VOID FRACTION:	0.980
START FO FOR BEST-FIT:	0.050
END FO FOR BEST-FIT:	0.400
TEMPERATURE (DEGREES C):	40.000

*** CALCULATED VALUES ***

BEST FIT : FO= 31.251E-5*T + -0.015	
SAMPLE AREA (IN CM**2):	8.973
NUMBER OF DATA POINTS IN BEST-FIT RANGE	72
SAMPLE EFF. HALF-THICKNESS (IN CM):	0.202
EQUILIBRIUM SORPTION PARAMETER, G:	0.835
EQUILIBRIUM PRESSURE	0.545
FOAM SOLUBILITY RATIO	0.818
FOAM SOLUBILITY COEFFICIENT	0.779
POLYMER SOLUBILITY RATIO	-8.078
POLYMER SOLUBILITY	-7.691
DIFFUSION COEFFICIENT (x10**8)	1278.695
PERMEABILITY COEFFICIENT (x10**8)	996.375

*** TRANSIENT PRESSURE DATA ***

TIME (SEC)	(P(T)-P1)/(P2-P1)
5.	0.998
30.	0.961
55.	0.931
79.	0.908
104.	0.888
129.	0.869
153.	0.854
178.	0.838
203.	0.827
228.	0.816
252.	0.805
277.	0.791
302.	0.784
327.	0.776
351.	0.767
376.	0.759
401.	0.751
415.	0.747
428.	0.744
440.	0.740
607.	0.701
857.	0.659
1107.	0.628
1357.	0.610
1607.	0.597
2606.	0.568
3606.	0.556
4606.	0.552
5605.	0.549
6605.	0.548
7604.	0.547
8604.	0.546
9604.	0.545

Plotting frame

1

META OPTION :

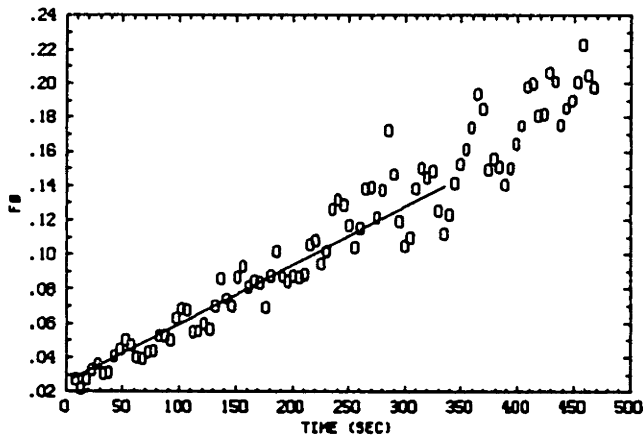
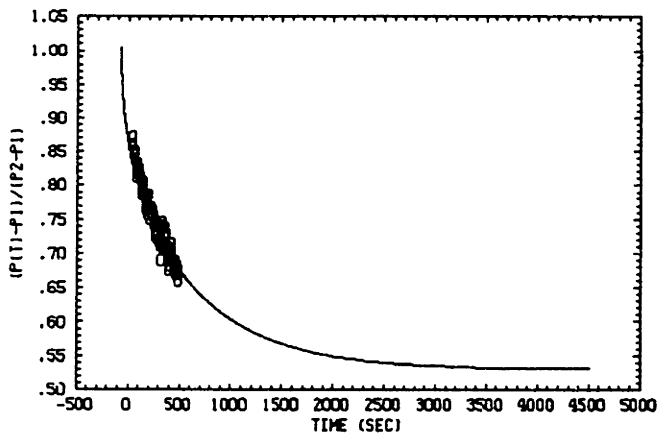


Figure F-25: O₂, 80°C Data Plot Sample 14A.

SAMPLE # 14A-22
GAS TESTED: O2
TEST DATE: 7-14-89

*** INPUT PARAMETERS ***

SAMPLE DIAMETER (IN CM):	3.250
TOTAL CHAMBER VOLUME (IN CM**3):	9.130
CHAMBER GAS VOLUME, ZERO DEF. (IN CM**3):	4.600
CHAMBER GAS VOLUME, MAX. DEF. (IN CM**3):	4.600
FOAM VOID FRACTION:	0.980
START FO FOR BEST-FIT:	0.020
END FO FOR BEST-FIT:	0.140
TEMPERATURE (DEGREES C):	80.000

*** CALCULATED VALUES ***

BEST FIT : FO=	34.191E-5*T +	0.026
SAMPLE AREA (IN CM**2):		8.296
NUMBER OF DATA POINTS IN BEST-FIT RANGE		63
SAMPLE EFF. HALF-THICKNESS (IN CM):		0.273
EQUILIBRIUM SORPTION PARAMETER, G:		0.886
EQUILIBRIUM PRESSURE		0.530
FOAM SOLUBILITY RATIO		0.900
FOAM SOLUBILITY COEFFICIENT		0.760
POLYMER SOLUBILITY RATIO		-4.000
POLYMER SOLUBILITY		-3.377
DIFFUSION COEFFICIENT (x10**8)		2548.796
PERMEABILITY COEFFICIENT (x10**8)		1936.507

*** TRANSIENT PRESSURE DATA ***

TIME (SEC)	(P(T)-P1) / (P2-P1)
5.	0.859
30.	0.851
55.	0.819
79.	0.810
104.	0.788
129.	0.784
153.	0.758
178.	0.763
203.	0.764
228.	0.748
252.	0.746
277.	0.716
302.	0.740
327.	0.727
351.	0.698
376.	0.702
401.	0.689
425.	0.670
450.	0.673

Plotting frame

1

META OPTION :

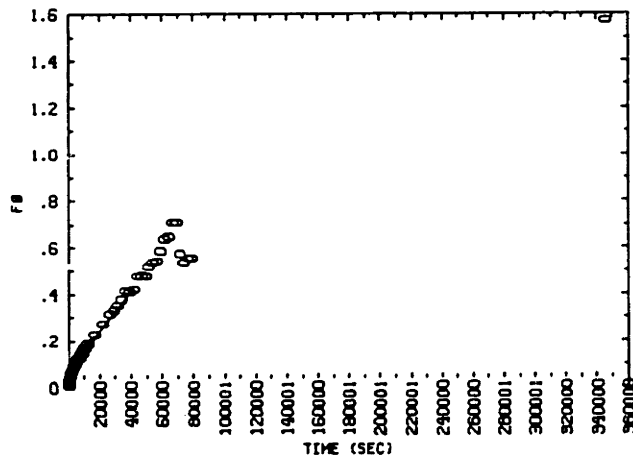
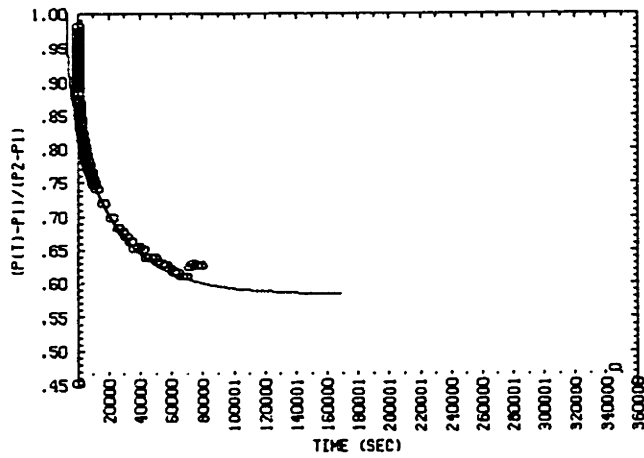


Figure F-26: CFC-11, 80°C Data Plot Sample 14A.

SAMPLE # 14B-P2
 GAS TESTED: CFC-11
 TEST DATE: 9-20-89

*** INPUT PARAMETERS ***

SAMPLE DIAMETER (IN CM):	3.380
TOTAL CHAMBER VOLUME (IN CM**3):	7.190
CHAMBER GAS VOLUME, ZERO DEF. (IN CM**3):	3.560
CHAMBER GAS VOLUME, MAX. DEF. (IN CM**3):	3.560
FOAM VOID FRACTION:	0.980
START FO FOR BEST-FIT:	0.100
END FO FOR BEST-FIT:	0.400
TEMPERATURE (DEGREES C):	80.000

*** CALCULATED VALUES ***

BEST FIT : FO=	0.890E-5*T + 0.063	
SAMPLE AREA (IN CM**2):		8.973
NUMBER OF DATA POINTS IN BEST-FIT RANGE		69
SAMPLE EFF. HALF-THICKNESS (IN CM):		0.202
EQUILIBRIUM SORPTION PARAMETER, G:		0.714
EQUILIBRIUM PRESSURE		0.584
FOAM SOLUBILITY RATIO		0.700
FOAM SOLUBILITY COEFFICIENT		0.591
POLYMER SOLUBILITY RATIO		-14.000
POLYMER SOLUBILITY		-11.819
DIFFUSION COEFFICIENT (x10**8)		36.419
PERMEABILITY COEFFICIENT (x10**8)		21.521

*** TRANSIENT PRESSURE DATA ***

TIME (SEC)	(P(T)-P1) / (P2-P1)
5.	0.977
30.	0.962
55.	0.954
79.	0.950
104.	0.944
129.	0.938
153.	0.936
203.	0.927
228.	0.924
252.	0.922
302.	0.913
327.	0.911
351.	0.908
401.	0.901
425.	0.900
450.	0.896
745.	0.871
1245.	0.847
1744.	0.835
2744.	0.820
3744.	0.803
4743.	0.789
5743.	0.781
6743.	0.774
7742.	0.763
8742.	0.757
9742.	0.751
10241.	0.748
12374.	247 0.736
44004.	0.634
69004.	0.606
345600.	0.469

Blank Page

F.4 Foam No. 15

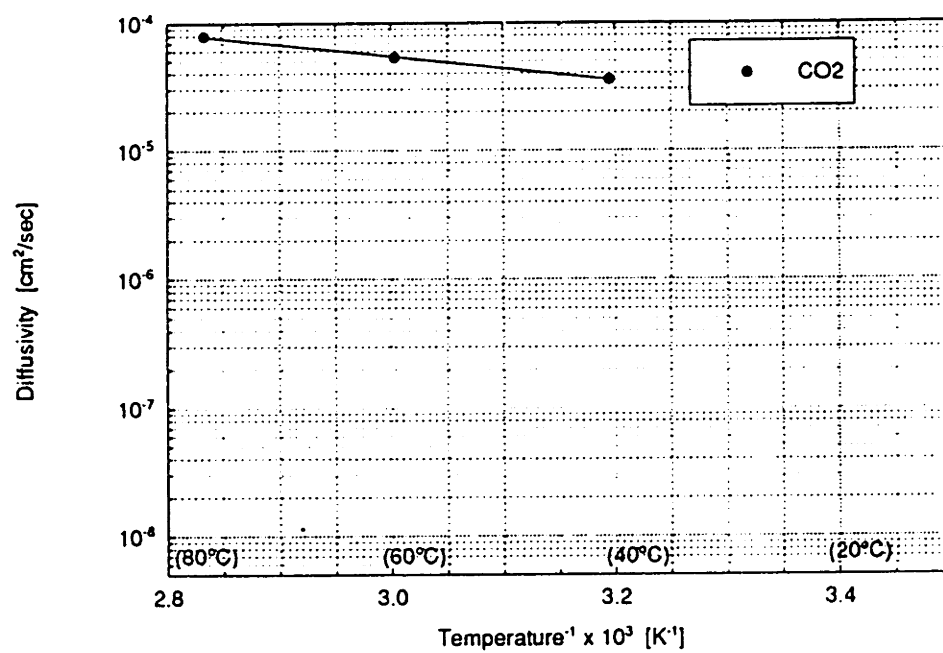


Figure F-27: $\text{Log}(D_{eff})$ versus $1/T$ for all test results, Foam 15.

Plotting frame

5

META OPTION :

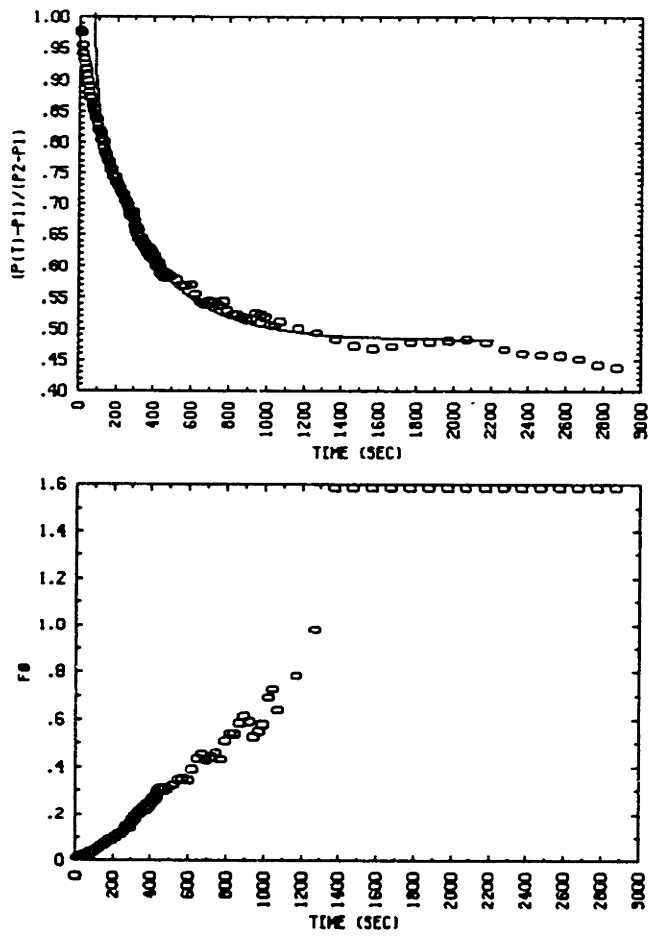


Figure F-28: CO₂, 81°C Data Plot Sample 15B.

SAMPLE # 15B-P3
GAS TESTED: CO2
TEST DATE: 8-30-89

*** INPUT PARAMETERS ***

SAMPLE DIAMETER (IN CM):	3.160
TOTAL CHAMBER VOLUME (IN CM**3):	10.170
CHAMBER GAS VOLUME, ZERO DEF. (IN CM**3):	5.030
CHAMBER GAS VOLUME, MAX. DEF. (IN CM**3):	5.030
FOAM VOID FRACTION:	0.982
START FO FOR BEST-FIT:	0.025
END FO FOR BEST-FIT:	0.300
TEMPERATURE (DEGREES C):	80.000

*** CALCULATED VALUES ***

BEST FIT : FO=	73.915E-5*T +	-0.060	
SAMPLE AREA (IN CM**2):			7.843
NUMBER OF DATA POINTS IN BEST-FIT RANGE		120	
SAMPLE EFF. HALF-THICKNESS (IN CM):			0.328
EQUILIBRIUM SORPTION PARAMETER, G:			1.073
EQUILIBRIUM PRESSURE			0.482
FOAM SOLUBILITY RATIO			1.050
FOAM SOLUBILITY COEFFICIENT			0.886
POLYMER SOLUBILITY RATIO			3.778
POLYMER SOLUBILITY			3.189
DIFFUSION COEFFICIENT (x10**8)			7937.274
PERMEABILITY COEFFICIENT (x10**8)			7035.618

*** TRANSIENT PRESSURE DATA ***

TIME (SEC)	(P(T)-P1)/(P2-P1)
5.	0.974
30.	0.920
55.	0.875
79.	0.844
104.	0.816
129.	0.795
153.	0.767
178.	0.749
203.	0.729
228.	0.710
252.	0.700
272.	0.674
284.	0.680
297.	0.659
309.	0.656
322.	0.638
334.	0.632
346.	0.625
359.	0.619
371.	0.623
396.	0.604
420.	0.594
445.	0.580
470.	0.583
571.	0.563
696.	0.540
821.	0.518
946.	0.520
1071.	0.506
1571.	0.462
2071.	0.478
2571.	0.452

Plotting frame

3

META OPTION :

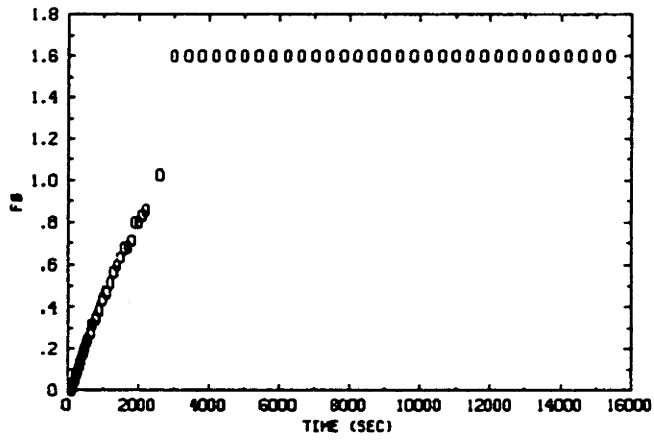
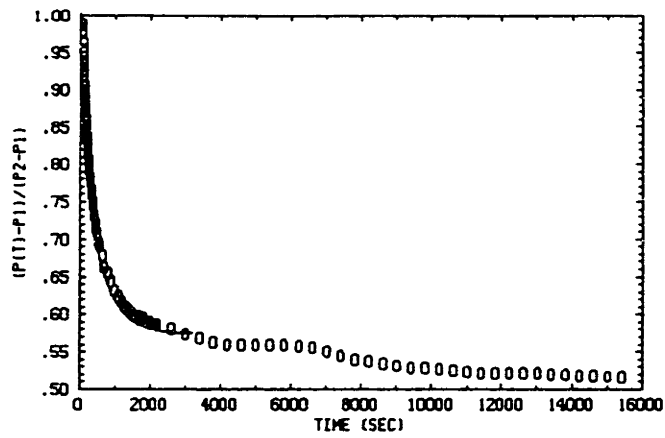


Figure F-29: CO₂, 60°C Data Plot Sample 15B.

SAMPLE # 15B-P3
GAS TESTED: CO2
TEST DATE: 8-30-89

*** INPUT PARAMETERS ***

SAMPLE DIAMETER (IN CM):	3.160
TOTAL CHAMBER VOLUME (IN CM**3):	10.170
CHAMBER GAS VOLUME, ZERO DEF. (IN CM**3):	5.030
CHAMBER GAS VOLUME, MAX. DEF. (IN CM**3):	5.030
FOAM VOID FRACTION:	0.982
START FO FOR BEST-FIT:	0.050
END FO FOR BEST-FIT:	0.500
TEMPERATURE (DEGREES C):	60.000

*** CALCULATED VALUES ***

BEST FIT : FO=	49.807E-5*T +	0.004	
SAMPLE AREA (IN CM**2):			7.843
NUMBER OF DATA POINTS IN BEST-FIT RANGE		78	
SAMPLE EFF. HALF-THICKNESS (IN CM):			0.328
EQUILIBRIUM SORPTION PARAMETER, G:			0.741
EQUILIBRIUM PRESSURE			0.574
FOAM SOLUBILITY RATIO			0.725
FOAM SOLUBILITY COEFFICIENT			0.649
POLYMER SOLUBILITY RATIO			-14.278
POLYMER SOLUBILITY			-12.777
DIFFUSION COEFFICIENT (x10**8)			5348.470
PERMEABILITY COEFFICIENT (x10**8)			3470.081

*** TRANSIENT PRESSURE DATA ***

TIME (SEC)	(P(T)-P1)/(P2-P1)
5.	0.988
30.	0.934
55.	0.898
79.	0.870
104.	0.849
129.	0.830
153.	0.810
178.	0.796
203.	0.784
228.	0.772
252.	0.761
277.	0.750
302.	0.738
327.	0.732
351.	0.723
376.	0.714
401.	0.708
425.	0.700
450.	0.695
541.	0.678
1009.	0.624
1509.	0.598
2009.	0.587
3708.	0.563
5719.	0.559
7726.	0.539
9726.	0.528
11725.	0.522
13724.	0.519

plotting frame

2

META OPTION :

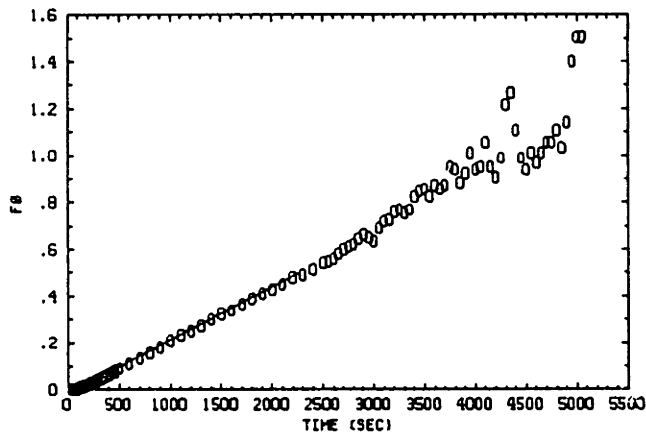
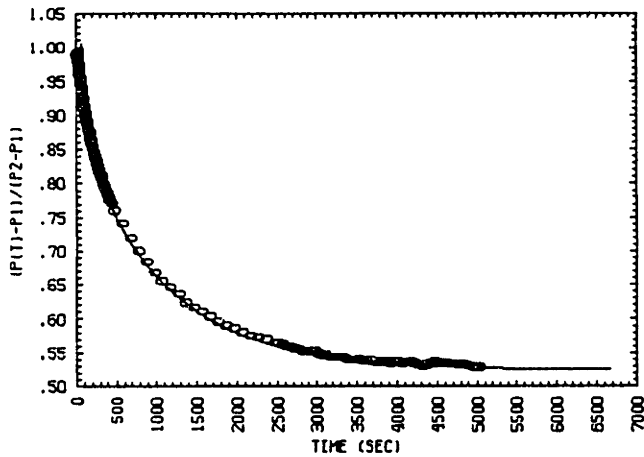


Figure F-30: CO₂, 40°C Data Plot Sample 15A

SAMPLE # 15A-P3
GAS TESTED: CO2
TEST DATE: 6-30-89

*** INPUT PARAMETERS ***

SAMPLE DIAMETER (IN CM):	3.258
TOTAL CHAMBER VOLUME (IN CM**3):	10.170
CHAMBER GAS VOLUME, ZERO DEF. (IN CM**3):	3.590
CHAMBER GAS VOLUME, MAX. DEF. (IN CM**3):	3.590
FOAM VOID FRACTION:	0.982
START FO FOR BEST-FIT:	0.050
END FO FOR BEST-FIT:	0.500
TEMPERATURE (DEGREES C):	40.000

*** CALCULATED VALUES ***

BEST FIT : FO=	22.901E-5*T +	-0.019	
SAMPLE AREA (IN CM**2):			8.337
NUMBER OF DATA POINTS IN BEST-FIT RANGE			47
SAMPLE EFF. HALF-THICKNESS (IN CM):			0.395
EQUILIBRIUM SORPTION PARAMETER, G:			0.907
EQUILIBRIUM PRESSURE			0.524
FOAM SOLUBILITY RATIO			0.495
FOAM SOLUBILITY COEFFICIENT			0.471
POLYMER SOLUBILITY RATIO			-27.071
POLYMER SOLUBILITY			-25.773
DIFFUSION COEFFICIENT (x10**8)			3566.690
PERMEABILITY COEFFICIENT (x10**8)			1679.983

*** TRANSIENT PRESSURE DATA ***

TIME (SEC)	(P(T)-P1) / (P2-P1)
5.	0.985
30.	0.970
55.	0.945
79.	0.924
104.	0.906
129.	0.890
153.	0.875
178.	0.860
203.	0.850
228.	0.838
252.	0.829
277.	0.819
302.	0.809
327.	0.802
351.	0.793
376.	0.785
401.	0.777
425.	0.770
671.	0.715
1171.	0.642
1671.	0.599
2170.	0.571
2570.	0.558
2820.	0.549
3070.	0.542
3320.	0.539
3570.	0.534
3820.	0.534
4070.	0.529
4320.	0.526
4570.	0.531
4820.	0.529

Blank Page

F.5 Foam No. 16

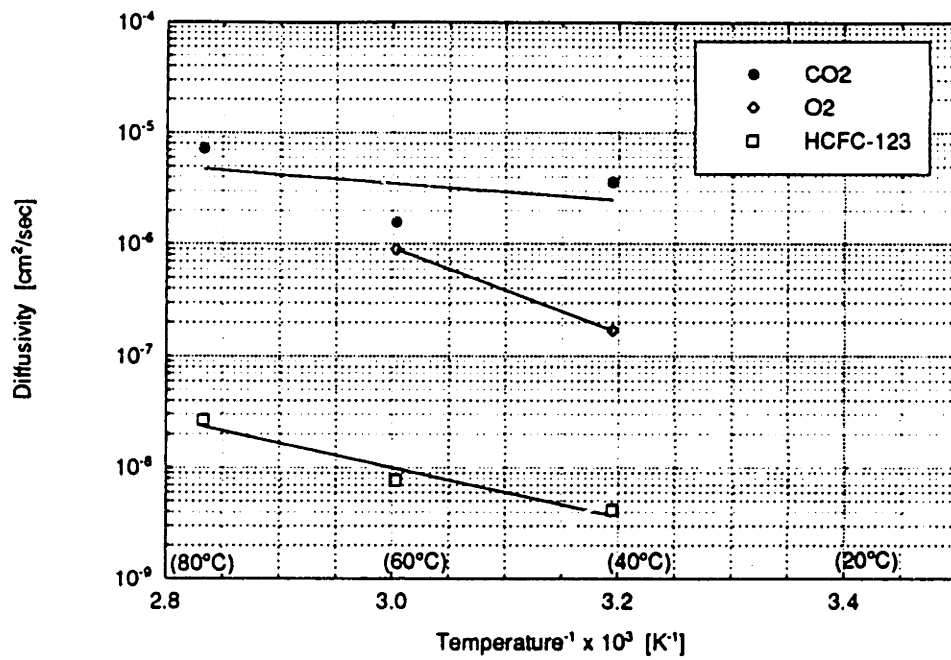


Figure F-31: $\text{Log}(D_{eff})$ versus $1/T$ for all test results, Foam 16.

Plotting frame

3

META OPTION :

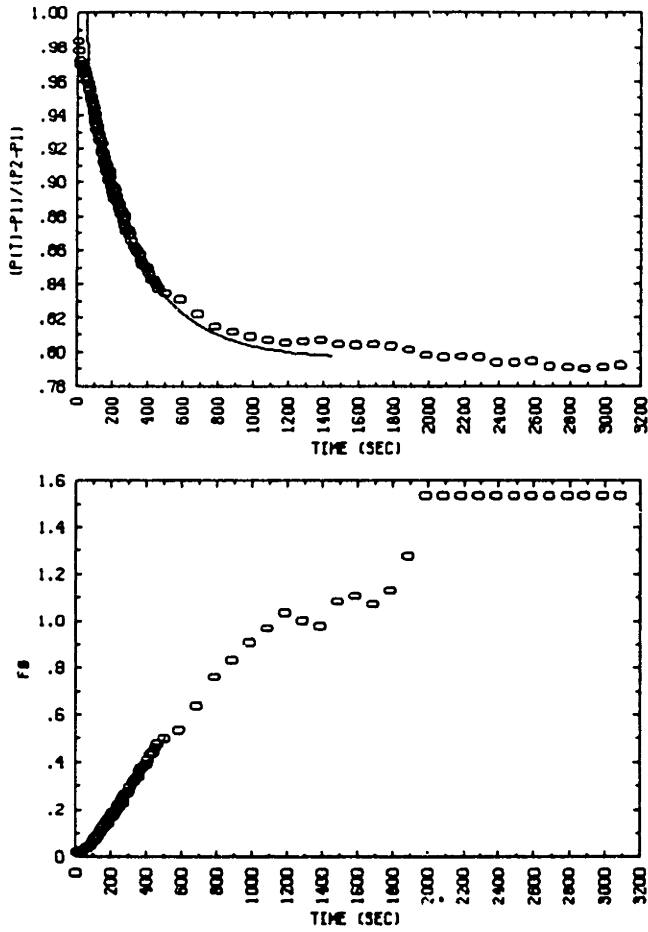


Figure F-32: CO₂, 80°C Data Plot Sample 16A.

SAMPLE # 16A-P2
GAS TESTED: CO2
TEST DATE: 10-3-89

*** INPUT PARAMETERS ***

SAMPLE DIAMETER (IN CM):	3.470
TOTAL CHAMBER VOLUME (IN CM**3):	5.260
CHAMBER GAS VOLUME, ZERO DEF. (IN CM**3):	3.730
CHAMBER GAS VOLUME, MAX. DEF. (IN CM**3):	3.730
FOAM VOID FRACTION:	0.977
START FO FOR BEST-FIT:	0.020
END FO FOR BEST-FIT:	0.500
TEMPERATURE (DEGREES C):	80.000

*** CALCULATED VALUES ***

BEST FIT : FO=	109.854E-5*T +	-0.060
SAMPLE AREA (IN CM**2):		9.457
NUMBER OF DATA POINTS IN BEST-FIT RANGE	109	
SAMPLE EFF. HALF-THICKNESS (IN CM):		0.081
EQUILIBRIUM SORPTION PARAMETER, G:		0.256
EQUILIBRIUM PRESSURE		0.796
FOAM SOLUBILITY RATIO		0.625
FOAM SOLUBILITY COEFFICIENT		0.528
POLYMER SOLUBILITY RATIO		-15.304
POLYMER SOLUBILITY		-12.920
DIFFUSION COEFFICIENT (x10**8)		718.857
PERMEABILITY COEFFICIENT (x10**8)		379.284

*** TRANSIENT PRESSURE DATA ***

TIME (SEC)	(P(T)-P1)/(P2-P1)
5.	0.982
30.	0.968
55.	0.960
74.	0.949
87.	0.945
99.	0.939
111.	0.930
124.	0.924
136.	0.921
149.	0.914
161.	0.905
173.	0.905
186.	0.905
198.	0.896
210.	0.893
223.	0.889
235.	0.886
247.	0.881
260.	0.876
272.	0.873
292.	0.870
341.	0.858
391.	0.848
440.	0.840
685.	0.821
1185.	0.804
1684.	0.803
2184.	0.796
2684.	0.790

plotting frame

2

META OPTION :

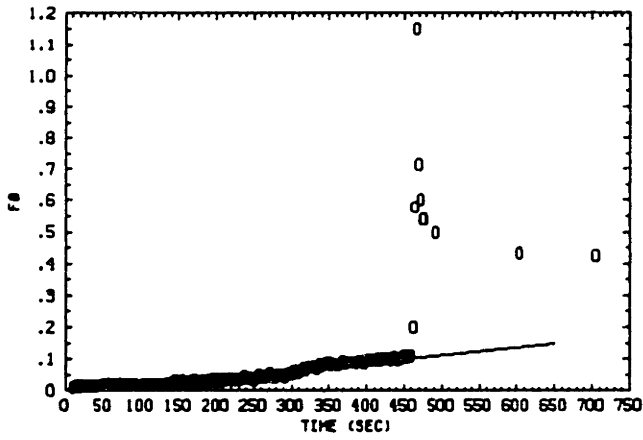
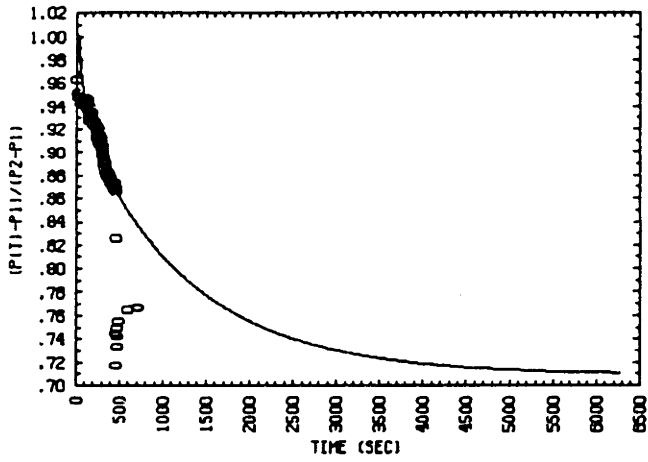


Figure F-33: CO₂, 60°C Data Plot Sample 16A

SAMPLE # 16A-P2
GAS TESTED: CO2
TEST DATE: 10-5-89

*** INPUT PARAMETERS ***

SAMPLE DIAMETER (IN CM):	3.470
TOTAL CHAMBER VOLUME (IN CM**3):	5.260
CHAMBER GAS VOLUME, ZERO DEF. (IN CM**3):	3.730
CHAMBER GAS VOLUME, MAX. DEF. (IN CM**3):	3.730
FOAM VOID FRACTION:	0.977
START FO FOR BEST-FIT:	0.010
END FO FOR BEST-FIT:	0.150
TEMPERATURE (DEGREES C):	60.000

*** CALCULATED VALUES ***

BEST FIT : FO=	24.387E-5*T +	-0.008	
SAMPLE AREA (IN CM**2):			9.457
NUMBER OF DATA POINTS IN BEST-FIT RANGE		158	
SAMPLE EFF. HALF-THICKNESS (IN CM):			0.081
EQUILIBRIUM SORPTION PARAMETER, G:			0.410
EQUILIBRIUM PRESSURE			0.709
FOAM SOLUBILITY RATIO			1.000
FOAM SOLUBILITY COEFFICIENT			0.895
POLYMER SOLUBILITY RATIO			1.000
POLYMER SOLUBILITY			0.895
DIFFUSION COEFFICIENT (x10**8)			159.579
PERMEABILITY COEFFICIENT (x10**8)			142.807

*** TRANSIENT PRESSURE DATA ***

TIME (SEC)	(P(T)-P1)/(P2-P1)
5.	0.960
30.	0.945
55.	0.942
79.	0.944
104.	0.943
126.	0.943
139.	0.933
151.	0.925
163.	0.924
176.	0.930
188.	0.924
200.	0.923
213.	0.922
225.	0.918
238.	0.914
250.	0.911
262.	0.910
275.	0.909
287.	0.910
299.	0.895
312.	0.890
324.	0.886
336.	0.882
349.	0.879
361.	0.876
373.	0.876
386.	0.874
398.	0.870
411.	0.869
423.	0.869
435.	0.870
448.	0.867
460.	0.743

Plotting frame

1

META OPTION :

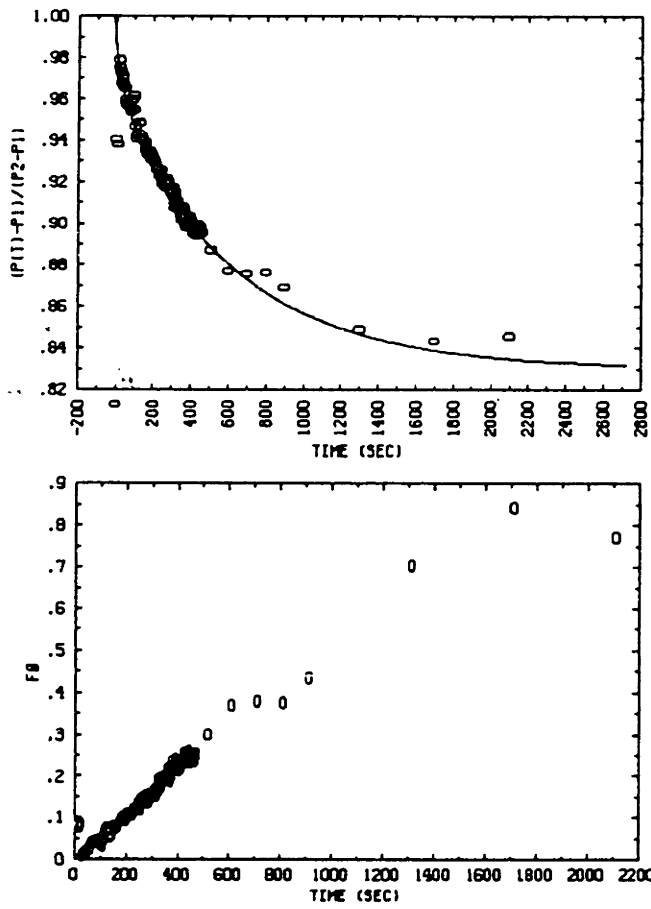


Figure F-34: CO₂, 40°C Data Plot Sample 16A

SAMPLE # 16A-P2
CAS TESTED: CO2
TEST DATE: 10-8-89

*** INPUT PARAMETERS ***

SAMPLE DIAMETER (IN CM):	3.470
TOTAL CHAMBER VOLUME (IN CM**3):	5.260
CHAMBER GAS VOLUME, ZERO DEF. (IN CM**3):	3.730
CHAMBER GAS VOLUME, MAX. DEF. (IN CM**3):	3.730
FOAM VOID FRACTION:	0.977
START FO FOR BEST-FIT:	0.001
END FO FOR BEST-FIT:	0.250
TEMPERATURE (DEGREES C):	40.000

*** CALCULATED VALUES ***

BEST FIT : FO=	55.180E-5*T +	0.004	
SAMPLE AREA (IN CM**2):			9.457
NUMBER OF DATA POINTS IN BEST-FIT RANGE		128	
SAMPLE EFF. HALF-THICKNESS (IN CM):			0.081
EQUILIBRIUM SORPTION PARAMETER, G:			0.205
EQUILIBRIUM PRESSURE			0.830
FOAM SOLUBILITY RATIO			0.500
FOAM SOLUBILITY COEFFICIENT			0.476
POLYMER SOLUBILITY RATIO			-20.739
POLYMER SOLUBILITY			-19.745
DIFFUSION COEFFICIENT (x10**8)			361.082
PERMEABILITY COEFFICIENT (x10**8)			171.889

*** TRANSIENT PRESSURE DATA ***

TIME (SEC)	(P(T)-P1) / (P2-P1)
5.	0.939
30.	0.970
55.	0.956
79.	0.952
104.	0.945
129.	0.947
153.	0.937
178.	0.932
203.	0.929
228.	0.924
242.	0.922
255.	0.920
267.	0.915
280.	0.917
292.	0.916
304.	0.914
317.	0.906
329.	0.906
341.	0.905
354.	0.904
366.	0.897
378.	0.897
391.	0.901
403.	0.898
415.	0.893
428.	0.894
440.	0.894
453.	0.895
697.	0.874
2097.	0.844

plotting frame

3

META OPTION :

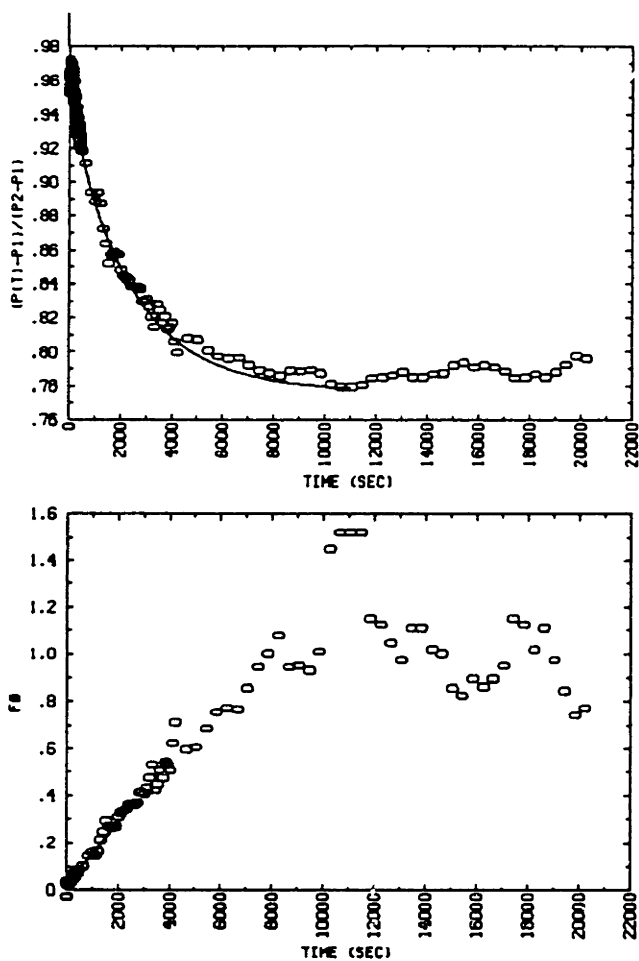


Figure F-35: O₂, 60°C Data Plot Sample 16A

SAMPLE # 16A-P2
GAS TESTED: O2
TEST DATE: 11-15-89

*** INPUT PARAMETERS ***

SAMPLE DIAMETER (IN CM):	3.470
TOTAL CHAMBER VOLUME (IN CM**3):	5.260
CHAMBER GAS VOLUME, ZERO DEF. (IN CM**3):	3.730
CHAMBER GAS VOLUME, MAX. DEF. (IN CM**3):	3.730
FOAM VOID FRACTION:	0.977
START FO FOR BEST-FIT:	0.010
END FO FOR BEST-FIT:	0.260
TEMPERATURE (DEGREES C):	60.000

*** CALCULATED VALUES ***

BEST FIT : $FO = 13.701E-5 * T + 0.007$

SAMPLE AREA (IN CM**2):	9.457
NUMBER OF DATA POINTS IN BEST-FIT RANGE	104
SAMPLE EFF. HALF-THICKNESS (IN CM):	0.081
EQUILIBRIUM SORPTION PARAMETER, G:	0.287
EQUILIBRIUM PRESSURE	0.777
FOAM SOLUBILITY RATIO	0.700
FOAM SOLUBILITY COEFFICIENT	0.626
POLYMER SOLUBILITY RATIO	-12.043
POLYMER SOLUBILITY	-10.778
DIFFUSION COEFFICIENT (x10**8)	89.657
PERMEABILITY COEFFICIENT (x10**8)	56.163

*** TRANSIENT PRESSURE DATA ***

TIME (SEC)	(P(T)-P1) / (P2-P1)
5.	0.955
30.	0.953
55.	0.968
79.	0.956
104.	0.959
129.	0.952
153.	0.958
178.	0.948
203.	0.936
228.	0.942
252.	0.939
277.	0.933
302.	0.932
327.	0.933
351.	0.926
376.	0.932
401.	0.920
425.	0.926
450.	0.920
842.	0.892
1442.	0.862
1942.	0.855
2442.	0.837
2942.	0.828
3441.	0.827
3941.	0.813
5041.	0.805
7040.	0.790
9039.	2650.787
11039.	0.778
13038.	0.786
15037.	0.790
17037.	0.787

plotting frame

1

META OPTION :

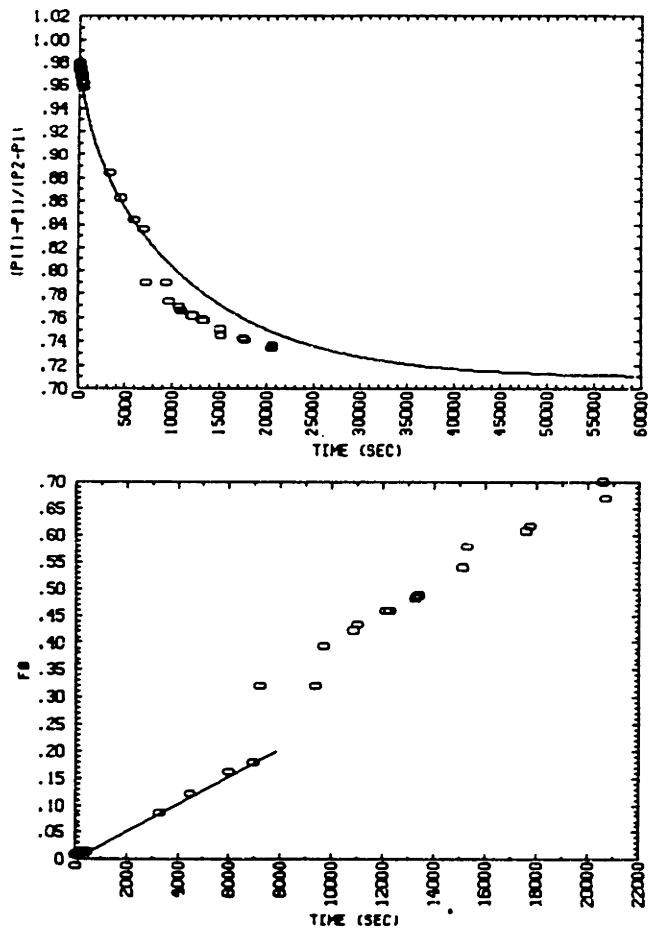


Figure F-36: O₂, 40°C Data Plot Sample 16A

SAMPLE # 16A-P2
 GAS TESTED: O2
 TEST DATE: 11-28-89

*** INPUT PARAMETERS ***

SAMPLE DIAMETER (IN CM):	3.470
TOTAL CHAMBER VOLUME (IN CM**3):	5.260
CHAMBER GAS VOLUME, ZERO DEF. (IN CM**3):	3.730
CHAMBER GAS VOLUME, MAX. DEF. (IN CM**3):	3.730
FOAM VOID FRACTION:	0.977
START FO FOR BEST-FIT:	0.010
END FO FOR BEST-FIT:	0.200
TEMPERATURE (DEGREES C):	40.000

*** CALCULATED VALUES ***

BEST FIT : FO=	2.577E-5*T +	-0.001	
SAMPLE AREA (IN CM**2):			9.457
NUMBER OF DATA POINTS IN BEST-FIT RANGE			5
SAMPLE EFF. HALF-THICKNESS (IN CM):			0.081
EQUILIBRIUM SORPTION PARAMETER, G:			0.410
EQUILIBRIUM PRESSURE			0.709
FOAM SOLUBILITY RATIO			1.000
FOAM SOLUBILITY COEFFICIENT			0.952
POLYMER SOLUBILITY RATIO			1.000
POLYMER SOLUBILITY			0.952
DIFFUSION COEFFICIENT (x10**8)			16.863
PERMEABILITY COEFFICIENT (x10**8)			16.055

*** TRANSIENT PRESSURE DATA ***

TIME (SEC)	(P(T)-P1)/(P2-P1)
5.	0.971
30.	0.975
55.	0.976
79.	0.972
104.	0.967
129.	0.973
153.	0.971
178.	0.970
203.	0.967
228.	0.965
252.	0.965
277.	0.965
302.	0.961
327.	0.962
351.	0.965
376.	0.960
401.	0.959
425.	0.958
450.	0.957
7185.	0.787
12100.	0.759
15240.	0.743

plotting frame

3

META OPTION :

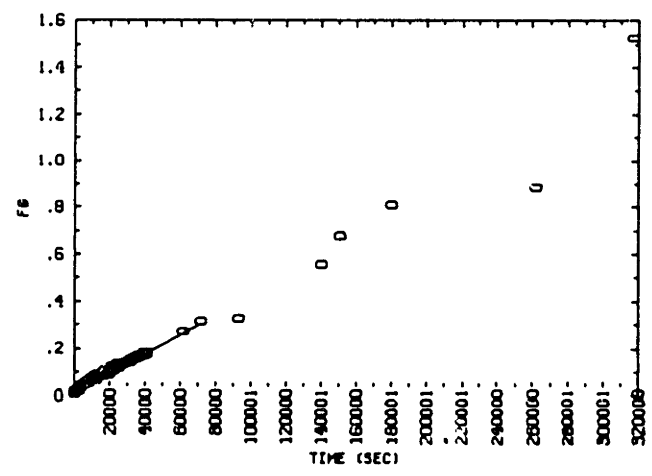
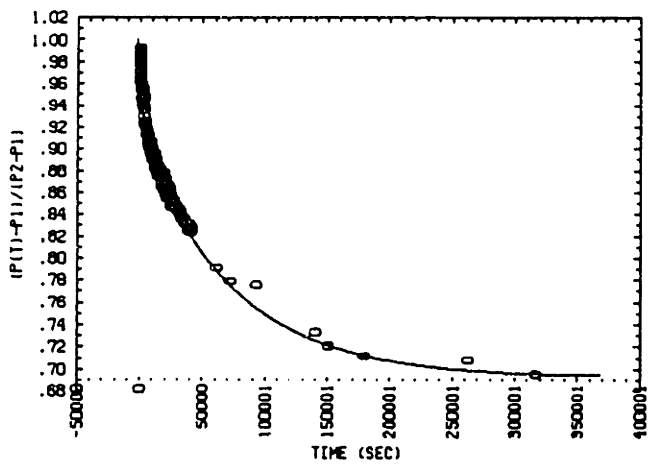


Figure F-37: HCFC-123, 80°C Data Plot Sample 16A

SAMPLE # 16A-P2
 GAS TESTED: HCFC-123
 TEST DATE: 12-16-89

*** INPUT PARAMETERS ***

SAMPLE DIAMETER (IN CM): 3.470
 TOTAL CHAMBER VOLUME (IN CM**3): 5.260
 CHAMBER GAS VOLUME, ZERO DEF. (IN CM**3): 3.730
 CHAMBER GAS VOLUME, MAX. DEF. (IN CM**3): 3.730
 FOAM VOID FRACTION: 0.977
 START FO FOR BEST-FIT: 0.001
 END FO FOR BEST-FIT: 0.300
 TEMPERATURE (DEGREES C): 80.000

*** CALCULATED VALUES ***

BEST FIT : FO= 0.409E-5*T + 0.011
 SAMPLE AREA (IN CM**2): 9.457
 NUMBER OF DATA POINTS IN BEST-FIT RANGE 599
 SAMPLE EFF. HALF-THICKNESS (IN CM): 0.081
 EQUILIBRIUM SORPTION PARAMETER, G: 0.444
 EQUILIBRIUM PRESSURE 0.692
 FOAM SOLUBILITY RATIO 1.083
 FOAM SOLUBILITY COEFFICIENT 0.914
 POLYMER SOLUBILITY RATIO 4.610
 POLYMER SOLUBILITY 3.892
 DIFFUSION COEFFICIENT (x10**8) 2.676
 PERMEABILITY COEFFICIENT (x10**8) 2.447

*** TRANSIENT PRESSURE DATA ***

TIME (SEC)	(P(T)-P1)/(P2-P1)	TIME (SEC)	(P(T)-P1)/(P2-P1)
5.	0.990	13250.	0.883
55.	0.988	14250.	0.880
104.	0.982	15249.	0.875
153.	0.977	16499.	0.871
203.	0.971	17499.	0.871
277.	0.967	18498.	0.869
376.	0.963	18998.	0.868
425.	0.961	19248.	0.863
639.	0.952	20248.	0.857
1139.	0.956	20498.	0.863
1639.	0.947	21011.	0.857
2138.	0.937	21262.	0.859
2638.	0.946	22012.	0.863
3138.	0.935	23011.	0.859
3638.	0.920	24011.	0.855
4638.	0.917	25510.	0.846
5637.	0.914	26360.	0.851
6137.	0.907	28359.	0.844
7736.	0.900	30359.	0.843
8986.	0.895	32374.	0.838
9736.	0.898	37372.	0.828
10486.	0.891	40371.	0.824
11001.	0.885	61620.	0.789
12001.	0.893	179563.	0.709

plotting frame

2

META OPTION :

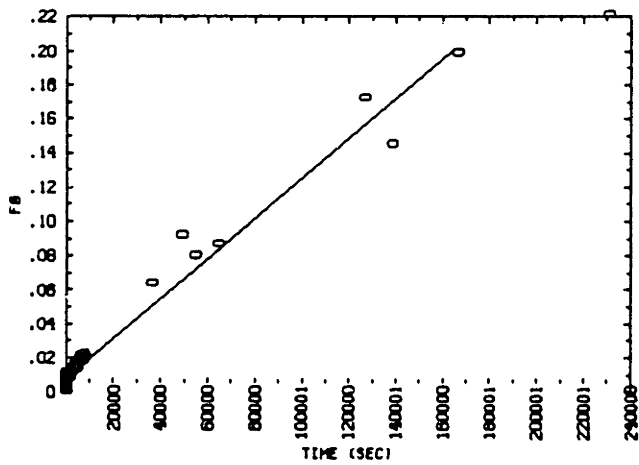
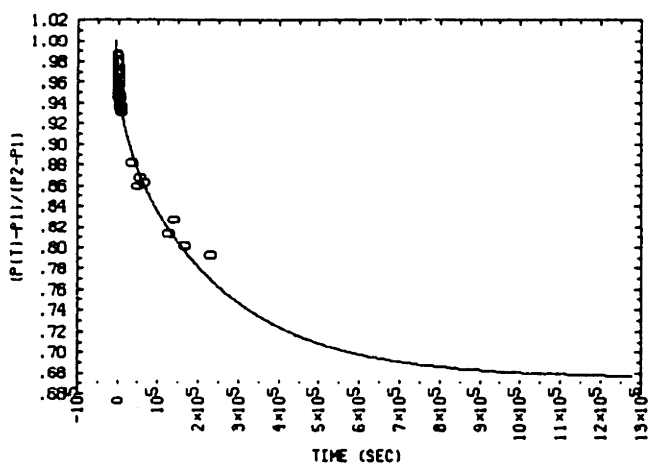


Figure F-38: HCFC-123, 60°C Data Plot Sample 16A

SAMPLE # 16A-P2
 GAS TESTED: HCFC-123
 TEST DATE: 1-9-90

*** INPUT PARAMETERS ***

SAMPLE DIAMETER (IN CM):	3.470
TOTAL CHAMBER VOLUME (IN CM**3):	5.260
CHAMBER GAS VOLUME, ZERO DEF. (IN CM**3):	3.730
CHAMBER GAS VOLUME, MAX. DEF. (IN CM**3):	3.730
FOAM VOID FRACTION:	0.977
START FO FOR BEST-FIT:	0.005
END FO FOR BEST-FIT:	0.200
TEMPERATURE (DEGREES C):	60.000

*** CALCULATED VALUES ***

BEST FIT : FO=	0.117E-5*T +	0.008	
SAMPLE AREA (IN CM**2):			9.457
NUMBER OF DATA POINTS IN BEST-FIT RANGE		142	
SAMPLE EFF. HALF-THICKNESS (IN CM):			0.081
EQUILIBRIUM SORPTION PARAMETER, G:			0.480
EQUILIBRIUM PRESSURE			0.676
FOAM SOLUBILITY RATIO			1.170
FOAM SOLUBILITY COEFFICIENT			1.047
POLYMER SOLUBILITY RATIO			8.391
POLYMER SOLUBILITY			7.509
DIFFUSION COEFFICIENT (x10**8)			0.768
PERMEABILITY COEFFICIENT (x10**8)			0.804

*** TRANSIENT PRESSURE DATA ***

TIME (SEC)	(P(T)-P1)/(P2-P1)
5.	0.976
30.	0.983
55.	0.972
79.	0.968
104.	0.967
129.	0.966
178.	0.964
228.	0.962
277.	0.960
327.	0.963
401.	0.960
452.	0.957
892.	0.958
1392.	0.959
1892.	0.952
2392.	0.948
2891.	0.946
3404.	0.942
3904.	0.941
4904.	0.939
5403.	0.937
5915.	0.934
6415.	0.929
6915.	0.932
7415.	0.933
7914.	0.931
64390.	0.860

Plotting frame

1

META OPTION :

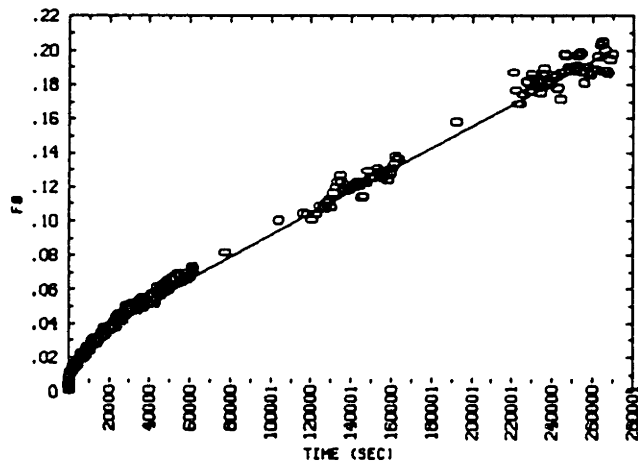
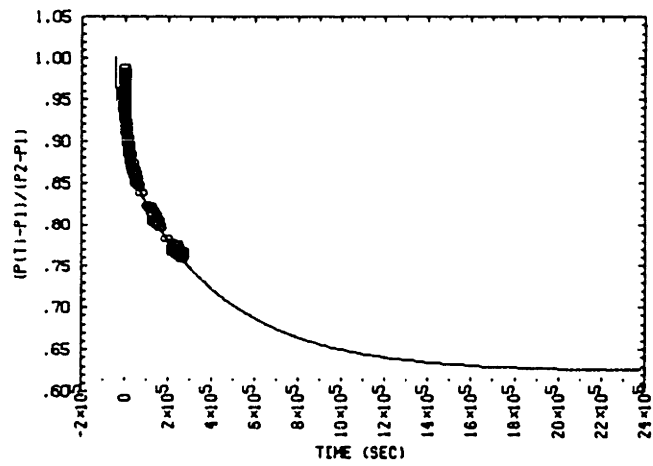


Figure F-39: HCFC-123, 40°C Data Plot Sample 16A

SAMPLE * 16A-P2
 GAS TESTED: HCFC-123
 TEST DATE: 2-14-90

*** INPUT PARAMETERS ***

SAMPLE DIAMETER (IN CM): 3.470
 TOTAL CHAMBER VOLUME (IN CM**3): 5.260
 CHAMBER GAS VOLUME, ZERO DEF. (IN CM**3): 3.730
 CHAMBER GAS VOLUME, MAX. DEF. (IN CM**3): 3.730
 FOAM VOID FRACTION: 0.977
 START FO FOR BEST-FIT: 0.040
 END FO FOR BEST-FIT: 0.200
 TEMPERATURE (DEGREES C): 40.000

*** CALCULATED VALUES ***

BEST FIT : FO= 0.064E-5*T + 0.028
 SAMPLE AREA (IN CM**2): 9.457
 NUMBER OF DATA POINTS IN BEST-FIT RANGE 281
 SAMPLE EFF. HALF-THICKNESS (IN CM): 0.081
 EQUILIBRIUM SORPTION PARAMETER, G: 0.602
 EQUILIBRIUM PRESSURE 0.624
 FOAM SOLUBILITY RATIO 1.468
 FOAM SOLUBILITY COEFFICIENT 1.398
 POLYMER SOLUBILITY RATIO 21.348
 POLYMER SOLUBILITY 20.325
 DIFFUSION COEFFICIENT (x10**8) 0.416
 PERMEABILITY COEFFICIENT (x10**8) 0.581

*** TRANSIENT PRESSURE DATA ***

TIME (SEC)	(P(T)-P1)/(P2-P1)	TIME (SEC)	(P(T)-P1)/(P2-P1)
5.	0.984	10416.	0.904
30.	0.973	12415.	0.899
55.	0.968	14414.	0.895
79.	0.964	16414.	0.891
104.	0.962	18413.	0.892
129.	0.960	20412.	0.887
153.	0.958	22428.	0.881
178.	0.955	25427.	0.874
203.	0.955	27426.	0.875
228.	0.952	29425.	0.873
252.	0.952	31425.	0.869
302.	0.951	38422.	0.862
327.	0.952	49435.	0.851
351.	0.948	59431.	0.848
376.	0.947	61430.	0.843
401.	0.950	118115.	0.816
470.	0.948	127114.	0.813
1419.	0.935	137113.	0.806
2419.	0.930	147113.	0.802
3418.	0.928	157112.	0.799
4418.	0.923	162111.	0.792
5418.	0.917	237723.	0.767
6417.	0.912	247722.	0.763
7417.	0.914	257721.	0.763
8417.	0.910	267720.	0.764
9416.	0.904		

Blank Page

F.6 Foam No. 17

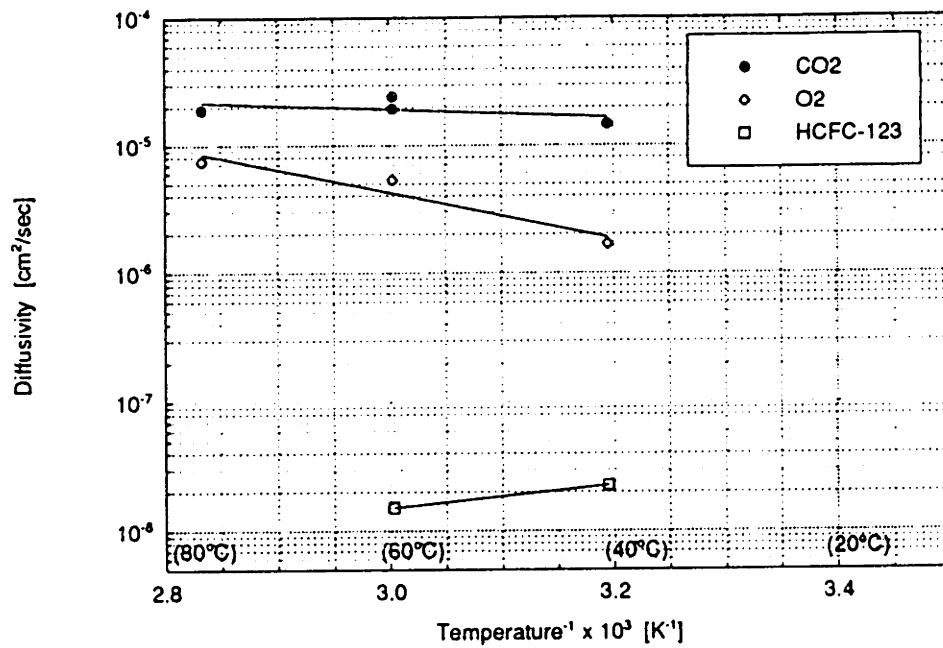


Figure F-40: $\text{Log}(D_{eff})$ versus $1/T$ for all test results, Foam 17.

Plotting frame

4

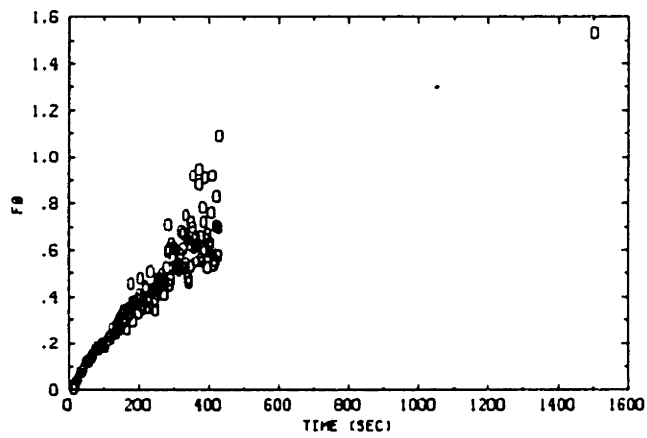
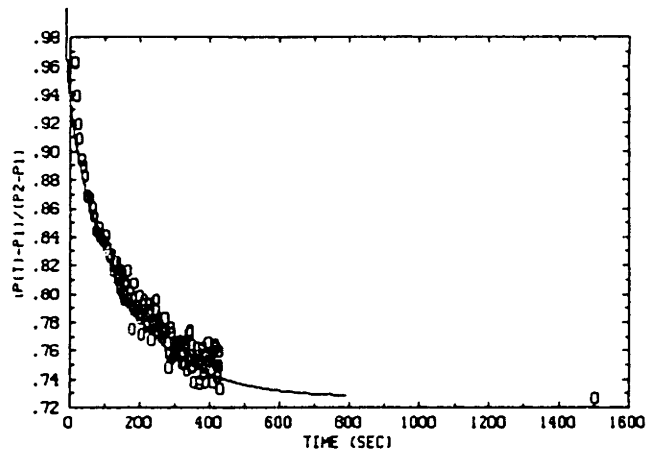


Figure F-41: CO₂, 80°C Data Plot Sample 17A.

SAMPLE # 17A-P3
GAS TESTED: CO2
TEST DATE: 10-8-89

*** INPUT PARAMETERS ***

SAMPLE DIAMETER (IN CM):	3.470
TOTAL CHAMBER VOLUME (IN CM**3):	5.540
CHAMBER GAS VOLUME, ZERO DEF. (IN CM**3):	3.657
CHAMBER GAS VOLUME, MAX. DEF. (IN CM**3):	3.657
FOAM VOID FRACTION:	0.979
START FO FOR BEST-FIT:	0.000
END FO FOR BEST-FIT:	0.250
TEMPERATURE (DEGREES C):	80.000

*** CALCULATED VALUES ***

BEST FIT : FO= 191.652E-5*T + 0.025

SAMPLE AREA (IN CM**2):	9.457
NUMBER OF DATA POINTS IN BEST-FIT RANGE	24
SAMPLE EFF. HALF-THICKNESS (IN CM):	0.100
EQUILIBRIUM SCORPTION PARAMETER, G:	0.376
EQUILIBRIUM PRESSURE	0.727
FOAM SOLUBILITY RATIO	0.730
FOAM SOLUBILITY COEFFICIENT	0.616
POLYMER SOLUBILITY RATIO	-11.851
POLYMER SOLUBILITY	-10.004
DIFFUSION COEFFICIENT (x10**8)	1899.573
PERMEABILITY COEFFICIENT (x10**8)	1170.851

*** TRANSIENT PRESSURE DATA ***

TIME (SEC)	(P(T)-P1)/(P2-P1)
5.	0.963
30.	0.890
55.	0.860
79.	0.840
104.	0.826
126.	0.812
139.	0.816
151.	0.798
163.	0.802
176.	0.788
188.	0.786
200.	0.793
213.	0.779
225.	0.768
238.	0.796
250.	0.778
262.	0.782
275.	0.748
287.	0.761
299.	0.758
312.	0.750
324.	0.763
336.	0.755
349.	0.756
361.	0.737
373.	0.744
386.	0.766
398.	0.745
411.	0.749
1494.	0.727

Plotting frame 2

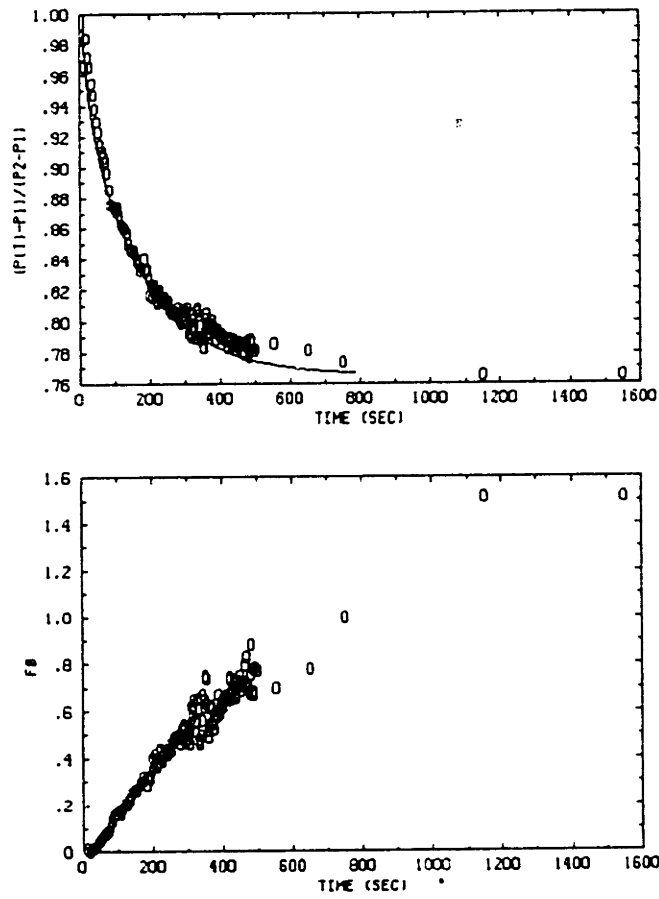


Figure F-42: CO₂, 60°C (Test A) Data Plot Sample 17A

SAMPLE # 17A-P3
GAS TESTED: CO2
TEST DATE: 10-6-89

*** INPUT PARAMETERS ***

SAMPLE DIAMETER (IN CM):	3.470
TOTAL CHAMBER VOLUME (IN CM**3):	5.540
CHAMBER GAS VOLUME, ZERO DEF. (IN CM**3):	3.657
CHAMBER GAS VOLUME, MAX. DEF. (IN CM**3):	3.657
FOAM VOID FRACTION:	0.979
START FO FOR BEST-FIT:	0.010
END FO FOR BEST-FIT:	0.400
TEMPERATURE (DEGREES C):	60.000

*** CALCULATED VALUES ***

BEST FIT : $FO = 196.411E-5 * T + -0.022$

SAMPLE AREA (IN CM**2):	9.457
NUMBER OF DATA POINTS IN BEST-FIT RANGE	44
SAMPLE EFF. HALF-THICKNESS (IN CM):	0.100
EQUILIBRIUM SORPTION PARAMETER, G:	0.307
EQUILIBRIUM PRESSURE	0.765
FOAM SOLUBILITY RATIO	0.597
FOAM SOLUBILITY COEFFICIENT	0.534
POLYMER SOLUBILITY RATIO	-18.195
POLYMER SOLUBILITY	-16.283
DIFFUSION COEFFICIENT (x10**8)	1946.744
PERMEABILITY COEFFICIENT (x10**8)	1039.887

*** TRANSIENT PRESSURE DATA ***

TIME (SEC)	(P(T)-P1)/(P2-P1)
5.	0.965
30.	0.947
55.	0.910
79.	0.876
104.	0.869
129.	0.850
153.	0.839
178.	0.832
196.	0.823
208.	0.820
220.	0.816
233.	0.815
245.	0.812
257.	0.806
270.	0.809
282.	0.804
294.	0.806
307.	0.793
319.	0.789
331.	0.797
344.	0.784
356.	0.793
369.	0.801
381.	0.794
393.	0.792
406.	0.790
430.	0.788
443.	0.785
455.	0.781
480.	0.787
741.	0.773

Plotting frame

3

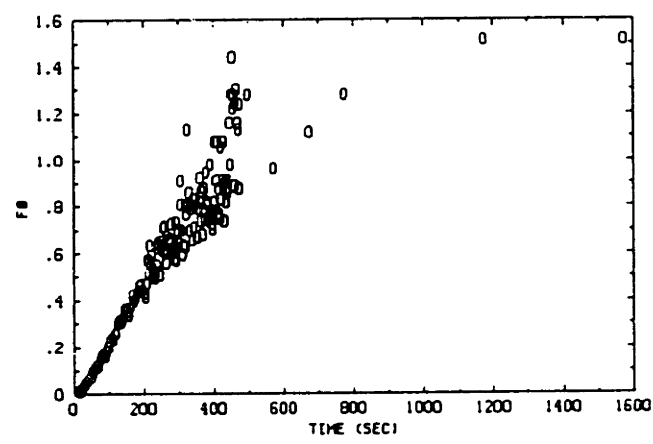
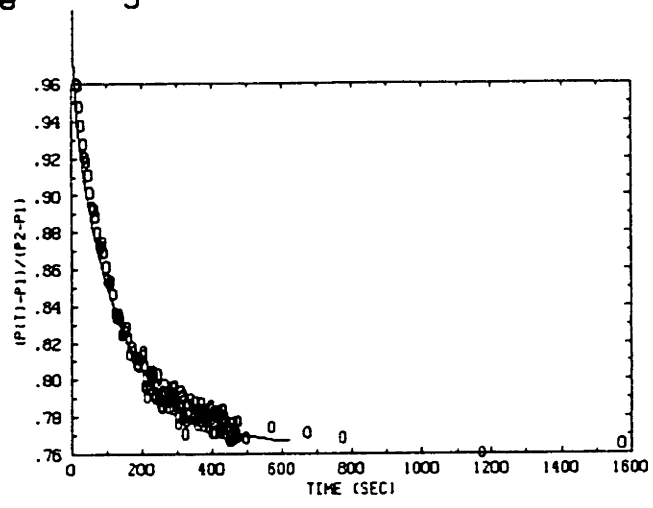


Figure F-43: CO₂, 60°C (Test B) Data Plot Sample 17A

SAMPLE # 17A-P3
GAS TESTED: CO2
TEST DATE: 10-8-89

*** INPUT PARAMETERS ***

SAMPLE DIAMETER (IN CM):	3.470
TOTAL CHAMBER VOLUME (IN CM**3):	5.540
CHAMBER GAS VOLUME, ZERO DEF. (IN CM**3):	3.657
CHAMBER GAS VOLUME, MAX. DEF. (IN CM**3):	3.657
FOAM VOID FRACTION:	0.979
START FO FOR BEST-FIT:	0.010
END FO FOR BEST-FIT:	0.500
TEMPERATURE (DEGREES C):	60.000

*** CALCULATED VALUES ***

BEST FIT : FO= 245.531E-5*T + -0.009	
SAMPLE AREA (IN CM**2):	9.457
NUMBER OF DATA POINTS IN BEST-FIT RANGE	43
SAMPLE EFF. HALF-THICKNESS (IN CM):	0.100
EQUILIBRIUM SORPTION PARAMETER, G:	0.307
EQUILIBRIUM PRESSURE	0.765
FOAM SOLUBILITY RATIO	0.596
FOAM SOLUBILITY COEFFICIENT	0.533
POLYMER SOLUBILITY RATIO	-18.247
POLYMER SOLUBILITY	-16.329
DIFFUSION COEFFICIENT (x10**8)	2433.602
PERMEABILITY COEFFICIENT (x10**8)	1297.570

*** TRANSIENT PRESSURE DATA ***

TIME (SEC)	(P(T)-P1)/(P2-P1)
5.	0.960
30.	0.921
55.	0.892
79.	0.874
104.	0.854
129.	0.833
153.	0.822
178.	0.809
198.	0.807
210.	0.797
223.	0.805
235.	0.803
247.	0.793
260.	0.793
272.	0.792
284.	0.797
297.	0.780
309.	0.791
322.	0.786
334.	0.786
346.	0.788
359.	0.787
371.	0.780
383.	0.782
396.	0.782
408.	0.783
420.	0.784
433.	0.778
445.	281 0.769
458.	0.770
560.	0.775

Plotting frame 1

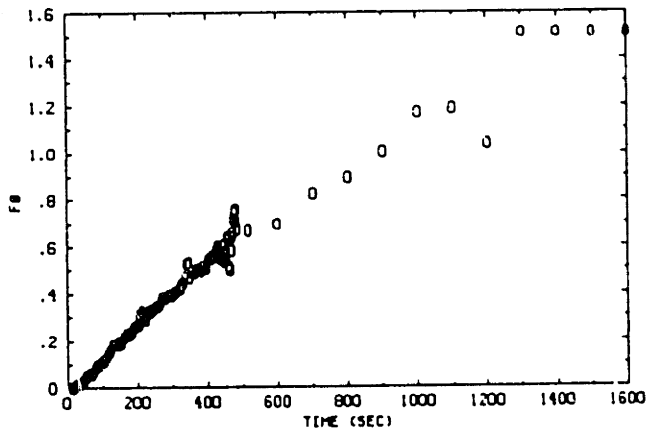
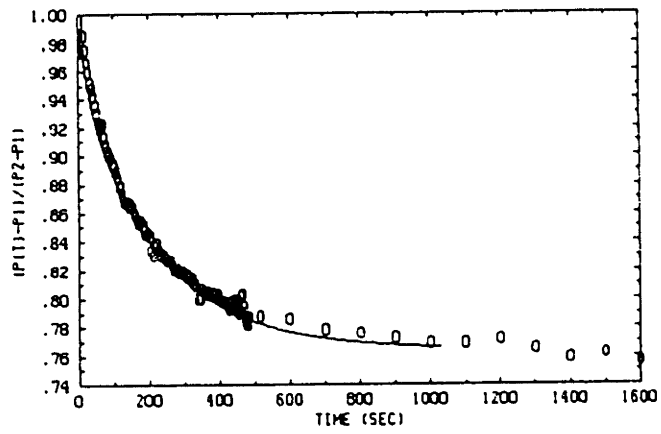


Figure F-44: CO₂, 40°C Data Plot Sample 17A

SAMPLE # 17A-P3
 GAS TESTED: CO2
 TEST DATE: 10-8-89

*** INPUT PARAMETERS ***

SAMPLE DIAMETER (IN CM):	3.470
TOTAL CHAMBER VOLUME (IN CM**3):	5.540
CHAMBER GAS VOLUME, ZERO DEF. (IN CM**3):	3.657
CHAMBER GAS VOLUME, MAX. DEF. (IN CM**3):	3.657
FOAM VOID FRACTION:	0.979
START FO FOR BEST-FIT:	0.010
END FO FOR BEST-FIT:	0.400
TEMPERATURE (DEGREES C):	40.000

*** CALCULATED VALUES ***

BEST FIT : FO=	148.282E-5*T +	-0.016	
SAMPLE AREA (IN CM**2):			9.457
NUMBER OF DATA POINTS IN BEST-FIT RANGE			57
SAMPLE EFF. HALF-THICKNESS (IN CM):			0.100
EQUILIBRIUM SORPTION PARAMETER, G:			0.308
EQUILIBRIUM PRESSURE			0.764
FOAM SOLUBILITY RATIO			0.599
FOAM SOLUBILITY COEFFICIENT			0.570
POLYMER SOLUBILITY RATIO			-18.095
POLYMER SOLUBILITY			-17.228
DIFFUSION COEFFICIENT (x10**8)			1469.704
PERMEABILITY COEFFICIENT (x10**8)			838.163

*** TRANSIENT PRESSURE DATA ***

TIME (SEC)	(P(T)-P1)/(P2-P1)
5.	0.985
30.	0.948
55.	0.922
79.	0.900
104.	0.884
129.	0.867
153.	0.858
178.	0.847
203.	0.830
228.	0.831
252.	0.826
277.	0.819
302.	0.816
327.	0.807
351.	0.804
376.	0.801
401.	0.798
420.	0.797
433.	0.799
445.	0.799
458.	0.795
470.	0.782
692.	0.779
1192.	0.772

Plotting frame 3

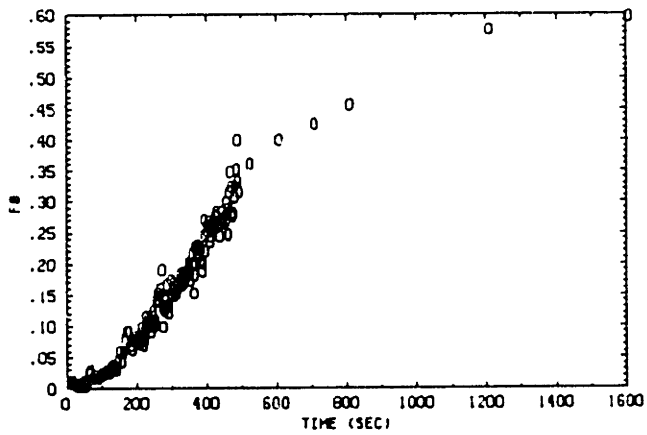
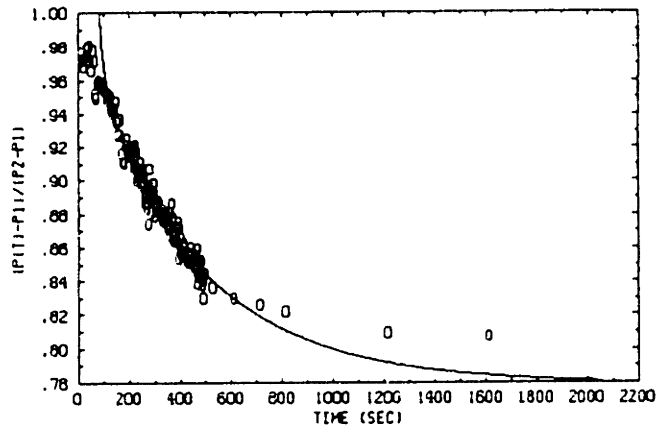


Figure F-45: O₂, 80°C Data Plot Sample 17A.

SAMPLE # 17A-P3
GAS TESTED: O2
TEST DATE: 11-8-89

*** INPUT PARAMETERS ***

SAMPLE DIAMETER (IN CM):	3.470
TOTAL CHAMBER VOLUME (IN CM**3):	5.450
CHAMBER GAS VOLUME, ZERO DEF. (IN CM**3):	3.657
CHAMBER GAS VOLUME, MAX. DEF. (IN CM**3):	3.657
FOAM VOID FRACTION:	0.979
START FO FOR BEST-FIT:	0.050
END FO FOR BEST-FIT:	0.300
TEMPERATURE (DEGREES C):	80.000

*** CALCULATED VALUES ***

BEST FIT : $FO = 83.304E-5 \cdot T + -0.070$

SAMPLE AREA (IN CM**2):	9.457
NUMBER OF DATA POINTS IN BEST-FIT RANGE	106
SAMPLE EFF. HALF-THICKNESS (IN CM):	0.095
EQUILIBRIUM SORPTION PARAMETER, G:	0.270
EQUILIBRIUM PRESSURE	0.788
FOAM SOLUBILITY RATIO	0.550
FOAM SOLUBILITY COEFFICIENT	0.464
POLYMER SOLUBILITY RATIO	-20.429
POLYMER SOLUBILITY	-17.246
DIFFUSION COEFFICIENT (x10**8)	748.632
PERMEABILITY COEFFICIENT (x10**8)	347.594

*** TRANSIENT PRESSURE DATA ***

TIME (SEC)	(P(T)-P1) / (P2-P1)
5.	0.972
30.	0.980
55.	0.952
79.	0.957
104.	0.948
129.	0.943
153.	0.928
178.	0.925
200.	0.921
213.	0.917
225.	0.902
238.	0.897
250.	0.887
262.	0.874
275.	0.890
287.	0.888
299.	0.888
312.	0.883
324.	0.876
336.	0.872
349.	0.867
361.	0.867
373.	0.865
386.	0.860
398.	0.855
411.	0.855
423.	0.853
435.	0.855
448.	285 0.848
460.	0.843
472.	0.843
514.	0.836
1599.	0.807

Plotting frame 2

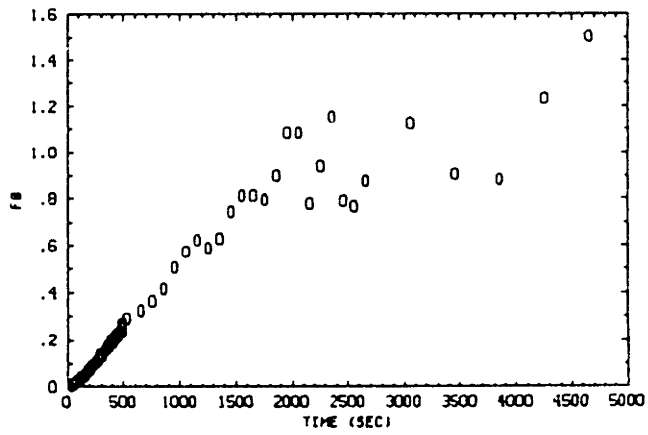
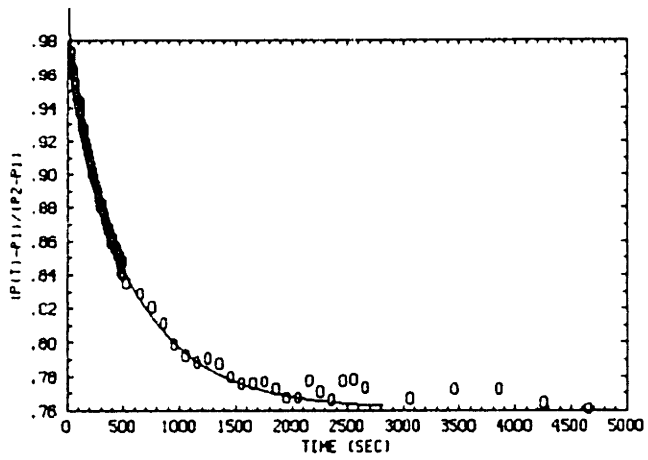


Figure F-46: O_2 , 60°C Data Plot Sample 17A

SAMPLE # 17A-P3
 GAS TESTED: O2
 TEST DATE: 11-18-89

*** INPUT PARAMETERS ***

SAMPLE DIAMETER (IN CM):	3.470
TOTAL CHAMBER VOLUME (IN CM**3):	5.540
CHAMBER GAS VOLUME, ZERO DEF. (IN CM**3):	3.657
CHAMBER GAS VOLUME, MAX. DEF. (IN CM**3):	3.657
FOAM VOID FRACTION:	0.979
START FO FOR BEST-FIT:	0.010
END FO FOR BEST-FIT:	0.200
TEMPERATURE (DEGREES C):	60.000

*** CALCULATED VALUES ***

BEST FIT : FO= 53.864E-5*T + -0.010	
SAMPLE AREA (IN CM**2):	9.457
NUMBER OF DATA POINTS IN BEST-FIT RANGE	73
SAMPLE EFF. HALF-THICKNESS (IN CM):	0.100
EQUILIBRIUM SORPTION PARAMETER, G:	0.314
EQUILIBRIUM PRESSURE	0.761
FOAM SOLUBILITY RATIO	0.610
FOAM SOLUBILITY COEFFICIENT	0.545
POLYMER SOLUBILITY RATIO	-17.595
POLYMER SOLUBILITY	-15.745
DIFFUSION COEFFICIENT (x10**8)	533.877
PERMEABILITY COEFFICIENT (x10**8)	291.201

*** TRANSIENT PRESSURE DATA ***

TIME (SEC)	(P(T)-P1) / (P2-P1)
5.	0.973
30.	0.962
55.	0.946
79.	0.939
104.	0.928
129.	0.927
153.	0.916
178.	0.908
203.	0.902
228.	0.893
252.	0.880
277.	0.882
302.	0.873
327.	0.868
351.	0.859
376.	0.860
401.	0.856
425.	0.852
450.	0.842
627.	0.829
1126.	0.788
1625.	0.776
2125.	0.778
2625.	0.773
4624.	0.761

Plotting frame 1

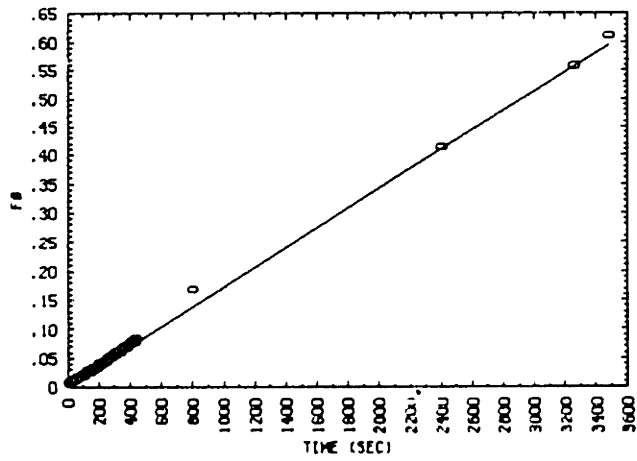
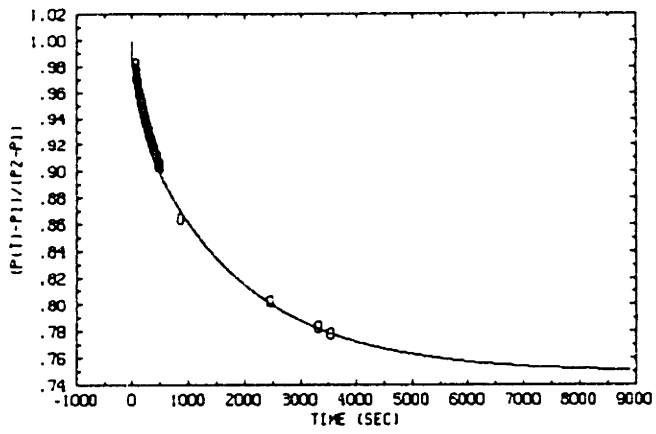


Figure F-47: O₂, 40°C Data Plot Sample 17A

SAMPLE # 17A-P3
 GAS TESTED: O2
 TEST DATE: 11-28-89

*** INPUT PARAMETERS ***

SAMPLE DIAMETER (IN CM):	3.470
TOTAL CHAMBER VOLUME (IN CM**3):	5.540
CHAMBER GAS VOLUME, ZERO DEF. (IN CM**3):	3.657
CHAMBER GAS VOLUME, MAX. DEF. (IN CM**3):	3.657
FOAM VOID FRACTION:	0.979
START FO FOR BEST-FIT:	0.050
END FO FOR BEST-FIT:	0.600
TEMPERATURE (DEGREES C):	40.000

*** CALCULATED VALUES ***

BEST FIT : FO=	16.972E-5*T +	0.003
SAMPLE AREA (IN CM**2):		9.457
NUMBER OF DATA POINTS IN BEST-FIT RANGE		33
SAMPLE EFF. HALF-THICKNESS (IN CM):		0.100
EQUILIBRIUM SORPTION PARAMETER, G:		0.335
EQUILIBRIUM PRESSURE		0.749
FOAM SOLUBILITY RATIO		0.650
FOAM SOLUBILITY COEFFICIENT		0.619
POLYMER SOLUBILITY RATIO		-15.667
POLYMER SOLUBILITY		-14.916
DIFFUSION COEFFICIENT (x10**8)		168.223
PERMEABILITY COEFFICIENT (x10**8)		104.105

*** TRANSIENT PRESSURE DATA ***

TIME (SEC)	(P(T)-P1) / (P2-P1)
5.	0.982
30.	0.969
55.	0.963
79.	0.957
104.	0.952
129.	0.947
153.	0.942
178.	0.940
203.	0.933
228.	0.931
252.	0.927
277.	0.923
302.	0.917
327.	0.917
351.	0.913
376.	0.911
401.	0.906
425.	0.905
210.	0.864
2400.	0.803
3260.	0.783
3480.	0.778

Plotting frame 2

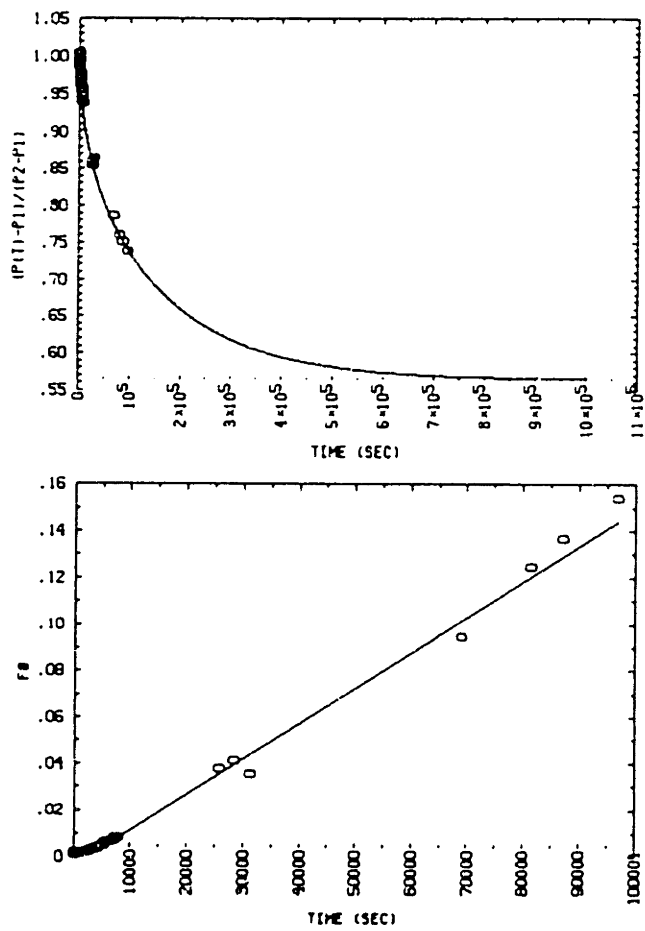


Figure F-48: HCFC-123, 60°C Data Plot Sample 17A

SAMPLE # 17A-P3
 GAS TESTED: HCFC-123
 TEST DATE: 1-8-90

*** INPUT PARAMETERS ***

SAMPLE DIAMETER (IN CM):	3.470
TOTAL CHAMBER VOLUME (IN CM**3):	5.540
CHAMBER GAS VOLUME, ZERO DEF. (IN CM**3):	3.657
CHAMBER GAS VOLUME, MAX. DEF. (IN CM**3):	3.657
FOAM VOID FRACTION:	0.073
START FO FOR BEST-FIT:	0.001
END FO FOR BEST-FIT:	0.150
TEMPERATURE (DEGREES C):	60.000

*** CALCULATED VALUES ***

BEST FIT : FO=	0.152E-5*T + -0.004	
SAMPLE AREA (IN CM**2):		9.457
NUMBER OF DATA POINTS IN BEST-FIT RANGE		64
SAMPLE EFF. HALF-THICKNESS (IN CM):		0.100
EQUILIBRIUM SORPTION PARAMETER, G:		0.772
EQUILIBRIUM PRESSURE		0.564
FOAM SOLUBILITY RATIO		1.500
FOAM SOLUBILITY COEFFICIENT		1.342
POLYMER SOLUBILITY RATIO		24.809
POLYMER SOLUBILITY		22.202
DIFFUSION COEFFICIENT (x10**8)		1.507
PERMEABILITY COEFFICIENT (x10**8)		2.023

*** TRANSIENT PRESSURE DATA ***

TIME (SEC)	(P(T)-P1)/(P2-P1)
5.	0.990
30.	0.983
55.	0.982
79.	0.989
104.	0.983
129.	0.985
153.	0.993
178.	0.992
203.	0.993
228.	0.995
252.	0.998
590.	0.994
1090.	0.986
1589.	0.983
2089.	0.976
2589.	0.971
3102.	0.967
3602.	0.963
4101.	0.962
4601.	0.955
5101.	0.948
5614.	0.948
6114.	0.944
6613.	0.939
7113.	0.942
7613.	0.934
31269.	0.860

Plotting frame 1

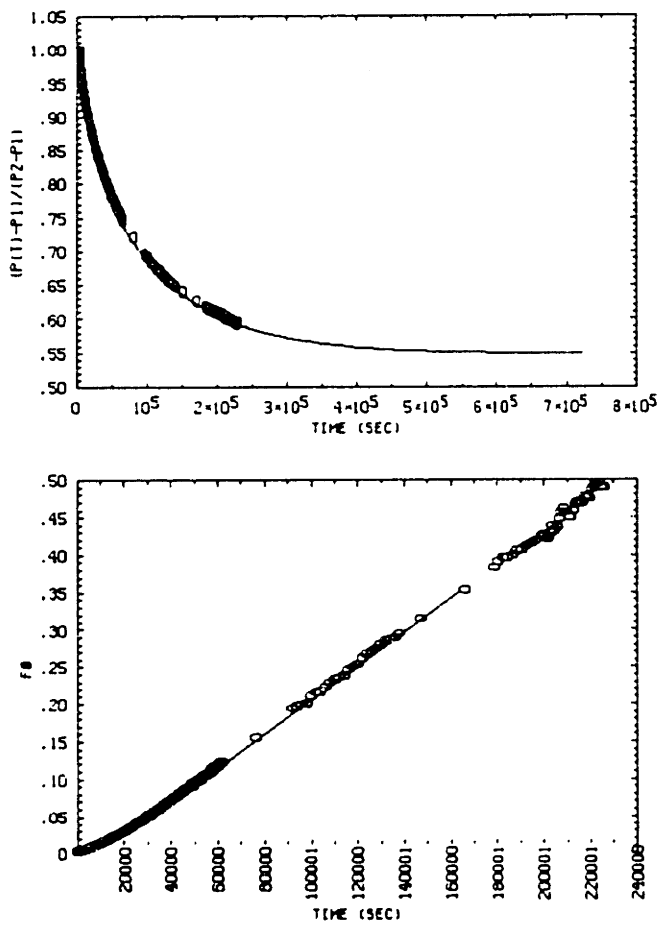


Figure F-49: HCFC-123, 40°C Data Plot Sample 17A

SAMPLE # 17A-P3
 GAS TESTED: HCFC-123
 TEST DATE: 2-11-90

*** INPUT PARAMETERS ***

SAMPLE DIAMETER (IN CM): 3.470
 TOTAL CHAMBER VOLUME (IN CM**3): 5.540
 CHAMBER GAS VOLUME, ZERO DEF. (IN CM**3): 3.657
 CHAMBER GAS VOLUME, MAX. DEF. (IN CM**3): 3.657
 FOAM VOID FRACTION: 0.979
 START FO FOR BEST-FIT: 0.050
 END FO FOR BEST-FIT: 0.350
 TEMPERATURE (DEGREES C): 40.000

*** CALCULATED VALUES ***

BEST FIT : FO= 0.227E-5*T + -0.021
 SAMPLE AREA (IN CM**2): 9.457
 NUMBER OF DATA POINTS IN BEST-FIT RANGE 180
 SAMPLE EFF. HALF-THICKNESS (IN CM): 0.100
 EQUILIBRIUM SORPTION PARAMETER, G: 0.824
 EQUILIBRIUM PRESSURE 0.548
 FOAM SOLUBILITY RATIO 1.600
 FOAM SOLUBILITY COEFFICIENT 1.523
 POLYMER SOLUBILITY RATIO 29.571
 POLYMER SOLUBILITY 28.154
 DIFFUSION COEFFICIENT (x10**8) 2.255
 PERMEABILITY COEFFICIENT (x10**8) 3.434

*** TRANSIENT PRESSURE DATA ***

TIME (SEC)	(P(T)-P1)/(P2-P1)	TIME (SEC)	(P(T)-P1)/(P2-P1)
38.	0.975	11892.	0.901
64.	0.979	12892.	0.899
89.	0.985	13891.	0.891
113.	0.988	14891.	0.887
138.	0.991	15890.	0.884
163.	0.992	16890.	0.878
188.	0.993	17890.	0.874
212.	0.994	18889.	0.871
237.	0.994	19889.	0.865
262.	0.991	20895.	0.861
286.	0.994	25903.	0.842
311.	0.996	30901.	0.827
336.	0.994	40898.	0.794
361.	0.993	50911.	0.769
385.	0.992	60907.	0.747
410.	0.992	76341.	0.721
896.	0.985	99874.	0.686
1895.	0.973	109873.	0.675
2895.	0.960	119872.	0.665
3895.	0.952	129872.	0.654
4894.	0.943	146808.	0.640
5894.	0.935	184555.	0.615
6894.	0.930	194554.	0.611
7893.	0.924	201554.	0.609
8893.	0.918	216553.	0.598
9893.	0.912	221552.	0.594
10892.	0.906		

Blank Page

F.7 Foam No. 18

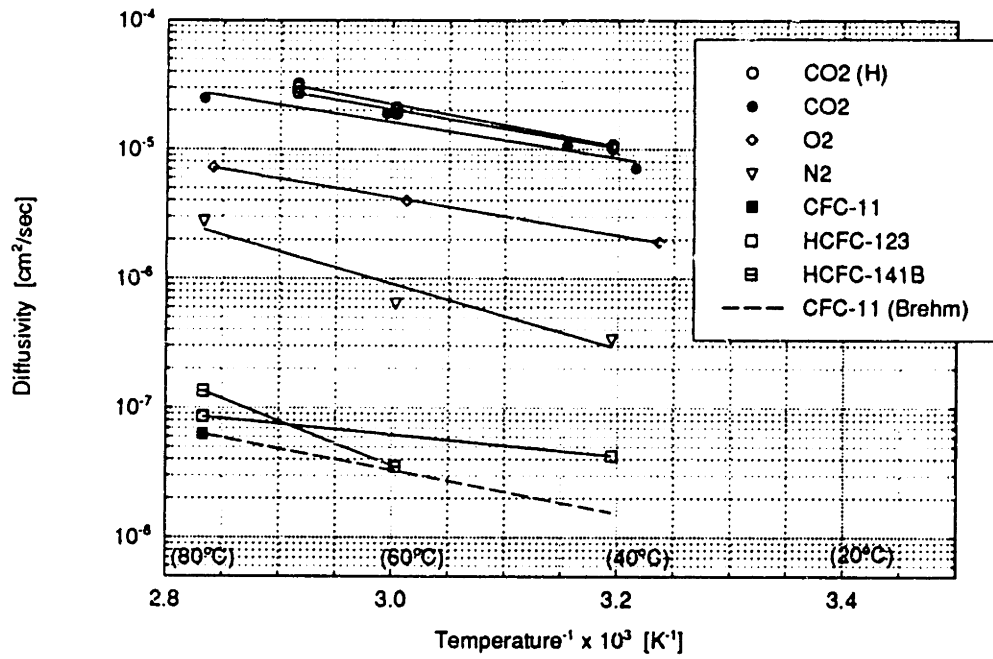


Figure F-50: $\text{Log}(D_{eff})$ versus $1/T$ for all test results, Foam 18.

Plotting frame

4

META OPTION :

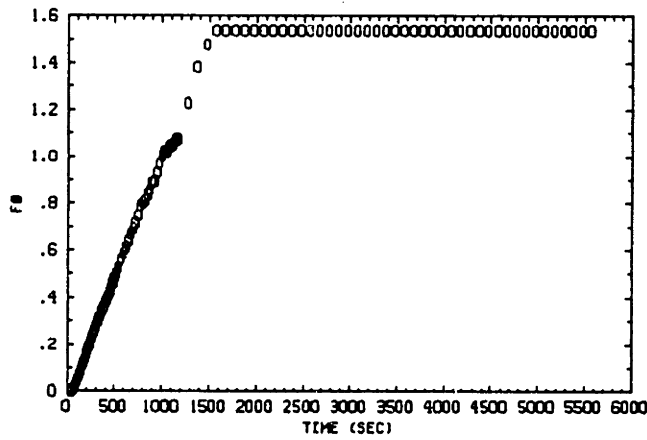
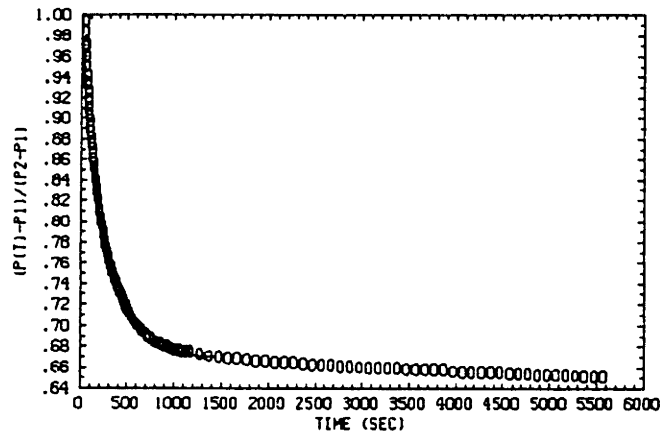


Figure F-51: CO₂, 80°C Data Plot Sample 18A.

SAMPLE # 18A-P4
GAS TESTED: CO2
TEST DATE: 8-14-89

*** INPUT PARAMETERS ***

SAMPLE DIAMETER (IN CM):	3.300
TOTAL CHAMBER VOLUME (IN CM**3):	6.385
CHAMBER GAS VOLUME, ZERO DEF. (IN CM**3):	3.210
CHAMBER GAS VOLUME, MAX. DEF. (IN CM**3):	3.310
FOAM VOID FRACTION:	0.980
START FO FOR BEST-FIT:	0.010
END FO FOR BEST-FIT:	0.500
TEMPERATURE (DEGREES C):	80.000

*** CALCULATED VALUES ***

BEST FIT : FO= $109.793E-5 \cdot T + -0.025$

SAMPLE AREA (IN CM**2):	8.553
NUMBER OF DATA POINTS IN BEST-FIT RANGE	129
SAMPLE EFF. HALF-THICKNESS (IN CM):	0.151
EQUILIBRIUM SORPTION PARAMETER, G:	0.497
EQUILIBRIUM PRESSURE	0.663
FOAM SOLUBILITY RATIO	0.735
FOAM SOLUBILITY COEFFICIENT	0.620
POLYMER SOLUBILITY RATIO	-12.250
POLYMER SOLUBILITY	-10.341
DIFFUSION COEFFICIENT (x10**8)	2487.904
PERMEABILITY COEFFICIENT (x10**8)	1543.699

*** TRANSIENT PRESSURE DATA ***

TIME (SEC)	(P(T)-P1)/(P2-P1)
5.	0.970
30.	0.951
55.	0.911
79.	0.881
104.	0.857
129.	0.836
153.	0.819
178.	0.804
203.	0.790
228.	0.778
252.	0.769
277.	0.760
292.	0.756
317.	0.750
329.	0.745
341.	0.742
366.	0.736
391.	0.731
415.	0.727
440.	0.719
465.	0.716
490.	0.712
611.	0.696
736.	0.685
861.	0.680
986.	0.676
1111.	0.675
1536.	0.669
2036.	0.665
2535.	0.663
3535.	0.658
4535.	0.655
5534.	0.652

Plotting frame

3

META OPTION :

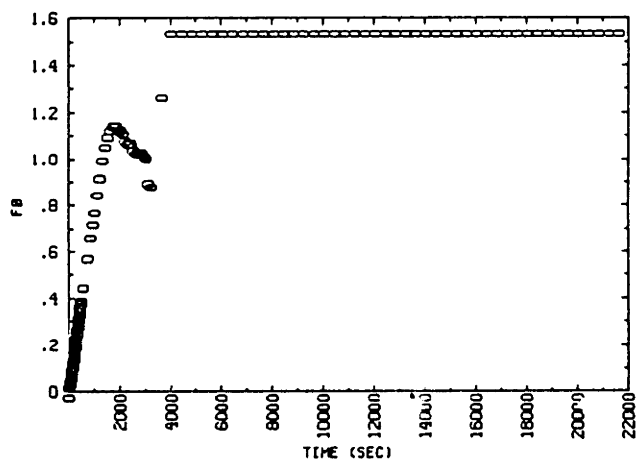
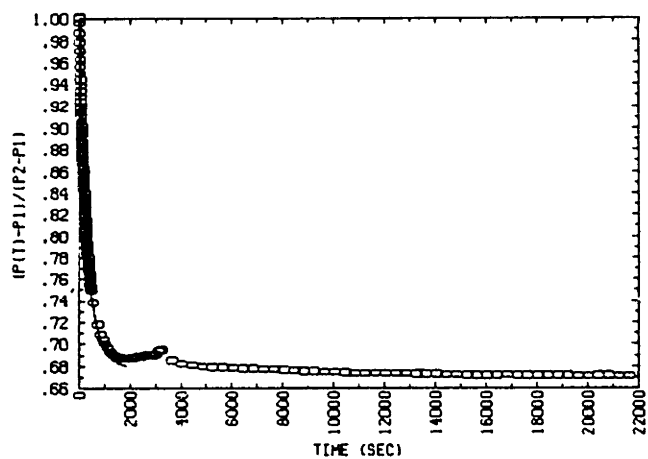


Figure F-52: CO₂, 61°C Data Plot Sample 18A

SAMPLE # 12A-P4
 GAS TESTED: CO2
 TEST DATE: 8-15-89

*** INPUT PARAMETERS ***

SAMPLE DIAMETER (IN CM):	3.300
TOTAL CHAMBER VOLUME (IN CM**3):	6.335
CHAMBER GAS VOLUME, ZERO DEF. (IN CM**3):	3.810
CHAMBER GAS VOLUME, MAX. DEF. (IN CM**3):	3.810
FOAM VOID FRACTION:	0.980
START FO FOR BEST-FIT:	0.010
END FO FOR BEST-FIT:	0.350
TEMPERATURE (DEGREES C):	61.000

*** CALCULATED VALUES ***

BEST FIT : FO= 83.046E-5*T + -0.036	
SAMPLE AREA (IN CM**2):	8.553
NUMBER OF DATA POINTS IN BEST-FIT RANGE	85
SAMPLE EFF. HALF-THICKNESS (IN CM):	0.151
EQUILIBRIUM SORPTION PARAMETER, G:	0.473
EQUILIBRIUM PRESSURE	0.679
FOAM SOLUBILITY RATIO	0.700
FOAM SOLUBILITY COEFFICIENT	0.625
POLYMER SOLUBILITY RATIO	-14.000
POLYMER SOLUBILITY	-12.491
DIFFUSION COEFFICIENT (x10**8)	1881.808
PERMEABILITY COEFFICIENT (x10**8)	1175.285

*** TRANSIENT PRESSURE DATA ***

TIME (SEC)	(P(T)-P1) / (P2-P1)
5.	0.998
30.	0.968
55.	0.936
79.	0.912
104.	0.892
129.	0.875
153.	0.860
178.	0.846
203.	0.834
228.	0.823
252.	0.813
277.	0.803
302.	0.794
327.	0.787
351.	0.780
376.	0.772
401.	0.766
425.	0.760
450.	0.755
475.	0.749
842.	0.706
1342.	0.688
1842.	0.684
2342.	0.686
2841.	0.687
3641.	0.683
5640.	0.676
7640.	0.674
9639.	0.672
13638.	0.670
17636.	0.669
21659.	0.668

Plotting frame

2

META OPTION :

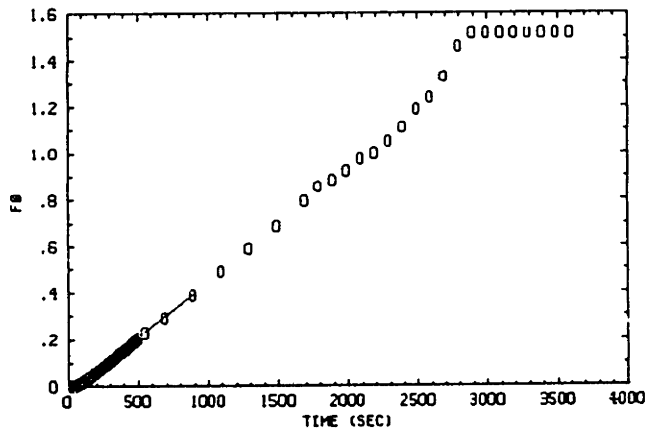
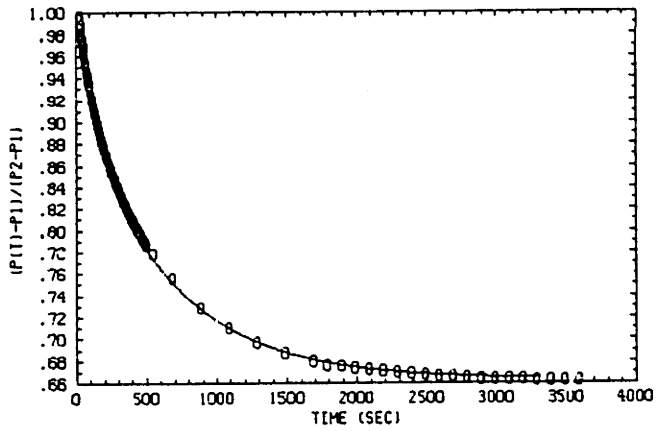


Figure F-53: CO₂, 44°C Data Plot Sample 18A

SAMPLE # 18A-P4
 GAS TESTED: CO2
 TEST DATE: 8-23-89

*** INPUT PARAMETERS ***

SAMPLE DIAMETER (IN CM):	3.300
TOTAL CHAMBER VOLUME (IN CM**3):	6.385
CHAMBER GAS VOLUME, ZERO DEF. (IN CM**3):	3.810
CHAMBER GAS VOLUME, MAX. DEF. (IN CM**3):	3.810
FOAM VOID FRACTION:	0.980
START FO FOR BEST-FIT:	0.010
END FO FOR BEST-FIT:	0.400
TEMPERATURE (DEGREES C):	44.000

*** CALCULATED VALUES ***

BEST FIT : FO= 46.808E-5*T + -0.021	
SAMPLE AREA (IN CM**2):	8.553
NUMBER OF DATA POINTS IN BEST-FIT RANGE	90
SAMPLE EFF. HALF-THICKNESS (IN CM):	0.151
EQUILIBRIUM SORPTION PARAMETER, G:	0.508
EQUILIBRIUM PRESSURE	0.663
FOAM SOLUBILITY RATIO	0.752
FOAM SOLUBILITY COEFFICIENT	0.707
POLYMER SOLUBILITY RATIO	-11.398
POLYMER SOLUBILITY	-10.715
DIFFUSION COEFFICIENT (x10**8)	1060.669
PERMEABILITY COEFFICIENT (x10**8)	749.846

*** TRANSIENT PRESSURE DATA ***

TIME (SEC)	(P(T)-P1)/(P2-P1)
5.	0.997
30.	0.969
55.	0.946
79.	0.927
104.	0.911
129.	0.898
153.	0.885
178.	0.875
203.	0.864
228.	0.855
252.	0.846
277.	0.838
302.	0.830
327.	0.823
351.	0.816
376.	0.810
401.	0.804
425.	0.797
450.	0.792
475.	0.786
1063.	0.710
1863.	0.675
2363.	0.669
2863.	0.664
3363.	0.662

Plotting frame

1

META OPTION :

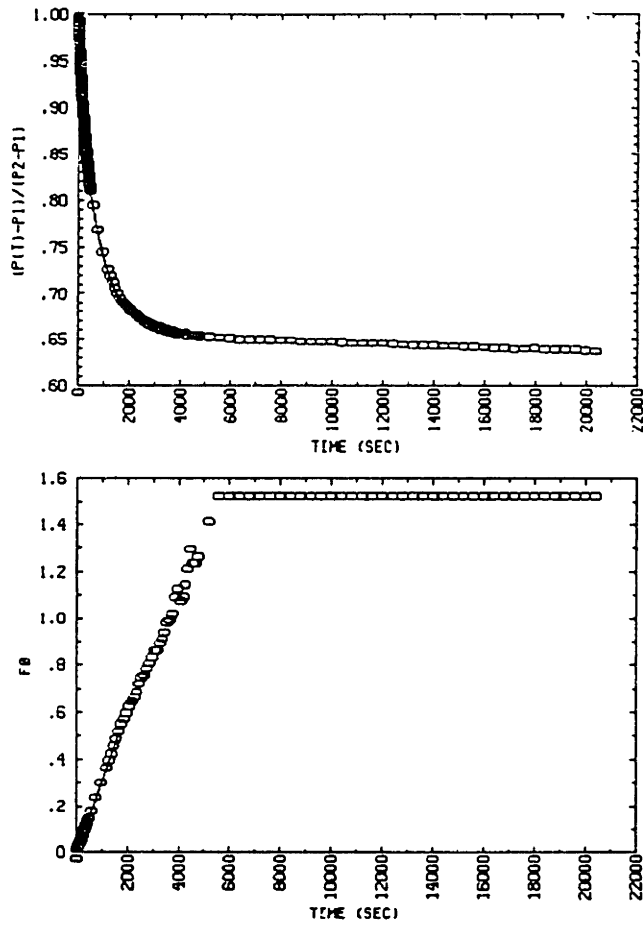


Figure F-54: CO₂, 38°C Data Plot Sample 18A

SAMPLE # 18A-P4
 GAS TESTED: CO2
 TEST DATE: 8-24-89

*** INPUT PARAMETERS ***

SAMPLE DIAMETER (IN CM):	3.300
TOTAL CHAMBER VOLUME (IN CM**3):	6.385
CHAMBER GAS VOLUME, ZERO DEF. (IN CM**3):	3.810
CHAMBER GAS VOLUME, MAX. DEF. (IN CM**3):	3.810
FOAM VOID FRACTION:	0.930
START FO FOR BEST-FIT:	0.010
END FO FOR BEST-FIT:	0.500
TEMPERATURE (DEGREES C):	38.000

*** CALCULATED VALUES ***

BEST FIT : FO= 31.382E-5*T + -0.017	
SAMPLE AREA (IN CM**2):	8.553
NUMBER OF DATA POINTS IN BEST-FIT RANGE	94
SAMPLE EFF. HALF-THICKNESS (IN CM):	0.151
EQUILIBRIUM SORPTION PARAMETER, G:	0.544
EQUILIBRIUM PRESSURE	0.648
FOAM SOLUBILITY RATIO	0.805
FOAM SOLUBILITY COEFFICIENT	0.771
POLYMER SOLUBILITY RATIO	-8.750
POLYMER SOLUBILITY	-8.384
DIFFUSION COEFFICIENT (x10**8)	711.103
PERMEABILITY COEFFICIENT (x10**8)	548.510

*** TRANSIENT PRESSURE DATA ***

TIME (SEC)	(P(T)-P1)/(P2-P1)
5.	0.996
30.	0.972
55.	0.953
79.	0.937
104.	0.925
129.	0.912
153.	0.902
178.	0.892
203.	0.885
228.	0.875
252.	0.867
277.	0.859
302.	0.851
327.	0.845
351.	0.839
376.	0.834
401.	0.828
425.	0.822
450.	0.817
475.	0.811
768.	0.765
1967.	0.681
2967.	0.663
3967.	0.653
4467.	0.651
5566.	0.649
7565.	0.646
9565.	0.644
11579.	0.643
13578.	0.641
15577.	0.639
17577.	0.637
19576.	0.636

Plotting frame

3

META OPTION :

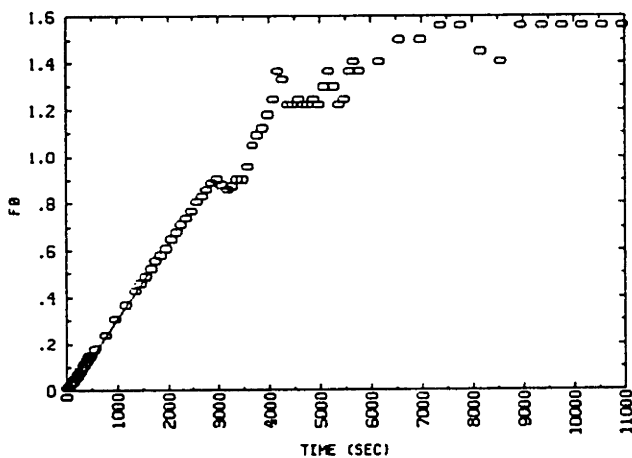
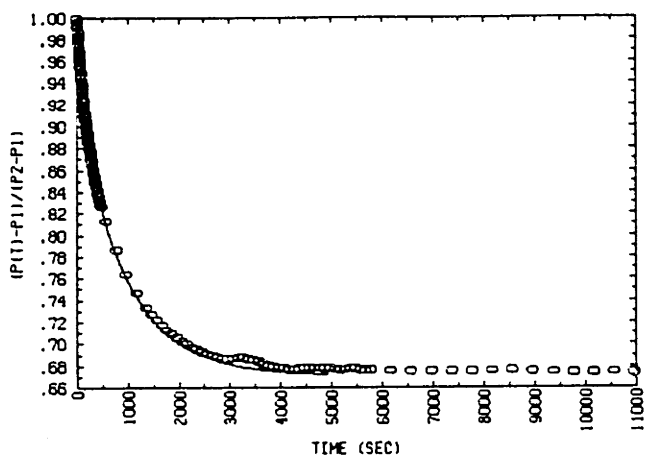


Figure F-55: O₂, 79°C Data Plot Sample 18A.

SAMPLE # 18A-P4
GAS TESTED: O2
TEST DATE: 8-24-89

*** INPUT PARAMETERS ***

SAMPLE DIAMETER (IN CM):	3.300
TOTAL CHAMBER VOLUME (IN CM**3):	6.385
CHAMBER GAS VOLUME, ZERO DEF. (IN CM**3):	3.810
CHAMBER GAS VOLUME, MAX. DEF. (IN CM**3):	3.810
FOAM VOID FRACTION:	0.980
START FO FOR BEST-FIT:	0.010
END FO FOR BEST-FIT:	0.500
TEMPERATURE (DEGREES C):	79.000

*** CALCULATED VALUES ***

BEST FIT : FO=	$31.934E-5 \cdot T + -0.016$	
SAMPLE AREA (IN CM**2):		8.553
NUMBER OF DATA POINTS IN BEST-FIT RANGE		86
SAMPLE EFF. HALF-THICKNESS (IN CM):		0.151
EQUILIBRIUM SORPTION PARAMETER, G:		0.490
EQUILIBRIUM PRESSURE		0.671
FOAM SOLUBILITY RATIO		0.725
FOAM SOLUBILITY COEFFICIENT		0.613
POLYMER SOLUBILITY RATIO		-12.774
POLYMER SOLUBILITY		-10.815
DIFFUSION COEFFICIENT (x10**8)		723.626
PERMEABILITY COEFFICIENT (x10**8)		443.847

*** TRANSIENT PRESSURE DATA ***

TIME (SEC)	(P(T)-P1) / (P2-P1)
5.	0.989
30.	0.980
55.	0.963
79.	0.947
104.	0.934
129.	0.922
153.	0.911
178.	0.901
203.	0.892
228.	0.884
252.	0.876
277.	0.869
302.	0.862
327.	0.856
351.	0.849
376.	0.843
401.	0.838
425.	0.832
450.	0.827
762.	0.784
1562.	0.720
2062.	0.699
2561.	0.688
3061.	0.684
3561.	0.681
4061.	0.675
4561.	0.675
5060.	0.674
5560.	0.674
6960.	0.673
8959.	0.673
10958.	0.671

plotting frame

2

META OPTION :

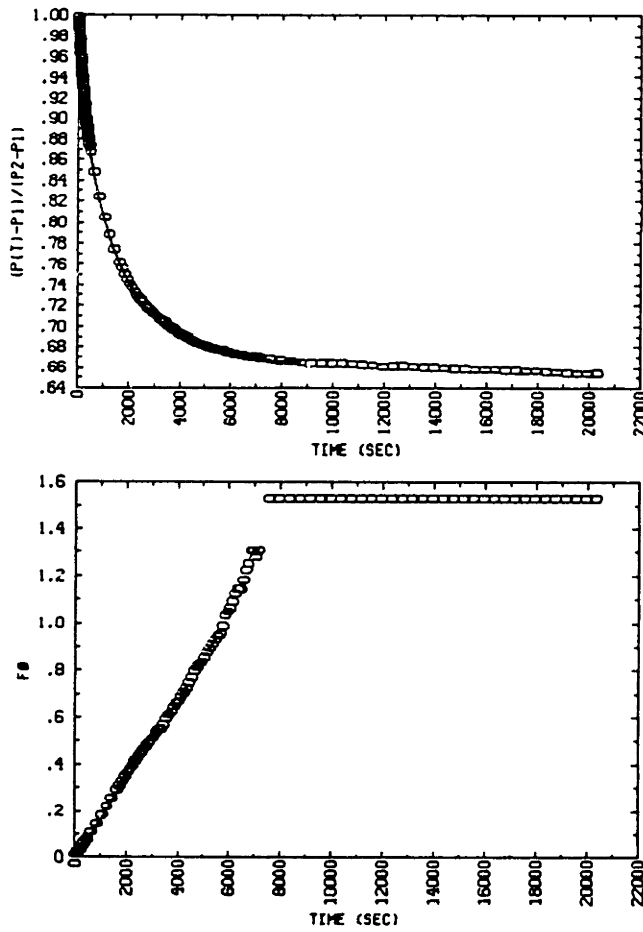


Figure F-56: O₂, 59°C Data Plot Sample 18A

SAMPLE # 18A-P4
 GAS TESTED: O2
 TEST DATE: 8-29-89

*** INPUT PARAMETERS ***

SAMPLE DIAMETER (IN CM):	3.300
TOTAL CHAMBER VOLUME (IN CM**3):	6.385
CHAMBER GAS VOLUME, ZERO DEF. (IN CM**3):	3.810
CHAMBER GAS VOLUME, MAX. DEF. (IN CM**3):	3.810
FOAM VOID FRACTION:	0.980
START FO FOR BEST-FIT:	0.020
END FO FOR BEST-FIT:	0.500
TEMPERATURE (DEGREES C):	59.000

*** CALCULATED VALUES ***

BEST FIT : FO= 17.569E-5*T + -0.016	
SAMPLE AREA (IN CM**2):	8.553
NUMBER OF DATA POINTS IN BEST-FIT RANGE	76
SAMPLE EFF. HALF-THICKNESS (IN CM):	0.151
EQUILIBRIUM SORPTION PARAMETER, G:	0.507
EQUILIBRIUM PRESSURE	0.664
FOAM SOLUBILITY RATIO	0.750
FOAM SOLUBILITY COEFFICIENT	0.673
POLYMER SOLUBILITY RATIO	-11.500
POLYMER SOLUBILITY	-10.322
DIFFUSION COEFFICIENT (x10**8)	398.112
PERMEABILITY COEFFICIENT (x10**8)	268.006

*** TRANSIENT PRESSURE DATA ***

TIME (SEC)	(P(T)-P1) / (P2-P1)
5.	0.995
30.	0.985
55.	0.973
79.	0.962
104.	0.953
129.	0.945
153.	0.937
178.	0.930
203.	0.923
228.	0.918
252.	0.911
277.	0.906
302.	0.900
327.	0.895
351.	0.890
376.	0.886
401.	0.881
425.	0.877
450.	0.872
511.	0.864
1450.	0.771
2550.	0.720
3549.	0.698
4549.	0.682
5549.	0.674
6548.	0.668
7048.	0.667
8747.	0.662
10747.	0.660
12746.	0.658
14745.	0.656
18744.	0.652

plotting frame

1

META OPTION :

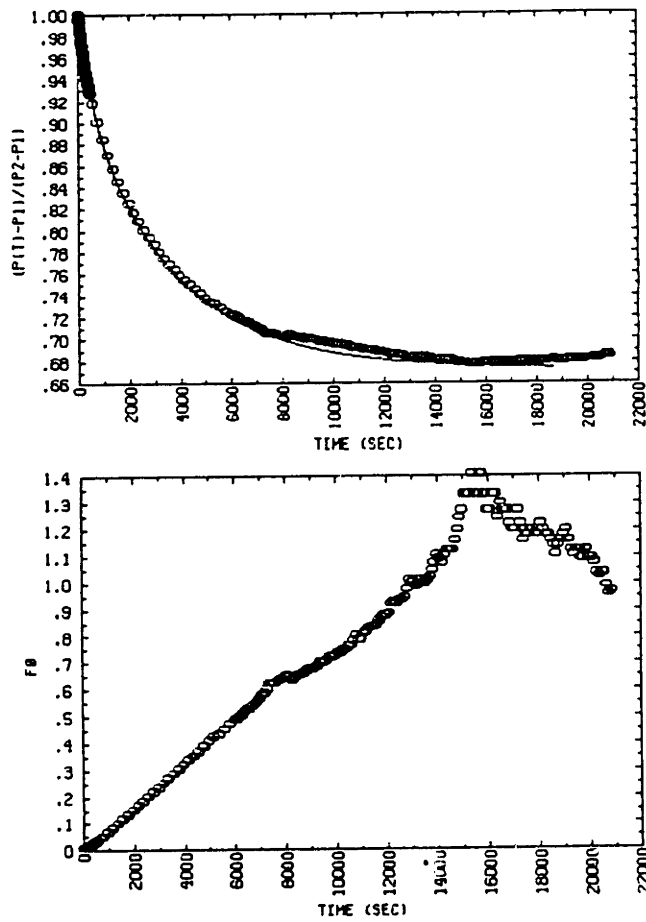


Figure F-57: O₂, 36°C Data Plot Sample 18A

SAMPLE # 18A-24
GAS TESTED: O2
TEST DATE: 9-12-89

*** INPUT PARAMETERS ***

SAMPLE DIAMETER (IN CM):	3.300
TOTAL CHAMBER VOLUME (IN CM**3):	6.385
CHAMBER GAS VOLUME, ZERO DEF. (IN CM**3):	3.810
CHAMBER GAS VOLUME, MAX. DEF. (IN CM**3):	3.810
FOAM VOID FRACTION:	0.980
START FO FOR BEST-FIT:	0.050
END FO FOR BEST-FIT:	0.400
TEMPERATURE (DEGREES C):	36.000

*** CALCULATED VALUES ***

BEST FIT : FO=	8.484E-5*T +	-0.024	
SAMPLE AREA (IN CM**2):			8.553
NUMBER OF DATA POINTS IN BEST-FIT RANGE			20
SAMPLE EFF. HALF-THICKNESS (IN CM):			0.151
EQUILIBRIUM SORPTION PARAMETER, G:			0.487
EQUILIBRIUM PRESSURE			0.673
FOAM SOLUBILITY RATIO			0.720
FOAM SOLUBILITY COEFFICIENT			0.694
POLYMER SOLUBILITY RATIO			-13.000
POLYMER SOLUBILITY			-12.537
DIFFUSION COEFFICIENT (x10**8)			192.251
PERMEABILITY COEFFICIENT (x10**8)			133.493

*** TRANSIENT PRESSURE DATA ***

TIME (SEC)	(P(T)-P1)/(P2-P1)
5.	0.997
30.	0.993
55.	0.988
79.	0.983
104.	0.978
129.	0.973
153.	0.969
178.	0.965
203.	0.961
228.	0.957
252.	0.953
277.	0.951
302.	0.946
327.	0.944
351.	0.939
376.	0.937
401.	0.934
425.	0.931
450.	0.927
567.	0.916
1551.	0.843
2550.	0.799
3550.	0.767
4550.	0.744
5549.	0.727
6749.	0.712
7749.	0.702
8748.	0.699
10755.	0.689
12761.	0.682
16760.	0.676
20759.	0.683

plotting frame

3

META OPTION :

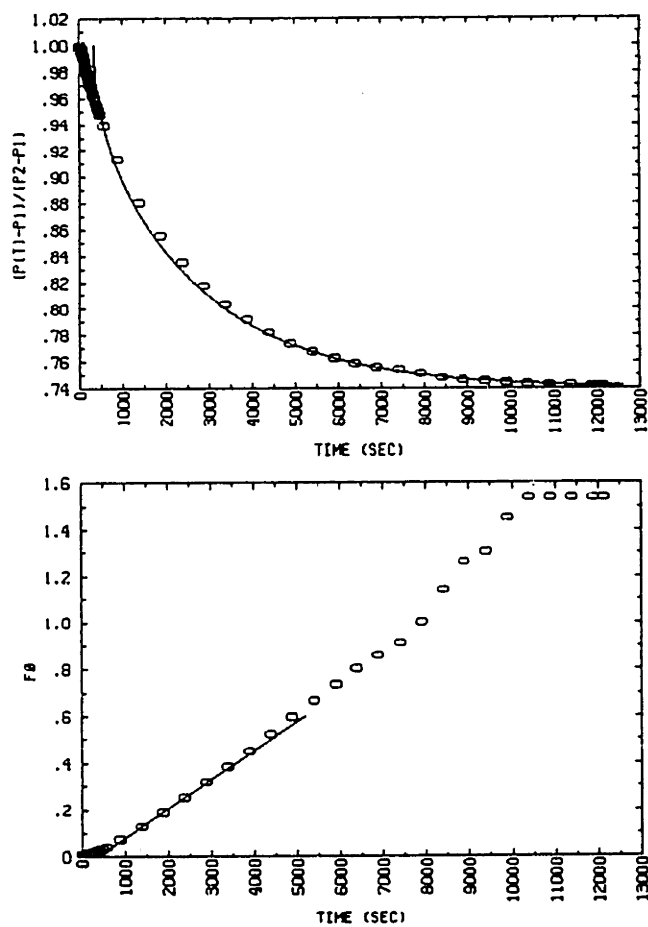


Figure F-58: N₂, 80°C Data Plot Sample 18A.

SAMPLE # 1JA-P4
 GAS TESTED: N2
 TEST DATE: 9-16-89

*** INPUT PARAMETERS ***

SAMPLE DIAMETER (IN CM):	3.300
TOTAL CHAMBER VOLUME (IN CM**3):	6.385
CHAMBER GAS VOLUME, ZERO DEF. (IN CM**3):	3.810
CHAMBER GAS VOLUME, MAX. DEF. (IN CM**3):	3.810
FOAM VOID FRACTION:	0.980
START FO FOR BEST-FIT:	0.020
END FO FOR BEST-FIT:	0.600
TEMPERATURE (DEGREES C):	80.000

*** CALCULATED VALUES ***

BEST FIT : FO= 12.448E-5*T + -0.044	
SAMPLE AREA (IN CM**2):	8.553
NUMBER OF DATA POINTS IN BEST-FIT RANGE	16
SAMPLE EFF. HALF-THICKNESS (IN CM):	0.151
EQUILIBRIUM SORPTION PARAMETER, G:	0.351
EQUILIBRIUM PRESSURE	0.740
FOAM SOLUBILITY RATIO	0.520
FOAM SOLUBILITY COEFFICIENT	0.439
POLYMER SOLUBILITY RATIO	-23.001
POLYMER SOLUBILITY	-19.418
DIFFUSION COEFFICIENT (x10**8)	282.064
PERMEABILITY COEFFICIENT (x10**8)	123.814

*** TRANSIENT PRESSURE DATA ***

TIME (SEC)	(P(T)-P1)/(P2-P1)
5.	0.994
30.	0.997
55.	0.996
79.	0.991
104.	0.989
129.	0.985
153.	0.981
178.	0.978
203.	0.975
228.	0.972
252.	0.969
277.	0.966
302.	0.964
327.	0.960
351.	0.958
376.	0.955
401.	0.952
425.	0.949
450.	0.948
475.	0.945
1885.	0.853
4384.	0.780
6883.	0.754
9382.	0.743
11881.	0.740

plotting frame

2

META OPTION :

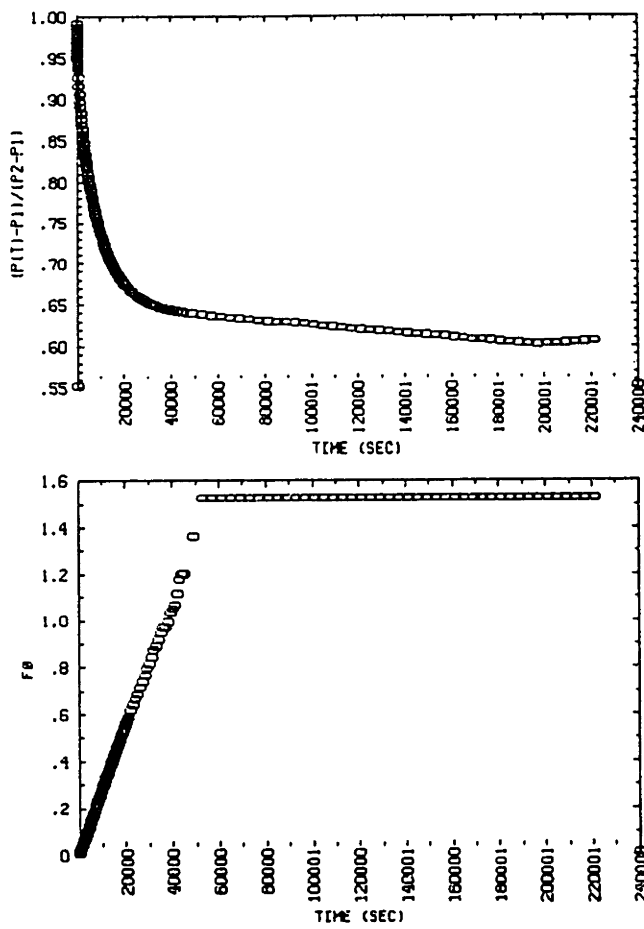


Figure F-59: N₂, 60°C Data Plot Sample 18A

SAMPLE # 18A-P4
 GAS TESTED: N2
 TEST DATE: 11-10-89

*** INPUT PARAMETERS ***

SAMPLE DIAMETER (IN CM): 3.300
 TOTAL CHAMBER VOLUME (IN CM**3): 6.385
 CHAMBER GAS VOLUME, ZERO DEF. (IN CM**3): 3.810
 CHAMBER GAS VOLUME, MAX. DEF. (IN CM**3): 3.810
 FOAM VOID FRACTION: 0.980
 START FO FOR BEST-FIT: 0.050
 END FO FOR BEST-FIT: 0.300
 TEMPERATURE (DEGREES C): 60.000

*** CALCULATED VALUES ***

BEST FIT : FO= 2.868E-5*T + -0.006
 SAMPLE AREA (IN CM**2): 8.553
 NUMBER OF DATA POINTS IN BEST-FIT RANGE 44
 SAMPLE EFF. HALF-THICKNESS (IN CM): 0.151
 EQUILIBRIUM SORPTION PARAMETER, G: 0.578
 EQUILIBRIUM PRESSURE 0.634
 FOAM SOLUBILITY RATIO 0.855
 FOAM SOLUBILITY COEFFICIENT 0.765
 POLYMER SOLUBILITY RATIO -6.250
 POLYMER SOLUBILITY -5.593
 DIFFUSION COEFFICIENT (x10**8) 64.982
 PERMEABILITY COEFFICIENT (x10**8) 49.720

*** TRANSIENT PRESSURE DATA ***

TIME (SEC)	(P (T) -P1) / (P2-P1)	TIME (SEC)	(P (T) -P1) / (P2-P1)
5.	0.988	14666.	0.696
30.	0.977	15665.	0.691
55.	0.973	16665.	0.686
79.	0.970	17664.	0.681
104.	0.967	18664.	0.677
129.	0.964	19664.	0.673
178.	0.959	20663.	0.669
203.	0.956	28078.	0.653
252.	0.952	38077.	0.642
277.	0.949	57076.	0.633
327.	0.945	77074.	0.628
376.	0.941	97073.	0.624
425.	0.937	137070.	0.613
450.	0.936	177066.	0.604
1270.	0.894	217063.	0.602
2270.	0.860		
3270.	0.834		
4269.	0.812		
5269.	0.793		
6269.	0.778		
7268.	0.763		
8268.	0.751		
10267.	0.729		
11667.	0.717		
12666.	0.710		
13666.	0.702		

Plotting frame

i

META OPTION :

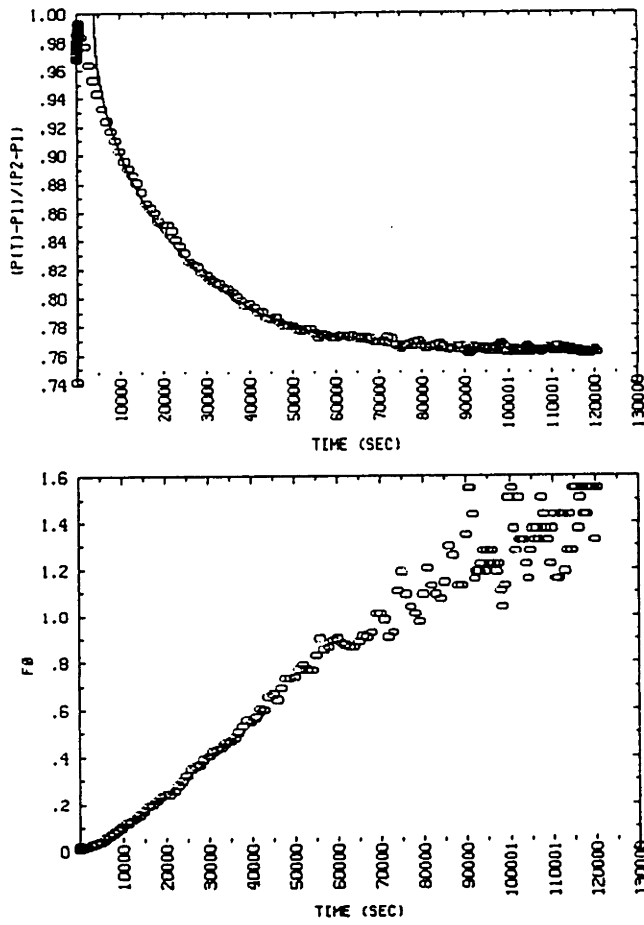


Figure F-60: N₂, 40°C Data Plot Sample 18A

SAMPLE # 18A-P4
 GAS TESTED: N2
 TEST DATE: 10-11-89

*** INPUT PARAMETERS ***

SAMPLE DIAMETER (IN CM): 3.300
 TOTAL CHAMBER VOLUME (IN CM**3): 6.385
 CHAMBER GAS VOLUME, ZERO DEF. (IN CM**3): 3.810
 CHAMBER GAS VOLUME, MAX. DEF. (IN CM**3): 3.810
 FOAM VOID FRACTION: 0.980
 START FO FOR BEST-FIT: 0.025
 END FO FOR BEST-FIT: 0.600
 TEMPERATURE (DEGREES C): 40.000

*** CALCULATED VALUES ***

BEST FIT : FO= 1.507E-5*T + -0.062
 SAMPLE AREA (IN CM**2): 8.553
 NUMBER OF DATA POINTS IN BEST-FIT RANGE 39
 SAMPLE EFF. HALF-THICKNESS (IN CM): 0.151
 EQUILIBRIUM SORPTION PARAMETER, G: 0.319
 EQUILIBRIUM PRESSURE 0.758
 FOAM SOLUBILITY RATIO 0.472
 FOAM SOLUBILITY COEFFICIENT 0.449
 POLYMER SOLUBILITY RATIO -25.400
 POLYMER SOLUBILITY -24.183
 DIFFUSION COEFFICIENT (x10**8) 34.156
 PERMEABILITY COEFFICIENT (x10**8) 15.349

*** TRANSIENT PRESSURE DATA ***

TIME (SEC)	(P(T)-P1)/(P2-P1)
5.	0.965
30.	0.968
79.	0.979
178.	0.981
252.	0.986
376.	0.991
401.	0.984
425.	0.981
450.	0.983
475.	0.984
953.	0.981
1857.	0.974
2858.	0.961
3858.	0.951
4859.	0.942
5858.	0.931
7858.	0.915
9859.	0.901
11859.	0.889
13860.	0.879
15860.	0.864
18861.	0.852
28862.	0.816
38864.	0.793
48866.	0.778
58882.	0.770
68884.	0.767
78886.	3150.768
88888.	0.764
99390.	0.760
109406.	0.763
119408.	0.759

Figure F-61: CFC-11, 80°C Data Plot Sample 18C

plotting frame

2

META OPTION :

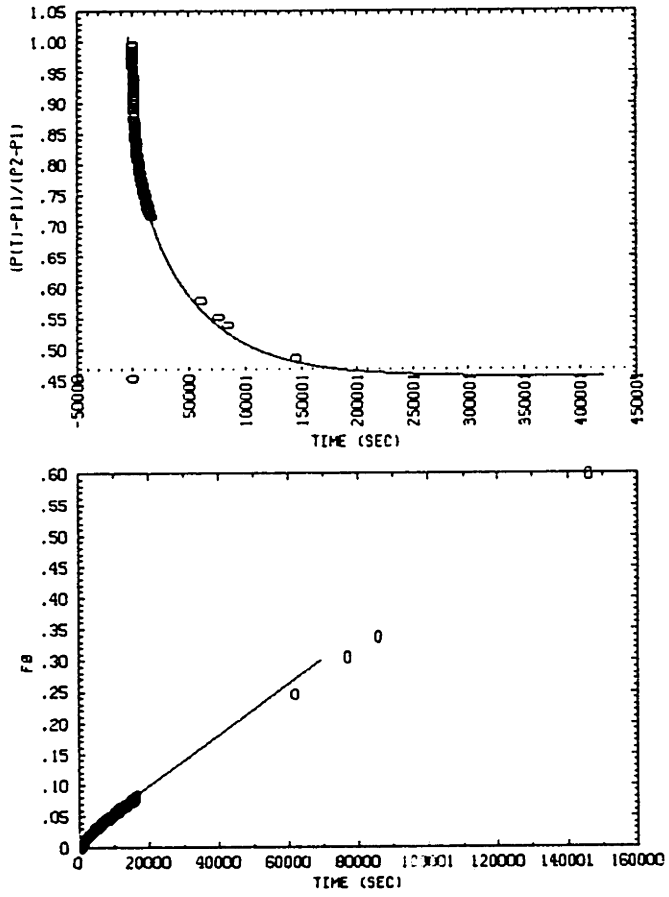


Figure F-62: HCFC-123, 80°C Data Plot Sample 18B

SAMPLE # 18B-P1
 GAS TESTED: HCFC-123
 TEST DATE: 12-15-89

*** INPUT PARAMETERS ***

SAMPLE DIAMETER (IN CM): 3.344
 TOTAL CHAMBER VOLUME (IN CM**3): 5.189
 CHAMBER GAS VOLUME, ZERO DEF. (IN CM**3): 2.655
 CHAMBER GAS VOLUME, MAX. DEF. (IN CM**3): 2.655
 FOAM VOID FRACTION: 0.980
 START FO FOR BEST-FIT: 0.020
 END FO FOR BEST-FIT: 0.300
 TEMPERATURE (DEGREES C): 80.000

*** CALCULATED VALUES ***

BEST FIT : FO= 0.412E-5*T + 0.016
 SAMPLE AREA (IN CM**2): 8.783
 NUMBER OF DATA POINTS IN BEST-FIT RANGE 276
 SAMPLE EFF. HALF-THICKNESS (IN CM): 0.144
 EQUILIBRIUM SORPTION PARAMETER, G: 1.193
 EQUILIBRIUM PRESSURE 0.456
 FOAM SOLUBILITY RATIO 1.250
 FOAM SOLUBILITY COEFFICIENT 1.055
 POLYMER SOLUBILITY RATIO 13.500
 POLYMER SOLUBILITY 11.397
 DIFFUSION COEFFICIENT (x10**8) 8.565
 PERMEABILITY COEFFICIENT (x10**8) 9.038

*** TRANSIENT PRESSURE DATA ***

TIME (SEC)	(P(T)-P1) / (P2-P1)	TIME (SEC)	(P(T)-P1) / (P2-P1)
5.	0.991	3590.	0.812
30.	0.978	4090.	0.810
55.	0.970	4590.	0.801
79.	0.967	5090.	0.796
104.	0.960	5599.	0.786
129.	0.955	6105.	0.782
153.	0.950	6605.	0.778
178.	0.947	7105.	0.771
203.	0.943	7605.	0.769
252.	0.936	8104.	0.766
277.	0.933	8604.	0.761
327.	0.927	9104.	0.756
376.	0.921	9604.	0.751
401.	0.919	10104.	0.749
425.	0.915	10604.	0.741
591.	0.899	11118.	0.742
841.	0.878	11618.	0.736
1091.	0.868	12118.	0.732
1341.	0.860	12618.	0.731
1591.	0.855	13117.	0.726
1841.	0.846	13617.	0.725
2091.	0.842	14117.	0.720
2341.	0.836	14617.	0.717
2591.	0.833	15117.	0.718
3090.	0.824	15617.	0.714
3340.	0.817	75952.	0.546

Plotting frame 1

META OPTION :

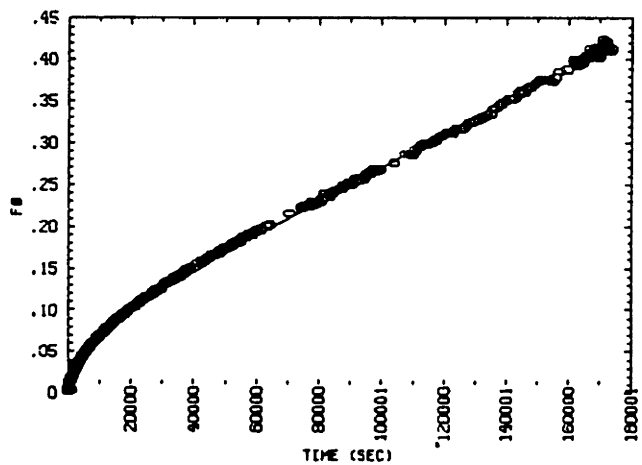
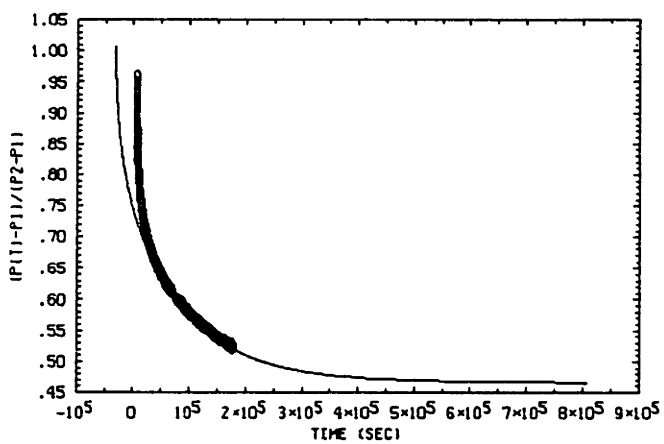


Figure F-63: HCFC-123, 40°C Data Plot Sample 18B

SAMPLE # 18B-P1
 GAS TESTED: HCFC-123
 TEST DATE: 3-3-90

*** INPUT PARAMETERS ***

SAMPLE DIAMETER (IN CM): 3.344
 TOTAL CHAMBER VOLUME (IN CM**3): 5.189
 CHAMBER GAS VOLUME, ZERO DEF. (IN CM**3): 2.655
 CHAMBER GAS VOLUME, MAX. DEF. (IN CM**3): 2.655
 FOAM VOID FRACTION: 0.980
 START FO FOR BEST-FIT: 0.100
 END FO FOR BEST-FIT: 0.300
 TEMPERATURE (DEGREES C): 40.000

*** CALCULATED VALUES ***

BEST FIT : FO= 0.205E-5*T + 0.065
 SAMPLE AREA (IN CM**2): 8.783
 NUMBER OF DATA POINTS IN BEST-FIT RANGE 269
 SAMPLE EFF. HALF-THICKNESS (IN CM): 0.144
 EQUILIBRIUM SORPTION PARAMETER, G: 1.145
 EQUILIBRIUM PRESSURE 0.466
 FOAM SOLUBILITY RATIO 1.200
 FOAM SOLUBILITY COEFFICIENT 1.142
 POLYMER SOLUBILITY RATIO 11.000
 POLYMER SOLUBILITY 10.473
 DIFFUSION COEFFICIENT (x10**8) 4.260
 PERMEABILITY COEFFICIENT (x10**8) 4.866

*** TRANSIENT PRESSURE DATA ***

TIME (SEC)	(P(T)-P1)/(P2-P1)	TIME (SEC)	(P(T)-P1)/(P2-P1)
140.	0.959	20164.	0.697
270.	0.934	21180.	0.695
375.	0.919	22180.	0.691
465.	0.910	23179.	0.687
585.	0.899	25179.	0.682
705.	0.890	27178.	0.677
795.	0.883	28177.	0.674
945.	0.875	29177.	0.672
1050.	0.869	31176.	0.665
1320.	0.858	33176.	0.662
2170.	0.833	35175.	0.658
3170.	0.811	37174.	0.655
4170.	0.797	39174.	0.650
5169.	0.783	43187.	0.643
6169.	0.772	46186.	0.636
7169.	0.763	50185.	0.631
8168.	0.756	54184.	0.625
9168.	0.747	61181.	0.616
10168.	0.742	78808.	0.596
11167.	0.737	88810.	0.584
12167.	0.729	99547.	0.575
13167.	0.726	115715.	0.560
14166.	0.720	125714.	0.554
15166.	0.716	135714.	0.546
16165.	0.713	145713.	0.539
17165.	0.709	155712.	0.534
18165.	0.704	169343.	0.526
19164.	0.700	173092.	0.524

Plotting frame

5

META OPTION :

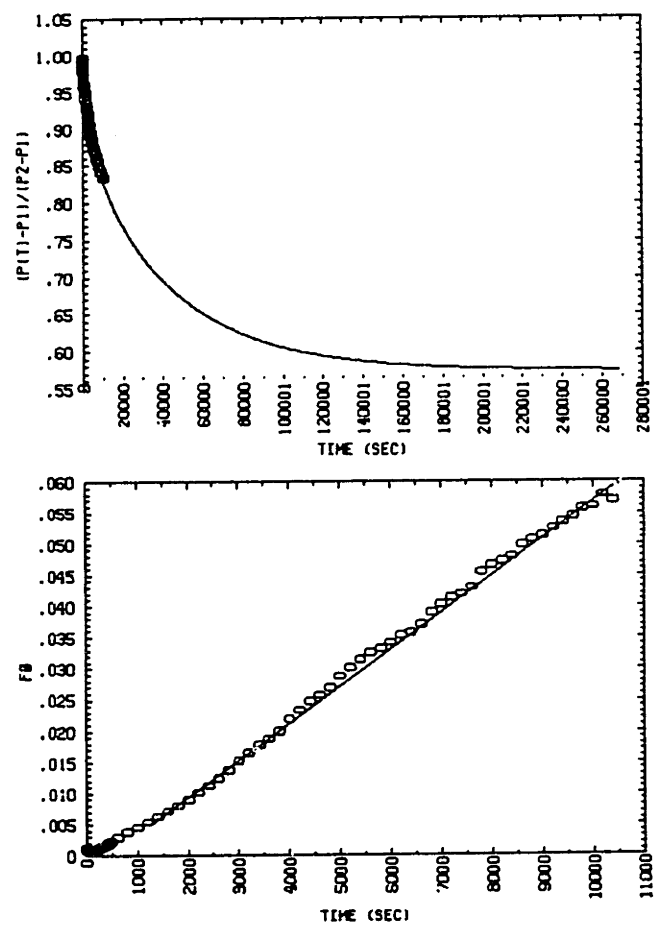


Figure F-64: HCFC-141b, 80°C Data Plot Sample 18A

SAMPLE # 18A-P4
 GAS TESTED: HCFC-141B
 TEST DATE: 112-13-89

*** INPUT PARAMETERS ***

SAMPLE DIAMETER (IN CM):	3.300
TOTAL CHAMBER VOLUME (IN CM**3):	6.385
CHAMBER GAS VOLUME, ZERO DEF. (IN CM**3):	3.810
CHAMBER GAS VOLUME, MAX. DEF. (IN CM**3):	3.810
FOAM VOID FRACTION:	0.990
START FO FOR BEST-FIT:	0.005
END FO FOR BEST-FIT:	0.700
TEMPERATURE (DEGREES C):	80.000

*** CALCULATED VALUES ***

BEST FIT : FO=	0.595E-5*T +	-0.003	
SAMPLE AREA (IN CM**2):			8.553
NUMBER OF DATA POINTS IN BEST-FIT RANGE			46
SAMPLE EFF. HALF-THICKNESS (IN CM):			0.151
EQUILIBRIUM SORPTION PARAMETER, G:			0.743
EQUILIBRIUM PRESSURE			0.574
FOAM SOLUBILITY RATIO			1.100
FOAM SOLUBILITY COEFFICIENT			0.929
POLYMER SOLUBILITY RATIO			6.000
POLYMER SOLUBILITY			5.065
DIFFUSION COEFFICIENT (x10**8)			13.491
PERMEABILITY COEFFICIENT (x10**8)			12.528

*** TRANSIENT PRESSURE DATA ***

TIME (SEC)	(P(T)-P1)/(P2-P1)
5.	0.982
30.	0.989
55.	0.992
79.	0.992
104.	0.990
129.	0.990
153.	0.988
178.	0.987
203.	0.985
228.	0.982
252.	0.982
277.	0.981
302.	0.980
327.	0.978
351.	0.978
376.	0.976
401.	0.975
425.	0.974
450.	0.973
609.	0.964
1605.	0.940
2605.	0.919
3604.	0.899
4604.	0.883
5604.	0.869
6603.	0.861
7603.	0.851
8602.	0.841
9602.	0.834

Figure F-65: HCFC-141b, 60°C Data Plot Sample 18A

SAMPLE # 18A-P4
 GAS TESTED: HCFC-141B
 TEST DATE: 12-13-89

*** INPUT PARAMETERS ***

SAMPLE DIAMETER (IN CM):	3.300
TOTAL CHAMBER VOLUME (IN CM**3):	6.385
CHAMBER GAS VOLUME, ZERO DEF. (IN CM**3):	3.810
CHAMBER GAS VOLUME, MAX. DEF. (IN CM**3):	3.810
FOAM VOID FRACTION:	0.980
START FO FOR BEST-FIT:	0.001
END FO FOR BEST-FIT:	0.040
TEMPERATURE (DEGREES C):	60.000

*** CALCULATED VALUES ***

BEST FIT : FO=	0.154E-5*T + -0.001	
SAMPLE AREA (IN CM**2):		8.553
NUMBER OF DATA POINTS IN BEST-FIT RANGE		27
SAMPLE EFF. HALF-THICKNESS (IN CM):		0.151
EQUILIBRIUM SORPTION PARAMETER, G:		0.743
EQUILIBRIUM PRESSURE		0.574
FOAM SOLUBILITY RATIO		1.100
FOAM SOLUBILITY COEFFICIENT		0.984
POLYMER SOLUBILITY RATIO		6.000
POLYMER SOLUBILITY		5.369
DIFFUSION COEFFICIENT (x10**8)		3.488
PERMEABILITY COEFFICIENT (x10**8)		3.434

*** TRANSIENT PRESSURE DATA ***

TIME (SEC)	(P(T)-P1)/(P2-P1)
396.	0.996
420.	0.995
3901.	0.952
8902.	0.914
13912.	0.890
18916.	0.873
23917.	0.862
28929.	0.854
33930.	0.848
211905.	0.817

The End